Novel Microwave-Mediated Luminescent Chromophore Synthesis for Photophysical Study

Thesis Submitted for the Degree of Doctor of Philosophy at Cardiff University

Zhifan Lin

October 2010

UMI Number: U564679

UMI

Dissertation Publishing

ProQuest
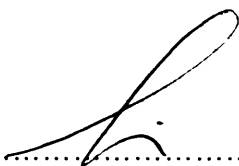
DECLARATION

This work has not previously been accepted in substance for any degree and is not concurrently submitted in candidature for any degree.

Signed .... (candidate)   Date .... 12 | 4 | 2011
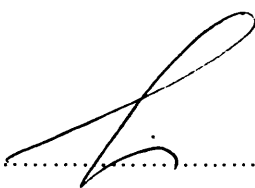
STATEMENT 1

This thesis is being submitted in partial fulfillment of the requirements for the degree of PhD

Signed .... (candidate)   Date ...... 12 | 4 | 2011
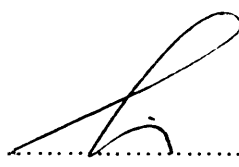
STATEMENT 2

This thesis is the result of my own independent work/investigation, except where otherwise stated. Other sources are acknowledged by explicit references.

Signed .... (candidate)   Date ...... 12 | 4 | 2011

STATEMENT 3

I hereby give consent for my thesis, if accepted, to be available for photocopying and for inter library loan, and for the title and summary to be made available to outside organisations.

Signed .... (candidate)   Date ...... 12 | 4 | 2011

ABSTRACT

Nicotinonitrile chromophores with tunable photophysical properties and solvatochromic behaviour can be prepared quickly and efficiently by microwave-assisted tandem oxidation/Bohlmann–Rahtz heteroannulation followed by copper(I)-mediated N-arylation.

Synthesis of 2,4,6-trisubstituted pyrimidines by tandem oxidation/heterocyclocondensation of propargylic alcohols and amidines was also achieved rapidly under microwave dielectric heating using barium manganate as an novel oxidant. Irradiation at 150 °C in ethanol–acetic acid for 45 min resulted in a dramatic improvement of synthetic yield over the conventional manganese dioxide-mediated condition and established a facile route to synthesize triarylpyrimidines in investigating their photophysical properties.

The synthesis of fluorescent 2,2':6',2''-terpyridine zinc sensors with desirable photophysical properties from β-aminocrotononitrile and diverse 2,6-bis(alkynone)pyridines was established by a one-pot Bohlmann-Rahtz reaction in excellent yields.

Finally, a series of novel cyanobipyridine-derived zinc(II) bis(thiolate) complexes were prepared excellently by a microwave-assisted cross-coupling/complexation sequence and display luminescence that can be modulated using intrinsic functionality and ancillary ligands.

ACKNOWLEDGMENTS

ABBREVIATIONS

Abs.	Absorption
Ac	Acetyl
APcI	atmospheric pressure chemical ionization
aq.	Aqueous
Ar	Unspecified aryl substituent
Bu	Butyl
BuLi	Butyllithium
cat.	Catalytic/catalyst
CF	Continuous Flow
CI	Chemical Ionization
DMF	N,N–Dimethylformamide
DMSO	Dimethyl sulfoxide
ε	Molar absorbtivity
EI	Electron Impact
Em.	Emission
equiv. or eq.	Equivalent
Et	Ethyl
Ex.	Excitation
Fl.	Fluorescence
FTIR	Fourier Transform Infra Red
g	Grams
h	Hour/s
HPLC	High Pressure Liquid Chromatography
HRMS	High Resolution Mass Spectrometry
Hz	Hertz
IBX	o-Iodoxybenzoic acid
IC	Internal Conversion
ICT	Intra-molecular Charge Transfer State
ILCT	Intra-ligand Charge Transfer State
IR	Infra Red
ISC	Intersystem Crossing
J	Coupling constant (in Hz)
LDA	Lithium di *iso*–propylamide
LE	Locally Excited Electronic State

lit.	Literature
LLCT	Ligand-ligand Charge Transfer State
LRMS	Low Resolution Mass Spectrometry
M	Molar
MAOS	Microwave–Assisted Organic Synthesis
Me	Methyl
MHz	Megahertz
min	Minutes
MLCT	Metal-ligand Charge Transfer State
μM	Micromolar
mol	Mole
Mp	Melting point
MS	Mass Spectrometry
nm	Nanometer
NMR	Nuclear Magnetic Resonance
ns	Nanosecond
P	*Para*
Ph	Phenyl
PhMe	Toluene
Ppm	Parts per million
ps	Picosecond
quant.	Quantitative
R	Specified substituent
RT	Room Temperature
Silica/SiO₂	Merck Kieselgel 60 H silica or Matrex silica 60
sp.	Species
SPOT	Solid Phase Organic Transformation
Tert	Tertiary
TFA	Trifluoroacetic acid
THF	Tetrahydrofuran
TLC	Thin Layer Chromatography
TMS	Trimethylsilyl
Ts	Tosyl (*para*–toluene sulphonyl)
UV	Ultraviolet
VR	Vibrational Relaxation
Vs.	Versus

TABLE OF CONTENTS

Chapter One – Introduction

First described more than two decades ago, microwave-assisted synthesis has been developed from a laboratory curiosity to an established synthetic method that nowadays is widely used in academia and the chemical/pharmaceutical industry. One of the most valuable advantages of using controlled microwave dielectric heating for chemical synthesis is the dramatically reduced reaction times: from days and hours to minutes, even seconds. As will be explained in this thesis, there are also many more good reasons why scientists nowadays should incorporate dedicated microwave reactors into their daily research and development routines.

During the past 25 years, there has been a great increase in the use of the photoluminescence technique in biological and biomedical related sciences.[1(a)-(c)] Initially introduced as an analytical tool to determine concentrations of various species in solution (neutral or ionic), photoluminescence has now evolved into a valuable research method used extensively in the areas of biochemistry, flow cytometry, medical diagnostics, DNA sequencing and genetic analysis. Furthermore, there has also been a remarkable growth in the use of photoluminescence for cellular and molecular imaging (Figure 1). Luminescence imaging can actually reveal the structure and dynamics of intracellular living systems in vivo, typically validating at single molecule detection levels.

Photoluminescence technology is used by scientists from many disciplines. This thesis describes the principles of the microwave-assisted synthesis of luminescent chromophores and therefore, provides new potential in the organic, photophysical and biological sciences. Throughout the discussion, we have included many examples that illustrate how the fundamental principles can be used resourcefully, in various research applications.
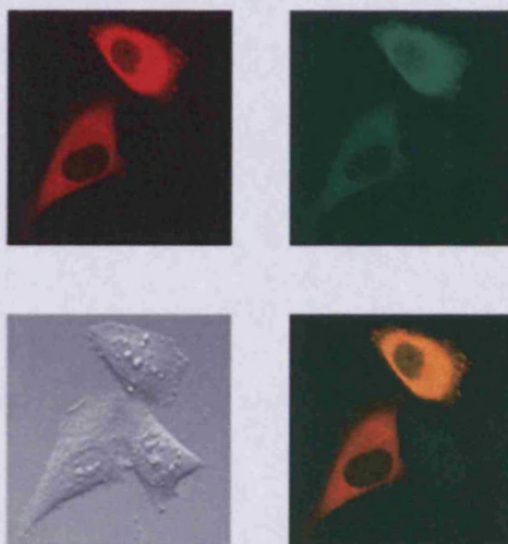
Figure 1. Multi-colour live cell fluorescence imaging using a single genetic building block. The technique is based on the formation of a covalent bond between a protein fusion tag and a synthetic ligand, and therefore designed to enable the understanding of proteins' photophysical characteristics in an intracellular-like environment.[1(d)]

1.1 Microwave theory

In an ideal world, chemical transformations occur at room temperature, reach full conversion within a few minutes, and provide quantitative isolated yields. The reality, however, is quite different. Many synthetically relevant processes require elevated temperatures in order to activate a transformation, with reaction times of several hours or even days to drive a reaction to completion not being uncommon. Until recently, heating reaction mixtures on a laboratory scale was typically performed by using oil baths often under reflux conditions where the reaction temperature is limited by the boiling point of the solvent. This traditional form of heating is a rather slow and inefficient method for transferring energy into a reaction mixture, since it depends on the thermal conductivity of various external materials present in the system, and quite often, will result in the temperature of the external vessel cell being higher than the reaction mixture itself.

In contrast, microwave irradiation produces efficient internal heating by the direct coupling of microwave energy with the target molecules present in the mixture.[2-3] Microwave irradiation actually triggers heating by two major mechanisms — dipolar polarization and ionic conduction. Whereas the dipoles in the reaction mixture (*e.g.*, polar solvents) are primarily involved with the polarization movement, the charged particles in the mixture (*e.g.*, ions) can be largely affected by the ionic conduction.

1.1.1 Dipolar polarization mechanism

If two samples, one containing water and one dioxane, are heated in a single-mode microwave cavity at a fixed power and for a fixed irradiation time, the final temperature will be higher in the water sample, as shown in Figure 2.

Figure 2. The temperature increases of water and dioxane, respectively, at 150 W microwave irradiation.[4]

2

In order to understand why this phenomenon occurs, it is necessary to appreciate the underlying principles of the microwave dielectric heating mechanism. As with all electromagnetic radiation, microwave radiation can be divided into an electric field component and a magnetic field component. The former electric field is responsible for the dielectric heating, which is mainly effected via the dipolar polarization mechanism.[4]

For a substance to generate heat when coupled with the microwave irradiation, it must possess a relatively 'long-lasting' dipole moment, as has the water molecule. A dipole is sensitive to the external electric field and will attempt to align itself with the field by undergoing the 'dipolar orientational rotation' (Figure. 3).
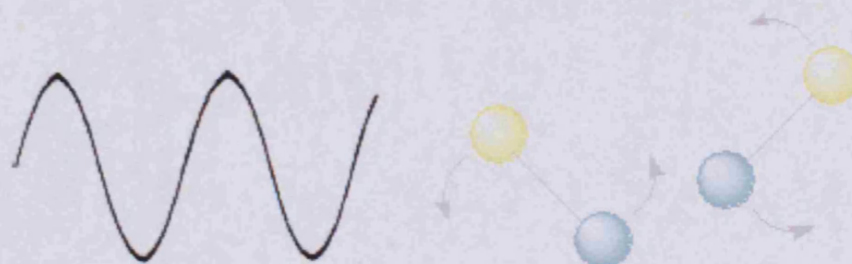
Figure 3. Dipolar molecules will try to align with an oscillating electric field.

The applied field provides the energy for such a rotation. In gaseous phase for example, molecules are spaced far apart from each other and therefore their alignments with the applied field are rapid and efficient, whilst in the solution phase, instantaneous alignment can be frequently prohibited by the presence of other substrates in the system (i.e. the solvents). Therefore the ability of solutes to align itself with the applied field will vary with irradiation frequencies and viscosities of various reaction media.

Under irradiation with low frequency radiation, the solute will submissively rotate in phase with the external oscillating field, and gain some energy thereafter, although the overall heating efficiency generated by such 'total alignment' is really small.

Alternatively, under the influence of high frequency radiation, the dipoles actually do not have sufficient time to respond to the oscillating field and just stop rotating. Since no motion can be induced into the reaction mixture, therefore no energy transfer will occur and eventually no heating will be facilitated.

If the applied field is however, targeted upon the microwave energy scale, a balanced phenomenon will actually occur between these two extremes. Under the microwave dielectric heating, the irradiation frequency is low enough, so that all the reacting dipoles will have the time to respond to the external electric field and undergo the 'in phase' rotation.

The frequency is, however, not high enough that can allow such rotation to follow precisely the direction of the electric field, so as the dipole re-orientates to align itself with the external field, the field has already changed and will produce a newly emanated 'phase difference' between itself and the 'just modified' dielectric property of the reacting dipole.

Such a phase difference can actually cause a kinetic energy loss due to the random collision among various particles in the reaction system, which will consequently generate a large amount of the *kinetic* heat that is required to facilitate a chemical reaction to successfully occur.

Thus in the previous example, it becomes clear that why dioxane that lacks any dipolar orientational characteristics that are demanded to mediate an efficient microwave dielectric interaction (*between the field and the reacting particle*), does not heat whilst water, which has a large dipole moment, heats dramatically.

Similarly, this explains why the gaseous system can not be heated by the microwave irradiation, since the distance between two activated molecules therein is apparently long enough for them to follow perfectly any transient changes of the external electric field, so that as a consequence, no phase differences occur afterwards.

1.1.2 Ionic conducting mechanism

If two samples containing distilled water and tap water, respectively, are heated in a single mode microwave cavity at a fixed power and for a fixed time, the final temperature will be higher in the sample containing tap water (Figure 4).
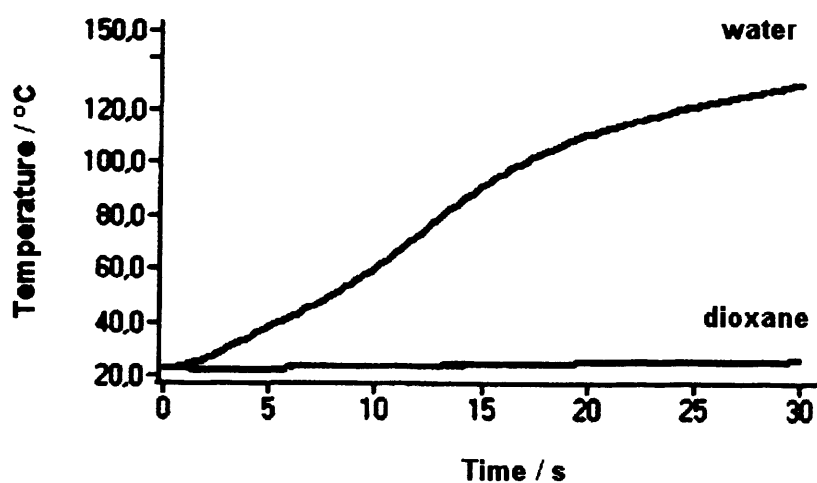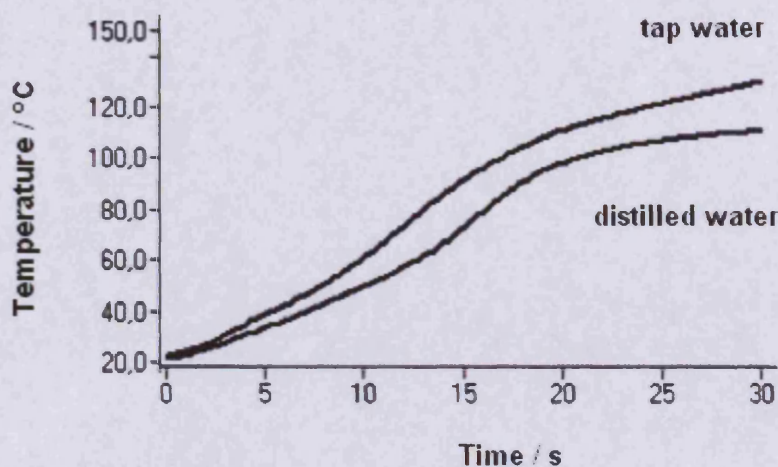

Figure 4. The temperature increases of distilled water and tap water, respectively, at 150 W microwave irradiation.[4]

This phenomenon is due to a second characteristic interaction between the external electric field and the reaction mixture, the ionic conducting mechanism (Figure 5). If a solution contains ionic species, or even a single isolated ion with a hydrogen-bonded cluster, all the ions will move orderly through the solution after the electric field is applied to the mixture. This will result in an increased reaction temperature due to the enhanced collision rate, converting much kinetic energy into reaction heat.
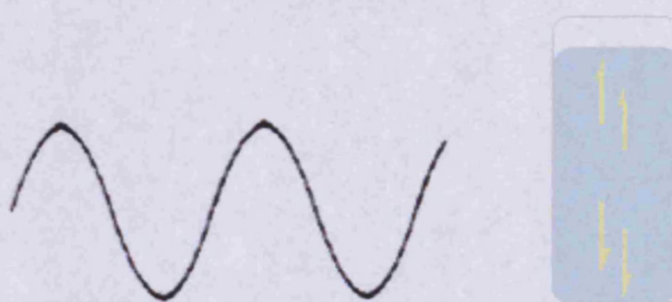
Figure 5. Charged particles in a solution will follow the applied electric field.

The conducting mechanism is a much more versatile interaction than the dipolar mechanism in the regard of generating the thermal energy. In the example above, the heat generated by the conducting mechanism will actually multiply the reacting enthalpy produced initially via the 'field-dipole' interaction, resulting in an even higher end temperature in the tap water mixture.[4]

1.1.3 Loss angle

As mentioned above, permanent dipolar and ionic species are required to mediate microwave dielectric heating. How does the microwave heating effect vary among different solvents? Actually the microwave-assisted dielectric polarization primarily depends upon the ability of different reacting molecules (solutes and solvents) in re-orientating their own dipole moments in order to harmonize with the external electric field.[4]

Table 1. Dielectric constants and loss tangent values for some organic solvents.

Solvent	Dielectric constant $(\varepsilon_s)^a$	Loss tangent (tan δ)^b
Acetic acid	6.1	0.091
Ethyl acetate	6.2	0.174
THF	7.6	0.059
Methylene Chloride	9.1	0.047
Acetone	20.6	0.042
Methanol	32.7	0.941
Acetonitrile	36	0.659
Dimethylformamide	36.7	0.062
DMSO	47	0.161
Water	80.4	0.123

^{a} The dielectric constant ε_s equals to relative permittivity ε', at room temperature and under the influence of a static electric field; ^{b} Values determined at 2.45 GHz and room temperature.

It would be reasonable to deduce that the more polar the solvent is (i.e. the higher dielectric constant value it possesses), the more readily that the microwave irradiation can be absorbed and therefore the higher the reaction temperature that can be achieved. This should correspond well to what is actually observed in section 1.11 (water vs dioxane). If however, two solvents with comparable dielectric constant ε_s, such as acetone and methanol (Table 1), are heated under the same irradiating power and for a same period of time, the end temperature in methanol is nevertheless much higher than that of acetone, as shown in Figure 6.
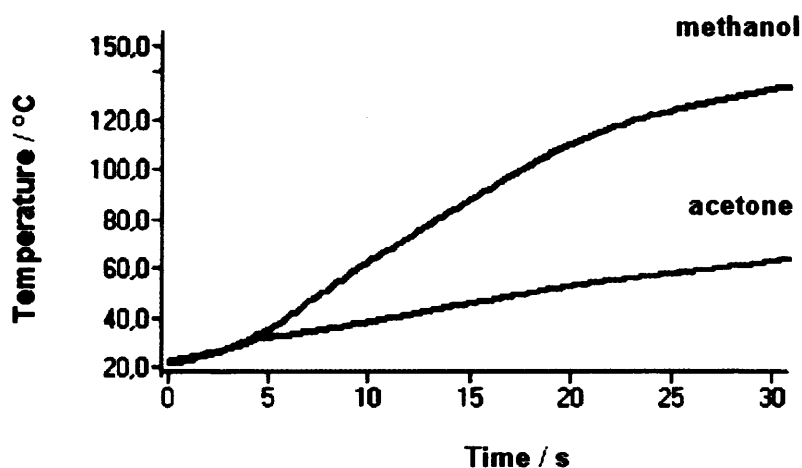
Figure 6. The temperature increases of ethanol and acetone, respectively, at 150 W microwave irradiation.[4]

In order to compare the abilities of various solvents in generating the heat from microwave irradiation, their capacities in aligning with the external dielectric field and converting the collisional oscillation into the corresponding thermal energy must be taken into account and these factors can be well understood in the term of the loss angle δ, as given in the expression (Eqt. 1).

$$\tan \delta = \frac{\varepsilon''}{\varepsilon'}$$

(1)

In this equation, the relative permittivity ε', is equivalent to the dielectric constant ε_s. The dielectric loss factor ε'' quantifies the efficiency with which the absorbed energy can be converted into heat. For solvents with comparable values of ε' and ε'', the loss factor tan δ actually provides a convenient way of comparing the ability of different media in terms of converting microwave energy into the required thermal kinetic drive. The dielectric constants of acetone and methanol are indeed, in the same range (Table 1); however methanol possesses a much higher loss tangent than acetone, for which, it couples better with the microwave irradiation and will result in a much more rapid increase of temperature. By applying the same principle, polar additives such as ionic liquids or passive heating elements made out of strongly microwave absorbing materials (e.g., SiC) can be added to otherwise low absorbing media in order to increase the overall absorbance level of the coupling system.[5] Since the reaction vessels employed in microwave chemistry are made out of essentially microwave transparent materials (e.g., Teflon, tan δ < 0.01), as a result, only the reaction mixture and not the vessel will be affected by the microwave irradiation (Figure 7).
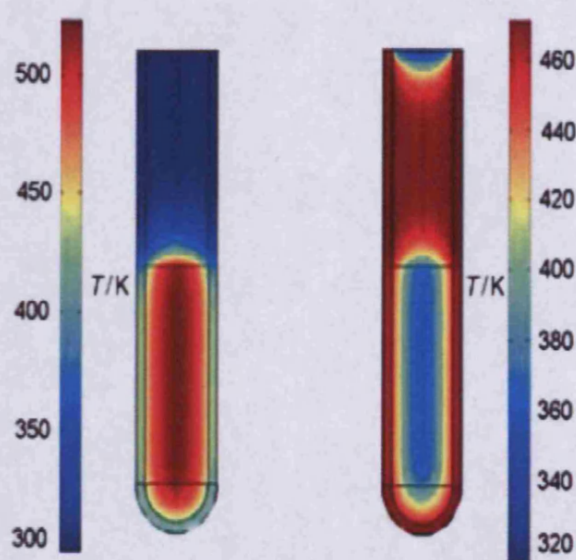
Figure 7. The temperature profile after 60 sec as affected by microwave irradiation (left) compared to treatment in an oil bath (right). Microwave irradiation raises the temperature of the entire reaction system simultaneously, whereas in the conductive heating tube, the areas in close contact with the vessel wall are heated first.[4]

1.1.4 Microwave effect

Dramatic rate accelerations and yield enhancements resulting from the microwave irradiation have not always been observed under conventional heating conditions, however most, if not all, are still attributed to some underlying thermal effects. They are actually due to the characteristics of the microwave dielectric heating, defined as 'specific microwave effects', arising from superheating, the selective absorption of heterogeneous catalysts or reagents in a less polar medium that can generate so-called 'hot spots'.[6]

'Hot spot' is a thermal effect caused by an inhomogeneous field, often resulting in high temperature areas formed within the irradiated sample. In theory,[6-7] a hot spot could be caused by the dielectric differences of reaction mixture, uneven distributions of electro-magnetic strength, or dissimilar abilities of the target medium in absorbing volumetric dielectric heating through the microwave irradiation.

A representative reaction coordinate shows that the reactants must reach the higher energy level of the transition state, by absorbing thermal energy from the nearby system, in order to be transformed into the corresponding chemical products (Figure 8).
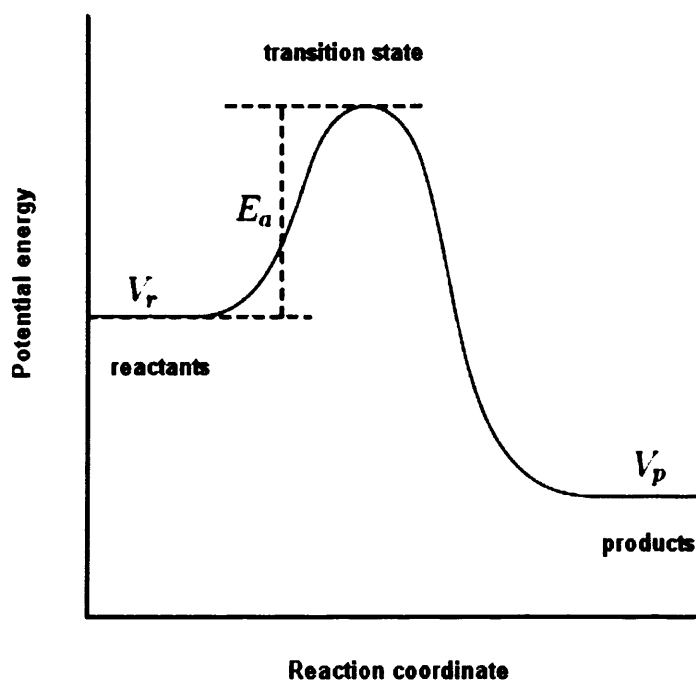
Figure 8. Typical reaction profile for the transformation of the reactants to products passing through the transition state.[7]

In the above figure, the rate related to a 'total transformation' can be actually calculated by using the Arrhenius equation:

$$k = Ae^{\frac{-E_a}{RT}}$$ (2)

where k is the rate constant, A is the frequency of collisions corresponding to a correct orientation for a reaction to occur, E_a is the activation energy, R is the gas constant and T is the reaction temperature.

Such an exponential correlation represents the fraction of molecules with the minimum energy required to overcome the activation barrier and allow the reaction to take place.

Based on this equation, Mingos and Baghurst calculated the accelerating rate caused by the increase of temperature for a first order reaction and they worked out that on average, a rise in temperature from 77 °C to 177 °C resulted in a 1000-fold rate enhancement (13.4 h *vs.* 23.4 s).[8]

Clearly, this experimental statement clarified what many others had observed, that rapid heating, greatly increased temperature and astonishingly enhanced reaction rate under microwave mediated conditions, actually can be rationalized in terms of a simple thermal/kinetic effect.

However, at the same time, some authors have indeed suggested the existence of a 'non-thermal microwave effect' (in some terms, referred as the *athermal* effect).[4(b)] In general, non-thermal effects can be classified as the rate acceleration that can not be directly explained in the term of either a purely thermal/kinetic, or specific microwave heating effect.

Such a non-thermal effect essentially results from a close interaction of the external electric field with target molecules in the reaction mixture. It has also been argued that the presence of an electric field actually can lead to the orientational effect of various dipolar molecules (presumably existing both in the reactants and the medium) and therefore, change the pre-exponential factor A and/or the activation energy E_a (in the term of $\Delta S°$) from the Arrhenius equation.[9]

Synchronizing with such a statement, a similar phenomenon should also be observed from the dipolar collision mechanism (section 1.11), where the polarity is increased going from the ground

state to the activated transition state, resulting in a great enhancement of the transformation rate, by lowering the activation barrier of the entire reacting system.[9]

Nevertheless, microwave effects are the subject of considerable current debate and controversy,[10] and it is evident that extensive investigating efforts will be required in order to comprehensively appreciate the underlying principles and maximize the great potential of this innovative technique, both in academic research and the drug-manufacturing industry.

1.1.5 Synthetic applications

As we have seen, in recent years, the use of microwave dielectric heating in synthetic chemistry has emerged as a valuable alternative to conventional conductive heating methods.[11] This field of chemistry is known as the 'Microwave-Assisted Organic Synthesis' (MAOS). With no direct contact between the chemical reactants and the energy source, microwave-assisted chemistry can be more efficient, in terms of the energy used, capable of providing faster heating rates and able to improve reaction rates and efficiencies. Recent advances in instrumentation, with the introduction of dedicated ovens for organic synthesis that focus microwaves in a monomodal cavity, have increased the popularity and reproducibility of microwave chemistry, increasing the methodology available for the development of new synthetic reactions and optimisation of existing procedures.[12]

For example, recently MAOS was employed in the synthesis of a variety of flavonoid-derived heterocyclic compounds in supporting an 'Anti-Methicillin Resistant *Staphylococcus Aureus*' (MRSA) drug discovery project,[13] which can ultimately lead to the improved treatment of fungal infection to human bodies and similar biological related diseases, *e.g.*, microbial invasion by plant pathogens or bacterial drug resistant strains (*i.e.* towards vancomycin, which is a mainstay of the MRSA therapy).

Following a classic Baker-Venkataraman rearrangement,[14] Brown *et al.* coupled acetyl chlorides with a range of *o*-hydroxyacetophenones. While 1-(2-hydroxyaryl)propane-1,3-dione intermediates were formed, they were subsequently converted into the flavonoid derivatives upon microwave-assisted 'metal-free' cyclisation (Scheme 1).
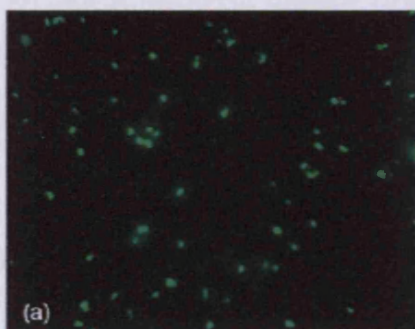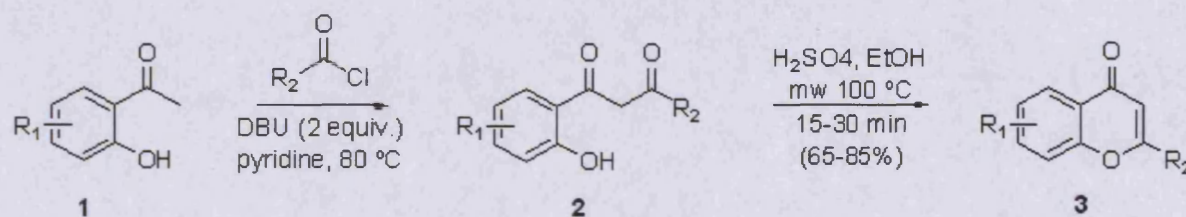
Scheme 1. Microwave-assisted synthesis of flavonoid-derived heterocycles.[13] *Inset: (a) Baclight image of MRSA – total cells (stained by Syto9 fluorescent dye); (b) After exposure to one of the flavonoid derivatives – dead cells (stained by propidium iodide).* This result clearly showed the loss of the membrane integrity in MRSA cells upon exposure to the target drug, indicating the remarkable bactericidal character of these flavonoid-derived compounds.

Under a conventional heating approach, such a synthesis would take 1 to 2 days to complete, while under the optimised microwave conditions, the final cyclisation step was achieved in only 30 min, in 65-85% isolated yield.

More recently, Burgess *et al.* also illustrated the advantages of MAOS in synthesizing the regioisomerically pure rhodamine chromophores by developing a facile microwave-assisted 2-component condensation of 4-bromobenzaldehyde with various phenolic amines.[15]

When the aldehyde was reacted with a sample amine under thermal condition (90 °C) for 18 hours, cyclodehydration only occurred in 35% yield, accompanied by the formation of a wide range of side-products that made the subsequent ^{1}H NMR interpretation nearly impossible. Higher temperatures and longer reaction times merely resulted in diminished yields and for some specific reactions investigated, decompositions occurred.[15]

However, by using microwave-assisted conditions for the condensation between 4-bromobenzaldehyde and a phenolic amine at 150 °C for 10 minutes, followed by an *in situ* oxidation with Chloranil, the Burgess group successfully isolated the regioisomerically pure 4-

11

bromorhodamine derivatives in 53-73% yield, without the requirement for further chromatographic purification (Scheme 2).
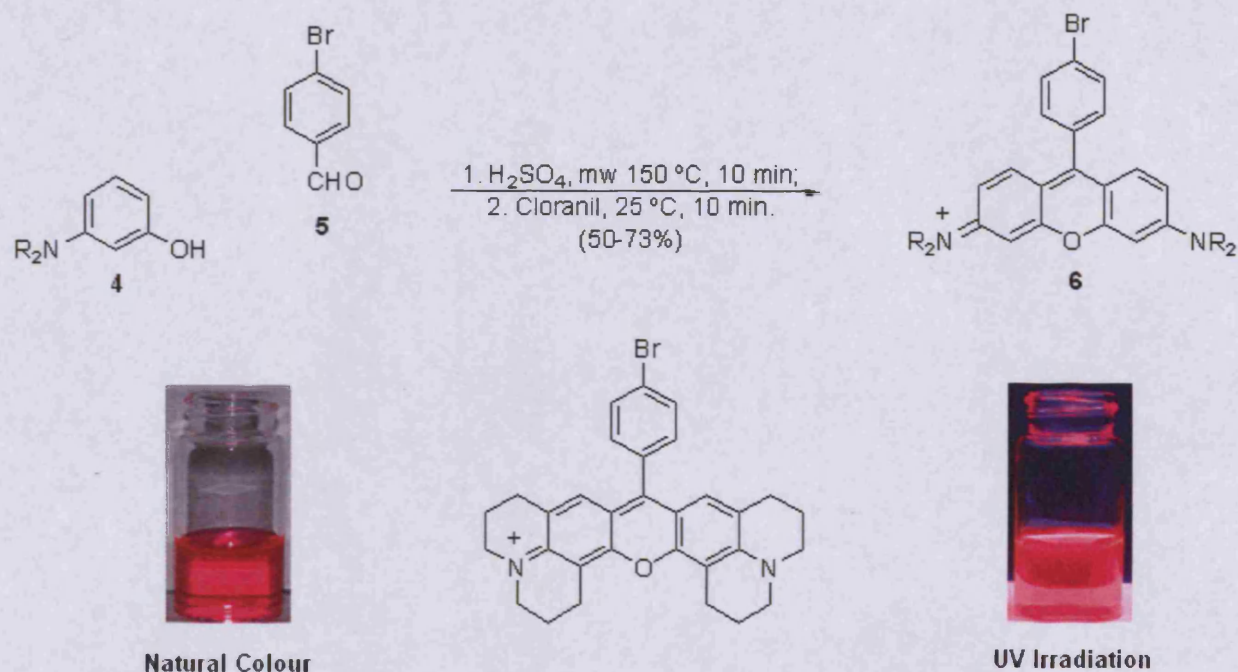
Scheme 2. Microwave-assisted synthesis of regioiomerically pure bromorhodamine derivatives.

The rhodamine dyes synthesized via such a method are highly colourful and the ambient state emission spectra span the range 532 - 616 nm in polar protic solvents.[15] Such luminescence response will actually make them attractive candidates in designing novel light-harvesting charge/energy transfer cassettes,[16] and as a result, will enable a range of photophysical investigations for various biomedical applications (*e.g.*, multiplexing,[17] high throughput DNA sequencing[18] etc).

1.2 Principles of photoluminescence[1]

Photoluminescence is the emission of photons from electronically excited states. Generally, photoluminescence can be divided into two categories, depending upon the nature of the ground and the excited states. In a singlet excited state, the electron in the higher-energy orbital has the opposite spin orientation to the second electron in the lower orbital. These two electrons are said to be paired. In a triplet state these electrons are unpaired, that is, their spins have the same orientational characteristics. Return to the ground state from an excited singlet state does not require an electron to change its spin orientation. A change in spin orientation is however, needed for a triplet state to return back to the singlet ground state.[1&19]

Fluorescence (Figure 7) is the emission which results from the return to the lower orbital of the paired electron. Such transitions are quantum mechanically 'allowed' and the emissive rates result in fluorescence life time near 10^{-8} s or 10 ns. The lifetime is the average period of time a chromophore remains in the excited state. Phosphorescence is the emission which results from the transition between states of different multiplicity, generally from a triplet excited state returning to a singlet ground state. Such transitions are 'not allowed' and the emissive rates are slow. Typical phosphorescence lifetimes range from milliseconds to seconds, depending primarily upon the nature of non-radiative deactivation processes other than the radiative emission.
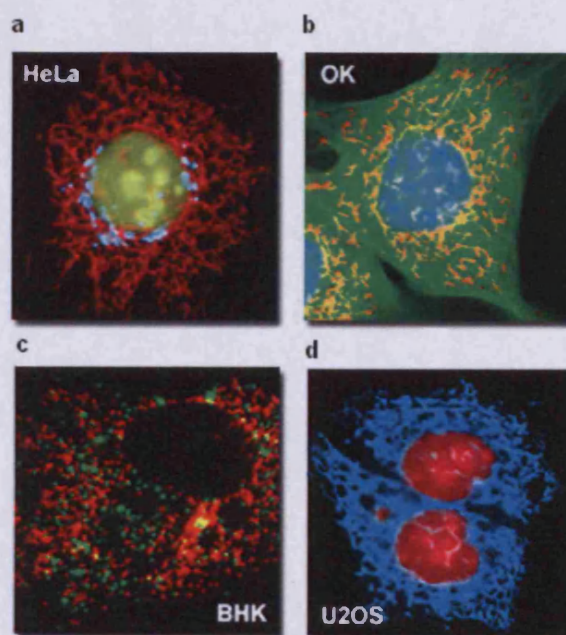
Figure 7. Intracellular imaging simultaneously labelled by multi-colour fluorescent proteins, *e.g.*, the opossum kidney epithelial cells in (b) were labelled by EGFP (tubulin), ECFP (nucleus) and DsRed2FP (mitochondria)

targeting different intracellular functions and clearly separated by wide-field photoluminescence filtering combinations used in manipulating the live cell imaging (Nikon CFP, YFP HYQ and Cy3 HYQ).[20]

1.2.1 Jablonski diagram

The Perrin-Jablonski diagram is convenient for visualizing in a simple way any possible radiative and non-radiative processes among various electronic states: *e.g.*, photon absorption, internal conversion, fluorescence, intersystem crossing, phosphorescence, delayed fluorescence and triplet-triplet transitions. The singlet electronic states are denoted as S_0 (fundamental electronic state), S_1, S_2 ... and the triplet states, T_1, T_2 ... Vibrational levels are associated with each electronic state. It is important to note that absorption is very fast ($\approx 10^{-15}$ s) with respect to all other processes (so that there is no concomitant displacement of nucleic configurations between the ground state and the initially excited singlet state, according to the Frank-Condon principle.[21]).
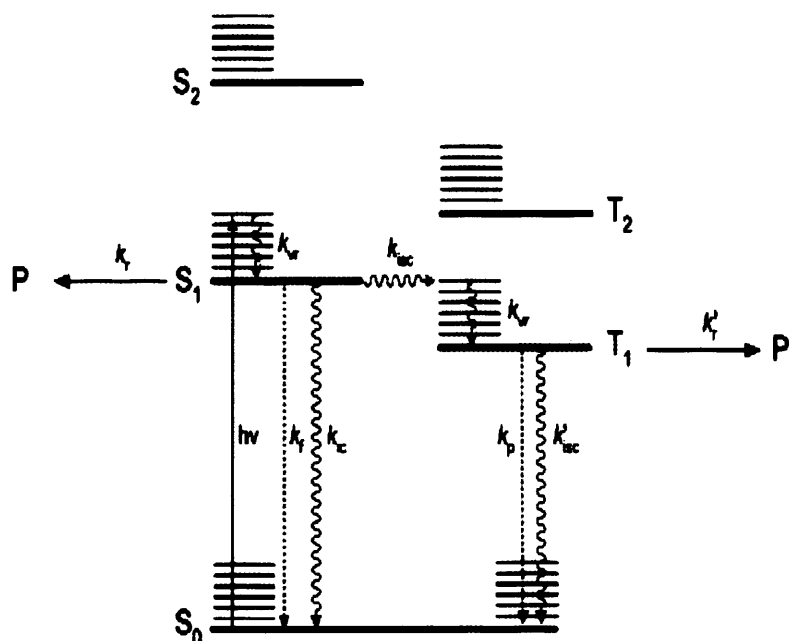
Figure 8. Jablonski diagram (IC: internal conversion; ISC: intersystem crossing; S: singlet excited state; T: triplet excited state; P & P': formation of photo-chemical products, an alternative channel of the non-radiative decay).

Following light absorption, several de-excitation processes may occur as a consequence. A chromophore is usually excited to some higher vibrational levels of either S_1 or S_2 states and then, molecules in condensed phases rapidly relax to the lowest vibrational level of S_1 state, which is defined as internal conversion and generally occurs in 10^{-12} s. Since fluorescence lifetimes are typically near 10^{-8} s, internal conversion is generally complete prior to emission. Hence the fluorescence emission essentially results from the thermally equilibrated S_1 state.

As for absorption, the electronic transition down to the lowest electronic level also results in an excited vibrational state (Figure 8). This state will reach thermal equilibrium in about 10^{-12} s. An interesting consequence of these considerations is that the absorption spectrum of the chromophore actually reflects the vibrational levels of the electronically excited states, and the emission spectrum reflects the vibrational levels of the ground state.[1] Generally, electronic excitation does not greatly alter the spacing of the vibrational levels. As a result, the vibrational structures seen in the absorption and emission spectra are similar.

Molecules in the S_1 state can also undergo conversion to the first triplet state T_1. Emission from T_1 is termed as phosphorescence, and is spontaneously shifted to longer wavelengths (lower energy region) relative to the fluorescence. Conversion of S_1 to T_1 is called inter system crossing (ISC). Transition from T_1 to the ground state is forbidden, and as a result the rate constant for such emission is several orders of magnitude smaller than those of fluorescence ($k_p \ll k_f$).

1.2.2 Stokes shift & mirror image rule

In general, the differences between the vibrational levels are similar in the ground and excited states, so that the fluorescence spectrum often resembles the first absorption band. The gap between the maximum of the first absorption band and the maximum of fluorescence is defined as the Stokes shift (Figure 9).
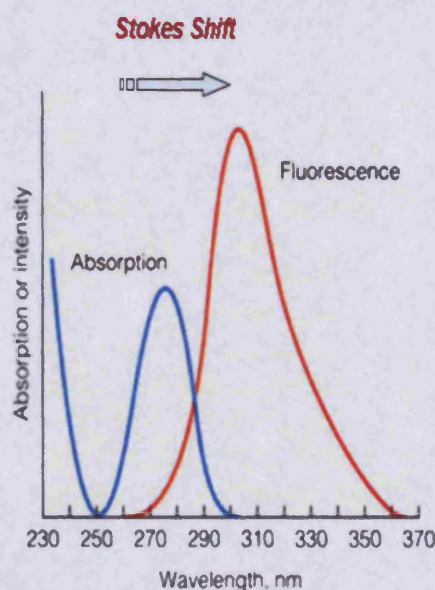
Figure 9. The simplified definition of Stokes shift; In real calculation, however Δv should be in the unit of wavenumber (cm^{-1}) rather than wavelength (nm).

Due to the energy loss between the excitation and emission processes observed universally in the solution phase, one common cause of the Stokes shift is the rapid non-radiative deactivation to the lowest vibrational level of the emitting excited state (vibrational relaxation). In addition, chromophores generally decay to the excited vibrational levels of ground state S_0 (Fig. 7), resulting in even more loss of energy. Besides these effects, chromophores can also display further Stokes shifts either due to solvent effects or excited state reactions.[22]

One interesting observation is that, differing from the large energy loss observed in the solution phase, chromophores generally do not shown any Stokes shifts in the gaseous phase. An un-shifted emission can be observed when the gas concentrations are sufficiently small so that the excited chromophore does not collide with any other molecules prior to the emission, whereas in the solution phase, such collisional deactivations are continuous and the non-radiative energy loss is somehow inevitable.

Generally, the fluorescence emission spectrum appears to be a mirror image of the absorption spectrum, especially the absorption representing the $S_0 \rightarrow S_1$ transition. This is particularly evident for various chromophores possessing conjugated aromatic hydrocarbon functionalities, *e.g.*, 1,3,6,8-tetraisopropylpyrene shown in Figure 10.[23]
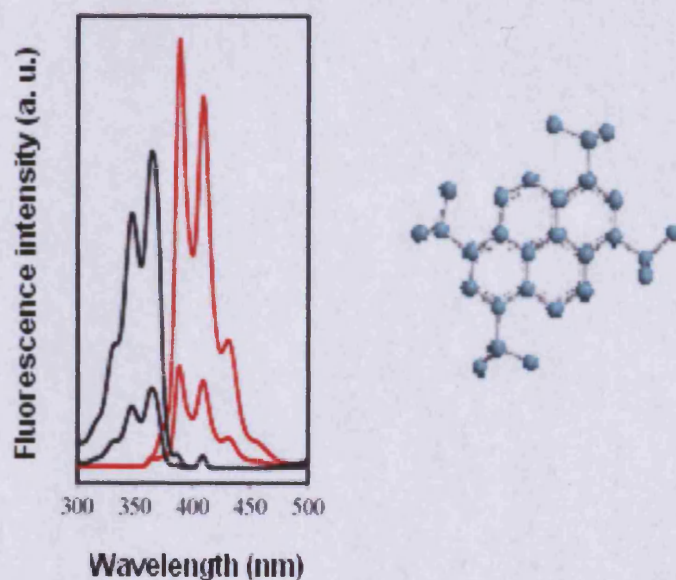
Figure 10. Selected absorption (black lines) and emission (red lines) of 1,3,6,8-tetraisopropylpyrene in CH_2Cl_2 ranging from 1.66×10^{-6} M to 1.0×10^{-5} M.[23] As can be seen, the formation of an excimer is not observed due to steric repulsion of the isopropyl groups in this de novo designed molecular framework.

The general symmetric nature of these spectra is a result of the same electronic transitions being involved in both absorption and emission, together with the similarity of different vibrational levels of the S_0 and S_1 states.

In many chromophores, these energy levels are *not* significantly altered by the diverse distributions of electronic surfaces between S_0 and S_1. Thus again, according to the Franck-Condon principle,[21] all electronic transitions should be expected as vertical, which means that they could have already occurred in the first place, without actually changing the position of the chromophore's nucleic configuration.

As a result, if a particular transition probability between the 0 and 2nd vibrational level is largest in absorption, the reciprocal transition should also be most probable in emission (Figure 11).[1]
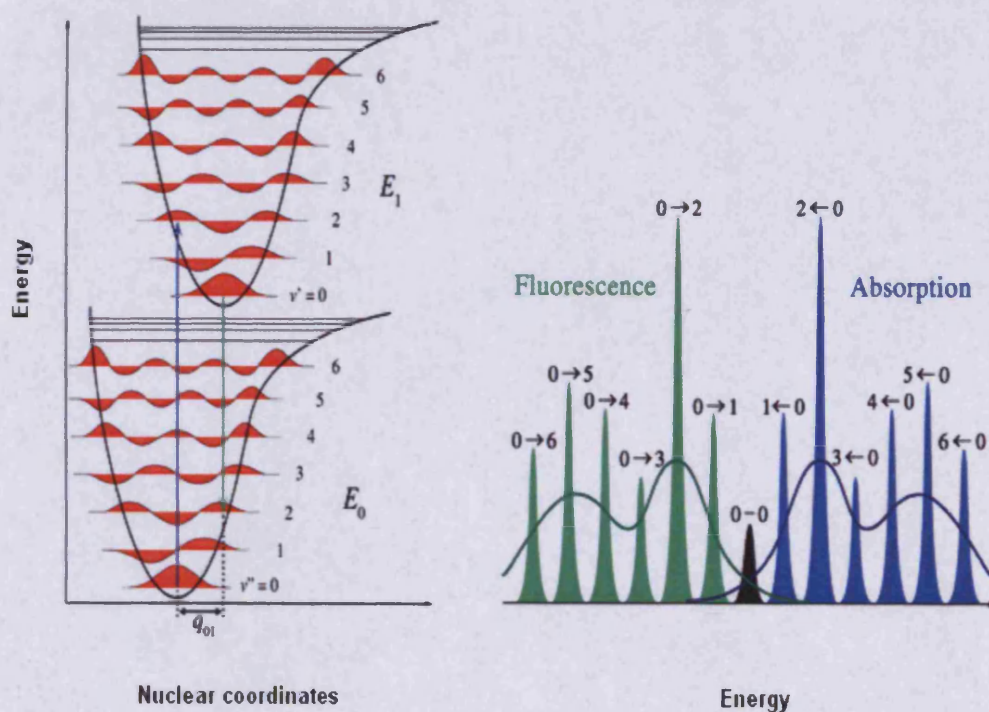
Figure 11. Mirror image rule and Franck-Condon factors: since electronic transitions are very fast compared with nuclear motions, vibrational levels are favored when they correspond to a minimal change in the nucleic configuration. Electronic transitions between the lowest vibrational levels of the electronic states (the 0-0 transition) have the same energy in both absorption and fluorescence.

1.2.3 Fluorescence lifetime (τ) and quantum yield (Φ_f)

The fluorescence lifetimes and quantum yields of chromophores are frequently measured for various research purposes.[24] The meaning of these parameters can be best illustrated by referring to a modified Jablonski diagram (Figure 12).
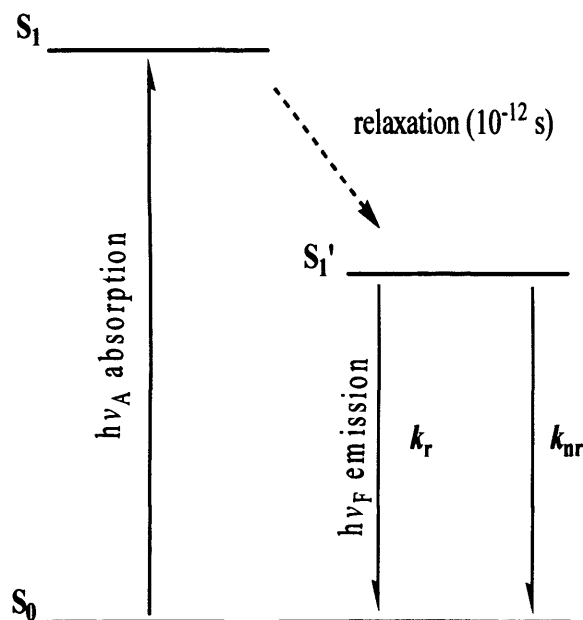
Figure 12. Modified Jablonski diagram and an illustration of radiative *vs* non-radiative deactivation processes.

In this diagram, we do not explicitly explore the individual relaxation processes leading to the relaxed S_1 state. Instead, we primarily focused on those processes which are responsible for returning to the ground state S_0. In particular, we are interested in the radiative (k_r) and non-radiative (k_{nr}) rate constants of the chromophore deactivating to the ground state at room temperature.

The fluorescence quantum yield is the ratio of the number of photons emitted to the number absorbed. The rate constants k_r and k_{nr} both *de-populate* the excited state. The fraction of chromophores which decay through the singlet emission and therefore yield the fluorescence quantum energy, is given by:

$$\Phi_f = \frac{k_r}{k_r + k_{nr}} \tag{3}$$

This quantum yield can be close to unity if the non-radiative rate of deactivation is much smaller than the rate of the radiative deactivation ($k_{nr} \ll k_r$). We have already noticed that the energy yield of fluorescence is always less than unity because of the Stokes loss. So herein, for convenience we have denoted all possible non-radiative de-excitation processes into a single rate constant as k_{nr}.

The lifetime of the excited state is defined by the average time the molecule spends in the excited state prior to return to the ground state. Generally, fluorescence lifetimes are near 10 ns. For the chromophore illustrated in Fig. 11, the lifetime can be calculated as:

$$\tau = \frac{1}{k_r + k_{nr}} \qquad\qquad (4)$$

One should always bear in mind that the fluorescence emission actually is a random process, and few chromophores actually emit their photons exactly at $t = \tau$. Thus the fluorescence lifetime can be viewed as an average value of the time spent in the excited state. For a radiative decay with a single exponential characteristic, 63% of the excited species have deactivated prior to $t = \tau$ and 37% deactivated at $t > \tau$.[1]

Of course the quantum yield and lifetime can be affected by many factors which can influence either of the rate constants. For example, a molecule maybe non-fluorescent as a direct result of a large rate of internal conversion or a slow rate of radiative emission.

Scintillators are generally chosen for their high quantum yields, which is a result of the large k_r values and, therefore, their fluorescence lifetimes are surprisingly short, merely near 1 ns.[1] The fluorescence emission of aromatic substrates containing $-NO_2$ groups are generally weak, primarily as a result of the large value of k_{nr}.

The quantum yields of phosphorescence (Φ_p) are extremely small in solution phase at room temperature. The triplet-to-singlet transition is actually forbidden by the spin symmetry and the rates of spontaneous emission k_r are about 10^3 s^{-1} or even smaller. Since k_{nr} values are near 10^9 s^{-1}, therefore quantum yields of phosphorescence are really insignificant at room temperature, especially under aerated conditions.

1.2.4 Effects of solvents on fluorescence emission spectra

The fluorescence emission spectra of many chromophores are sensitive to the polarity of their nearby environment. For example, if the emission spectrum of a probe such as 2-pyrenol (2-PyOH) is examined in solvents of varying polarities,[25] one finds that the emission spectrum shifts to shorter wavelengths (*hypothochromic / blue shifts*) as the solvent polarity is decreased.

Conversely, increasing solvent polarity generally results in shifts of the emission spectrum to longer wavelengths (*bathochromic / red shifts*). Typical solvatochromic spectra of 2-pyrenol are shown in Figure 13. Interestingly, bathochromic shifts are often, but not always, accompanied by the decrease of fluorescence quantum yields.
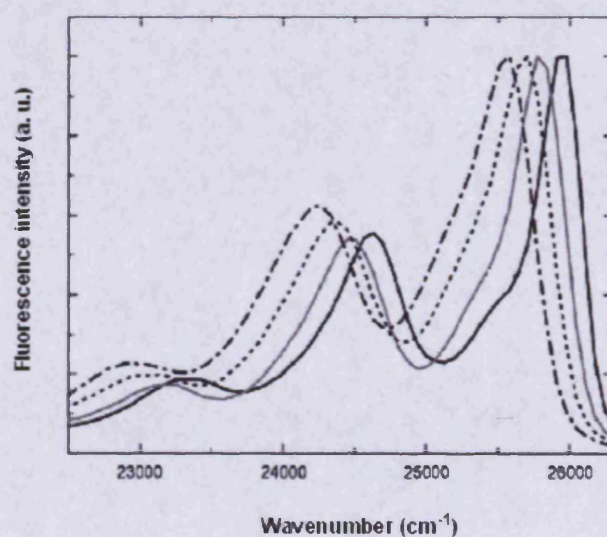
Figure 13. Fluorescence emission spectra of 2-pyrenol (λ_{exc} = 365 - 375 nm). From left to right the solvents are hexamethyl-phosphoric triamide, dimethyl formamide, propylene carbonate and toluene.[25]

1.2.4.1 Stokes shift and solvent relaxation

The emission from chromophores generally occurs at wavelengths which are longer than those of light absorption. As mentioned above, this loss of energy between absorption and re-emission of light, or Stokes shift, is a result of several excited state relaxation dynamics,[1] which may include energy loss due to dissipation of vibrational energy, re-distribution of electrons in the surrounding solvent molecules induced by the altered dipole movement of the excited chromophore, re-orientation of the solvent molecules around the excited state dipole, and also can be any specific interactions such as hydrogen bonding and formation of a charge transfer complex (exciplex).[26]

Precise interpretation of the solvent sensitivity indeed requires a broad understanding of the 'solvato-effects' on both the ground state and excited state energy levels of the chromophore. Nevertheless, one can certainly use the most simplified theories such as the 'solvent-chromophore interaction' to explain those interesting spectral properties (Figure 14), typically by analysing the dipolar difference upon the thermodynamically equilibrated microenvironment surrounding the chromophore (*i.e.*, the so called solvent cage).[1,22]
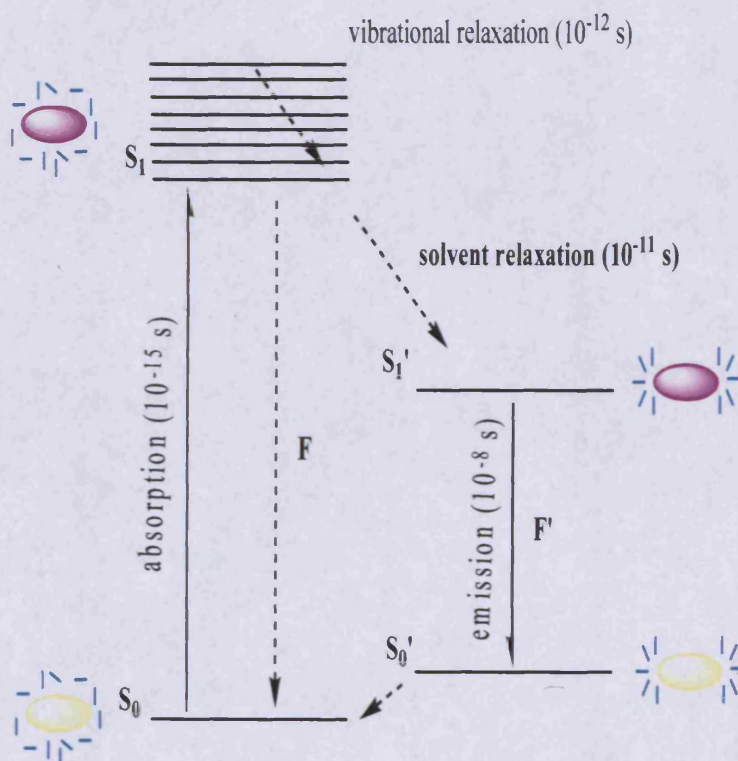
Figure 14. Jablonski diagram for the phenomenon of fluorescence and the difference between vibrational and solvent relaxation *(Inset symbol: yellow bar - chromophore in its ground state: Donor-Acceptor configuration; red bar - chromophore in its excited state where the ICT process has just occurred, D^+-A^-; blue line: nearby solvent).*

Due to the simple 'Donor-Acceptor' type chromophore, absorption of light occurs in about 10^{-15} s, a time too short for a significant displacement of its nucleic configuration, but evidently enough for re-distributing its electrons from the donor to the acceptor.[27]

As a result, the chromophore in its electronically excited state (S_1, Figure 14) will possess a dipole moment (μ_e) much larger than that in its ground state S_0 ($\mu_e \gg \mu_g$), which means that the initial light absorption will actually result in an instantaneously evolved dipolar species with great charge transfer character (D^+-A^-) and consequently perturbing the 'solvent cage' nearby, which had already formed prior to the photon excitation.

Solvent molecules of course will quickly respond this newly emerged 'dipolar difference' by re-organising the cage into a more stabilized configuration (precisely according to the $D^+ - A^-$ electronic configuration presented on the chromophore), leading to a much more relaxed state with minimum free energy ($S_1 \rightarrow S_1'$, Figure 14).

The higher the polarity of the solvent, the lower the energy of the relaxed state and the larger the bathochromic shift that can be observed from the emission spectrum. Such a process is actually called *solvent relaxation* and the time scale of this is entirely dependent upon the physical and chemical properties of the solvent.[22]

For instance, viscosity can be a critical factor which will effectively influence the rate of the solvent relaxation. If the time required for re-organising solvent molecules around the chromophore is short with respect to its excited state lifetime, fluorescence will essentially be emitted from chromophores in equilibrium with their solvent shell (F', Figure 14).

As emission of a fluorescence photon is almost quasi-instantaneous, this means that the chromophore will be inclined to recover its initial dipole orientation (D–A) and a new relaxation process will actually lead to the most stabilized electronic configuration presented originally by the 'chromophore-cage' system in its ground state ($S_0' \rightarrow S_0$, Figure 14).

Alternatively, if the medium is too viscous to allow solvent molecules to re-distribute, emission will consequently arise from the initially populated Frank-Condon state (S_1, as in the case of a nonpolar medium) and no shifts of the fluorescence spectrum will be observed (F, Figure 14).

Finally, if the solvent's re-organisation time is of the order of the excited state lifetime, the first emitted photons will correspond to wavelengths shorter than those emitted at longer times. In this case, the fluorescence spectrum observed under continuous inspection will be shifted but the position of the maximum can not be directly related to the solvent polarity.

It is also interesting to note that during the re-organisation of solvent molecules, the 'time evolution' of the fluorescence intensity depends on the observation wavelength, but once the stabilized 'chromophore-cage configuration' is attained, the fluorescence decay only reflects the depopulation of the relaxed excited state (S_1').

From the time-resolved fluorescence intensities recorded at various wavelengths, the fluorescence spectrum at a given time can be re-constructed, so that the 'time evolution' of the fluorescence spectrum can be monitored during the course of the solvent relaxation. This means that fluorescence can be actually utilized as a great tool for detecting the response time of various solvents (or any polar species in the microenvironment) following the excitation of a probing chromophore, whose dipole moment can be instantaneously modified upon the initial photon absorption.[22]

1.3 A selected application:

Microwave-assisted synthesis of dimethylaminostyryl borondipyrromethylene derived luminescent chromophores and their related photophysical study[28]

A common misconception about microwave-assisted synthesis is that due to the high temperatures that are often employed, such technology could not be applied directly into more sensitive reactions, such as asymmetric synthesis or the preparation of delicate luminescent chromophores which have been incorporated with labile electron-transporting functionalities.

While comparatively few luminescent dye syntheses have been reported in the past under microwave-assisted conditions, this number is steadily increasing.

As we know, in a conventional synthetic approach using the thermal heating, if a high temperature is required in order to promote a chemical transformation, a solvent with a high boiling point must be selected which might prove difficult to remove during the following work-up stage.

In contrast, using sealed vessel microwave heating, the boiling point of the solvent is less important since the solvent can be superheated above its regular boiling point under microwave irradiation.[4(b)]

Therefore with microwave-assisted synthesis, it is the dielectric property of various reaction media that need to be considered in order to maximise the thermal conductive potential of this novel technology.

For example, an interesting correlation between the temperature and the dielectric property of various irradiating systems was explored through the facile microwave-assisted synthesis of the BODIPY-derived luminescent sensor **9**, as shown in Scheme 4.[28]
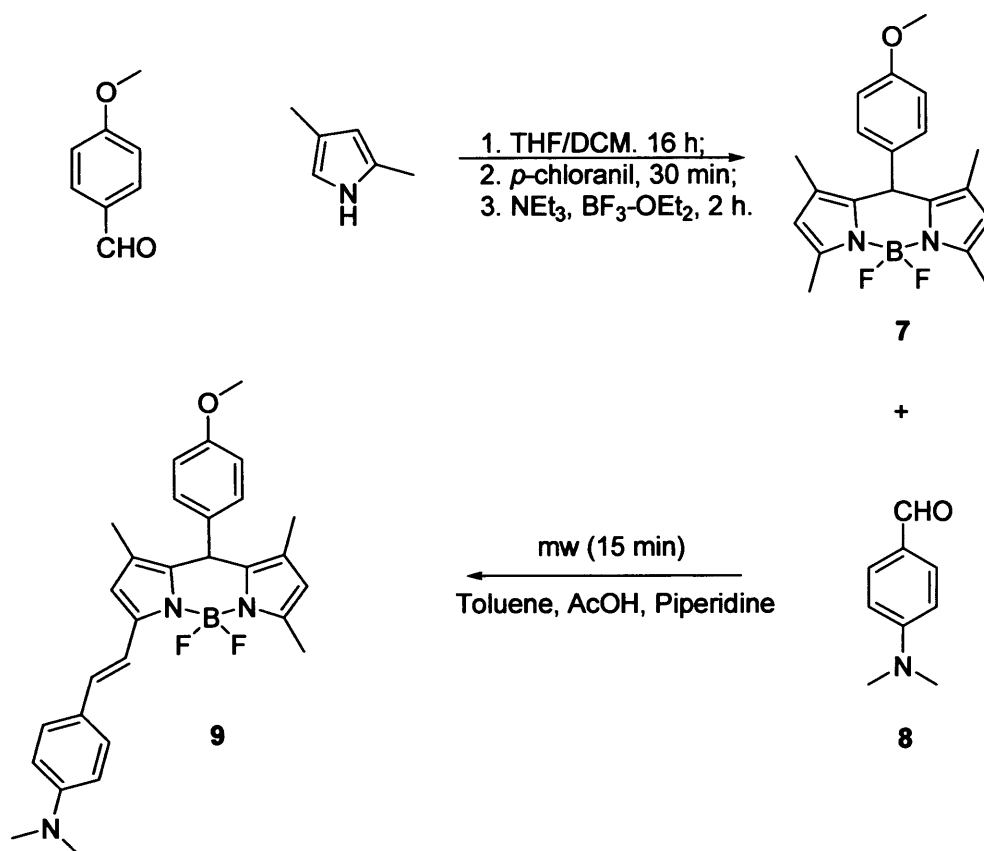
Scheme 4. Novel microwave-assisted synthesis of dimethylaminostyryl borondipyrromethene fluorescent sensor **9**.

Under conventional reflux conditions using DMSO as a solvent (bp 189 °C), the condensation between *p-N,N*-dimethylaminobenzaldehyde **8** and 1,3,5,7-tetramethyl-substituted-tetramethyl-3a,4a-diaza-4-bora-*s*-indacene **7** typically required 26 to 28 hours to complete. Since there is no need to choose a high boiling solvent using a microwave-assisted approach, the solvent was initially changed to distilled toluene (bp 110.6 °C).

Toluene is not a very efficient microwave absorbing solvent as compared to DMSO and therefore the temperature of the mixture upon microwave heating only reached a maximum of 150 °C, requiring several minutes to reach the ceiling point.

Under these conditions, the condensation leading to the BODIPY-derived luminescent sensor **9** required approximately 1 hour to complete. In order to further increase the temperature and reduce the reaction time, the sample system was carefully modified by adding a moderate amount of a 'strong microwave absorbing medium' - acetic acid as the heating catalyst. As mentioned

above, acetic acid can actually interact effectively with the microwave electric field on its own (*through the dipolar polarisation mechanism - section 1.11*) and be rapidly heated at rates easily exceeding 10 °C per second.[29]

As such, by adding a small amount of acetic acid as the 'boiling agent', the general dielectric property of the reaction mixture was fine tuned to provide 'rapid heating' – within less than 2 minutes – to 170 °C. Under these conditions, the overall time for the final condensation step was significantly reduced from 26 hours to 15 minutes (!), providing a near identical yield of the compound produced via the thermal conductive heating procedure.

Such an example clearly demonstrated the versatility of microwave chemistry in enhancing the reaction rate by rapidly increasing the temperature in such a fashion that is not typically attainable under thermal conditions.

The UV/vis absorption and steady-state fluorescence spectra of chromophore **9** measured in various solvents are shown in Figure 15.
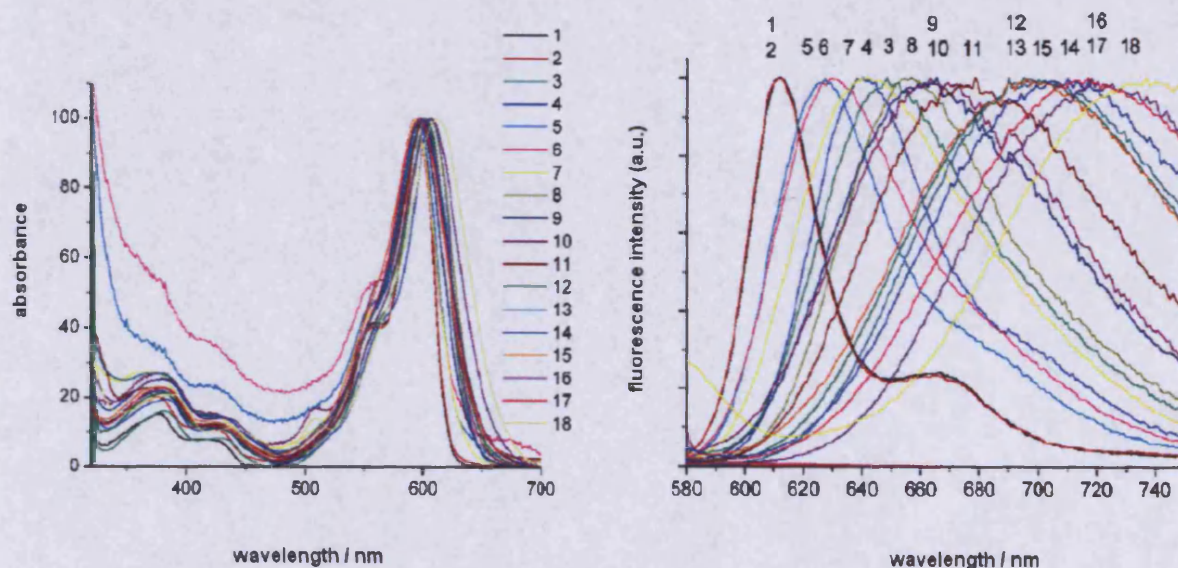
Figure 15. Normalized absorption and emission spectra of **9** (λ_{exc} = 560 nm) in several solvents. The numbers refer to the solvents explored: 1. methylcyclohexane; 2. cyclohexane; 3. 1,4-dioxane; 4. toluene; 5. dibutyl ether; 6. diisopropyl ether; 7. diethyl ether; 8. chloroform; 9. ethyl acetate; 10. tetrahydrofuran (THF); 11. 1-butanol; 12. acetone; 13. butanenitrile (butyronitrile); 14. propanenitrile (propionitrile); 15. methanol; 16. *N,N*-dimethylformamide (DMF); 17. acetonitrile; 18. dimethyl sulfoxide (DMSO).[28]

As shown, a slight increase in the solvent polarity resulted in a dramatic loss of the well-resolved fluorescence band located at 665 nm, which primarily corresponds to the BODIPY based $\pi \rightarrow \pi^*$ transition,[30] and in concomitant appearance of a newly formed emission located at lower energy.

Under the same conditions, the ground state UV/vis spectra remained essentially insensitive to the solvent polarity and, in particular, there was no indication that another absorption band had formed in the low energy region.

Tanle 2. Photophysical properties of **9** in general aprotic solvents.[a]

Entry	Solvent	λ_{abs} (nm)	λ_{em} (nm)	Δv (cm^{-1})	Φ_f[b] ($\times 10^{-3}$)	τ_1[c] (ns)	τ_2 (ps)	k_r (10^{8}s^{-1})	k_{nr} (10^{8}s^{-1})
1	cyclohexane	597	612	411	9.7 ± 0.03	3.50	-	2.77	0.09
2	THF	600	664	1606	5.6 ± 0.04	3.00	-	1.87	1.47
3	acetonitrile	597	717	2803	0.9 ± 0.02	1.20	-	0.75	7.58

[a] For the time-resolved fluorescence measurements, the sample were excited at 580 nm; [b] Quantum yield values were determined by excitation at 560 nm; [c] The standard error: ≤ 15 ps.

The long wavelength fluorescence band detected in polar solvents was structureless, fairly broad and could be fitted reasonably well into a single exponential decay curve among selected solvents (Table 2).

Fluorescence quantum yields (Φ_f) calculated for this newly formed emission were $\leq$ 0.001 in polar solvent (*e.g.*, acetonitrile), which was significantly different from the quantum yield estimated for the locally excited singlet state (^1L_b) that was most likely existing within the range 0.005 – 0.008.[31] Interestingly, unlike the vivid solvatochromism observed from this newly emanated low energy emission band, in principle, ^1L_b fluorescence did not show any solvent dependences at all.

Such positive solvatochromic behaviour of **9** detected in polar solvents clearly suggests that the occurrence of an intra-molecular charge transfer (ICT) process is responsible for its high solvent sensitivity: the dimethylaminostyryl group is an electron donor and the boradiazaindacene group is an electron-acceptor, allowing for the formation of a singlet excited state with great charge transfer character.

In polar aprotic solvents (Table 2), it appears that the rate of forming a CT state (^1L_a) competes fairly well with the inherent radiative as well as non-radiative processes that can possibly affect the deactivation pathway of the initially formed Frank-Condon state (^1L_b), lowering the energy level of the singlet emitting excited state and, therefore, shifting the room temperature fluorescence to a longer wavelength.

For all of the polar aprotic solvents investigated, most ^1L_a lifetimes (τ_1) were detected over a few nanoseconds and analysed quantitatively, in terms of the energy-gap law,[32] *i.e.*, τ_1 decreased simultaneously with reduced S_1-S_0 energy difference, which was meanwhile accompanied by an increased rate of non-radiative decay (k_{nr}).

In aerated protic solvents at room temperature, where the hydrogen bonding between the solvent and amino sp^3 lone pair electrons is expected to take place, a second, short-lasting decay component (τ_2) was observed (Entry 1 & 2, Table 3).

Table 3. Photophysical properties of **9** in both protic and aprotic solvents.[a]

Entry	Solvent	λ_{abs} (nm)	λ_{em} (nm)	$\Delta\nu$ (cm^{-1})	Φ_f[b] (%)	τ_1[c] (ns)	τ_2[c] (ps)	k_r (10^{8}s^{-1})	k_{nr} (10^{8}s^{-1})
1	1-butanol	601	678	1890	0.59 ± 0.03	2.45	106	-	-
2	methanol	596	696	2411	0.16 ± 0.01	0.85	14	-	-
3	acetonitrile	597	717	2803	0.09 ± 0.002	1.20	-	0.75	7.58

[a] For the time-resolved fluorescence measurements, the sample were excited at 580 nm; [b] Quantum yield values were determined by excitation at 560 nm; [c] The standard errors on τ_1: ≤ 15 ps and on τ_2: ≤ 3 ps.

Such decay components can be detected in methanol but not in an aprotic analogue (*e.g.*, acetonitrile) that has similar orientational polarizability, nor in THF which possesses virtually identical solvent viscosity.[33]

So as a result, the origin of this newly observed excited state (τ_2) was rationalized in terms of the conformational re-arrangement of the hydrogen bonding, which arose immediately after the excited state relaxation ($^1L_b \rightarrow {}^1L_a$) had occurred, rather than the conventional approach in analysing the formation of delayed fluorescence (*i.e.*, $^1L_a \rightarrow T_1 \rightarrow {}^1L_a \rightarrow S_0$).[28]

Such a statement can be further verified through the emission model shown in Figure 15.
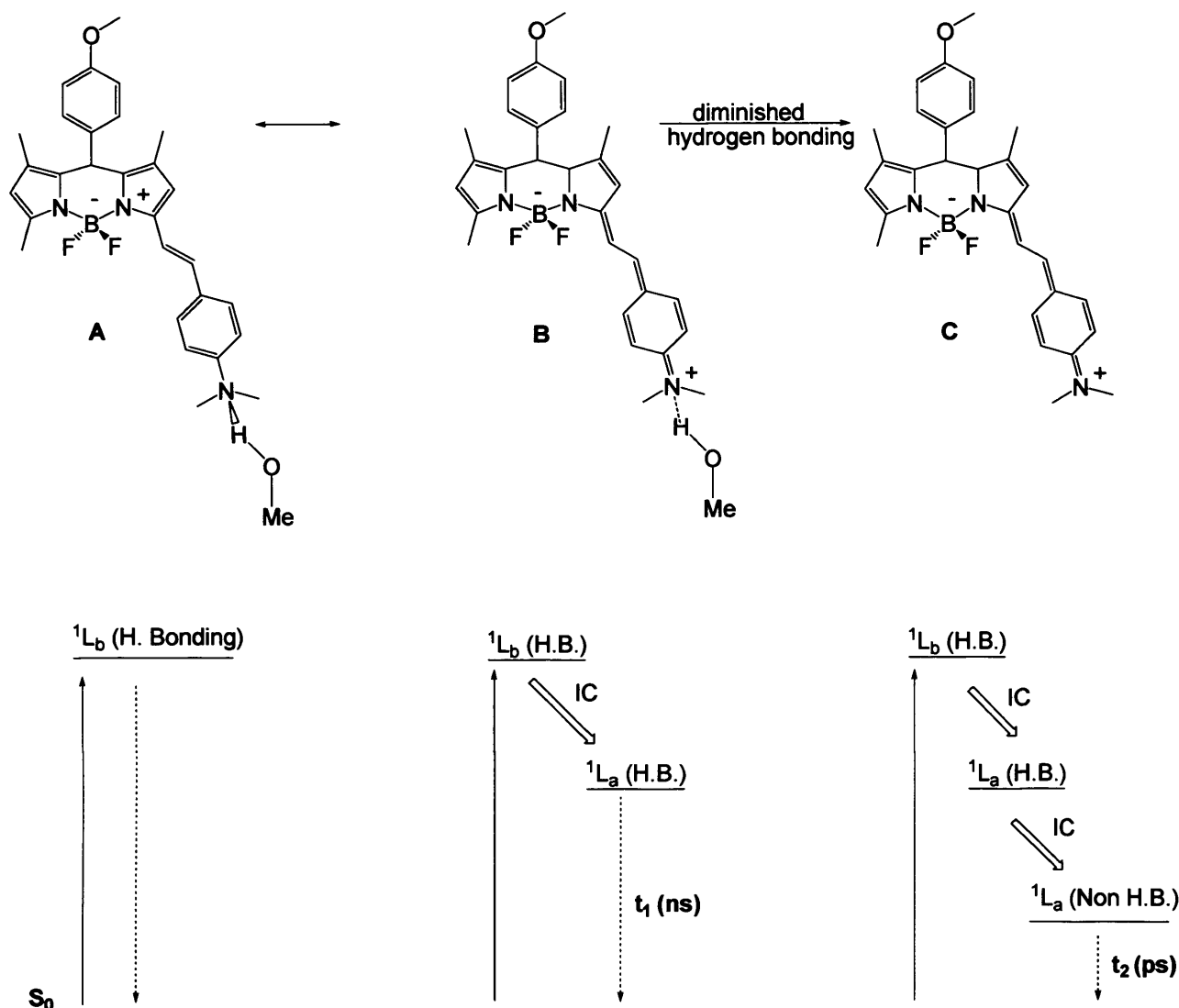
Figure 15. Delocalized structures of 9 contributing to its real structure in the ground and excited states (protic media).

Clearly, in structure B, a positive charge is presented on the delocalized aniline nitrogen atom and its dynamics upon re-distributing the electron density from the aminostyryl donor to the boradiazaindacene acceptor, must correspond well to the weakening of the hydrogen bonding interactions between the solvent and the aniline nitrogen after the initial ICT process has taken place.

Weakened hydrogen bonding interactions will certainly make the amino group a better donor and lower the energy level of the just populated charge transfer state [^1L_a(H.B.)], leading to a red shift of room temperature fluorescence, and ultimately the formation of a second, short-lived emitting excited state over the time scale of a few picoseconds [^1L_a(Non H.B.)].

Indeed, such an explanation has been verified through the experimental detail recorded by Fukuzumi et al., in their *photo-induced electron transfer* study of the luminescent ferrocene-

quinone like system.[34] At shorter wavelength, the emission mainly originated from a hydrogen-bonded charge transfer state (Structure B, Figure 15) which could quickly evolve into a non hydrogen-bonded CT state emitting at lower energy (Structure C). In totally relaxed excited-state configuration (C), nitrogen lone pair electrons are no longer available for hydrogen bonding; therefore the interaction between the solvent and the chromophore would be expected to be negligible, either compared to the ground state S_0 or the initially populated LE state [^1L_b(H.B.)]. This actually means that hydrogen bonding will stabilize the ground state 'zwitterionic-like' structure (A) more effectively than the CT state 'quinoid-like' structure (C), which will simultaneously lead to the observation that room temperature fluorescence measured in methanol is always shorter (*i.e.*, in wavelength) than that in acetonitrile, even though both solvents possess a very comparable orientational polarisability (Entry 2 & 3, Table 3).

1.4 Conclusions

Microwave technology is emerging as an alternative energy source powerful enough to accomplish syntheses in minutes, instead of hours or even days. For this reason, microwave irradiation is currently seeing an exponential increase in acceptance as a leading technique, for accelerating various chemical transformations on the research scale.

Although some questions relating to the existence of a 'special microwave effect',[35] the scalability[36] and the overall energy efficiency of microwave assisted synthesis are still under scrutiny, there is little doubt that microwave chemistry will eventually become a standard synthetic-platform at most research installations in the very near future.

As seen in the discussion, an entirely new arena of application in the synthesis of photo-luminescent compounds can be investigated widely and easily using this novel methodology.

References

1. (a) Lakowicz, J. R. *'Principles of Fluorescence Spectroscopy'* 3rd Ed, Springer, New York, **2006**.; (b) Sameiro, M.; Gonçalves, T. *Chem. Rev.*, **2009**, *109*, 190.; (c) Stains, C. I.; Porter, J. R.; Ooi, A. T.; Segal, D. J.; Ghosh, I. *J. Am. Chem. Soc.*, **2005**, *127*, 10782.; (d) Promega Digital Gallery: HaloTag® fluorescent intracellular imaging.

2. Kappe, C. O.; Dallinger, D. *Chem. Rev.* **2007**, *107*, 2563.

3. Loupy, A. *'Microwaves in Organic Synthesis'* 2nd Ed, Wiley-VCH, Weinheim, **2006**.

4. (a) Tierney, J. P.; Lidstrom, P. *'Microwave Assisted Organic Synthesis'* 1st Ed, Blackwell, Oxford, **2005**.; (b) Kappe, C. O. *Angew. Chem. Int. Ed.*, **2004**, *43*, 6250.

5. Kremsner, J. M.; Kappe, C. O. *J. Org. Chem.* **2006**, *71*, 4651.

6. Zhang, X.; Hayward, D. O.; Mingos, D. M. P. *J. Chem. Soc., Chem. Commun.* **1999**, 975.

7. Zhang, X.; Hayward, D. O.; Mingos, D. M. P. *Catal. Lett.* **2003**, *88*, 33.

8. Baghurst, D. R.; Mingos, D. M. P. *Chem. Soc. Rev.* **1991**, *20*, 1.

9. Perreux, L, ; Loupy, A. *Tetrahedron*, **2001**, *57*, 9199.

10. (a) Kuhnert, N. *Angew. Chem.* **2002**, *114*, 1943.; (b) Strauss, C. R. *Angew. Chem.* **2002**, *114*, 3741.

11. Bagley, M. C.; Glover, C.; Merritt, E. A. *Synlett.* **2007**, *16*, 2459.

12. Galema, S. A. *Chem. Soc. Rev.* **1997**, *26*, 233.

13. Abdel Ghani, S. B. *Bioorg. Med. Chem. Lett.* **2008**, *18*, 518

14. Mahal, H. S.; Venkataraman, K. *J. Chem. Soc.* **1934**, 1767.

15. Burgess, K.; Jiao, G-S.; Castro, J. C.; Thoresen, L. H. *Org. Lett.*, **2003**, *5*, 3675.

16. Skene, W. G.; Dufresne, S. *Org. Lett.*, **2004**, *6*, 2949.

17. Burgess, K.; Burghart, A.; Chen, J.; Wan, C-W. *'New Chemistry of BODIPY Dyes, and BODIPY Dye Cassettes Featuring Through-Bond Energy Transfer'* 1st Ed, San Jose, Canada, **2000**.

18. Burghart, A.; Thoresen, L. H.; Chen, J.; Burgess, K.; Johansson, L. B-A. *J. Chem. Soc., Chem. Commun.* **2000**, 2203.

19. Rendell, D. *'Fluorescence and Phosphorescence'* 1st Ed, John Wiley & Sons, New York, **1987**.

20. Microscopyu Digital Gallery.

21. Balzani, V.; Carrassiti, V. *'Photochemistry of Coordination Compounds'* 1st Ed, Academic Press, London & New York, **1970**.

22. Valeur, B. *'Molecular Fluorescence'* 1st Ed, Wiley-VCH, New York, **2002**.

23. Banerjee, M.; Vyas, V. S.; Lindeman, S. V.; Rathore, R. *J. Chem. Soc., Chem. Commun.* **2008**, 1889.

[24.] Grabowski, Z. R.; Rotkiewicz, K.; Rettig, W. *Chem. Rev.*, **2003**, *103*, 3899.

[25.] Jung, G.; Gerharz, S.; Schmitt, A. *Phys. Chem. Chem. Phys.*, **2009**, *11*, 1416.

[26.] Reichardt, C. *'Solvent Effect in Organic Chemistry'* 1st Ed, Verlag Chemie, Weiheim, **1988**.

[27.] Banwell, C. N. *'Fundamentals of Molecular Spectroscopy'* 3rd Ed, McGraw-Hill Book, London, **1983**.

[28.] Baruah, M.; Qin, W.; Basaric, N.; De Borggraeve, W. M.; Boens, N. *J. Phys. Chem. A*, **2006**, *110*, 5998.

[29.] Kappe, C. O.; Dallinger, D.; Murphree, S. S. *'Practical Microwave Synthesis for Organic Chemistry – Strategies, Instruments, and Protocols'* 1st Ed, Wiley-VCH, Weinheim, **2008**.

[30.] Baruah, M.; Qin, W.; Basaric', N.; De Borggraeve, W. M.; Boens, N. *J. Org. Chem.* **2005**, *70*, 4152.

[31.] Rettig, W.; Letard, J-F.; Lapouyade, R. *Chem. Phys. Lett.* **1994**, *222*, 209.

[32.] Caspar, J. V.; Meyer, T. J. *J. Phys. Chem.* **1983**, *87*, 952.

[33.] Nakamura, H.; Anada, T.; Morozumi, T. *J. Phys. Chem. B*, **2001**, *105*, 2923.

[34.] Fukuzumi, S.; Yoshida, Y.; Okamoto, K.; Imahori, H.; Araki, Y.; Ito, O. *J. Am. Chem. Soc.* **2002**, *124*, 6794.

[35.] De-La-Hoz, A.; Moreno, A. *Chem. Soc. Rev.* **2005**, *34*, 164.

[36.] Bowman, M. D.; Holcomb, J. L. *Org. Process Res. Dev.* **2008**, *12*, 41.

Chapter Two – Results and Discussion

2 Microwave chemistry in the synthesis of pyridine–containing chromophores

A series of modifications of the Bohlmann-Rahtz methodology developed by Bagley & co-workers led to various facile routes to tri- & tetrasubstituted pyridines using an assortment of conditions (*e.g., thermal conductive heating or microwave dielectric irradiation*) and synthetic catalysts (*e.g., zinc bromide, acetic acid or Amberlyst 15 ion exchange resin*).[11] These methods can proceed in a single step without the need for isolation of the aminodienone intermediate[37] and can avoid the use of toxic solvents which were always required under conventional conditions to mediate the 'alkynone-enamine C-alkylation' and subsequent cyclodehydration steps in order to yield the pyridine target.

As part of this ongoing investigation in the search of alternative methods, our aims were to explore a novel microwave-assisted tandem oxidation/Bohlmann-Rahtz heteroannulation approach [*which is accompanied by the copper(I)-mediated N-arylation*] for the rapid synthesis of pyridine-containing luminescent chromophores that bear tunable D-A functionalities and can display CT-based emission characteristics with significant Stokes shifts, excellent RT quantum efficiencies and unusual solvatochromic properties.
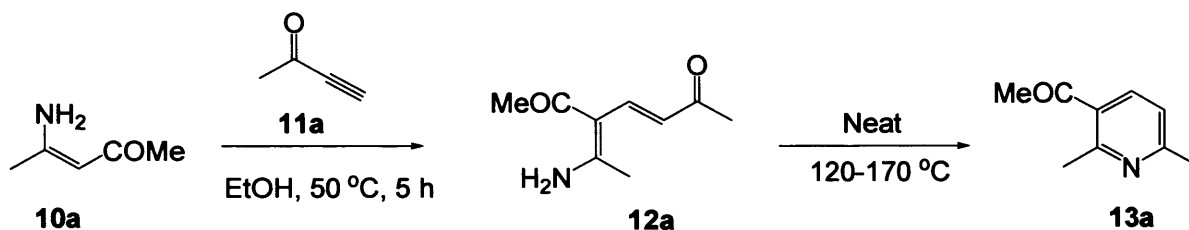
2.1 Discovery: The Bohlmann-Rahtz pyridine synthesis

Many different methods for the synthesis of pyridines are available, encompassing a number of prominent procedures that have earned their inventors great acclaim for the discovery of useful heterocyclic methodology. Invariably these procedures are judged on a number of familiar criteria: efficiency, selectivity (including regio–, chemo– and stereoselectivity), substrate tolerance, opportunities for diversity and ecological value. However, inevitably, with so many varied routes to these targets being revealed throughout the years, some transformations following their discovery, in spite of having the potential to satisfy most if not all of the criteria, become largely forgotten. The Bohlmann–Rahtz pyridine synthesis, first reported in 1957,[37] until very recently was one such procedure.

Trisubstituted pyridines are synthesized in a two–step procedure by the reaction of enamines **10a** and alkynyl ketone **11a**, (Scheme 5). Bohlmann and Rahtz observed that the condensation of **10a** and **11a** is completely regioselective and proceeds by Michael addition and enamine *C*–alkylation to give an aminodiene intermediate **12** that can be isolated in high yield. In a subsequent procedure, heating intermediates **12** to a temperature of 120–170 °C, induces spontaneous

cyclodehydration to give 2,3,6–trisubstituted pyridines **13** in excellent yield and with total regiocontrol. Although it is related to the corresponding reaction of enamines with enones and hence to the well–known Hantzsch dihydropyridine synthesis,[38] the use of ynones leads to the heteroaromatic product directly thus obviating the need for a final aromatizing oxidative step.[39]

Scheme 5. The traditional Bohlmann-Rahtz pyridine synthesis


2.2 Recent improvements in methodology

Within the last decade the potential of the Bohlmann–Rahtz pyridine synthesis has begun to be unravelled. Bagley and co–workers have published many works regarding methodology improvement, including a range of catalytic and solvent effects, tandem processes and microwave technology. The immediate result of these works is the identification of modified Bohlmann–Rahtz procedures that offer a growing range of tri– and tetrasubstituted pyridines that are regio–, chemo– and even stereospecific. In addition, the modified procedures offer the potential for greater application in synthetic chemistry due to milder, improved reaction conditions compared to the original Bohlmann–Rahtz pyridine synthesis. This section will primarily summarize the contributions made from the literature since Bohlmann–Rahtz first discovered the reaction in 1957.

2.2.1 Microwave-assisted synthesis

As mentioned above, the use of microwave dielectric heating in synthetic chemistry has emerged as a valuable alternative to conventional conductive heating methods[40] and the recent advances in instrumentation, with the introduction of dedicated ovens for organic synthesis that focus microwaves in a monomodal cavity, have increased the popularity and reproducibility of microwave chemistry, increasing the methodology available for the development of new synthetic reactions and optimisation of existing procedures.[41]

In order to expand further the versatility of the Bohlmann–Rahtz reaction and in an effort to explore a microwave–assisted process, Bagley, Lunn and Xiong carried out investigations in a self–tuning single–mode CEM Discover™ Focused Synthesizer.[42] A solution of ethyl β–aminocrotonate **10b** and an excess of phenylpropynone **11b** (Scheme 6) was stirred in toluene or dimethyl sulfoxide (solvents that have been shown to promote the Michael addition for traditional Bohlmann–Rahtz reactions in previous studies)[11] at 170 °C by irradiating initially at 150 or 160 W.

Scheme 6. One-pot synthesis of pyridine **13b** under the thermal or microwave-assisted conditions
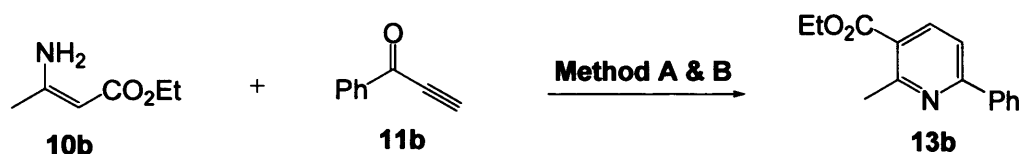
Method

A: Various solvents, sealed tube, 170 °C, 10-90 min;

B: Various solvents, microwave, 170 °C, 10-90 min.

Entry	Solvents	Time (min)	Yield (%)[a]	
			A	B
1	PhMe	90	54	76
2	DMSO	20	80	87
3	PhMe-ZnBr$_2$(15 mol%)	10	33	80
4	PhMe-AcOH (5:1)	10	95	98

[a] Isolated yield after the chromatographic purification

The reaction conducted in toluene was found to be sluggish at best, providing pyridine **13b** in 76% yield after 90 min (entry 1). The use of a more polar solvent, dimethyl sulfoxide that can couple more efficiently with microwave radiation, resulted in a more rapid reaction. Michael addition and spontaneous cyclodehydration was complete after 20 min, to give pyridine **13b** in 87% yield (entry 2). As expected reactions conducted in toluene were accelerated dramatically by the presence of zinc(II) bromide (15 mol%) providing the product in 80% yield after 10 min at 170 °C (entry 3). However, the optimum conditions for this transformation employed acetic acid. After stirring for 10 min in a solution of toluene–acetic acid (5:1) at 170 °C, pyridine **13b** was isolated in 98% yield (entry 4).

As described, all of the microwave–assisted experiments facilitated both Michael addition and cyclodehydration in a single synthetic step and generated the target pyridine **13b** as a single regioisomer. A further investigation was carried out in order to establish if traditional conductive heating methods could also facilitate a similar one–pot transformation. The same range of reactions was repeated in a sealed tube using an oil bath as an external heat source and the results were compared with the microwave–assisted reactions (Scheme 6). In almost all of the experiments, the microwave–assisted conditions gave the product in a higher yield, in particular for the reaction conducted in toluene in the presence of 15 mol% of zinc(II) bromide (entry 3), although in many instances comparable yields were obtained as well (entries 2 and 4).

In order to test the scope of the microwave–assisted reaction, ethyl β–aminocrotonate **10b** was reacted with a number of different alkynones **11c-f** by irradiating a solution of the reagents in dimethyl sulphoxide at 170 °C for 20 min (Scheme 7). In all of the experiments, a single regioisomeric pyridine was formed. Although the efficiency of the reaction of enamine **10b** and 4–phenylbutynone **11d** was low (entry 2),[42] this alkynone has been noted to be problematic in similar heteroannelation reactions.[43]

Scheme 7. Microwave-assisted synthesis of pyridine 13
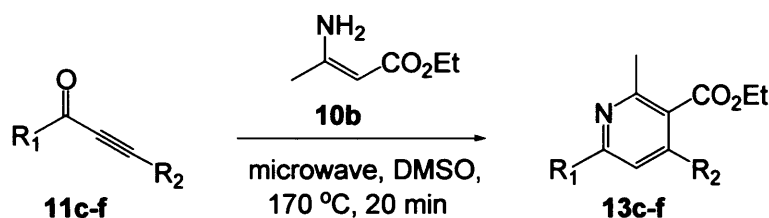
Entry	Alkynone 11	R^1	R^2	Pyridine 13	Yield (%)[a]
1	c	Me	Et	c	94
2	d	Me	Ph	d	24
3	e	4'-ClC₆H₄	H	e	75
4	f	4'-MeOC₆H₄	H	f	66

[a] Isolated yield after the chromatographic purification

The remaining microwave–assisted reactions gave pyridine products **13c, e-f** in good yields after purification by column chromatography (entries 3-4), illustrating that the one–pot microwave–assisted Bohlmann–Rahtz reaction represents a simple and highly–expedient route to tri– and tetrasubstituted pyridines. This is a new and extremely simple method to facilitate Michael addition and cyclodehydration in only 20 min using microwave irradiation, which proceeds with total control of regiochemistry.[42]

2.2.2 Continuous flow technique

From the early experiments in domestic ovens to the use of multimodal or monomodal instruments designed for organic synthesis, this technology has been implemented worldwide and continues to be developed.[41] However, although modern monomodal instruments dedicated for the microwave assisted organic synthesis (MAOS) are very successful in small scale operations, efforts to process this technology in continuous flow (CF) reactors are frustrated by the physical limitations of microwave heating, with a penetration depth of only a few centimetres and the limited dimensions of the standing wave cavity.

Current technology has attempted to overcome these obstacles with conventional instruments by the use of CF reactors that pump the reagents through a small heated coil that winds in and out of the cavity, with external temperature monitoring using a fibre optic sensor, although alternative methods, such as using a multimode batch or CF reactor, have also been described.[44]

More recently a new method for carrying out MAOS under CF processing using a commercially available monomodal microwave synthesizer has been described by Bagley, Jenkins, Lubinu, Mason and Wood.[44] The flow cell was inserted into the cavity of a self–tunable monomodal microwave synthesizer, irradiated, and stabilized at the required reaction temperature through moderation of microwave power before the introduction of reagents into the reactor (Figure 16).

The reactant, aminodienone **12b** was dissolved in solvent and introduced into the microwave cavity through a small tube (~5 mm internal diameter) via the HPLC pump. The solvent/reactant mixture was passed through a layer of sand (~10 g) (necessary to minimize dispersion and create micro–channels) via the small tube and coupled with microwave radiation in the reaction chamber at the bottom of the reaction tube (10 mL volume).

As a result of the continuous pressure exerted by the HPLC pump and that of the back pressure regulator (sand was prevented from escaping from the reaction tube by the presence of two frits, shown in white) the reacting mixture was forced up the reaction tube and heated. The mixture passed through the micro–channels in the sand and was collected in a flask and purified either by column chromatography or, following optimisation, the product, pyridine **13b** could be isolated as a single product by simply evaporating the solvent.

Figure 16. Schematic diagram of the CF microwave reactor
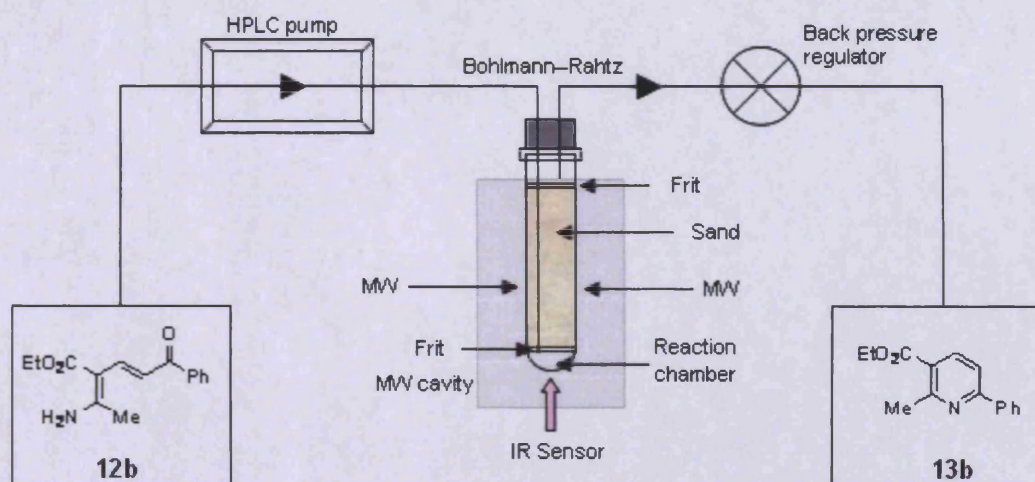
The development of a new microwave–assisted CF process shown above for the synthesis of pyridines based upon the Bohlmann–Rahtz reaction was one of the first systems to be tested. Aminodienone **12b** was prepared and cyclodehydrated with CF processing under homogeneous conditions in toluene–acetic acid (5:1) over sand, and the results compared to batch experiments carried out in a sealed tube (conventional microwave synthesis) and to the corresponding homogeneous CF process with a commercially available Teflon heating coil system (Scheme 8).

In order to compare CF and batch processing, conventional batch microwave synthesis (method A) using the same reaction tube (10 mL) as described above for the CF system, containing the solvent and reagent was sealed and irradiated for a fixed time and output. The product was purified by conventional methods; one shortfall as mentioned earlier is the fact that only a small amount of material could undergo reaction because of the small volume (10 mL) of the reaction tube.

Further comparisons were made using the commercially available Teflon heating coil system (method B). This processing system benefits from a continuous spiralling of the tube in the microwave cavity; it is also an open system similar to the one described in Figure 16 and is a more direct comparison to the CF system described (method C).

Scheme 8. Microwave-assisted Bohlmann-Rahtz synthesis of pyridine **13b**
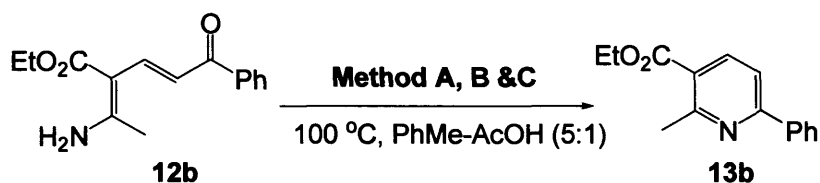
Method

A: microwaves (150 W), sealed tube, 2 min;

B: microwaves (300 W), CF in teflon heating coil, 1 mL/min;

C: microwaves (300 W), CF in glass tube charged with sand, 1-1.5 mL/min.

Under conditions that gave efficient conversion (>98%) to pyridine **13b**, the processing rates of material using the glass tube reactor (method C) were considerably higher (Table 4).

Table 4. Comparing MAOS of pyridine **13b** using sealed tube or CF processing.

	seal tube[a]	CF coil[b]	CF coil[b]	CF glass tube[c]	CF glass tube[c]
Isolated yield (%)	>98	>98	85[d]	>98	>98
residency time (min)[e]	2	5[f]	3.3[f]	3	2
flow rate (mL/min)		1	1.5	1	1.5
processing rate (mmol/min)		0.1	0.15	0.1	0.15
total energy (kJ)[g]		1411	762	850	735

[a] Batch experiment in a sealed glass tube; [b] CF processing in a Teflon heating coil; [c] CF processing in glass tube reactor charged with sand; [d] Based upon 1H NMR analysis of crude reaction mixture; [e] Residency in the microwave cavity; [f] Residency in the heating coil; [g] Energy delivered by the magneton in a flow reaction.

Additionally, CF reactions run at the same flow rate used less magnetron energy in a glass tube (method C) than in the Teflon heating coil (method B) (Table 4), demonstrating that a glass tube CF reactor offers (i) improved heating efficiency, (ii) the potential for operation on a large scale, (iii) successful transfer from batch (method A) to CF processing (method C), and (iv) improved performance over commercial Teflon heating coils. As a result of these findings based partially on the Bohlmann–Rahtz synthesis, the scene was set to transfer the process technology to large–scale operations and ultimately to an industrial based process, if required.

2.3 Literature methods for 3-cyanopyridine synthesis

The direct construction of carbon-carbon bonds has always been a central theme in synthetic chemistry; structural diversity and the biological importance of nitrogen-containing heterocycles have made them attractive targets for synthesis over many years. Of these, cyanopyridines have drawn continuing efforts in the development of novel synthetic strategies, such as involving vinamidium salts,[45] one-pot reactions,[46] or microwave[47] and ultrasound irradiation.[48]

The cyanopyridine motif is certainly a valuable heterocyclic component found in various therapeutic agents.[49] For example, it is a building block for the synthesis of nicotinic acid, its amide (nicotinamide) is used in pharmaceutical formulations, such as additives in food and animal feed. Cyanopyridines possess interesting photophysical properties, making them ideal candidates in developing versatile luminescent chromophores and highly selective biological sensing materials. Thus extensive efforts have been made over the years to develop new methodology for the synthesis of cyanopyridine derivatives.

Initial experiments for the synthesis of cyanopyridines date as far back as 1908, when Meyer prepared 2,4,6-trimethyl-3,5-dicyanopyridine **16** by reaction of acetaldehyde **15**; the intermediate dihydropyridine was oxidised to achieve the cyanopyridine target (Scheme 9).[50]

Scheme 9. Synthesis of 2,4,6-trimethyl-3,5-dicyanopyridine **16**.
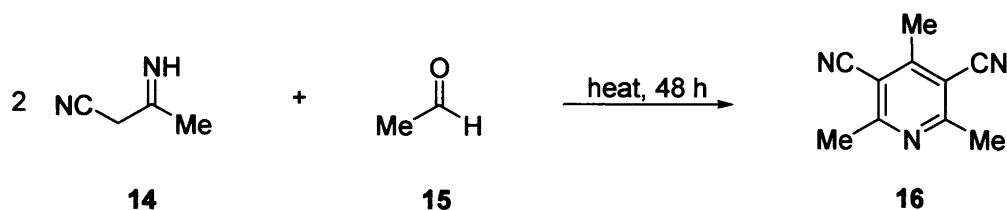
Many studies for the synthesis of cyanopyridines followed this initial discovery, including the production of a valuable intermediate for the synthesis of Vitamin B6 (pyridoxine) by Harris, Stiller and Folkers[51] from which extensive studies by Wenner and Platti found that two isomers were formed from the reaction, compromising 75% of the expected isomer **19** and 15% of isomeric 3-cyano-6-ethoxymethyl-4-methyl-2-hydroxypyridine **20** (Scheme 10).[52]

Scheme 10. Synthesis of cyanopyridine isomers **19** and **20**.
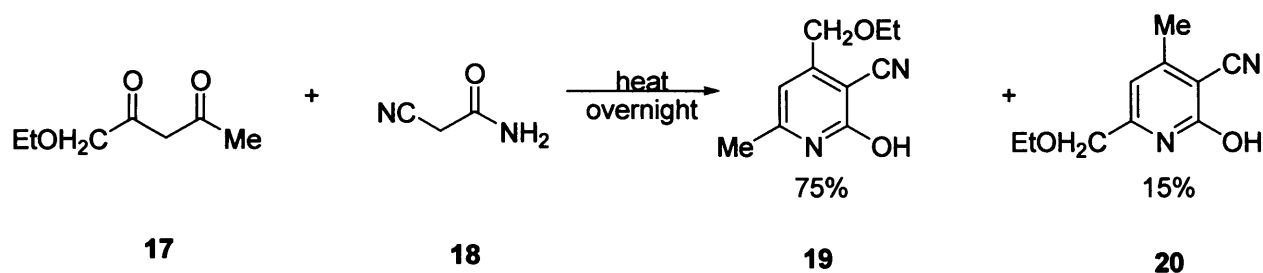
The synthesis of pyridine derivatives from malononitrile as a starting material can be carried out by several methods, such as by reacting dinitrile **21** with tetracyanopropene salt, obtained from orthoesters,[53] however the corresponding pyridine products required two steps to form, and the required orthoesters are not easily obtainable. In 1970, Alvares-Insúla, Lora-Tamato and Soto developed a method whereby the reaction of aldehydes and malonitrile in the presence of an alcohol/alkoxide provided a single step route for the synthesis of 4-substituted 2-amino-3,5-dicyano-6-alkoxypyridines **23** (Scheme 11).[54]

**Scheme 11.** Synthetic route to 3,5-dicyanopyridines **23**.
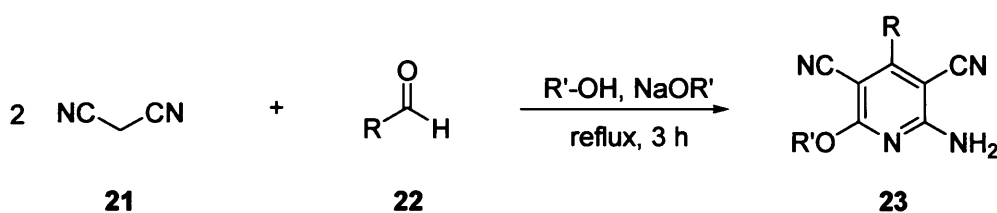
Various pyridines were prepared from aldehydes from this route and the pyridines were generated in moderate yields when aromatic aldehydes were employed (Table 5) whereas aliphatic and alicyclic aldehydes failed to produce the corresponding pyridines. Although this one-step reaction proceeds to the polysubstituted pyridines, the yields were moderate, and hence further research into the synthesis of pyridine derivatives continued.

Table 5. One-pot synthesis of pyridines from aldehydes.

Entry	Starting Aldehyde	R	Yield (%)
1	Acetaldehyde	Methyl	3
2	Propionaldehyde	Ethyl	7
3	Isobutyraldehyde	Isopropyl	32
4	Pivaldehyde	*tert*-Butyl	5
5	Valeraldehyde	*n*-Butyl	25
6	Benzaldehyde	Phenyl	50
7	*p*-Tolualdehyde	*p*-Tolyl	31
8	*m*-Tolualdehyde	*m*-Tolyl	49

Application of vinylogous iminium salts led to the synthesis of trisubstituted cyanopyridines in 1995 by Sikorski and co-workers. Previous work within the group used vinylogous iminium salts for the formation of five-membered rings such as pyrroles.[55] With the methodology established, combined with previous work reported by Jutz and co-workers[56] 2,3,6-trisubstitued pyridines were synthesized using the reaction of β-aminocrotononitrile **10c** with 2-substituted unsymmetrical vinamidinium salts **24** under basic conditions (Scheme 12).

Scheme 12. Synthesis of 3-cyanopyridines from β-aminocrotononitrile.
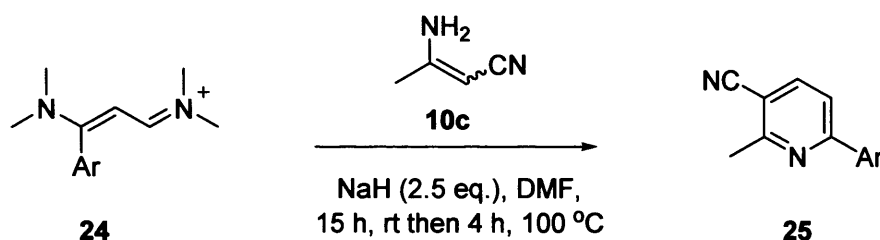


Two regioisomeric pyridines could be formed by the reaction of β-aminocrotononitrile **10c** and vinamidinium salts **24**. Nucleophilic attack on unsymmetrical vinamidinium salts has been shown to be under steric control; attack by the nitrogen of the enamine at the least sterically hindered carbon of the vinamidinium salts will result in 2,3,4-trisubtituted pyridine, whereas attack by the carbon of the enamine is favoured, resulting in 2,3,6-trisubstitued pyridine **25** as the major product.

**Table 6.** Synthesis of 2,3,6-trisubstituted pyridine **25**.

Entry	Ar	Yield (%)
1	4'-C_6H_4OMe	80
2	4'-C_6H_4Me	74
3	4'-C_6H_4Cl	58
4	4'-C_6H_4Br	49
5	Ph	67
6	4'-C_6H_4NO$_2$	52
7	4'-C_6H_4F	67
8	3',4'-C_6H_4(OMe)$_2$	65

The scope of this reaction was extended using a range of substrates and generated the trisubstituted pyridines in moderate to good yields. The use of symmetrical vinamidinium salts **26** gave the corresponding 2,3,5-trisubstituted pyridine **27** in 60% yield (Scheme 13).

Scheme 13. Synthesis of 2,3,5-trisubstituted pyridines.
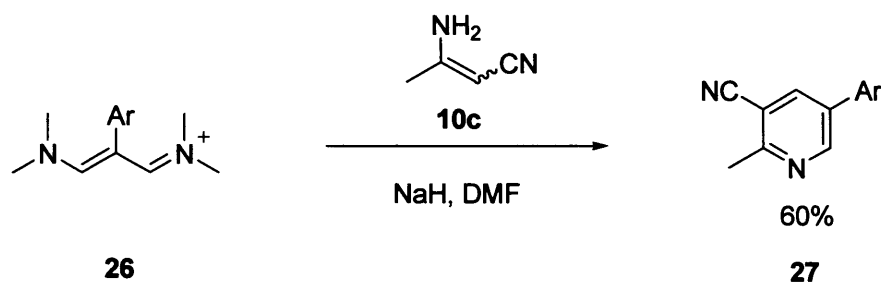
Although this methodology formed 2,3,5-trisubstituted **27** and 2,3,6-trisubstituted pyridines **25** in acceptable yields, it required the initial preparation of vinylogous salts in addition to inert, dry conditions, somehow limiting its applicability.

Other reactions incorporating enamine precursors for the formation of pyridine derivatives were reported by J. N. Chatterjea in 1952.[57] He reported two products were formed from the reaction of β-aminocrotononitrile with chalcone, namely compounds **30** and **31** although no yields were reported.

Scheme 14. Synthetic path to pyridines *via* Michael addition.
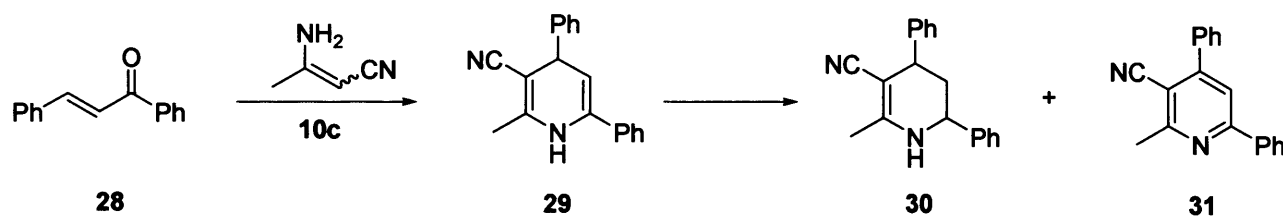
An alternative method emerged for the synthesis of 3-cyanopyridines by Gupta and co-workers in 1990, although this complicated procedure required dry conditions and the use of *n*-butyllithium (Scheme 15).[58]

Scheme 15. Reaction route for the synthesis of tetrasubstituted pyridine.
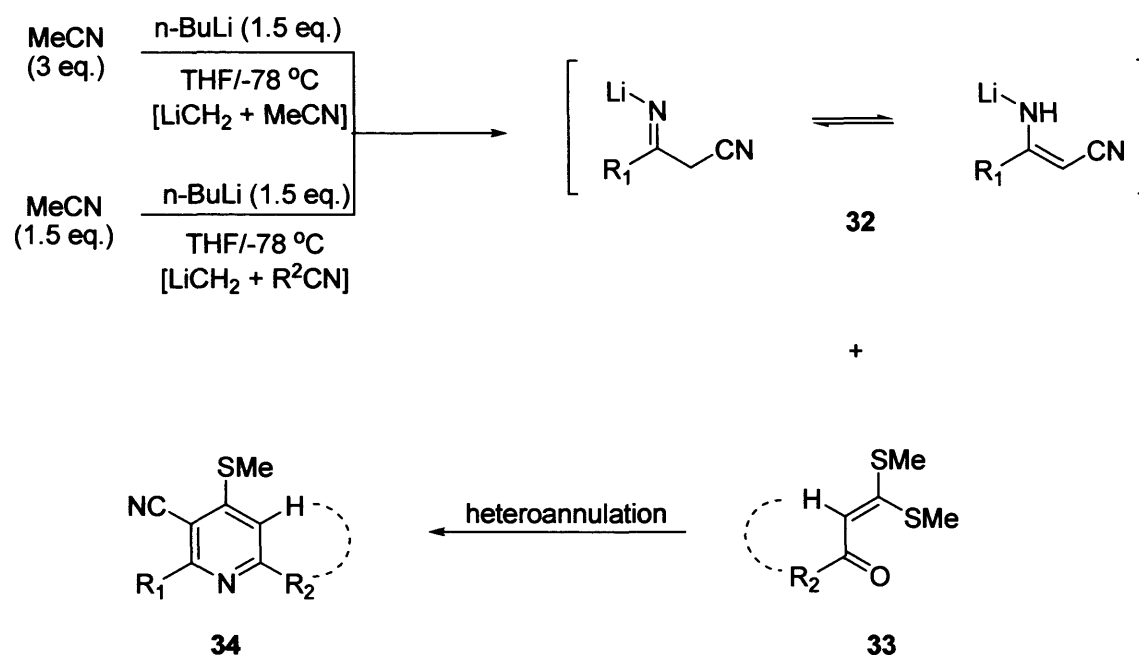
The lithiated β-amino-β-substituted acrylonitriles were first generated *in situ* by treating excess acetonitrile (3 eq) with n-butyllithium (1.5 eq), and this was reacted with a range of enones **33** generating cyanopyridines (Table 7). The overall yields produced from this method ranged from moderate to excellent, however the experimental procedure makes this method to some extent laborious.

Table 7. Synthesis of 2,6-substituted-4-(methylthio)-3-cyanopyridines **34**.

Entry	R_2	R_1	Yield (%)
1	Me	4'-C_6H_4OMe	92
2	Me	Ph	86
3	Me	4'-C_6H_4Cl	90
4	Me	2'-Naphthyl	92
5	Me	2'-Thienyl	82
6	Me	3'-Pyridyl	62
7	Ph	2'-Furyl	87
8	Ph	Me	57
9	2'-Thienyl	Ph	65
10	2'-Furyl	Ph	76

The fluorescent properties of cyanopyridines have sparked much interest in their synthesis to explore their photophysical potential in application. In 1992, a similar reaction to that reported by Chatterjea was found by Matsui and co-workers.[59]

4,6-disubstituted-3-cyano-2-methylpyridines **36** were prepared by the treatment of α,β-unsaturated compounds with β-aminocrotononitrile **10c** in the presence of tert-butoxide and these were found to show intense ambient state fluorescence in the region of 400-552 nm (Scheme 16).

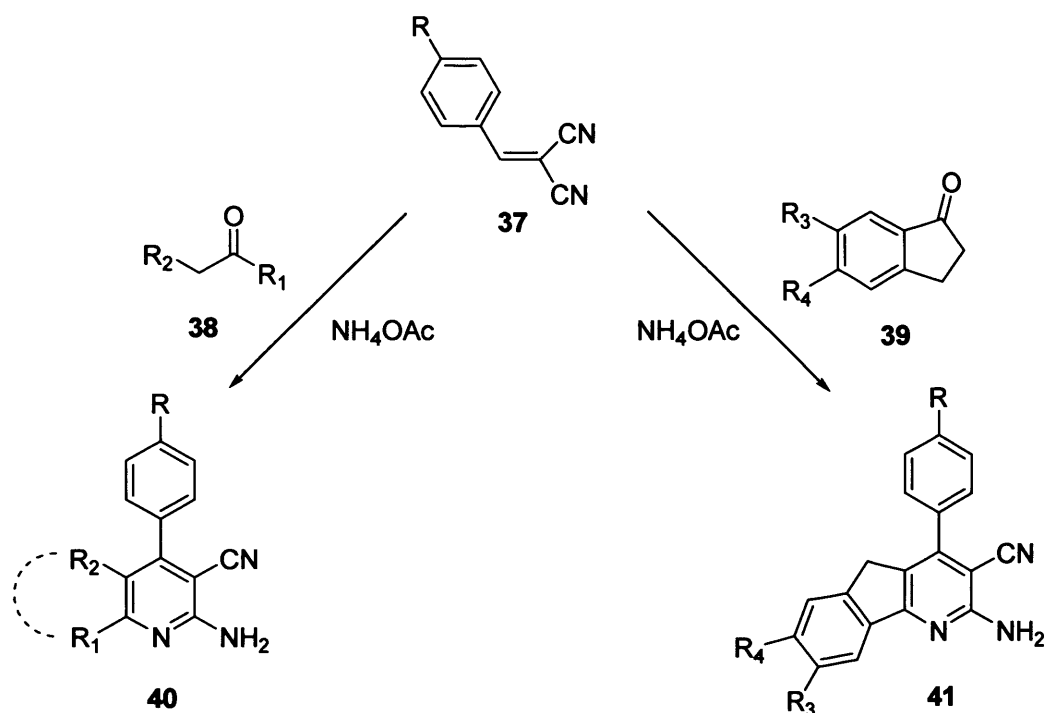**Scheme 16.** Synthesis of 3-cyanopyridines **36**.
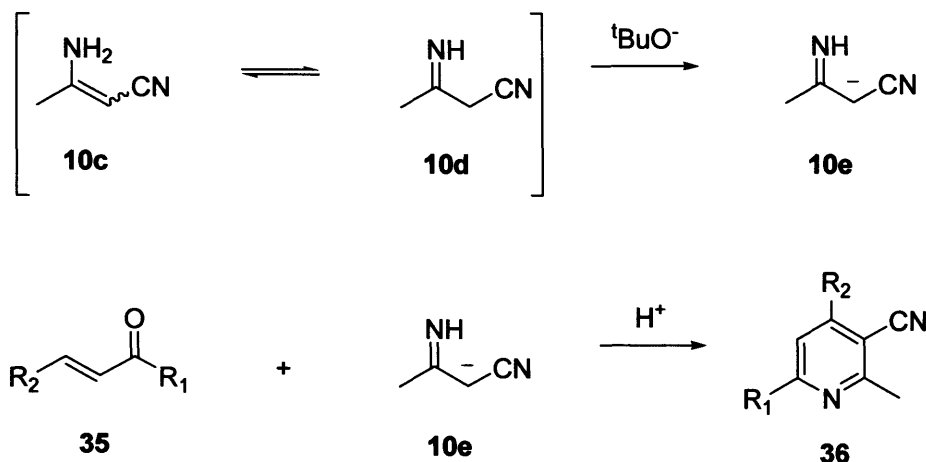
The mechanism proposed by Matsui and co-workers is very similar to the Bohlmann-Rahtz pyridine synthesis which has been discussed early in this chapter. β-Aminocrotononitrile can exist as an amino **10c** and imino **10d** isomer in solution. Michael addition of the carbanion of the imino isomer **10d** to **10e**, followed by cyclization with subsequent dehydration gave the 3-cyanopyridines **36** in good yields. A variety of 3-cyanopyridines was generated and their interesting luminescent properties were investigated.

Scheme 17. Proposed mechanism for the synthesis of 3-cyanopyridines.
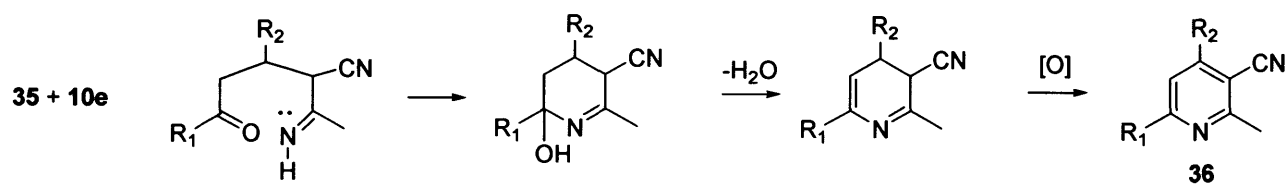
With a view to their pharmaceutical properties, use as important intermediates in preparing heterocyclic compounds and with various synthetic routes available for the synthesis of 2-amino-3-cyanopyridines, these derivatives continue to attract much interest. More recently, the use of microwave dielectric heating[41] has been observed as a valuable alternative to conventional conductive heating methods for the synthesis of cyanopyridines.

Scheme 18. Microwave-assisted synthesis of 2-amino-3-cyanopyridine derivatives.

An efficient and simple method was developed by Paul, Gupta and Loupy[60] in 1998 for the rapid synthesis of 2-amino-3-cyanopyridines from arylidenemalanonitriles **37** and ketones **38** or **39** in the presence of ammonium acetate without solvents/containing trace of solvent under microwave irradiation, reducing the reaction times and providing significant improvement to yields in comparison to conductive heating.

Table 8. Comparison of yields of 3-cyanopyridine products using different heating methods.

Product	Method A (%)	Method B (%)	Method C (%)
35a	52	72	49
35b	43	75	46
35c	58	78	69
35d	52	69	46

Method A: MW, no solvents; Method B: MW, trace solvents; Method C: conventional reflux in benzene.

The classical approach to the synthesis of cyanopyridines by this method is at reflux in benzene. The same reaction performed under microwave conditions required 3-5 minutes; the yields observed increased under microwave-assisted conditions and were enhanced further by the addition of small amounts of solvents.

Following on from this method, a few years later, Tu and co-workers prepared a series of 2-amino-3-cyanopyridines derivatives by one-pot condensation from malononitrile **21**, methyl ketone **42**, aromatic aldehyde **43** and ammonium acetate under microwave irradiation in the absence of solvents (Scheme 19).[61]

**Scheme 19.** One-pot synthesis of 2-amino-3-cyanopyridines.
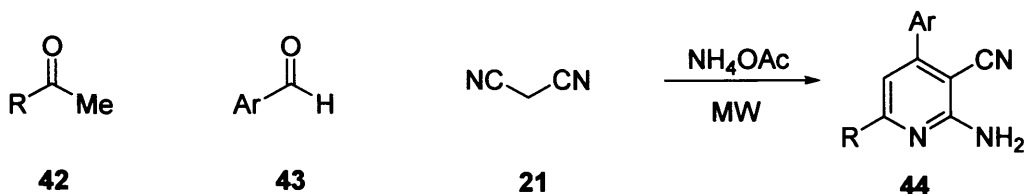
Entry	Ar	R	Time (min)	Yield (%)
1	4'-C_6H_4Cl	4'-C_6H_4OMe	8	83
2	4'-C_6H_4OMe	4'-C_6H_4OMe	7	80
3	4'-C_6H_4OMe	2',4'-$C_6H_4(Cl)_2$	7	75
4	4'-C_6H_4OMe	Ph	9	85
5	4'-C_6H_4Cl	2',4'-$C_6H_4(Cl)_2$	9	72
6	4'-C_6H_4Cl	4'-C_6H_4F	8	78
7	3'-Indolyl	4'-C_6H_4OMe	7	86
8	4'-C_6H_4Cl	Me	8	84

When a mixture of **42**, **43** and **21** with ammonium acetate was irradiated in a domestic microwave oven, reactions were almost complete in 7-9 min. The reaction mixtures were washed with a small amount of ethanol and crude products were recrystallized to afford cyanopyridine derivatives **44** in good yields (Scheme 19). This reaction proceeds *via* imine formation from aldehyde/ketone and ammonium acetate, followed by reaction of the corresponding enamine with the alkylidenemalononitrile formed by the condensation of aromatic aldehyde and malononitrile, followed by cyclization to form the 2-amino-3-cyanopyridines **44**.

Metallocenes are known to exhibit a wide range of biological properties, one being that ferrocene has attracted special attention since it is a neutral, chemically stable, non-toxic entity that is able to cross cell membranes.[62] The synthesis of 3-cyanopyridine compounds *via* the condensation of chalcone with malononitrile had been studied previously, but the reaction with ferrocenyl (Fc) substituents was not investigated until Ji[63] and co-workers developed an efficient synthesis of ferrocenyl substituted 3-cyanopyridine derivatives via the condensation of ferrocenyl substituted

chalcones **45** with malononitrile in a sodium alkoxide solution under ultrasonic irradiation (Scheme 20).

Scheme 20. Synthesis of ferrocenyl substituted 3-cyanopyridine derivatives.
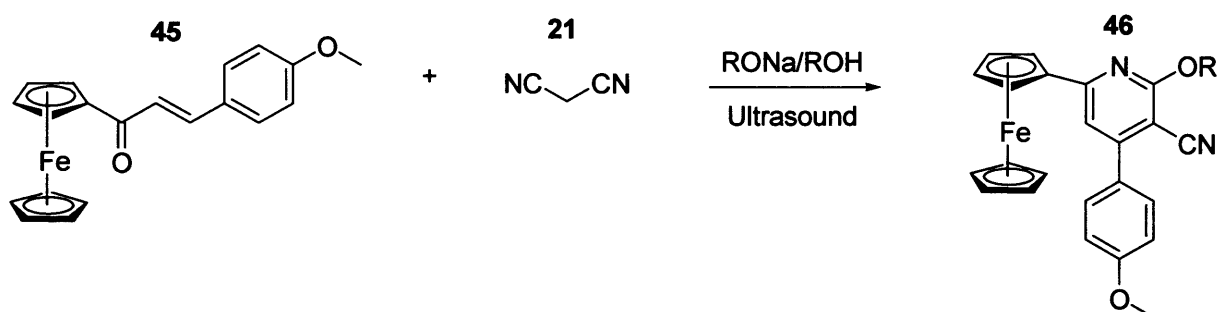
The acceleration of reactions by ultrasound to achieve higher yields, shorter reaction times and improved efficiency was applied to the reaction of chalcone and malononitrile by immersing the mixture into the water bath of a KQ-250E ultrasonic cleaner at 50-60 °C.

Table 9. Optimised yields for the ultrasound-assisted cyanopyridine synthesis.

Entry	Chalcone	Time (h)	Yield (%)
1		5	66
2		3	64
3		4	71
4		2	73
5		6	68

Ji and co-workers investigated the effects of ultrasonic irradiation on a range of substrate conducted in EtOH (Table 9). Both phenyl substituted chalcones and the heterocyclic ring containing chalcones reacted efficiently with malononitriles to afford the target products (entry 1-5) in moderate to good yields. It was concluded that a mild, efficient and ultrasound-assisted method for the synthesis of ferrocenyl substituted derivatives had been developed, and these could be used as intermediates, ligands for transition-metal ions or novel clinical medicines.

2.3.1 Synthetic Applications

As we have discussed, the synthesis of fluorescent chromophores with predictable and readily-modulated photophysical properties is essential to deliver new biologically compatible materials for application as responsive chemosensors in intracellular luminescence imaging. Not only can suitable dyes be utilized in their own rights, but their incorporation into metal–based architectures such as lanthanide–derived assemblies, enables the chromophore to function as a sensitizing component in lanthanide–based phosphorescence, with a wide range of fields for application. In all of these developments, the photophysical properties must be readily tuned by structural modification and the most straightforward way to achieve this would be by modulation of electronic properties. 3-Cyanopyridine dyes are currently being intensely investigated as photoactive materials for use in a variety of disciplines because of their excellent thermal and photochemical stability,[59] high luminescence efficiency and novel optoelectronic properties.[64] In particular, the photophysical potential of 3-cyanopyridines has been demonstrated recently by Bowman, Jacobsen and Blackwell.[65] In this elegant study, the SPOT synthesis of heterocyclic macroarrays identified fluorescent 3-cyanopyridines that exhibited promising photochemical stability, vivid ambient state luminescence and experimentally lowered physiological pH dependence (Scheme 21).

Scheme 21. Synthesis of cyanopyridine and deazalumazine chromophores from chalcone macroarrays.
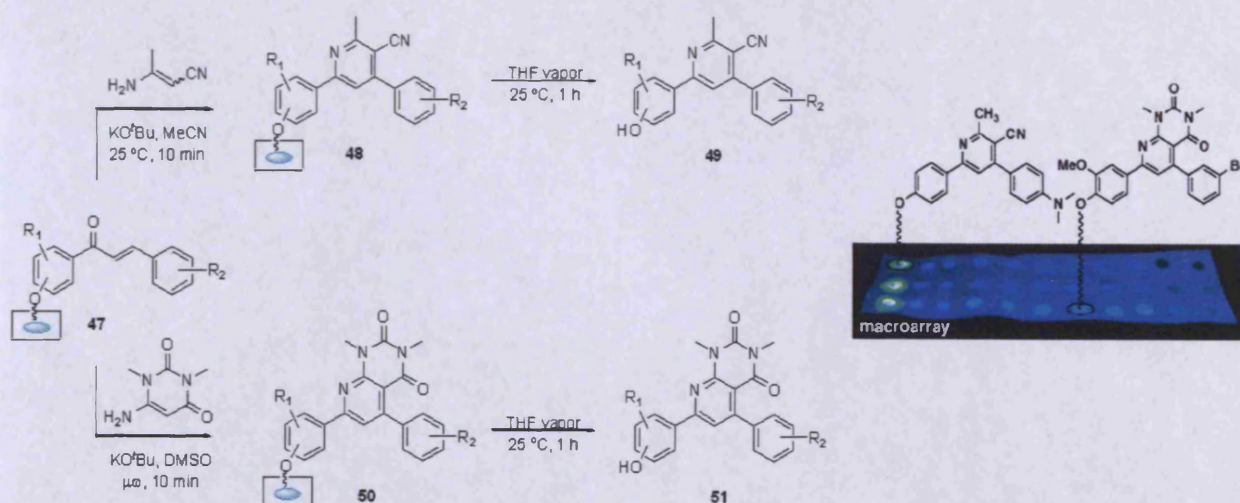
In their study, cyanopyridines and deazalumazines were generated in high purity via a spatially addressed synthesis on planar cellular supports. Chalcone macroarray **47** was converted into cyanopyridine macroarray **49** by treatment with 3-aminocrotononitrile generated *in situ* from acetonitrile and potassium tert-butoxide (Scheme 21). Spotting a pre-sonicated mixture of these reagents onto each individual chalcone array member at room temperature gave cyanopyridines in good yields (Table 10).

Table 10. Structures, purity data and photophysical properties of selected cyanopyridines **49**.

| Entry	R_1	R_2	λ_{ex} (nm)	λ_{em} (nm)	$\Phi_f{}^a$	Yield (%)^b
1	4'-OH	H	341	433	0.07	81
2	4'-OH	4'-F	342	430	0.06	81
3	4'-OH	4'-Br	342	440	0.12	82
4	4'-OH	4'-OMe	339	423	0.12	70
5	4'-OH	4'-NMe$_2$	366	524	0.09	74
6	3'-OMe, 4'-OH	H	351	469	0.03	74
7	3'-OMe, 4'-OH	3'-OMe	351	473	0.02	89
8	3'-OMe, 4'-OH	4'-Br	352	475	0.02	70

^{a} Relative quantum yields measured in ethanol; ^{b} Determined by integration of HPLC traces with UV detection at 254 nm.

Furthermore, the non–linear optical properties of a series of 2–(pyrrolidin–1–yl)nicotinonitrile derivatives have also been reported.[66] Despite these novel inventions, there is still a great demand for the development of a facile synthetic route for the preparation of 3-cyanopyridine dyes, with high environmental sensitivities (*e.g.*, for real-time imaging of complex intracellular processes) and containing extended π-heteroaromatic conjugation.

The electronic and structural properties of donor-acceptor-substituted organic chromophores are of considerable interest nowadays because of their potential applications in a variety of electooptic devices.[67] Both synthetic[68] and theoretical[69] studies have verified that replacing the benzene ring that acts as a chromophoric interlink with readily delocalized five/six-membered aromatic heterocycles, such as thieny, 4-methoxyphenyl, 4-aminophenyl and pyridyl, can result in an enhanced covalent hyperpolarizability over the entire D-A molecular framework. In particular, conjugated dialkylamine and pyrrolidine derivatives as donors substituted with appropriate electron accepting groups are promising candidates among such push-pull type molecules, which at the same time, exhibit fascinating electrochromic, photochromic, luminescent and nonlinear optical properties.[70,71]

2.4 Aim of this research

So as one of our ongoing studies, we set out to discover a novel synthetic pathway for the effective modulation of a wide range of electron-donating and electron-accepting functionalities into the existing cyanopyridine dye architecture, which generally emit at biologically detectable wavelengths and are suitable for extended π-heteroaromatic conjugation (Scheme 22).
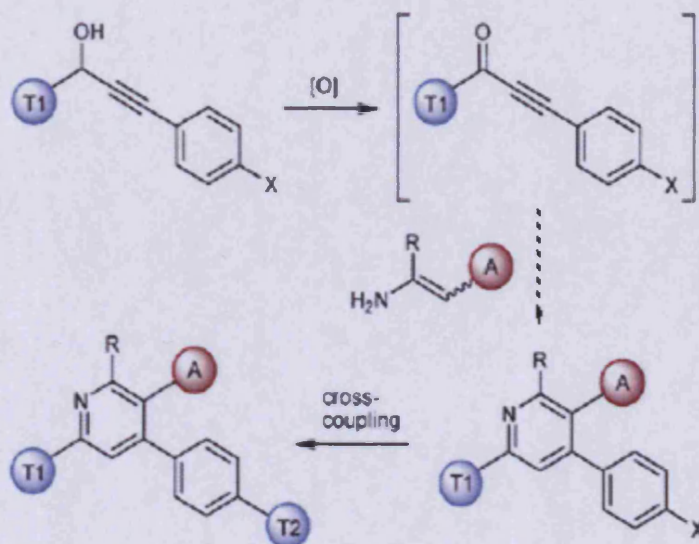
Scheme 22. Microwave-assisted strategy for the synthesis of electroluminescent frameworks with tunable D–A properties (T: tunable groups, containing at least one donor; A: acceptor group).

Recently, we reported that 2,4,6-trisubstitued pyrimidine chromophores can be prepared by tandem oxidation–heteroannulation of propargylic alcohols using manganese dioxide under microwave assisted conditions (Scheme 23).[72] In this method, an oxidant generated the ethynyl ketone *in situ* which was subsequently trapped in an acid–catalysed heterocyclocondensation with amidine derivatives to give the pyrimidine products in good overall yields, with total regiocontrol.
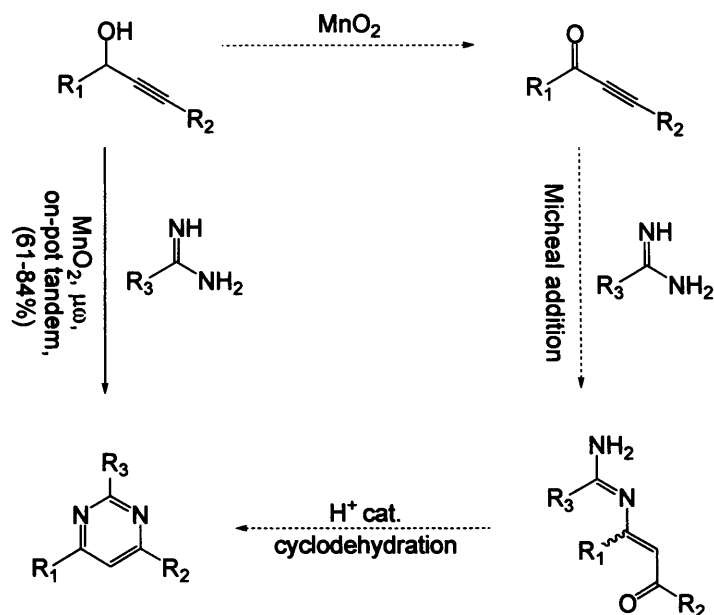
Scheme 23. Previous report on the tandem oxidation-heteroannulation of propargylic alcohols.

Although this approach for pyrimidine synthesis could be facilitated rapidly and efficiently using microwave dielectric heating to prepare the products in a one–pot tandem oxidation reaction. The corresponding process for pyridine synthesis was poorly efficient.[74] Given the success of our original two–step Bohlmann–Rahtz protocol for the synthesis of 3–cyanopyridines from β–aminocrotononitrile **10c**,[74] we set out to develop a facile one–step method for the preparation of 3–cyanopyridine dyes using a tandem oxidation–Bohlmann–Rahtz cyclocondensation under microwave irradiation in order to explore their photophysical potential.

2.4.1 Rapid synthesis of 3-cyanopyridine dyes

Many previous studies for tandem oxidation reactions have utilized manganese dioxide,[75] but it has been reported that barium manganate is a viable alternative reagent for the oxidation of benzylic, allylic and propargylic alcohols[76] that has been employed in a one pot tandem oxidation–Wittig reaction.[77] To explore its potential in tandem oxidation–heteroannulation reactions under microwave irradiation, a commercially–available propargylic alcohol **52a** and crotononitrile **10c** was submitted to a range of conditions (Scheme 24) for the synthesis of 3-cyanopyridine **53a** in the presence of $BaMnO_4$ and the findings compared to the use of IBX (entry 1) and MnO_2 (entries 2&4). In the solvents investigated (entries 5-10), ethanolic acetic acid (5:1) appeared to be optimum on irradiation at 170 °C for 45 min (entry 14, compared to entries 10-13).

The use of $BaMnO_4$ as an oxidant in 5:1 ethanolic acetic acid was considerable more efficient than either IBX under traditional conductive heating (entry 18) or MnO_2 in a comparable

microwave irradiation experiment (entry 15). Furthermore, at the high temperatures accessible under microwave irradiation, the reaction was much more efficient than comparable experiments using traditional reflux under conductive heating conditions (entry 16).

**Scheme 24.** Optimising conditions for the synthesis of **53a**.
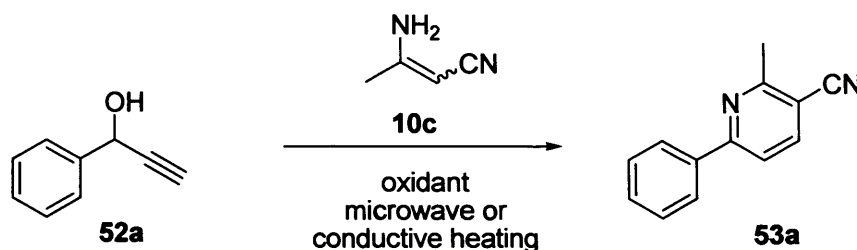
Entry	Reagents and Conditions[a]	Yield%[b]
1	IBX, PhMe, 65 °C, 18 h	10
2	MnO$_2$, PhMe, 65 °C, 18 h	12
3	BaMnO$_4$, PhMe, 65 °C, 18 h	30
4	MnO$_2$, PhMe, μW, 120 °C, 30 min	22
5	BaMnO$_4$, PhMe, μW, 120 °C, 30 min	51
6	BaMnO$_4$, DMSO, μW, 120 °C, 30 min	46
7	BaMnO$_4$, EtOH, μW, 120 °C, 30 min	56
8	BaMnO$_4$, EtOH-ZnBr$_2$ (15 mol%), μW, 120 °C, 30 min	58
9	BaMnO$_4$, EtOH-AcOH (1:1), μW, 120 °C, 30 min	64
10	BaMnO$_4$, EtOH-AcOH (5:1), μW, 120 °C, 30 min	69
11	BaMnO$_4$, EtOH-AcOH (5:1), μW, 150 °C, 30 min	72
12	BaMnO$_4$, EtOH-AcOH (5:1), μW, 170 °C, 30 min	76
13	BaMnO$_4$, EtOH-AcOH (5:1), μW, 170 °C, 60 min	80
14	**BaMnO$_4$, EtOH-AcOH (5:1), μW, 170 °C, 45 min**	**86**
15	MnO$_2$, EtOH-AcOH (5:1), μW, 170 °C, 45 min	54
16	BaMnO$_4$, EtOH-AcOH (5:1), reflux, 18 h	60
17	MnO$_2$, EtOH-AcOH (5:1), reflux, 18 h	24
18	IBX, EtOH-AcOH (5:1), reflux, 18 h	20

[a] 3 equivalent of the oxidant were used, unless otherwise stated; [b] Isolated yield after chromatographic purification.

The most efficient method from this study (Scheme 24, entry 14) was employed in the attempted synthesis of a small library of 3-cyanopyridines **53a-j** to explore their intriguing photophysical properties (Scheme 25). The subset of propargylic alcohols **52a-j** was prepared by the addition of lithium acetylide to the corresponding aldehydes according to the existing procedures developed by Tykwinski *et al.*[78]

**Scheme 25.** Microwave-assisted tandem synthesis of 3-cyanopyridines **53**.
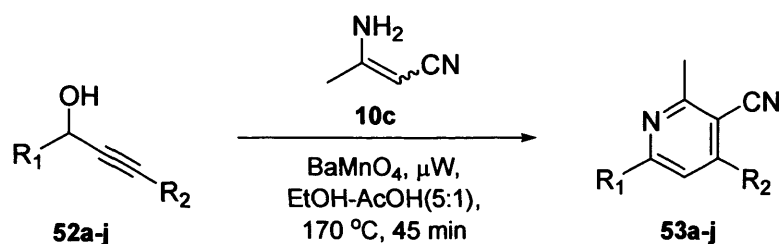
53	R^1	R^2	Yield%^{a}
a	Ph	H	86
b	4-MeOC$_6$H$_4$	4-Me$_2$NC$_6$H$_4$	88
c	4-MeOC$_6$H$_4$	4-MeOC$_6$H$_4$	92
d	4-MeOC$_6$H$_4$	4-BrC$_6$H$_4$	89
e	2-Pyridyl	4-Me$_2$NC$_6$H$_4$	84
f	2-Pyridyl	4-MeOC$_6$H$_4$	80
g	2-Pyridyl	4-BrC$_6$H$_4$	87
h	4-Piperidinophenyl	4-Me$_2$NC$_6$H$_4$	88
i	4-Piperidinophenyl	4-MeOC$_6$H$_4$	86
j	4-Piperidinophenyl	4-BrC$_6$H$_4$	82

^{a} Isolated yield after chromatographic purification on silica.

The barium manganate-mediated tandem oxidation Bohlmann-Rahtz reaction was found to be astonishingly effective for the synthesis of 3-cyanopyridines **53**, yielding the desired chromophores with a tunable substituent at the *6-position* of the heteroaromatic ring (*i.e.* EDG: **53b-d, 53h-j**; EWG: **53e-g**). Moreover, among all of the successful cases explored, only a single regioisomeric pyridine product was found. Of these, 4-(4-methoxyphenyl)-6-(4-methoxyphenyl)nictinonitrile **53c** was prepared in an outstanding 92% yield and, as studied previously,[65] would provide a valuable comparison to known photophysical data.

It is also noteworthy that this process can be effectively used to generate 4-(4-bromophenyl)-substituted cyanopyridines (**53d,g&j**) in excellent yields, which are viable building blocks for transition-metal-catalysed cross-coupling reactions[79] and thus could introduce a variety of electroluminescent functionalities into the existing cyanopyridine framework.

Attention was therefore given to the copper(I) mediated cross-coupling reactions between pyrrolidine and 4-(4-bromophenyl)-substituted synthetic intermediates (**53d,g&j**) in order to further develop their π-conjugated electron-transporting system (Scheme 26).

Scheme 26. Copper(I) mediated C-N bond cross-coupling of pyrrolidine and 3-cyanopyridines **53d,g&j**.
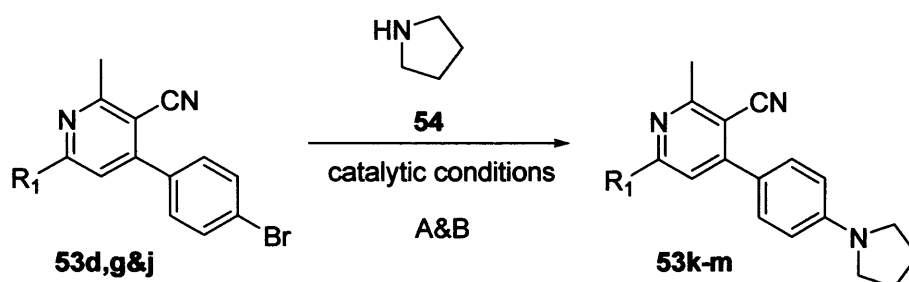
Condition

**A**: Cu(PPh$_3$)Br, neocuproine, ^{t}BuOK, toluene, 24 h;

B: Cu(neocup)(PPh$_3$)Br, ^{t}BuOK, toluene, 24 h.

Entry	Precursor 53	R^1	Product 53	Condition	Yield%^{a}
1	d	4-Methoxyphenyl	k	A	86
2	g	2-Pyridyl	l	B	72
3	j	4-Piperidinophenyl	m	A	88

^{a} Isolated yield after chromatographic purification on silica.

As expected, these reactions were found to be highly efficient under the general Ullmann condensation conditions.[80] In particular, reaction of **53d** and pyrrolidine in the presence of Cu(PPh$_3$)Br, neocuproine, ^{t}BuOK in toluene efficiently provided the luminescent dye, 4-(4-pyrrolidinophenyl)-6-(4-methoxyphenyl)nictinonitrile **53k**, in 86% yield. Pyrrolidine was also reacted with 4-(4-bromophenyl)-6-(4-piperidinophenyl)nictinonitrile **53j** to generate the coupling product **53m** in excellent yield. Although the highly electron-deficient precursor 4-(4-bromophenyl)-6-(2-pyridyl)nictinonitrile **53g** did not participate in a coupling reaction with pyrrolidine under similar Ullmann conditions (entry 2), whilst a catalytic combination of Cu(neocup)(PPh$_3$)Br (prepared according to the existing procedure[81]), ^{t}BuOK in toluene was applied, the reaction proceeded smoothly and provided the bright green luminescent crystals of 4-(4-pyrrolidinophenyl)-6-(2-pyridyl)nictinonitrile **53l** in 72% yield.

2.4.2 The photophysical study of 3-cyanopyridine dyes

53
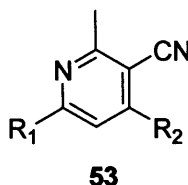
Photophysical studies revealed that the extended π-heteroaromatic conjugation has a great influence upon absorption maximum, emission maximum and fluorescent quantum yields of 3-cyanopyridine dyes (Table 11).

Table 11. Phtophysical properties of 3-cyanopyridine **53**.

53	R_1	R_2	λ_{max} (nm)	logε	λ_{max} (nm)	τ_0(ns)	$\Phi_f{}^b$
			UV/vis[a]		**Fluorescence[a]**		
h	4-$C_5H_{10}NC_6H_5$	4-$(CH_3)_2NC_6H_5$	364	4.60	468	2.19	0.56
m	4-$C_5H_{10}NC_6H_5$	4-$C_4H_8NC_6H_5$	370	4.58	470	2.89	0.28
b	4-$CH_3OC_6H_5$	4-$(CH_3)_2NC_6H_5$	374	4.15	472	3.98	0.54
k	4-$CH_3OC_6H_5$	4-$C_4H_8NC_6H_5$	386	4.03	482	4.38	0.24
f	2-Pyridyl	4-$CH_3OC_6H_5$	336	4.56	404	2.58	0.53
e	2-Pyridyl	4-$(CH_3)_2NC_6H_5$	385	4.38	488	8.79	0.30
l	2-Pyridyl	4-$C_4H_8NC_6H_5$	397	4.16	494	9.04	0.20

[a] Measured in $CHCl_3$ and the average concentration is 2.5×10^{-8} M; [b] External standard: fluorescein ($\Phi_f = 0.79$ in 0.1 M NaOH), estimated uncertainty: $\pm15\%$.

As expected, as the electron-donating ability of the 4-substituent (R_2) on the 3-cyanopyridine architecture increases (*e.g.*, **53** f$\rightarrow$e$\rightarrow$l), correspondingly larger bathochromic shifts of the absorption maximum in the UV-vis spectra were observed. This indicates an effective extension of the π-conjugating strength from the non-bonding electrons on the nitrogen, despite, theoretically,[82] the presence of two δ-bonds between donor and acceptor might moderately reduce the efficiency of the total charge transfer.

The position of the absorption bands is also influenced by the nature of the tunable group at the 6-substituent on the cyanopyridine framework. As expected, the introduction of a pyridyl electron-accepting group at the *6-position* (**53l**), relative to the 6-[4-(piperidinophenyl)]-substituted electron-donating analogue (**53m**), resulted in a 27 nm bathochromic shift in the absorption maximum, which is primarily due to an enhanced charge transfer rate, and therefore a much lowered S_0/S_1 energy difference.[83]

All of the donor-acceptor-substituted 3-cyanopyridine dyes were highly fluorescent. When they were dissolved in chloroform (10^{-6} M) and irradiated by ~ 385 nm UV light, intense visible luminescent-green emissions were observed (Figure 17).

Within compounds of the same class (*i.e.*, same 4-substituent on the cyanopyridine architecture), the emission wavelength was found to be highly dependent upon the nature of the 6-substituent. This is most pronounced in the compounds where R_1 = 4-methoxyphenyl (**53b&k**). Functionalization with an electron-donating group, **53k** for example where R_2 = 4-(pyrrolidino)phenyl, induced significant modulation of the fluorescence resulting in a bathochromic shift of the emission wavelength maximum [12 nm in this case, compared to the 4-(dimethylamino)phenyl substituted analogue **53b**].

2.4.2.1 The influence of the polarity on dye spectral properties of 53k

Given the electronic nature of **53k**, with both electron-accepting and electron-donating moieties within its architecture, we conducted some preliminary studies into the solvatochromic behaviour of this compound (Table 12).

Table 12. Solvatochromic data for **53k** in selected solvents.

| Solvent	UV/vis [a]			Fluorescence [a]			
	λ_{max} (nm)	logε	λ_{max} (nm)	τ_0(ns)	Φ_f [b]	k_{nr}/k_r [c]	Δv (cm^{-1})
Cyclohexane	368	3.89	420	2.15	0.42	1.38	3364
Chloroform	386	4.03	482	4.38	0.24	3.17	5160
DMSO	416	4.08	590	5.96	0.11	8.09	7089

[a] The average concentration: 2.5 × 10^{-8} M; [b] External standard: fluorescein (Φ_f = 0.79 in 0.1 M NaOH); estimated uncertainty: ±15%; [c] This value equals to $(1-\Phi_f) \times \Phi_f^{-1}$, assuming that phosphorescence is negligible.

For **53k**, a slight increase in the polarity of the solvent resulted in a dramatic decrease in fluorescence from the LE state (*i.e.* locally excited singlet state) and in the concomitant appearance of a fluorescence band situated at lower energy (Figure 17). This low-energy band is structureless, fairly broad and undergoes an evident bathochromic shift with increased solvent polarity.

The decrease in energy and consequent increase in the Stokes shift, with increased solvent polarity indicated that this newly formed state is significantly more polar than the corresponding ground state. This behaviour is consistent with the observed fluorescence emanating from an intramolecular charge transfer (ICT) state arising *via* charge transfer from the amine donor to the

3-cyanopyridine acceptor. As such, the position of the emission maximum reflects the extent of solvent stabilization of this largely polarized charge transfer state.

The rise in quantum yield from DMSO to cyclohexane is also consistent with the great CT character of **53k**. The large Stokes shift provided by polar solvent such as DMSO indicated a significant change in the molecular geometry from the ground (S^0) to the excited (S^1) state and therefore a sizable displacement of the S^1 potential energy surface relative to the S^0 surface. This would cause a larger overlap between the wave functions of the relaxed S^1 state and the higher vibrational levels of the S^0 state, leading to more efficient nonradiative processes and therefore lowering the quantum yield.
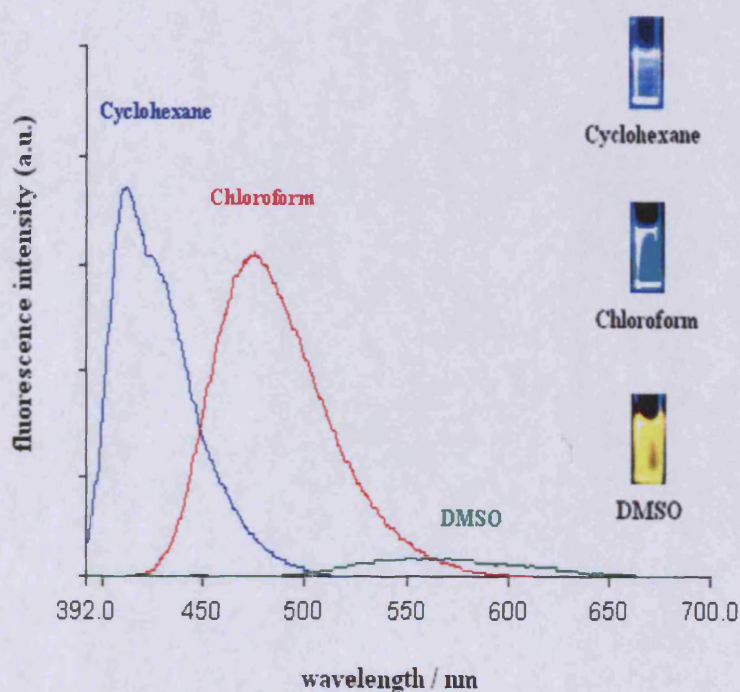
Figure 17. Emissive behaviour and fluorescent spectra of **53k** with various solvents.

This statement relies upon the assumption that $k_{nr} > k_r$, which is common in organic species[83] and is supported through this study. Conversely, nonpolar cyclohexane is associated with a significantly smaller Stokes shift; thus the pertinent wave functions will have only a small overlap, reducing the nonradiative rate constant and increasing the quantum yield of fluorescence.

2.4.2.2 The influence of the protic media on dye spectral properties of 53k

Considering the large Stokes shift of **53k** observed in acetonitrile, it is confirmed that the excited state in this solvent has considerable charge transfer character. Similarly large values in the Stokes shift have also been reported for 4-(N,N-dimethylamino)benzonitrile[84] and 4-(9-anthryl)-N,N-dimethylaniline[85] in their twisted intramolecular charge transfer (TICT) states.

The TICT excited state is formed by a twist of a bond between the donor and acceptor accompanied by nearly full intramolecular charge transfer, which is stabilized by re-orientating the surrounding solvent molecules. Since the TICT excited state is formed with a large structural change from the initially excited singlet (LE) state, the dynamic processes of the TICT state are remarkably sensitive to a microscopic environment, which can restrict these structural changes.

Table 13. The distinctive solvatochromic behaviours of **53k** in protic and aprotic media.

Solvent	UV/vis [a]		Fluorescence [a]				
	λ_{max} (nm)	$\log\varepsilon$	λ_{max} (nm)	τ_0(ns)	Φ_f [b]	k_{nr}/k_r [c]	Δv (cm^{-1})
Methanol	370	3.86	454	0.83	0.41	1.44	5001
Acetonitirle	404	4.06	582	5.06	0.16	5.25	7560

[a] The average concentration: 2.5×10^{-8} M; [b] External standard: fluorescein ($\Phi_f = 0.79$ in 0.1 M NaOH); estimated uncertainty: $\pm 15\%$; [c] This value equals to $(1-\Phi_f) \times \Phi_f^{-1}$, assuming that phosphorescence is negligible.

In alcohol solutions which can hydrogen bond to the nitrogen atom of the donor, it has been shown that the twisting process may be partially inhibited due to the requirements of simultaneous breakage of such a hydrogen bond.[86] Given the weak acidity of methanol compared to the non-acidic acetonitrile (pK_a values are 15.2 and 24, respectively), such hydrogen bonding is to be expected in methanol however may be absent (or only very weak) in acetonitrile, such that the formation of the TICT state may be inhibited in the former but not in the latter.

This difference is strikingly clear upon comparing the fluorescent quantum yields in two solvents: 0.41 and 0.16 for methanol and acetonitrile respectively. Given that the polarity parameters (Δf) for both solvent are virtually identical, the much larger quantum yield for **53k** in methanol is quite likely due to a reduction in the efficiency of forming the ICT state, followed by the formation of the LE state, rather than enhanced non-radiative deactivation to the (twisted) charge transfer state.

2.5 Conclusions

Over the last decade the Bohlmann-Rahtz pyridine synthesis has re-emerged as a viable route to substituted pyridines. The original report identified a useful two step method to target di- and trisubstituted pyridines. Due to intensive studies over the last ten years this has now been broadened by new procedures, implementing metal based Lewis acid and Brønsted acid catalysts. Some of these methods have been shown to be effective in various solvents including non-polar (toluene) and polar (ethanol and DMSO). Furthermore we have seen that the methods can be extended beyond the original reaction of an enamine and alkynone to incorporate facile one-pot oxidation-heteroannulation methodology to tri- and tetrasubstiuted pyridines with unique tunable photophysical properties, which arise due to intramolecular charge transfer character that is enhanced through π-heteroaromatic conjugation.

References

[37.] Bohlmann, F.; Rahtz, D. *Chem. Ber.* **1957**, *90*, 2265.

[38.] (a) Hantzsch, A.; *Liebigs Ann. Chem.* **1882**, *215*, 1; (b) Stout, D. M.; Meyers, A. I. *Chem Rev.* **1982**, *82*, 223–243; (c) Eisner, U.; Kuthan, J. *Chem. Rev.* **1972**, *72*, 1–42.

[39.] Bagley, M. C.; Bashford, K. E.; Hesketh, C. L.; Moody, C.J. *J. Am. Chem. Soc.* **2000**, *122*, 3301.

[40.] Gabriel, C.; Gabriel, S.; Grant, E. H.; Halstead, B. S. J.; Mingos, D. M. P. *Chem. Soc. Rev.* **1998**, *27*, 213.

[41.] Reviews on microwave chemistry include: (a) Kuhnert, N. *Angew. Chem., Int. Ed.* **2002**, *41*, 1863.; (b) Lidström, P.; Tierney, J.; Wathey, B.; Westman, J. *Tetrahedron* **2001**, *57*, 9225.; (c) Loupy, A.; Petit, A.; Hamelin, J.; Texier–Boullet, F.; Jacquault, P.; Mathé, D. *Synthesis* **1998**, 1213.; (d) Galema, S. A. *Chem. Soc. Rev.* **1997**, *26*, 233.; (e) Caddick, S. *Tetrahedron* **1995**, *51*, 10403.; (f) Stauss, C. R.; Trainor, R. W. *Aust. J. Chem.* **1995**, *48*, 1665.

[42.] Bagley, M. C.; Lunn, R.; Xiong, X.; *Tetrahedron Letts.* **2002**, *43*, 8331.

[43.] Bagley, M. C.; Dale, J. W.; Bower, J. *Synlett* **2001**, 1149.

[44.] Bagley, M. C.; Jenkins, R. L.; Lubinu, M. C.; Mason, C.; Wood, R. *J. Org. Chem.* **2005**, *70*, 7003.

[45.] Petrich, S. A.; Hicks, F. A.; Wilkison, D. R.; Tarrant, J. G.; Sikorski, J. *Tetrahedron* **1995**, *51*, 1575.

[46.] Alvares-Insula, A. S.; Lora-Tamayo, M.; Soto, J. L. *Synthesis of Organic Compounds II*, **1970**, 1308.

[47.] Shi, F.; Tu, S.; Fang, F.; Li, T. *ARKIVOC*, **2005**, 137.

[48.] Zhou, W. J.; Ji, S. J.; Shen, Z. L. *J. Organomet. Chem.*, **2006**, 1356.

[49.] Roth, H. J.; Kleemann, A. *Pharmaceutical Chemistry, Volume 1: Drug Synthesis*; John Wiley & Sons: New York, **1998**.

[50.] Meyer. *J. Prakt. Chem.*, **1908**, *78*, 497.

[51.] Harris; Stiller; Folkers. *J. Am. Chem. Soc.*, **1939**, *61*, 1242.

[52.] Wenner; Platti, J. *Org. Chem.*, **1946**, *11*, 751.

[53.] (a) Little. E. L.; Middleeton, W. J.; Coffman, D. D.; Sausen, G. N. *J. Am. Chem. Soc.*, **1958**, *80*, 3832.; (b) Cottis, S. G.; Tieckelmann, H. *J. Org. Chem.*, **1961**, *26*. 79.

[54.] Alvares-Insula, A. S.; Lora-Tamayo, M.; Soto. *Synthesis of Heterocyclics II.* **1970**, *7*, 1305.

[55.] Gupton, J.; Krolikowski, D.; Yu, R.; Sikorski, J. *J. Org. Chem.*, **1990**, 55.

[56.] Jutz, C.; Lobering. H.; Trinkl, K. *Synthesis*, **1977**, 326.

[57.] Chatterjea, J. N. *J. Indian. Chem. Soc.*, **1952**, *29*, 323.

[58.] Gupta, A. K.; Ila, H.; Junjappa, H. *Tetrahedron*, **1990**, *46*(10), 3703.

59. Matsui, M.; Oji, A.; Hiramatsu, K.; Shibata, K.; Maramatsu, H. *J. Chem. Soc., Perkin Trans. 2.*, **1992**, *2*, 201.

60. Paul, S.; Gupta, R.; Loupy, A. *J. Chem. Res.,* **1998**, *S*, 330.

61. Dombrowski, K. E.; Baldwin, W.; Sheats, J. *J. Organomet. Chem.*, **1986**, *302*, 281.

62. Pandya, S.; Yu, J.; Parker, D. *J. Chem. Soc., Dalton Trans.*, **2006**, 2757.

63. Zhou, W. J.; Ji, S. J.; Shen, Z. L. *J. Organomet. Chem.*, **2006**, *691*, 1356.

64. Mak, T. C. W.; Zhao, X-L. *J. Chem. Soc., Dalton Trans.*, **2004**, 3212.

65. Bowman, M. D.; Jacobsen, M. M.; Blackwell, H. E. *Org. Lett.*, **2006**, *8*, 1645.

66. Raghukumar, V.; Thirumalai, D.; Ramakrishnan, V. T.; Karunakara, V.; Ramamurthy, P. *Tetrahedron* **2003**, *59*, 3761.

67. Kanis, D. R.; Ratner, M. A.; Marks, T. J. *Chem. Rev.*, **1994**, *94*, 195.

68. (a) Rao, V. P.; Jen, A. K-Y.; Wong, K. Y.; Drost, K. J. *Tetrahedron Lett.*, **1993**, *34*, 1747. (b) Jen, A. K-Y.; Wong, K. Y.; Drost, K. J. *J. Chem. Soc., Chem. Commun.*, **1993**, 90.

69. (a) Varanasi, P. R.; Jen, A. K-Y.; Chandrasekhar, J.; Namboothiri, N. N. I.; Rathna, A. *J. Am. Chem. Soc.*, **1996**, *118*, 12443.

70. Facchetti, A.; Beverina, L.; Van-der Boom, M. E.; Dutta, E. G.; Pagani, G. A.; Marks, T. J. *J. Am. Chem. Soc.*, **2006**, *128*, 2142; and references cited therein.

71. Thompson, B. C.; About, K. A.; Reynolds, J. R.; Nakatani, K.; Audebert, P. *New J. Chem.*, **2005**, *29*, 1128.

72. Bagley, M. C.; Hughes, D. D.; Lubinu, M. C.; Merritt, E. A.; Taylor, P. H.; Tomkinson, N. C. O. *QSAR Comb. Sci.*, **2004**, *23*, 859.

73. Bagley, M. C.; Lunn, R.; Xiong, X. *Tetrahedron Lett.*, **2002**, *43*, 8331.

74. Bagley, M.C.; Hughes D.D.; Sabo, H. M.; Taylor, P. H.; Xiong, X. *Synlett*, **2003**, 1443.

75. (a) Smith, B. M.; Graham, A. E. *Tetrahedron Lett.*, **2007**, *48*, 4891. (b) Maki, B. E.; Chan, A.; Phillips, E. M.; Scheidt, K. A. *Org. Lett.*, **2007**, *9*, 371.

76. Firouzabadi, H.; Karimi, B.; Abbassi, A. *J. Chem. Res.*, **1999**, *236* and references therein.

77. Shuto, S.; Niizuma, S.; Matsuda, A. *J. Org. Chem.*, **1998**, *63*, 4489.

78. Shi Shun, A. L. K.; Chernick, E. T.; Eisler, S.; Tykwinski, R. R. *J. Org. Chem.*, **2003**, *68*, 1339.

79. Wolf, C.; Liu, S.; Mei, X.; August, A. T.; Casimir, M. D. *J. Org. Chem.*, **2006**, *71*, 3270.

80. Venkataraman, D.; Gujadhur, R. K.; Kintigh, J. T. *Tetrahedron Lett.*, **2001**, *42*, 4791.

81. Venkataraman, D.; Gujadhur, R. K.; Bates, C. G. *Org. Lett.*, **2001**, *3*, 4315.

82. Bixon, M.; Jortner, J. *J. Phys. Chem.*, **1993**, *97* (50), 13061.

83. Holmén, A.; Nordén, B.; Albinsson, B. *J. Am. Chem. Soc.*, **1997**, *119* (13), 3114.

84. Kosower, E. M.; Dodiuk, H. *J. Am. Chem. Soc.*, **1976**, *98* (4), 924.

85. Fox, M. A.; Britt, P. F. *J. Phys. Chem.*, **1990**, *94* (16), 6351.

86. Köhn, A.; Hättig, C. *J. Am. Chem. Soc.*, **2004**, *126* (23), 7399.

Chapter Three – Results and Discussion

3 New Strategy for the Preparation of Pyrimidine-Containing Luminescent Chromophores

3.1 Introduction

Azaheterocycles constitute a very important class of compounds. In particular, pyrimidine derivatives include a large number of natural products, bio-medically valuable compounds and photo-active OLED materials (Figure 18).[87] Several examples of biologically important compounds include trimethoprim **54**,[88] sulfadiazine **55**,[89] imatinib mesilate **56**[90] and capecitabine **57**.[91] In addition, novel light-emitting devices with highly electron-transporting capabilities **58** might also encompass pyrimidine-like functionalities.[67] While development of important methodologies for the synthesis of pyrimidines enjoys a profound history, the discovery of new strategies for the facile synthesis of pyrimidine-containing heterocycles remains a vibrant area of modern synthetic chemistry.

Figure 18. Representative compounds containing pyrimidine sub-structures.
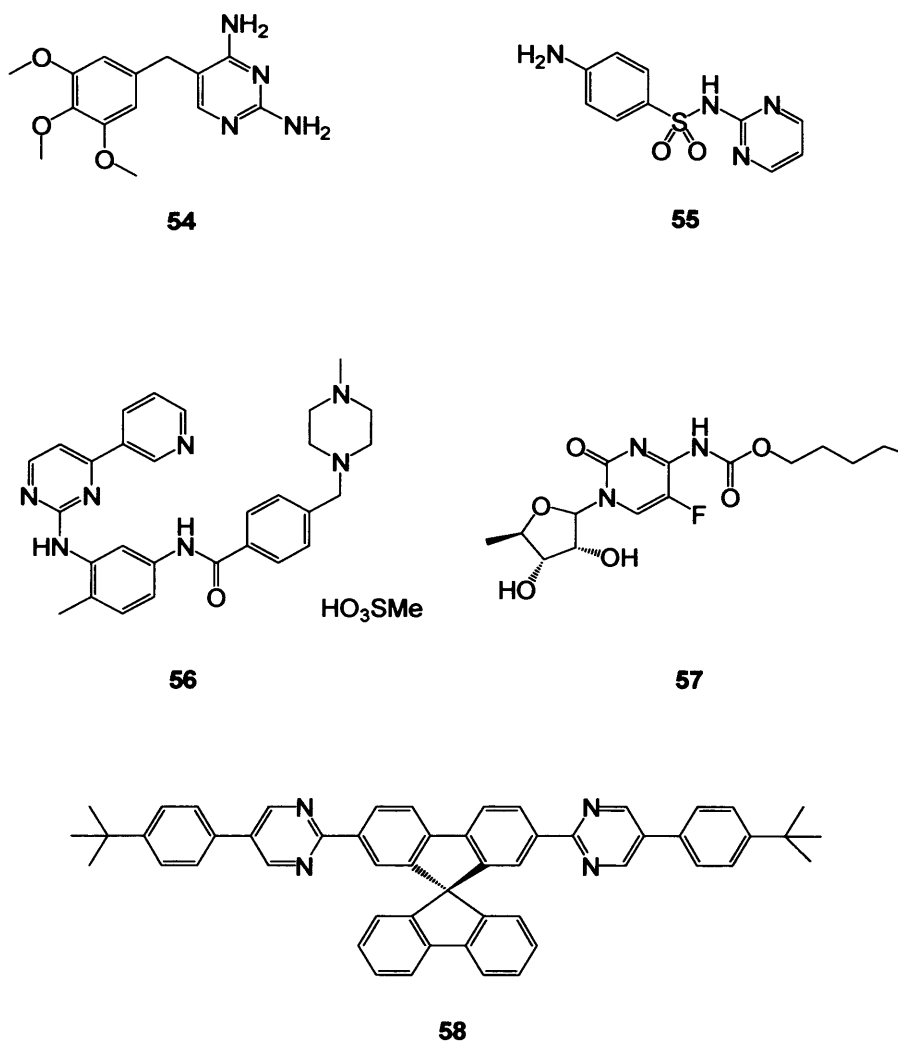
In 1818, Brugnatelli synthesized the first pyrimidine derivative, alloxan **59**, by nitric acid oxidative degradation of uric acid (Scheme 27).[92] Another early report, by Frankland and Kolbe in 1848, described the first synthesis of a pyrimidine cyanakine **60** by heating propionitrile with potassium metal.[93]

Since these early reports, many important contributions describing a variety of synthetic strategies for preparation of pyrimidine derivatives have also been published.[94]

Scheme 27. Early reports on the synthesis of pyrimidine derivatives.

Brugnatelli alloxan synthesis

59
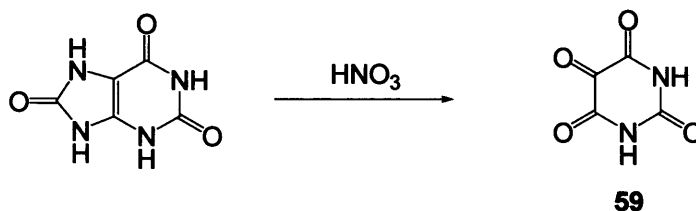
Frankland and Kolbe amino-pyrimidine synthesis

60
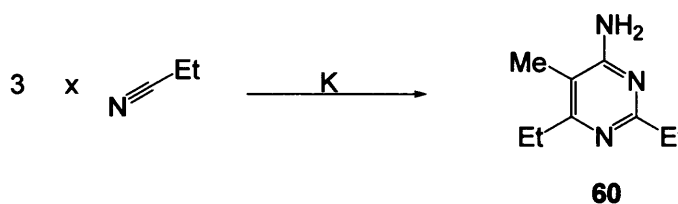
Many of these prevailing strategies rely on the condensation of N-C-N fragments, most often amidines or guanidines with 1,3-dicarbonyl derivatives (Scheme 28).[95]

Scheme 28. Typical pyrimidine synthesis by the condensation of 1,3-diketone and amidine.
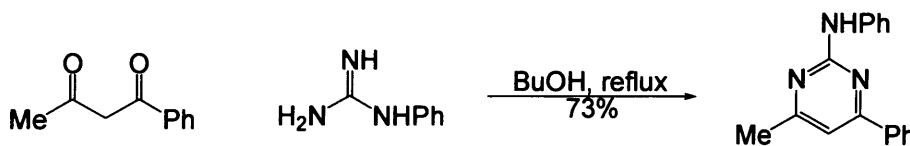
Another versatile approach to pyrimidine synthesis utilized N-C fragments. Nitriles are common N-C sources and have been used to form heterocycles in many syntheses. Cyanamide is a particularly versatile nitrile building block in the synthesis of pyrimidine derivatives (Scheme 29).[96]

Scheme 29. Typical pyrimidine synthesis by the condensation of 1,3-diketone and cyanamide.
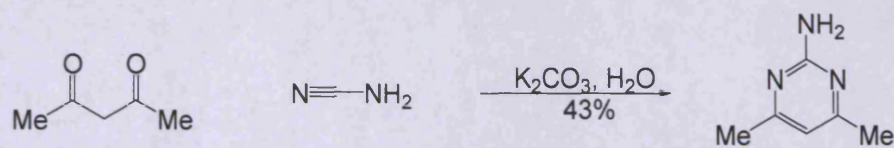
With advances in cross-coupling chemistry, the modification of substituents on the existing pyrimidine architecture has gained considerable attention: several recent publications have also described the up-to-date development of transition-metal mediated cross-coupling approaches to prepare photophysically robust pyrimidine-containing fluorescent chromophores.[97] Many of these procedures primarily rely upon the intrinsic reactivity associated with the extended pyrimidine π-heteroaromatic conjugation. For example, using activated heterocyclic cross-coupling reactions has been highly successful as a versatile strategy to develop novel luminescent oligomer light-emitting devices (Scheme 30).[98]
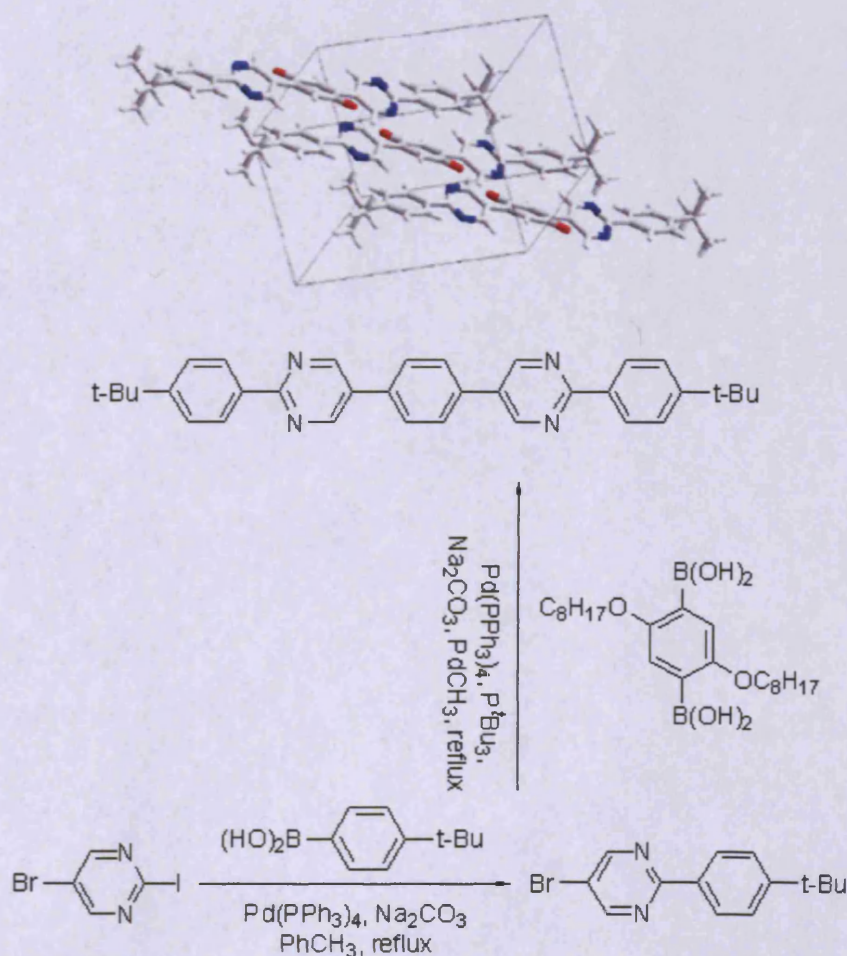
Scheme 30. Suzuki coupling approach for the synthesis of phenylene-pyrimidine based OLED materials. *(Inset: molecular packing diagram of the target oligomer, the long octyl chains are omitted for clarity.)*[98]

While these methods are very effective in the synthesis of extended π-heteroaromatic conjugation, the attention of this chapter will focuse on various strategies to construct the central pyrimidine heterocyclic ring and the diversity of different approaches to develop and evaluate novel pyrimidine-containing photo-luminescent chromophores.

3.2 Recent advances in versatile synthetic strategies to pyrimidines

A large amount of literature has described the synthetic advantages of the condensation between amidine and 1,3-dicarbonyl derivatives to access a diversity of pyrimidine-containing compound since this method was initially discovered over a century ago.[99]

Whereas most conventional approaches employed the direct condensation between 1,3-diketone and amidine derivatives (Scheme 31), some newly developed multi-component methods to afford the pyrimidine-containing heterocyclic compounds have also been published.[100]

Scheme 31. Traditional Pinner pyrimidine synthesis.
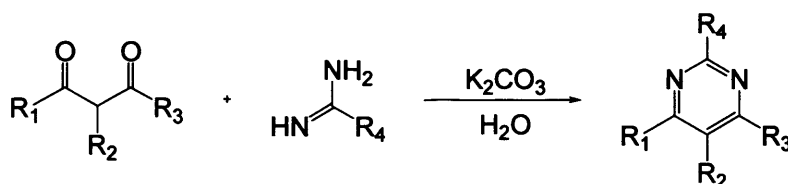
Ghosh and Katzenellenbogen reported an interesting modification to the traditional Pinner pyrimidine synthesis,[101] where N,N,N'-tris-(trimethylsilyl)amidines **62** (in place of the originally un-substituted amidines) were reacted with the 2-substituted-1,3-diketones **61** to form a variety of 2,4,6-trisubstituted and 2,4,5,6-tetrasubstituted pyrimidine products **63** in good yields (Scheme 32).[102]

Scheme 32. Modified Pinner pyrimidine synthesis using tris(trimethylsilyl)amidine **62**.
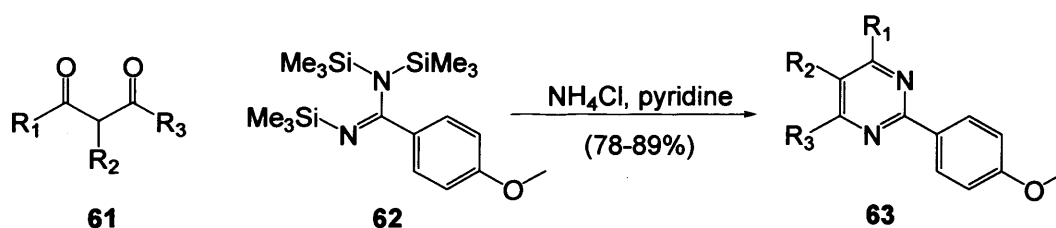
In such an approach, *N,N,N'*-tris-(trimethylsilyl)amidine **62** was thought to be less basic than the un-substituted amidine alternative, which could allow the use of milder reaction conditions and complete consumption of the air-sensitive, 1,3-diketone substrate. Furthermore, this procedure actually provided hexamethyldisiloxane in place of water by the end of the condensation, which was considered to be the major driving force that would drive the reaction forward.

Adamo *et al.* have also developed an alternative route to 2,4,6-trisubstituted pyrimidines **66** using amidinium chlorides **65** and diacetylenic ketoesters **64** (Scheme 33).[103]

Scheme 33. Novel synthesis of 2,4,6-trisubstituted pyrimidines **66** from diacetylenic ketoesters **64**.
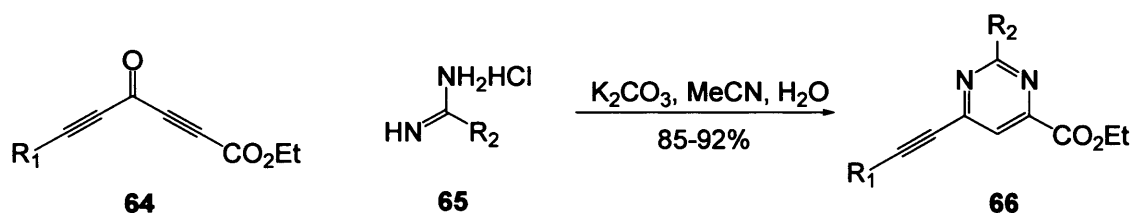
In this method, diacetylenic ketoesters **64** were prepared in two steps from aryl and alkyl propargylic aldehydes. Condensation with amidinium chloride **65** afforded the trisubstituted pyrimidine derivatives **66** with alkyl, aromatic and heteroaromatic substituents in good yield, with total regiocontrol.

3.2.1 Known methods for microwave-assisted synthesis of pyrimidines

As mentioned above, we have been interested in developing functionalized chromophoric compounds possessing tunable absorption and emission properties as they are essential in the search for materials for optoelectronic devices, light energy harvesting and fluorescent imaging microscopy.[104] Additionally, the use of a pyrimidine scaffold in this regard has received little attention, until recently when the fluorescent properties of π-extended pyrimidine systems was recognized.[105]

In the context of our work in this area, the Bagley group has developed a new method of combining conventional parallel synthesis and microwave-assisted organic synthesis (MAOS) for constructing diverse libraries of 2,6-disubstituted pyrimidines from the reaction of amidine hydrochlorides with various alkynones (Scheme 34, method A).[106]
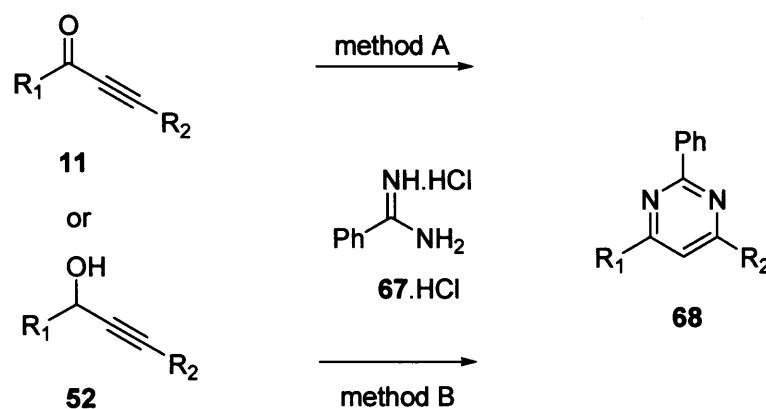
Scheme 34. Conventional methods for the synthesis of 2,4,6-triarylpyrimidines. Method A (cyclocondensation): Na_2CO_3, MeCN, microwave, 120 °C, 40 min; Method B (tandem oxidation): MnO_2, Na_2CO_3, MeCN, microwave, 150 °C, 45-60 min.

This method yielded some of the pyrimidines of interest by the microwave-assisted condensation of alkyones (**11**, where R^1 = Ph, Et, Me etc) with an excess of benzamidine hydrochloride **67**.HCl and sodium carbonate in acetonitrile, a method that gives good yields when the alkynone component is substituted only at one position (R^2 = H). This approach, however, was not universally efficient for the preparation of 2,4,6-trisubstituted pyrimidines (Table 14, entry 2).[107] Furthermore, the initial preparation of alkylnone starting materials are typically carried out in another two steps.[106,107] Thus, to address these problems, the Bagley group established a tandem oxidation-heteroannulation approach for the synthesis of 2,4,6-trisubstituted pyrimidines from propargylic alcohols using manganese dioxide as the oxidant under the microwave irradiation,[108] a route that generates the ethynyl ketone *in situ* as an intermediate, which could be trapped in an acid-catalysed cyclocondensation, using an amidine in the presence of acetonitrile to give the pyrimidine in a one-pot manner (Scheme 34, method B) in reasonable yields.

Table 14. Isolated yield of **68** using method A or B (Scheme 34).

Entry	R^1	R^2	Yield (A)%[a]	Yield (B)%[a]
1[b]	Ph	H	98	84
2[b]	Ph	SiMe₃	90[c]	_
3[d]	4-CH₃OC₆H₄	4-CH₃OC₆H₄	41	52
4[d]	4-CH₃OC₆H₄	4-(CH₃)₂NC₆H₄	_	19

[a] Isolated yield after chromatographic purification on silica; [b] Reaction developed by former members in the Bagley group; [c] Protodesilylated product (R^2=H) was obtained; [d] Reaction developed by the author of this thesis.

3.3 New methods for the microwave-assisted synthesis of triarylpyrimidine chromophores

It has been shown that barium manganate is a useful reagent for the oxidation of benzylic, allylic and propargylic alcohols[76] and, when used in a tandem oxidation/Wittig reaction,[77] was efficient and gave higher yields than manganese dioxide.[109] Following our previous observation that a related tandem oxidation/heteroannulation process was more facile under microwave irradiation with $BaMnO_4$ rather than with MnO_2, due to its more efficient coupling with the rapidly oscillating electric field,[110] the use of this oxidant (3 equiv.) was investigated in a microwave-assisted tandem oxidation/heterocyclocondensation of propargylic alcohol **52a** (1 equiv.) and benzamidine **67** (1 equiv.). It was thought that this would be a good substrate to study, as the heterocyclisation was highly efficient (Scheme 35).

Scheme 35. Optimising the oxidant for the microwave-assisted synthesis of pyrimidine **68a**.
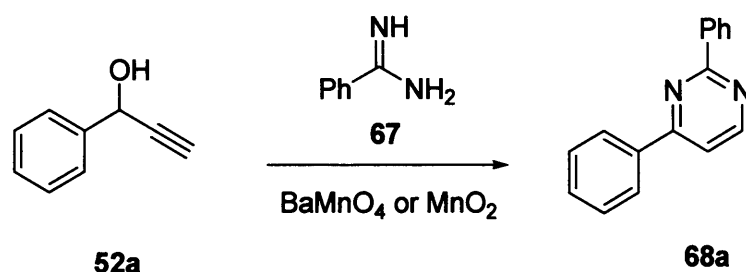
Entry	Oxidant	Condition	Yield %[a]
1	$BaMnO_4$	150 °C (150W), MeCN, 45 min	88
2	MnO_2	150 °C (150W), MeCN, 60 min	85
3	$BaMnO_4$	Reflux, MeCN, 10h	72
4	MnO_2	Reflux, MeCN, 10h	69

[a] Isolated yield after chromatographic purification on silica.

Not surprisingly, we have found that although the synthesis of 2,4-diphenylpyrimidine **68a** from barium manganate proceeded in excellent yield (88%), the reaction using manganese dioxide gave a slightly lower yield of the same pyrimidine and required chromatographic purification and a longer irradiation time, 60 min (Scheme 35, entry 2).

The same two experiments using propargylic alcohol **52a** and barium manganate or manganese dioxide were repeated under conductive heating conditions in the presence of acetonitrile. Each mixture was heated at reflux for 10 hours, cooled, filtered from the oxidant, the excess solvent was evaporated and the crude product was purified by chromatography on silica gel to give the pyrimidine product **68a** in acceptable yield (Scheme 35, entry 3 and 4).

Nevertheless it was found that the use of barium manganate as an oxidant was more efficient than manganese dioxide either under thermal or a similar microwave irradiation experiment. Furthermore, at the high temperatures accessible under microwave irradiation, this reaction was much more efficient than the corresponding traditional experiment carried out using conductive heating (Scheme 35, entry 1 and 3).

Although these results were promising, in terms of the reaction design, facility and efficiency, efforts were made to improve the yield further by carrying out the transformation in a series of alternative solvents to establish a system that had the optimum potential for the use of barium manganate as an oxidant in this microwave assisted tandem reaction (Table 15).

Table 15. Optimising the microwave-assisted cynthesis of pyrimidine **68a**.

Entry	Microwave-assisted conditions	Yield%[a]
1	150 °C (150W), MeCN, 45 min	88
2	150 °C (150W), MeOH, 45 min	50
3	150 °C (150W), EtOH, 45 min	62
4	120 °C (150W), EtOH-AcOH (5:1), 45 min	82
5	150 °C (150W), EtOH-AcOH (5:1), 30 min	64
6	**150 °C (150W), EtOH-AcOH (5:1), 45 min**	**92**

[a] Isolated yield after chromatographic purification on silica.

A mixture of benzamidine **67**, propargylic alcohol **52a** and BaMnO$_4$ was irradiated under different conditions in a sealed tube in a monomodal microwave synthesizer. In the solvents investigated (Table 15, entry 2-6), ethanolic acetic acid (entry 6) appeared to be optimum on irradiation at 150 °C (compared to entry 1 and 4) for 45 minutes (to entry 5), thus providing an alternative *in situ* tandem procedure for the rapid synthesis of pyrimidine targets.

In order to examine the scope of our novel microwave-assisted tandem reaction conditions, a mixture of benzamidine **67** and a range of different propargylic alcohols **52** (prepared by the addition of ethynylmagnesium bromide or lithium acetylide to the corresponding aldehydes according to existing methods[78]) was irradiated either with BaMnO$_4$ in ethanol-acetic acid (5:1) or MnO$_2$ in acetonitrile, and the results were compared with a study conducted using conventional heating methods (Scheme 36) and the reaction of chalcone precursors **47**, prepared according to the method of Matsui and co-workers.[59]

Scheme 36. Synthesis of pyrimidine **68a-g** by using the traditional conductive heating or novel microwave-assisted tandem method.
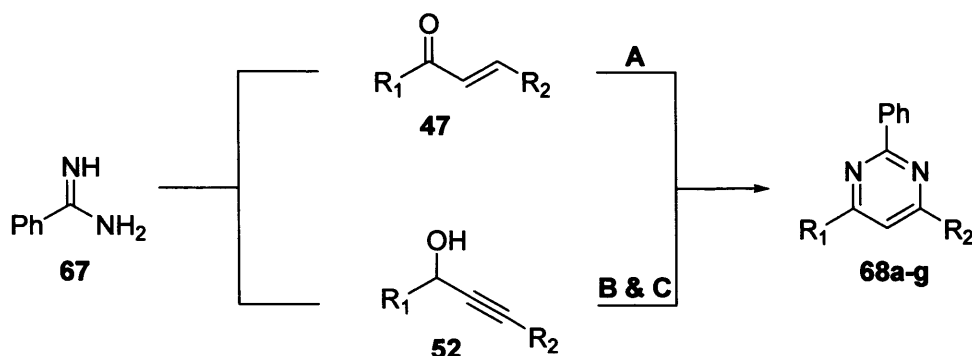
Condition

A: NaOH, EtOH, reflux, 10 h;

B: MnO_2, MW (150 W), 150 °C, MeCN, 45 min;

C: $BaMnO_4$, MW (150 W), 150 °C, EtOH-AcOH (5:1), 45 min

Although the microwave assisted procedure with MnO_2 (Table 2, method B) did afford the pyrimidine targets in some cases, the efficiency of reaction was comparable (entry 2, 4 & 5) or lower (entry 3) than an alternative thermal experiment carried out using chalcone precursors (method A). However, in all cases the microwave-assisted procedure with barium manganate in ethanolic acetic acid (method C) was highly efficient, giving the di- or tri-substituted pyrimidines **68 a-g** rapidly in good isolated yields, and moreover for one case investigated, even without the need for chromatographic purification (method C, entry 6). In comparison, the traditional experiment using conductive heating not only required much longer reaction times, but also gave a lower yield of product and always required purification by column chromatography.

Table 16. Synthesis of pyrimidine **68** under thermal or microwave-assisted conditions.

Enrty	product 68	R^1	R^2	Yield (A)%[a]	Yield (B)%[a]	Yield (C)%[a]
1	a	Ph	H	—	85[c]	92
2	b	$4\text{-CH}_3\text{OC}_6\text{H}_4$	$4\text{-CH}_3\text{OC}_6\text{H}_4$	30	42	72
3	c	$4\text{-CH}_3\text{OC}_6\text{H}_4$	3-Thienyl	11	10[c]	79
4	d	2-Thienyl	$4\text{-CH}_3\text{OC}_6\text{H}_4$	29	32	82
5	e	2-Thienyl	3-Thienyl	40	44	86
6	f	2-Naphthyl	$4\text{-CH}_3\text{OC}_6\text{H}_4$	31	48	73[b]
7	g	2-Naphthyl	3-Thienyl	24	36	68

[a] Results after column chromatography; [b] No purification procedures required; [c] The time of microwave irradiation at 150 °C was extended to 60 minutes.

With successful conditions established for the tandem process, a range of propargylic alcohols with π-conjugated functionalities **52h-m**, which had been shown to be effective building blocks

for fluorescent chromophores,[105] was submitted to the microwave-assisted *in situ* oxidation-heteroannulation reaction with benzamidine **67**, mediated by $BaMnO_4$ in EtOH-AcOH (5:1) at 150 °C. It was found that the efficiency of the reaction was highly dependent upon the nature of the propargylic alcohol, pyrimidine **68h-m** was generated in between 62-80% yield. Although the efficiency of the transformation was variable, in most instances it nevertheless compared very favourably with alternative traditional methods (Scheme 37, entry 2&5).

Scheme 37. Synthesis of pyrimidine **68h-m** using thermal or microwave-assisted conditions.
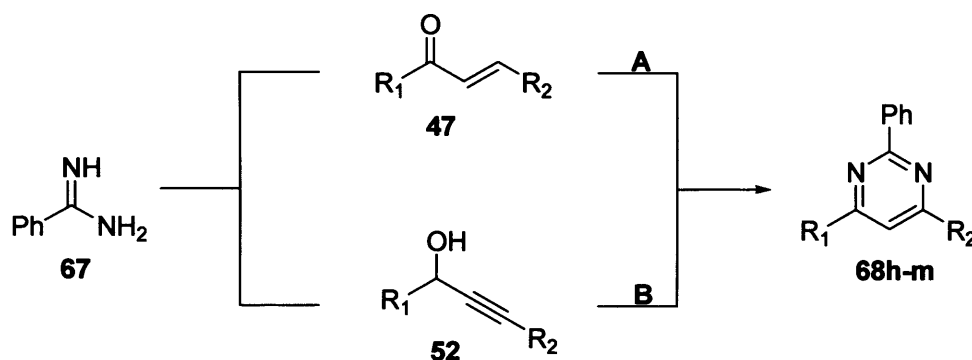
Condition

A: NaOH, EtOH, reflux, 10 h;

B: $BaMnO_4$, MW (150 W), 150 °C, EtOH-AcOH (5:1), 45 min

Enrty	product 68	R^1	R^2	Yield (A)%[a]	Yield (B)%[a]
1	h	$4\text{-}CH_3OC_6H_4$	$4\text{-}(CH_3)_2NC_6H_4$	24	72
2	i	2-Thienyl	$4\text{-}(CH_3)_2NC_6H_4$	_	68
3	j	2-Naphthyl	$4\text{-}(CH_3)_2NC_6H_4$	36	74
4	k	2-Naphthyl	$4\text{-}BrC_6H_4$	40	80
5	l	$4\text{-}CNC_6H_4$	$4\text{-}(CH_3)_2NC_6H_4$	_	62
6	m	$4\text{-}CNC_6H_4$	$4\text{-}BrC_6H_4$	22	76

[a] Results after column chromatography

Finally, in order to broaden the electronic profile of the π-extended pyrimidines accessible by this methodology, bromides **68k,m** were transformed by copper-mediated *N*-arylation[80] using the preformed Cu(I) catalyst $Cu(neocup)(PPh_3)Br$.[81] The original conductive heating procedure was modified and carried out in the presence of pyrrolidine and potassium *tert*-butoxide at 120 °C for one hour in toluene under microwave irradiation[111] to give pyrrolidino-derivatives **68n,o**, respectively, in excellent yields (Scheme 38).

Scheme 38. Further library diversification by copper-mediated *N*-arylation.

pyrrolidine, ^tBuOK,
toluene, Cu(neocup)(PPh₃)Br,
MW (120 °C), 60 min

68k R = 2-naphthyl
68m R = 4-cyanophenyl

68n R = 2-naphthyl (68%)
68o R = 4-cyanophenyl (74%)
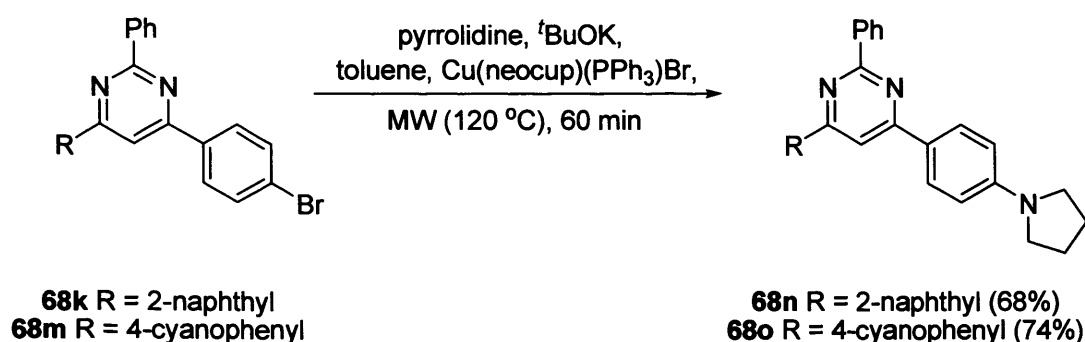
3.4 The photophysical study of 2,4,6-triarylpyrimidine dyes

68
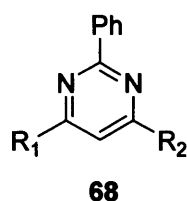
The photophysical properties of a selection of the functionalised pyrimidines were assessed. Majority of D-A type pyrimidines displayed solution-state (CHCl₃) fluorescence at room temperature (Table 17., with the exception of **68a**) and each possessed a single broad emission in the visible region following excitation at 360 nm.

Table 17. Photophysical properties of 2,4,6-triarylpyrimidine **68**.

68	R₁	R₂	UV/vis[a]		Fluorescence[a]		
			λ_{max} (nm)	logε	λ_{max} (nm)	τ (ns)	Φ_f[b]
a	C₆H₅	H	278	4.26	311[c]	0.55	0.51
h	4-CH₃OC₆H₅	4-(CH₃)₂NC₆H₅	365	4.54	453[d]	7.14	0.49
i	2-Thienyl	4-(CH₃)₂NC₆H₅	371	4.64	473[d]	6.96	0.46
l	4-NCC₆H₄	4-(CH₃)₂NC₆H₅	376	4.82	495[d]	3.46	0.44
o	4-NCC₆H₄	4-C₄H₈NC₆H₅	385	4.38	518[d]	3.33	0.23
j	2-Naphthyl	4-(CH₃)₂NC₆H₅	379	4.84	510[d]	2.43	0.40
n	2-Naphthyl	4-C₄H₈NC₆H₅	430	4.40	528[d]	2.37	0.19

[a] Measured in CHCl₃ and the average concentration is 2.0 × 10⁻⁶ M; [b] External standard: fluorescein (Φ_f = 0.79 in 0.1 M NaOH); estimated uncertainty: ±15%; [c] λ_{ex} = 280 nm; [d] λ_{ex} = 360 nm.

The short (<10 ns) emission lifetimes (mono-exponential, consistent with a single decaying excited state) were also characteristic of fluorescence in each case. With the exception of **68a**, notable Stokes shifts were attributed to the presence of the donor and acceptor groups, which are

74

likely to induce significant charge transfer character to the excited state. Consequently, the origin of the fluorescence in **68a** is more likely to be a locally excited singlet $\pi^* \rightarrow \pi$ transition.

3.4.1 The influence of the polarity on dye spectral properties of 68j

The most significant red shifts in both λ_{abs} and λ_{em} were achieved with a naphthyl unit as one component. Therefore the charge transfer character was confirmed by assessing the solvent dependence of the emission from **68j** in cyclohexane, chloroform and DMSO (Table 18).

Table 18. Solvatochromic data for **68j** in selected solvents

Solvent	UV/vis [a]		Fluorescence [a]				
	λ_{max} (nm)	$\log\varepsilon$	λ_{max} (nm)	τ (ns)	Φ_f [b]	k_{nr}/k_r [c]	$\Delta\nu$ (cm^{-1})
Cyclohexane	368	4.68	422	2.91	0.48	1.08	3490
Chloroform	379	4.84	510	2.43	0.40	1.50	6788
DMSO	382	4.92	599	1.63	0.22	3.55	9486

[a] The average concentration: 2.5×10^{-8} M; [b] External standard: fluorescein ($\Phi_f = 0.79$ in 0.1 M NaOH); estimated uncertainty: $\pm15\%$; [c] This value equals to $(1-\Phi_f) \times \Phi_f^{-1}$, assuming that phosphorescence is negligible.

The longer wavelength shift of the emission spectra can be interpreted in terms of the greatly changed molecular geometry of **68j** upon excitation with stabilization by the solvent cavity. Due to the transfer of electron density from the amino donor to the pyrimidyl acceptor, a dipole is clearly created in the excited state, much larger than that possessed by the ground state. DMSO is a polar solvent and therefore able to stabilize the polarized excited state by reorientation of the solvent molecules to accommodate the increased dipole, lowering the energy of the system. Such phenomena (*i.e.*, solvent relaxation and the subsequently varied Stokes shift with increased solvent polarity) are well known in the D-A type molecules.[97]

The radiative lifetime of the emitting excited state, τ, for **68j** in various solvent was calculated by measuring the decay of the emission maximum with time. In each case, the fluorescent decay can be fitted into a mono-exponential curve. The radiative lifetime of **68j** in cyclohexane is 2.91 ns, a value very close to the result of 4-*N,N*-dimethylanilinopyrimidine previously measured in similar solvent.[112] The radiative lifetimes of **68j** in polar solvents are clearly shorter than this and **68j** in DMSO has the shortest singlet lifetime of 1.63 ns.
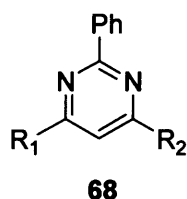
4-dimethylaminopyrimidine is known to undergo efficient intersystem crossing (ISC) below the 34 000 cm^{-1} region,[112-113] forming the high-lying triplet state with a short S_1 lifetime and fast non-radiative decay. This is due to its S_1 and T_1 states being almost isoenergetic and has been deemed as the reason for the astonishingly low quantum yield (*ca.* 0.009) observed in *n*-hexane.

For 4-N,N-dimethylanilinopyrimidine, the rate of ISC decreases because of an enhanced planarity of the fluorescent charge transfer state, which can lead to an increased energy difference between the S_1 and T_1 states,[112] and therefore the radiative lifetime increases. It is therefore reasonable to observe that the excited state of 2,4,6-trisubstituted pyrimidine **68j**, which has an equivalent conjugation length of five aromatic rings, has a longer lifetime than that for the monosubstituted pyrimidines because of a decrease in the rate of intersystem crossing and as such, an increase in the rate of the radiative fluorescence.

3.4.2 The influence of S_1/S_0 energy gap upon the radiative/non-radiative decaying characteristics

Processing both quantum yield and radiative lifetime data for these compounds allows the calculation of other photophysical parameters, namely the radiative rate constant k_r and the nonradiative rate constant k_{nr}.

Table 19. Radiative/non-radiative decaying rates of pyrimidines **68**.

68

68	R_1	R_2	$k_r (10^8 \text{ s}^{-1})^a$	$k_{nr} (10^8 \text{ s}^{-1})^b$	k_{nr}/k_r	Δv_{st} (cm^{-1})
a	C_6H_5	H	9.27	8.90	0.96	3816
h	4-$CH_3OC_6H_5$	4-$(CH_3)_2NC_6H_5$	0.69	0.71	1.04	5322
i	2-Thienyl	4-$(CH_3)_2NC_6H_5$	0.66	0.78	1.17	5813
l	4-NCC_6H_4	4-$(CH_3)_2NC_6H_5$	1.27	1.62	1.27	6394
o	4-NCC_6H_4	4-$C_4H_8NC_6H_5$	0.69	2.31	3.35	6670
j	2-Naphthyl	4-$(CH_3)_2NC_6H_5$	1.65	2.47	1.50	6788
n	2-Naphthyl	4-$C_4H_8NC_6H_5$	0.80	3.41	4.26	6833

[a] The value equals to $\Phi_f \times \tau^{-1}$, assuming that phosphoresence is negligible; [b] The value equals to $(1-\Phi_f) \times \tau^{-1}$.

As expected, **68a** has the highest k_r value but due to its combination of the lowest τ and highest Φ_f, it also has the highest k_{nr} value. It is therefore more useful to consider the ratio, k_{nr}/k_r.

It is apparent that the compounds with great charge transfer characters, **68j**, **68o** and **68n**, have the highest ratio ($k_{nr}/k_r = 1.50 - 4.26$) whereas **68a** has the lowest ($k_{nr}/k_r = 0.95$).

The higher proportion of k_{nr} observed for the CT compounds is consistent with their large Stokes shifts in chloroform and it seems likely these molecules have undergone a larger geometry change in the excited state, thereby displacing the S_1 potential energy surface, creating a greater S_0/S_1 wave function overlap and increasing the efficiency of the non-radiative deactivation. Indeed, **68n** has both the largest Stokes shift in chloroform and the highest k_{nr}/k_r ratio whereas **68a** has the lowest of both values.

The high k_r of **68a** can be linked to the very small Stokes shift observed for this molecule and hence this structure undergoes the smallest geometry change upon excitation. This point also supports the assumption that **68a** S_1 state is of $\pi \rightarrow \pi^*$ character rather than CT character, as observed for other compounds, which produce small k_r values and high k_{nr}/k_r ratios.

3.5 Conclusions

In conclusion, tandem oxidation/heterocyclocondensation of a propargylic alcohol and benzamidine using $BaMnO_4$ under microwave irradiation provides a rapid route to pyrimidines, which can be further derivatised by microwave-assisted copper-mediated N-arylation. The π-extended pyrimidines so-formed by this approach are highly fluorescent in the visible region, displaying solvent-dependent emission wavelengths suggestive of charge transfer-dominated excited states.

References

87. Erian, A. W. *Chem. Rev.*, **1993**, *93*, 1991.

88. Joffe, A. M.; Farley, J. D.; Linden, D.; Goldsand, G. *Am. J. Med.*, **1989**, *87*, 332.

89. Petersen, E.; Schmidt, D. R. *Expert Rev. Anti-Infect. Ther.*, **2003**, *1*, 175.

90. Nadal, E.; Olavarria, E. *Int. J. Clin. Pract.*, **2004**, *58*, 511.

91. Blum, J. L. *Oncologist*, **2001**, *6*, 56.

92. Brugnatelli, G. *Ann. Chim. Phys.*, **1818**, *8*, 201.

93. Frankland, E.; Kolbe, H. *Justus Liebigs Ann. Chem.*, **1848**, *65*, 269.

94. Gabriel, S.; Colman, J. *Ber. Dtsch. Chem. Ges.* **1899**, *32*, 1525.

95. Joule, J. A.; Mills, K. *Heterocyclic Chemistry, 4th ed.*, Blackwell, Cambridge, **2000**, 194.

96. Miller, A. *J. Org. Chem.*, **1984**, *49*, 4072.

97. Itami, K.; Yamazaki, D.; Yoshida, J. *J. Am. Chem. Soc.*, **2004**, *126*, 15396.

98. Wong, K.; Hung, T. S.; Lin, Y.; Wu, C.; Lee, G.; Peng, S.; Chou, C. H.; Su, Y. *Org. Lett.*, **2002**, *4*, 513.

99. Undheim, K.; Benneche, T. *Comprehensive Heterocyclic Chemistry II, Vol. 6*, Pergamon, Oxford, **1996**, 93.

100. Chinchilla, R.; Najera, C.; Yus, M. *Chem. Rev.*, **2004**, *104*, 2667.

101. Pinner, A.; *Ber. Dtsch. Chem. Ges.*, **1884**, *17*, 2519.

102. Ghosh, U.; Katzenellenbogen, J. A. *J. Heterocycl. Chem.*, **2002**, *39*, 1101.

103. Adamo, M. F. A.; Adlington, R. M.; Baldwin, J. E.; Pritchard, G. J.; Rathmell, R. E. *Tetrahedron*, **2003**, *59*, 2197.

104. Kanis, D. R.; Ratner, M. A.; Marks, T. J. *Chem. Rev.*, **1994**, *94*, 195.

105. Achelle, S.; Nouira, I.; Pfaffinger, B.; Ramondenc, Y. *J. Org. Chem.*, **2009**, *74*, 3711.

106. Bagley, M. C.; Hughes, D. D.; Taylor, P. H. *Synlett*, **2003**, 259.

107. Bagley, M. C.; Hughes, D. D.; Lubinu, M. C.; Merritt, E. A.; Taylor, P. H.; Tomkinson, N. C. O. *QSAR Comb. Sci.*, **2004**, *23*, 859.

108. Bagley, M. C.; Hughes, D. D.; Sabo, H. M.; Taylor, P. H.; Xiong, X. Synlett 2003, 1443.

109. Shuto, S.; Niizuma, S.; Matsuda, A. *J. Org. Chem.*, **1998**, *63*, 4489.

110. Bagley, M. C.; Lin, Z.; Phillips, D. J.; Graham, A. E. *Tetrahedron Lett.*, **2009**, *50*, 6823.

111. Bagley, M. C.; Dix, M. C.; Fusillo, V. *Tetrahedron Lett.*, **2009**, *50*, 3661 and references cited therein.

112. Herbich, J.; Waluk, J. *Chemical Physics.*, **1994**, *188*, 247.

[113.] a) Yamazaki, I.; Murao, T.; Yamanaka, T.; Yoshihara, K. *Faraday Discuss. Chem. Soc.*, **1983**, *75*, 395; b) Herbich, J.; Karpiuk, J.; Grabowski, Z. R.; Tamai, N.; Yoshihara, K. *J. Luminescence.*, **1992**, *54*, 165.

Chapter Four – Results and Discussion

4 New Strategy for the Preparation of 2,2':6',2''-Terpyridine Fluorescent Sensors for Zinc

4.1 Introduction

Quantitative analysis of trace metal ions using a selective analytical reagent has become extremely important for environmental and biological applications.[114] Remarkable improvements in fluorescent indicators have been made for biologically important divalent metal ions, in particular Ca^{2+} and Mg^{2+}, with several selective fluorophores such as Fura-2 **(69)**, Quin-2 **(70)** and Mag-Indol-1 **(71)**.[115,116]

69
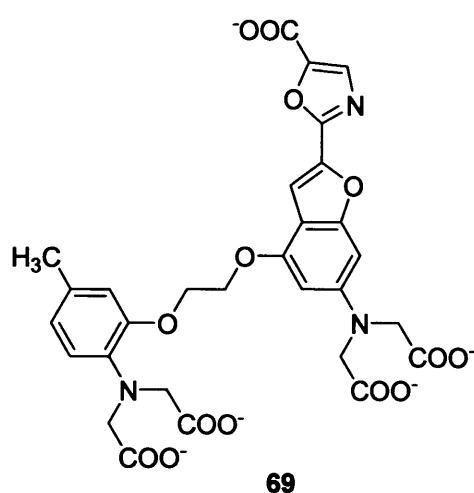
Fura-2
Emission: 505 nm
Excitation: 335 nm

70
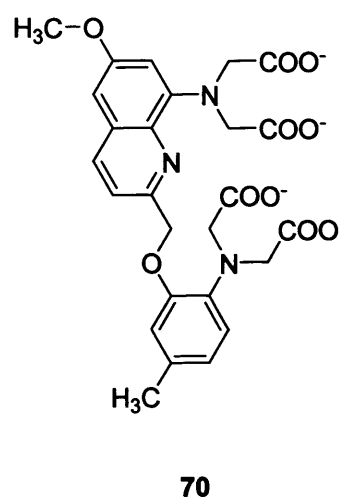
Quin-2
Emission: 495 nm
Excitation: 333 nm

71
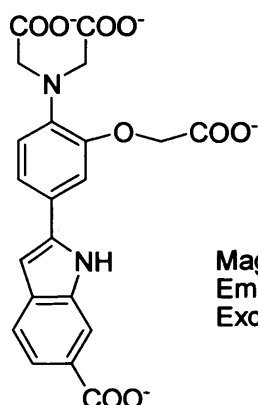
Mag-indol-1
Emission: 417 nm
Excitation: 330 nm

The criteria for these sensors are (1) stability, (2) metal selectivity, (3) metal affinity, (4) fluorescent signalling, (5) kinetically rapid sensitization and (6) synthetic applicability. For measurement of the dynamic mechanism of intracellular Ca^{2+}, the typical concentration in resting cells is 50–200 nm and the intracellular physiological range is 10 nm – 10 µm.[115] Therefore, as for

80

metal affinity, Ca^{2+}-selective biosensors should possess a K_d (dissociation constant) near the median concentration (*ca.* 10^{-6} M).[115] When a normal median concentration gives a 50% signal, one could most effectively detect both concentration increases and concentration decreases. Fura-2 and Quin-2, in this regard, are quite appropriate probes for the measurement of intracellular Ca^{2+} concentrations.[117]

As for the desired signalling properties of fluorescent probes, these are (1) intense fluorescence, (2) excitation wavelengths exceeding 340 nm (to pass through glass microscope objectives and minimize UV induced cell damage) with a wavelength corresponding to available laser sources,[117] and (3) emission wavelengths should shift by > 80 nm before and after complexation, so that ratiometric titration can be utilized (for quantification) rather than mere intensity changes. Fura-2, for example, fits these criteria.

The Zn(II) ion has been recognized as an important cation in biological systems (*e.g.* influencing DNA synthesis, apoptosis, gene expression, and protein structure and function).[118] The Zn(II) ion is also implicated in the formation of amyloid plaques during the onset of Alzheimer's disease.[118] The relative concentration of free Zn^{2+} within biological cells varies from about 1 nanomolar in the cytoplasm of many cells to about 1 millimolar in some vesicles.[118]

Clearly, a mechanism must be available for moving Zn^{2+} ions into complexation sites and for pumping it to elevated concentrations that allow triggering mechanisms to operate, as with Ca^{2+}.[118] Therefore the need for useful zinc-fluorophores to quantify trace Zn^{2+} ions is becoming increasingly important.

4.2 History of classical fluorescent zinc sensors

The first zinc-fluorophore TSQ (**72**)[119] was used as a histochemical stain for Zn^{2+} in various tissue sections of the brain, heart, and some other tissues. This stain was the only useful Zn(II)-specific fluorophore that worked in the presence of physiological concentrations of Ca^{2+} and Mg^{2+}.[119]
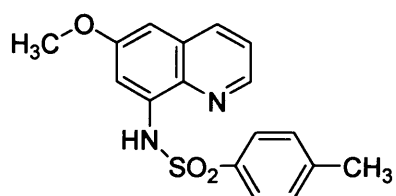

72

TSQ
Emission: 495 nm
Excitation: 334 nm

The complex of TSQ with free Zn^{2+} apparently has a stoichiometry of 2 : 1 TSQ/ Zn^{2+}, but a 1 : 1 complex may equilibrate with protein-bound Zn^{2+}.[119] These TSQ-Zn^{2+} complexes are not fully

identified nor fully characterized because of their complex structures and their stability constants have not been determined. The fluorescence intensity (*i.e.*, quantum yield) of the complexes varies with the media. Accordingly, TSQ was far from an ideal fluorophore for the quantitative analysis of Zn^{2+}.[119]

Whilst the TSQ-Zn^{2+} complexes were still chemically to be characterized, a modified TSQ, Zinquin **73** was developed and extensively used for cellular physiological studies by Zalewsky's group.[120,121] This was the first probe to visualize intracellular Zn^{2+} ions in living cells. An ester group is incorporated in **73**, so that after the neutral lipophilic probe permeates into the cell, the ester is hydrolyzed by intracellular esterases to become a carboxylate anionic form **74** and therefore can be retained for a long time within the cell (Scheme 39).[120] Thus, Zinquin became the first practical zinc-fluorophore to be used to determine the role of Zn^{2+} in the regulation of cell growth.
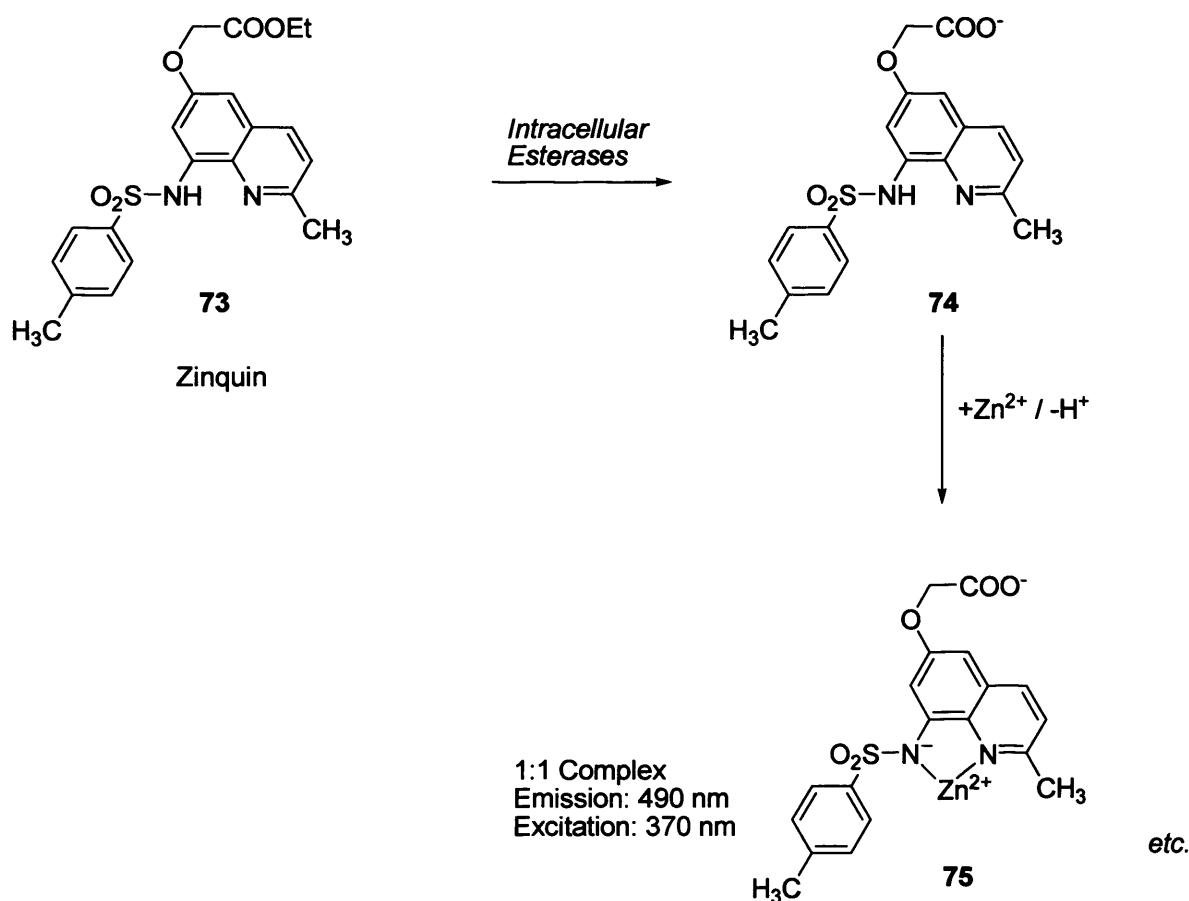
Scheme 39. Intracellular modification of Zinquin **73** to give the mental sensor **74**.

Zinquin **73** can monitor loosely bound, labile intracellular Zn^{2+} (not tightly bound Zn^{2+} in zinc enzymes or zinc-finger proteins) by fluorescence video image analysis or fluorometric

spectroscopy.[121] The importance of cellular Zn^{2+} distribution in the process of apoptosis was first revealed by Zinquin, for in zinc rich cells, such as hepatocytes and pancreatic islet b-cells,[121] the fluorescence is very intense.

By fluorometric titration, Zinquin was found to form both 1 : 1 and 2 : 1 complexes with Zn^{2+} with binding constants of $7.0 \times 10^6 \ M^{-1}$ and $11.7 \times 10^6 \ M^{-1}$ at pH 7.4.[120] However, the structure of these complexes was not determined, but on the basis of our following findings, **75** is a reasonable formula for the 1 : 1 complex, where the sulfonamide is deprotonated (Scheme 39).

It is certain, however, that the stability constants are not big enough to permit interaction of Zinquin with the tightly bound ($K_d \ll 1$ nanomolar) Zn^{2+} in metalloenzymes or zinc-finger proteins.[120] The intracellular Zn^{2+} chelator *N,N,N',N'*-tetrakis(2-pyridylmethyl) ethylendiamine (TPEN), which has a much higher affinity towards Zn^{2+}, can mask the Zn^{2+}-dependent Zinquin fluorescence.[120]

Very weak fluorescence (at 490 nm) of a 2 μM solution of Zinquin at pH 7.4 was increased at sub-nanomolar concentrations of free Zn^{2+} and was fully saturated at 1 μM Zn^{2+}.[119] Fluorescence was enhanced 20-fold by 1 μM Zn^{2+}. None of the other biologically relevant metal ions (Ca^{2+}, Mg^{2+}, Cu^{2+}, Fe^{2+}, Fe^{3+}, Mn^{2+}, Co^{2+}, *etc.*) affected the Zn^{2+}- dependent fluorescence of Zinquin.[120] However, when it comes to quantitative analysis of Zn^{2+} either in living cells or in other environments, Zinquin is still far from satisfactory, due to the mixed complexes it forms, with varying fluorescence intensity.

4.3 Development of new zinc sensors

Back in 1988, chelation-enhanced fluorescence (CHEF) was reported by Czarnik *et al.* with 9,10-bis(2,5-dimethyl-2,5-diazahexyl)anthracene **76** and Zn^{2+} in CH_3CN.[122] In 1990, **76** was extended to the macrocyclic system **77**.[123,124] A large CHEF effect by Zn^{2+} (14.4-fold) and Cd^{2+} (9-fold) was observed with **77** ($n = 2$) at pH 10 in aqueous solution, where the metal-free ligand is almost entirely a monoprotonated species.[123]
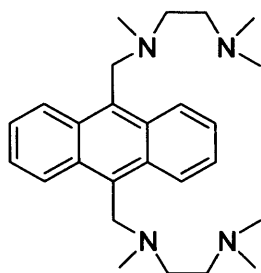
76
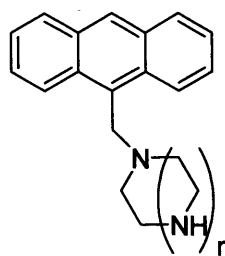
77   n = 1-5
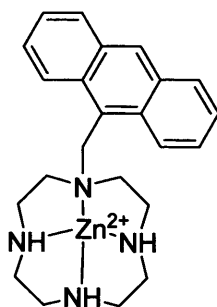
78

The fluorescence titration of **77** ($n = 3$) (10 μM) with Zn^{2+} (0–20 μM) in pH 12 buffer (highly alkaline), where **77** ($n = 3$) is unprotonated, showed the emission maximum at 416 nm (excited at λ_{ex} 335 nm) increases linearly until almost 1 : 1 complexation (to **78**). The reason why such a high pH was employed was to avoid the intrinsic competition between H^+ and Zn^{2+} for **77** at lower pH ranges.[123] The protonation(s) and metal complexation at the macrocyclic polyamine moiety commonly inhibit the quenching process by free nitrogen atoms: *e.g.*, the protonated ligand **77** ($n = 2$)·$2H^+$ at pH 7 showed an almost 120-fold larger fluorescence intensity than that of the free ligand **77** ($n = 2$) at pH 12.[123] Thus **77** ($n = 2$) cannot be a practical zinc-fluorophore under normal pH conditions.

4.4 Microwave assisted synthesis and photophysical studies: a highly selective, PCT based luminescent sensor for zinc

As mentioned above, a selective and sensitive sensor for selected transition metal ions has the potential to afford qualitative and quantitative information about the presence, distribution and concentration of these metal ions in a biological system.[114-116] For some years, we have been interested in the photophysical study of various ions, by using either steady state fluorescence or time-resolved lanthanide luminescence sensing.[124]

Our interest in the sensing of Zn(II) sprang from the fact that this ion plays a vital role in the neurological pathways in the brain. For instance, biologically relevant concentrations of labile

Zn(II) is thought to be several millimolar in the vesicles of presynaptic neutrons and as a consequence, the ion could be released easily by the synaptic activity of depolarization, modulating the functions of certain electronic channels within the brain cell.[125] It is well known that Zn(II) serves as a mediator for the cellular signalling in the central nervous system when the concentration of the ion in the tissue cell is high.[126] And also, Zn(II) is widely regarded as one of the most crucial co-factors in the regulation of apoptosis.[127]

For such an important ion, however, many existing sensors in the literature have inevitable drawbacks, such as being synthetically difficult to prepare, possessing a poor fluorescence response within detectable wavelengths, low quantum yield, small luminescent enhancement between the 'free' and the 'complexed' sensor, and poorly selective to group II ions, the later, as such, resulting in lowered Zn(II) selectivity. With this in mind, we set out to develop a new series of Zn(II) fluorescent sensors that would overcome all of these drawbacks.

Recent work by the Bagley group, and others, has showed that the microwave assisted Bohlmann-Rahtz type heteroannelation of functionally designed alkynones 11 is an efficient way of generating a variety of biologically important targets, which include pyridines (Scheme 40),[128] pyridazines,[129] pyrido[2,3-d]pyrimidines,[130] quinolines,[131] pyrazoles,[132] isoxazoles,[133] triazoles[134] and pyrimidines.[135]

**Scheme 40.** One-pot heteroannelation of alkynones 11 under the microwave assisted condition.
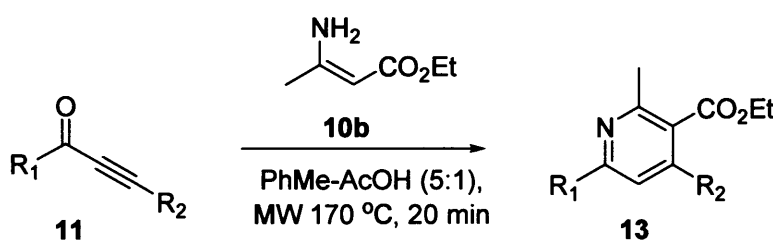
Entry	R_1	R_2	Yield (%)[a]
1	$4\text{-}ClC_6H_4$	H	75
2	Ph	H	87
3	Me	Et	94

[a] Isolated yield after the chromatographic purification.

4.4.1 Design & synthesis

Herein, we report on the use of the microwave assisted heterocyclization of 3-aminocrotonate **10c** and 3,3'-bis(4-bromophenyl)-1,1'-(pyridin-2-yl)-biprop-2-yn-1-one **79e**, to construct the novel 4,4''-(4-bromophenyl)-5,5''-nitrile-6,6''-methyl-2,2':6',2''-terpyridine **80e** in a highly facile manner (Scheme 41).
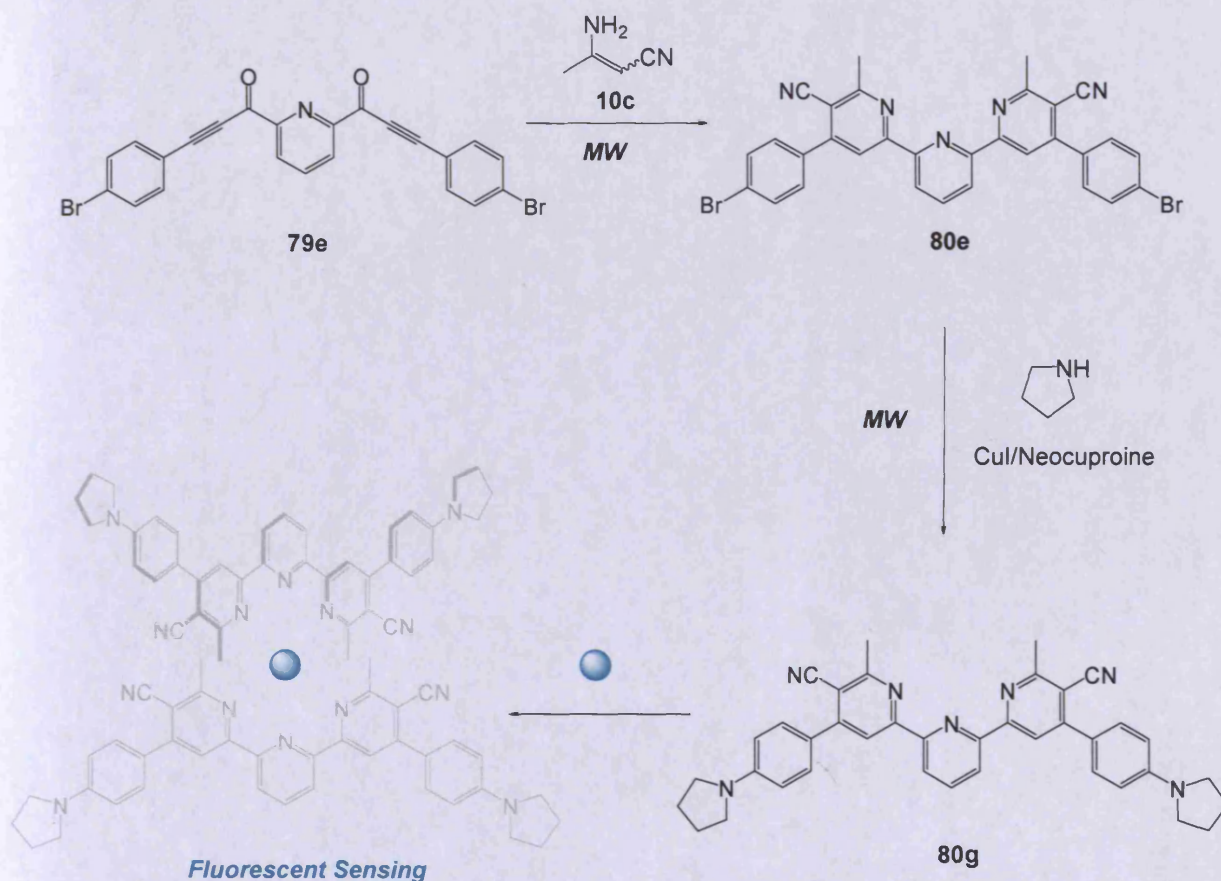
**Scheme 41.** Microwave assisted terpyridine synthesis and the subsequent complexation with Zn(II).

Generally these reactions are run under very mild conditions, are compatible with a range of different solvents and always provide the terpyridine products in good to excellent yields. The 4,4''-(4-bromophenyl) substituted terpyridine **80e** can also be further elaborated into a range of functionalized electro-luminescent materials by adopting the subsequent metal-catalysed C-N arylation reactions. In particular, such methodology has been used to prepare the compound 4,4''-(4-pyrrolidinophenyl)-5,5''-nitrile-6,6''-methyl-2,2':6',2''-terpyridine **80g**, a highly luminescent compound whose emissive character can be affected very distinctively upon the binding of zinc ions. This allows it to be further developed as a novel fluorescent sensor in the application of

detecting Zn(II) through the biologically competitive medium and as a result, facilitating a range of clinical or environmental investigations thereafter.

The bis-alkynone precursor 79e for this two-directional Bohnmann-Rahtz synthesis would be readily accessed by a double Sonogashira reaction, thus avoiding the need for a tandam oxidation approach.

Following the success of our modified Bohlmann-Rahtz conditions for the synthesis of 3-cyanopyridine 53 (Scheme 42), it was proposed that a similar microwave-assisted Michael addition-cyclodehydration strategy should be successful for the synthesis of novel 4,4''-aryl-substituted-2,2':6',2''-terpyridine compounds.

Scheme 42. Highly facile microwave assisted synthesis of 3-cyanopyridines.
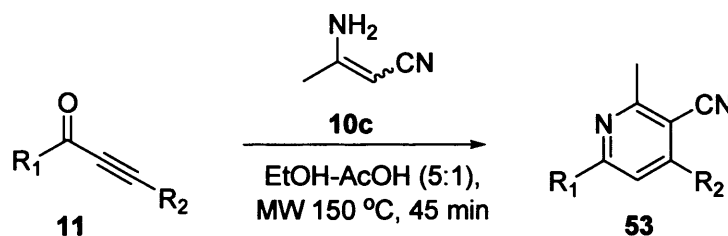
Entry	R_1	R_2	Yield (%)[a]
1	4-Piperidinophenyl	$4\text{-BrC}_6\text{H}_4$	76
2	4-Piperidinophenyl	$4\text{-MeOC}_6\text{H}_4$	78
3	4-Piperidinophenyl	$4\text{-Me}_2\text{NC}_6\text{H}_4$	84

[a] Isolated yield after the chromatographic purification.

Thus, in order to test the viability of the cyclocondensation reaction under the new/modified microwave-assisted conditions, a solution of 3-aminocrotononitrile 10c and 3,3'-(4-phenyl)-1,1'-(pyridin-2-yl)-biprop-2-yn-1-one 79a, which was easily prepared by the palladium/copper-catalysed Sonogashira coupling between pyridine-2,6-dicarboyl dichloride 82 and pheny-acetylene at microwave-assisted condition,[136] was irradiated in a solution of ethanol-acetic acid (5:1) at 150 °C. However, after 60 minutes, TLC and ^{1}H NMR spectroscopic analysis suggested that no reaction had occurred.
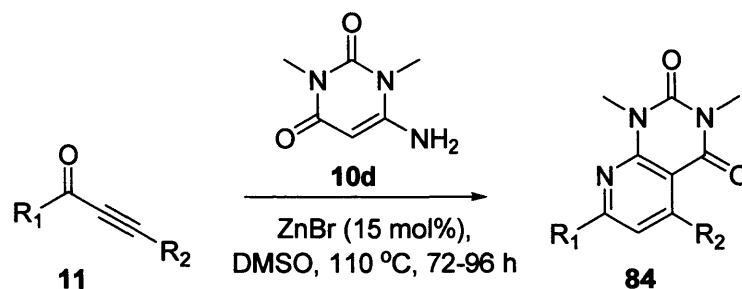
When the procedure was repeated at 170 °C using 1.5 equivalent of biprop-2-yn-1-one 79a, Micheal addition product 83a was generated in 86% isolated yield after chromatographic purification. When 83a was heated in the absence of solvent, according to the standard Bohlmann-Rahtz cyclodehydration procedure,[137] 4,4''-(4-phenyl)-5,5''-nitrile-6,6''-methyl-2,2':6',2''-terpyridine 80a was generated in 89% yield (Scheme 43).

This represents an overall yield for the transformation of 77% starting from 3-aminocrotononitrile **10c**, including two chromatographic purifications, and highlighted the great potential of the microwave assisted procedure for the formation of the synthetically viable intermediate, pyridine-dione **83a**.

**Scheme 43.** The Bohlmann-Rahtz type terpyridine synthesis catalysed by acetic acid.
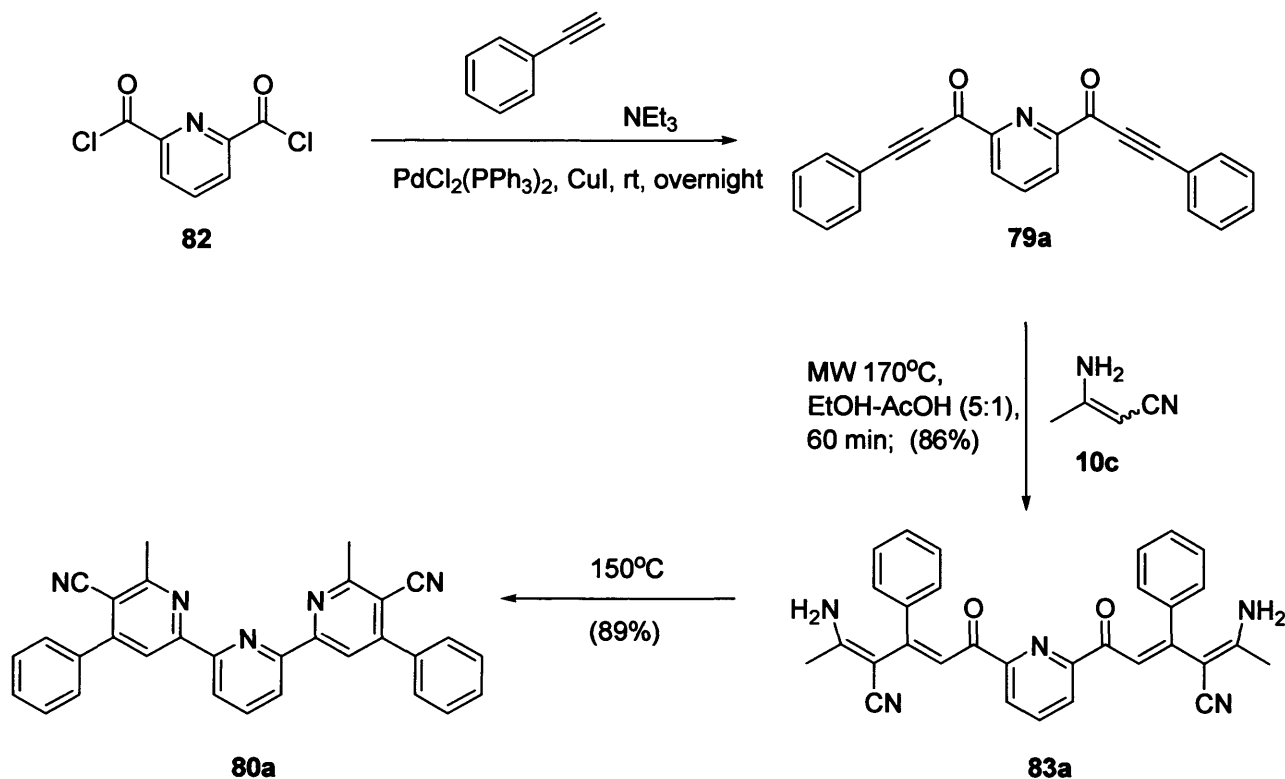
Following this success, it remained to be seen if a one-pot heteroannelation procedure could be facilitated in the presence of a Lewis acid catalyst. During a previous study within the group,[138] it was reported that zinc bromide catalysed heteroannelation, for the synthesis of pyrido[2,3-*d*]pyrimidine-2,4-diones **84** in very high yield, proceeding by cyclodcondensation of 6-amino-1,3-dimethyluracil **10d** and alkynone **11** in a single preparative step using a simple and facile experimental procedure (Scheme 44).

Scheme 44. One-pot synthesis of pyrido[2,3-*d*]pyrimidine-2,4-diones catalysed by $ZnBr_2$.

Entry	R_1	R_2	Yield (%)[a]	Time (h)
1[b]	Me	Et	75	72
2[b]	Me	Ph	72	72
3[c]	$CH_3OC_6H_4$	$(CH_3)_2NC_6H_4$	64	96

[a] Isolated yield after the chromatographic purification; [b] Reaction developed by former members in the Bagley group; [c] Reaction developed by the author of this thesis.

To this end, also in the search for alternative methods to affect the cyclodehydration that were compatible with other functionalities, bis-dienone intermediate **83a** was reacted with a number of Lewis acids under a variety of microwave assisted conditions (Scheme 45). In general the Lewis acid catalysed cyclodehydration appeared to be comparable or even less efficient than the corresponding non-catalytic process conducted under thermal conditions. However, using zinc bromide (15 mol%) in DMSO at 150 °C, terpyridine **80a** was prepared in 92% yield, showing that a Lewis acid catalysed one-step Bohlmann-Rahtz reaction was highly achievable and warranted further exploitation.

Scheme 45. The cyclodehydration of **83a** under different conditions.
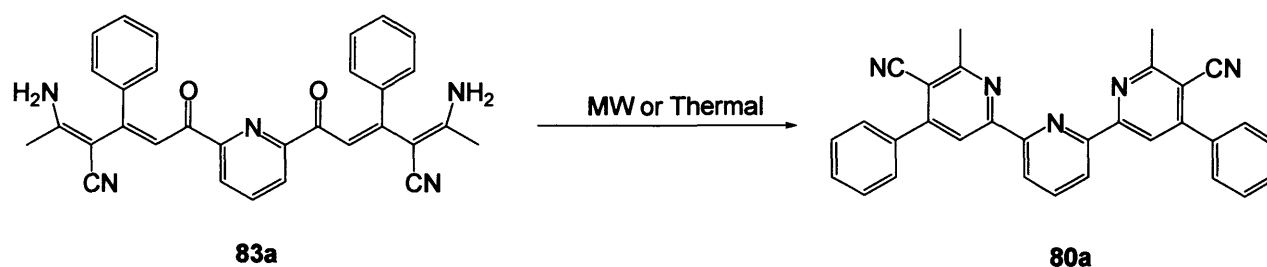
Entry	Lewis Acid	Condition	Yield (%)[a]
1	–	Oil bath 150 °C, overnight	89
2	–	MW 150 °C, DMSO-AcOH (5:1), 30 min	14
3	$FeCl_3$ (15 mol%)	MW 150 °C, DMSO, 30 min	23
4	$ZnCl_2$ (15 mol%)	MW 150 °C, DMSO, 30 min	44

| 5 | Yb(OTf)₃ (15 mol%) | MW 150 °C, DMSO, 30 min | 82 |
| 6 | ZnBr₂ (15 mol%) | MW 150 °C, DMSO, 30 min | 92 |

| 5 | $Yb(OTf)_3$ (15 mol%) | MW 150 °C, DMSO, 30 min | 82 |
| 6 | $ZnBr_2$ (15 mol%) | MW 150 °C, DMSO, 30 min | 92 |

[a] Isolated yield after the chromatographic purification

With a range of microwave-assisted conditions successfully established, it remained to examine whether such an approach was compatible with the initial Michael addition, so providing a new microwave-assisted Bohlmann-Rahtz type method to the facile synthesis of the 4,4''-aryl-substituted-2,2':6',2''-terpyridines in a single preparative step.

To this end, a solution of 3-aminocrotononitrile 10c and bis-alkynone 79a was irradiated under various conditions, which were all mediated by zinc bromide, a catalyst which should promote the cyclodehydration spontaneously in excellent yield (Scheme 46).

Scheme 46. The microwave assisted one-pot synthesis of terpyridine 80a catalysed by $ZnBr_2$.

79a   80a
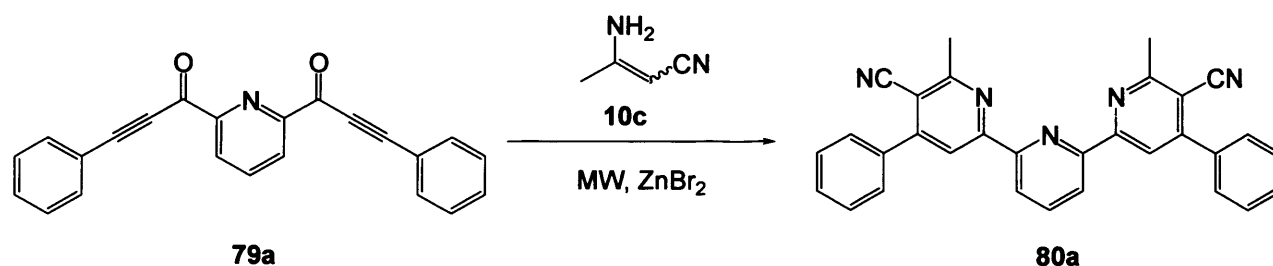
| Entry	Microwave assisted condition	Yield (%)[a]
1	$ZnBr_2$ (100 mol%), DMSO, 100 °C, 30 min	46
2	$ZnBr_2$ (20 mol%), DMSO, 100 °C, 30 min	40
3	$ZnBr_2$ (15 mol%), DMSO, 100 °C, 30 min	50
4	$ZnBr_2$ (15 mol%), Toluene, 100 °C, 30 min	54
5	$ZnBr_2$ (15 mol%), EtOH, 100 °C, 30 min	60
6	$ZnBr_2$ (15 mol%), EtOH, 120 °C, 30 min	63
7	$ZnBr_2$ (15 mol%), EtOH, 170 °C, 30 min	74
8	$ZnBr_2$ (15 mol%), EtOH, 150 °C, 30 min	77
9	$ZnBr_2$ (15 mol%), EtOH, 150 °C, 60 min	80
10	**$ZnBr_2$ (15 mol%), EtOH, 150 °C, 45 min**	**88**

[a] Isolated yield after the chromatographic purification.

Under all of the conditions explored, terpyridine 80a was formed in a single preparative step; the reaction catalysed by zinc bromide generating the product in good yield. The best conversion was achieved when a solution of enamine, bis-prop-2-yn-1-one and zinc bromide (15 mol%) in

ethanol was irradiated at 150 °C for 45 minutes to give the 4,4''-(4-phenyl)-5,5''-carbonitrile-6,6''-methyl-2,2':6',2''-terpyridine **80a** as the only product in 88% yield (Scheme 46, entry 10).

An excess of the bis-prop-2-yn-1-one **79a** (1.5 equivalent) was essential for optimising the yield of the one-pot transformation. Since no aminodienone intermediate **83a** had been isolated from any of these reactions, we concluded that, in the presence of zinc bromide, cyclodehydration was occurring spontaneously under the microwave-assisted conditions. The success of this transformation verified that Bohlmann-Rahtz terpyridine synthesis could be catalysed by zinc bromide under microwave irradiation in a single preparative step with excellent yield.

With this one-step heteroannelation methodology successfully established, it remained to compare the thermal non-catalytic and microwave-assisted catalytic processes (Scheme 47).

Scheme 47. The heteroannelation of pyridine-2,6-dialkynone **79** & enamine **10c** under various conditions.
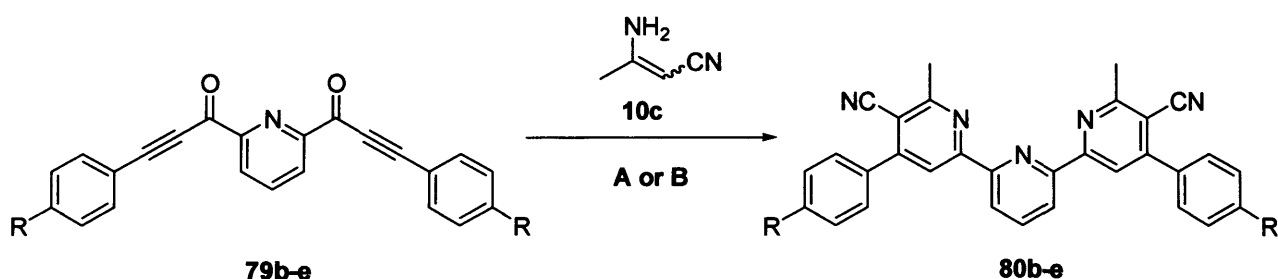
Conditions:

A: i. EtOH, 55 °C, overnight; ii. 150 °C, overnight;

B: MW 150 °C, ZnBr₂ (15 mol%), EtOH, 45 min.

Entry	80	R	Condition A		Condition B	
			Yield (%)[a]	Time (h)[b]	Yield (%)[a]	Time (h)
1	b	4-methoxy	50	48	82	0.75
2	c	4-dimethylamino	22	60[c]	64	0.75
3	d	4-chloro	62	48	86	0.75
4	e	4-bromo	66	48	84	0.75

[a] Isolated yield after the chromatographic purification; [b] Total reaction time between step i & ii; [c] On average, 24 h for step i and 36 h for step ii.

3-Aminocrotononitrile **10c** was reacted with a range of pyridine-2,6-dialkynones **79b-e**, which were prepared by a Sonogashira reaction,[136] using either the conventional thermal two-steps (Conditions A) or the novel microwave assisted one-step procedure (Conditions B). A representative number of reactions was carried out and the efficiency of the two different routes was investigated.

In almost all of the cases studied, the desired terpyridines was produced in acceptable yields. However, it was evident that the traditional two-step procedure was less efficient for the formation of terpyridine products; in particular, the introduction of a range of different aryl-substituents at the terminal positions of the dialkynone seemed as though it was affecting the synthetic outcome. When strongly electron-donating groups, dialkylamino for example, were attached onto the terminal positions of the dialkynone (Scheme 47, entry 2), the cyclodehydration was extended to 36 hours and the overall yield was sharply reduced.

On the other hand, considering the microwave-assisted reactions, it was apparent that the $ZnBr_2$-catalysed procedure was superior, increasing the efficiency of reaction dramatically in a much reduced time.

This comparison strongly supported the synthetic versatility of the newly developed conditions, and consolidated our modified Bohlmann-Rahtz methodology, which provides improved yields over the original method and avoids the harsh conditions of a prolonged heating period. The mild catalytic procedure can be applied directly to the synthesis of bi- or terpyridine luminescent targets in excellent yield, and, crucially, always affords the desired products in a single preparative step.

With successful experimental procedures established for this facile one-pot synthesis, it remained to investigate the scope of the microwave assisted methodology for the d-block metal mediated crossing-coupling reaction, which could bring a wide range of electron-transporting functionalities into the existing terpyridine architecture.

In the past few years, there has been a resurgence in interest in developing mild synthetic methods related with copper-based catalysts as an alternative to palladium(0) catalysts for the formation of aryl-heteroatom bonds.[139] Traditional palladium-mediated reactions can suffer from certain draw-backs such as high reaction temperatures, the use of palladium salts in greater than stoichiometric amounts, sensitivity to functional groups on the aryl-halide site, and irreproducibility.[140]

However, in comparison to palladium, a copper-based catalyst can be simple, mild, effective in the terms of accelerating the reaction and, also, an attractive contingency from an economic point of view. The applicability of such copper-based catalysts to the formation of aryl-heteroatom bonds, processed by microwave assisted cross coupling reactions, with terpyridine halides, was thus investigated.

We first chose to study the efficacy of the copper-based catalyst in the microwave assisted coupling reaction between 4,4''-(4-bromophenyl) substituted terpyridine **80e** and diethylamine in

DMSO. During one of our previous studies, we demonstrated the utility of some copper(I) complexes, *e.g.*, Cu(neocup)(PPh₃)Br, in synthesis of 2,4,6-triarylpyrimidine fluorescent chromophores which have strong amino electron-donating groups attached (Scheme 48).

**Scheme 48.** The microwave assisted C-N bond coupling catalyzed by Cu(neocup)(PPh₃)Br.
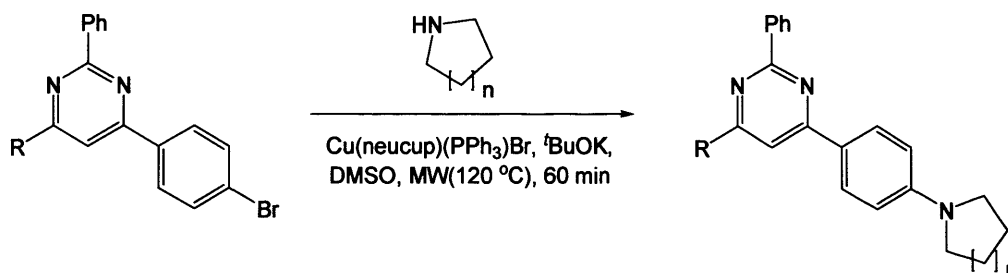
Entry	R	n	Yield (%)[a]
1	2-Naphthyl	1	56
2	2-Naphthyl	2	64
3	4-CNC₆H₄	1	62
4	4-CNC₆H₄	2	76

[a] Isolated yield after the chromatographic purification

This time, as part of our preliminary experiments, we replaced the Cu(neocup)(PPh₃)Br with 10 mol% CuI or CuI/neocuproine as catalyst and investigated its reactivity in the microwave-assisted C-N arylation to form a novel terpyridine luminescent product, 4,4''-(4-diethylaminophenyl)-5,5''-nitrile-6,6''-methyl-2,2':6',2''-terpyridine (**80f**) (Scheme 49).

Scheme 49. The microwave assisted synthesis of **80f** under various conditions.
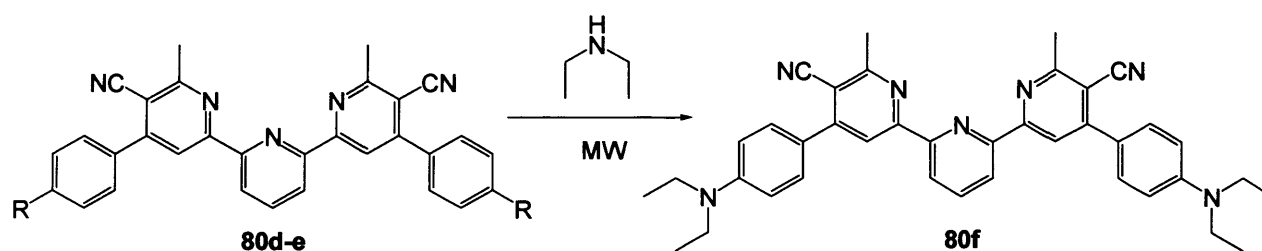
Entry	R	The Microwave Assisted Condition	Yield (%)[a]
1	Br	No catalyst, DMSO, 100 °C, 40 min	22[b]
2	Br	No catalyst, ᵗBuOK, DMSO, 100 °C, 40 min	23[b]
3	Br	Pd₂(dba)₃, racemic-BINAP, Cs₂CO₃, DMSO, 100 °C, 40 min	25[b]
4	Br	Cu(neocup)(PPh₃)Br, ᵗBuOK, DMSO, 100 °C, 40 min	36[b]
5	Br	Cu(PPh₃)₃Br, Neocuproine, ᵗBuOK, DMSO, 100 °C, 40 min	44[b]

6	Br	CuI, 'BuOK, DMSO, 100 °C, 40 min	31[b]
7	Br	CuI, Neocuproine, 'BuOK, DMSO, 100 °C, 40 min	46[b]
8	Br	CuI, Neocuproine, 'BuONa, DMSO, 100 °C, 40 min	51[b]
9	Br	CuI, Neocuproine, NaOEt, DMSO, 100 °C, 40 min	58[c]
10	Br	CuI, Neocuproine, NaOEt, IPA, 100 °C, 40 min	52[c]
11	Br	CuI, Neocuproine, NaOEt, Toluene, 100 °C, 40 min	64[c]
12	Br	CuI, Neocuproine, NaOEt, Toluene, 120 °C, 40 min	68[c]
13	Br	CuI, Neocuproine, NaOEt, Toluene, 150 °C, 40 min	80[c]
14	Br	CuI, Neocuproine, NaOEt, Toluene, 150 °C, 20 min	72[c]
15	**Br**	**CuI, Neocuproine, NaOEt, Toluene, 150 °C, 60 min**	**86[c]**
16	Cl	CuI, Neocuproine, NaOEt, Toluene, 150 °C, 60 min	64[c]

[a] Isolated yield of terpyridine **80f** after the chromatographic purification; [b] Both terpyridine halide and diethylamine were present in the crude product; [c] Excess diethylamine was present in the crude product.

We found that CuI/neocuproine (Scheme 49, entry 7) was more effective than Cu(neocoproine)(PPh₃)Br (entry 4). However, only a trace amount of the 4,4''-(4-diethylaminophenyl)-substituted product was isolated if CuI alone was used as the catalyst (entry 6). This observation indicated that the free neocuproine ligand was important in the terms of mediating the C-N bond forming reaction.

The initial choice of base was 'BuOK. We chose this system based on the study in our group that 'BuOK was essential in copper-based protocols for the formation of C-N bonds. In 40 minutes, although we observed the formation of terpyridine **80f** by TLC/^{1}H NMR spectroscopic analyses, the overall conversion was less than 50% (entry 4-7). When the 'BuOK was replaced with NaOEt, surprisingly we found complete consumption of the terpyridine starting material; when 10 mol% CuI/neocuproine was used as the catalyst, this led to a dramatically improved yield, 58%, after purification (entry 9).

It was also found that the use of a less polar solvent, toluene that would couple less efficiency with the microwave irradiation, resulted in a conversion with higher yield; C-N bond formation was complete after 40 minutes to give the terpyridine **80f** in 64% yield (entry 11). Reactions conducted in toluene were accelerated dramatically by increasing the temperature from 100 °C to 150 °C, providing the product in 80% yield (entry 13). However, the optimum condition for this transformation employed 60 minutes as the irradiation time, after stirring in a solution of toluene at 150 °C, 4,4''-(4-diethylaminophenyl)-substituted terpyridine **80f** was isolated in 86% yield following purification on silica; our most efficient result reported for the copper (I) mediated C-N coupling reaction to date (entry 15).

Finally, in a bid to explore the substrate selectivity, a mixture of 4,4''-(4-chlorophenyl)-substituted terpyridine **80d** and diethylamine was irradiated under the CuI/neocuproine catalysed conditions for 60 minutes to give the product in 64% yield (entry 16).

Although this experiment was not as efficient, we obtained a valuable insight that the copper (I) based C-N bond coupling reaction was more efficient with aryl bromides, rather than other halides, but was successful with chloride precursors.

On the basis of these observations, it was decided to use 10 mol% CuI /neocuproine as catalyst, NaOEt as the base and toluene as the solvent as a standard procedure in facilitating the microwave assisted coupling reaction between 4,4''-(4-bromophenyl)-substituted terpyridine **80e** and a range of different amines (Scheme 50).

Scheme 50. The microwave-assisted C-N bond forming reaction between **80e** and different amines.
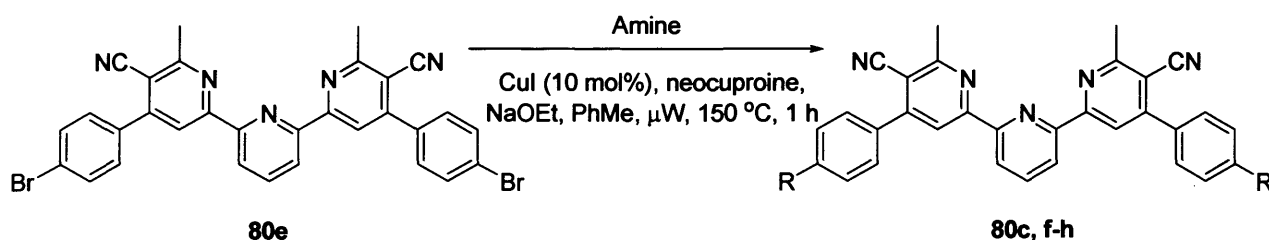
Entry	R	Product 80	Yield (%)[a]
1	$N(CH_3)_2$	c	71
2	$N(CH_2CH_3)_2$	f	86
3	NC_4H_8	g	84
4	NC_5H_{10}	h	89

[a] Isolated yield after the chromatographic purification.

It was pleasing to find that this method could be used successfully to couple amines that have strong electron-donating character, such as pyrrolidine, with **80e** in 84% yield (entry 3).

So far, we have shown a highly reliable and expedient protocol for the microwave-assisted formation of terpyridine aryl-nitrogen and aryl-oxygen bonds using a copper (I) catalyst. Such a protocol is most effective for terpyridine bromides and tolerates a wide range of functionalities. Additionally, in comparison to the thermal palladium catalysed procedure, our microwave assisted method is faster, milder and indeed avoids the use of air-sensitive conditions and the expensive BINAP ligand or other additives.

4.4.2 Photophysical study

Novel Fluorescent PCT (Photon-induced Charge Transfer) Sensor to Zn(II)

When a fluorophore contains an electron-donating group conjugated to an electron-withdrawing group, it undergoes intramolecular charge transfer from the donor to the acceptor upon photon excitation. The subsequent change upon the dipole moment results in a Stokes shift that largely depends on the microenvironment of the fluorophore; polarity probes have always been designed on this principle.[141] It can also be anticipated that cations in close interaction with the donor or acceptor will change the photophysical properties of the fluorophore because the complexed cation indeed affects the overall efficiency of the intramolecular charge transfer process.[142]

Figure 19. The principle of cation recognition by fluorescent PCT sensor.
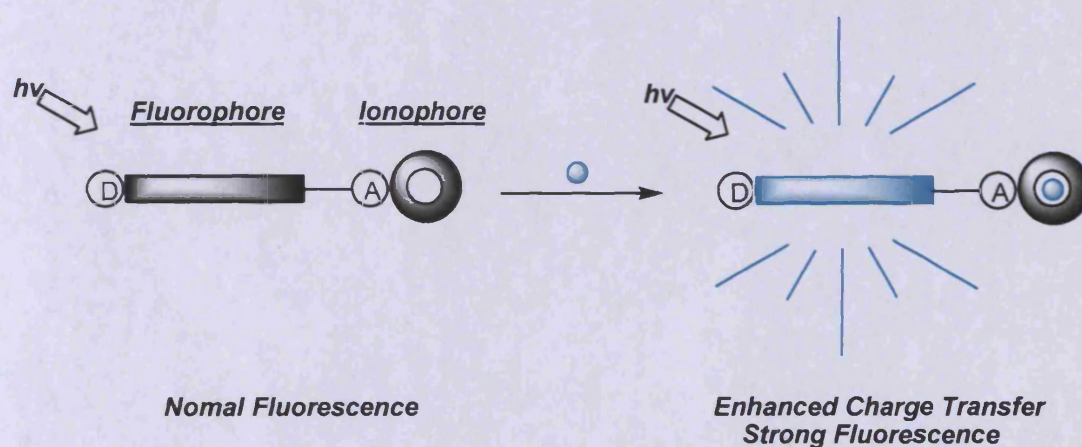
When a group playing the role of an electron donor within the fluorophore (*e.g.*, an amino group) interacts with the cation, the latter reduces the electron-donating character of this group; owing to the resulting reduction of conjugation, a blue shift of the absorption spectrum is expected together with a decrease of the extinction coefficient. Conversely, a cation interacting with the acceptor group enhances the electron-withdrawing character of this group; the absorption spectrum is thus red-shifted and the molar absorption coefficient is increased. The fluorescence spectra are in principle shifted in the same direction as those of the absorption spectra. In addition, changes in quantum yields and lifetimes can also be observed. All of these photophysical effects are strongly dependent on the nature of the cation and the selectivity between the cation and the receptor is somehow crucial (Figure 19).

The sensor **80g**, discussed herein, is functionally designed and based on the photon-induced charge transfer (PCT) principle where a fluorophore is connected to an ionophore by a δ bond. Here, 4-pyrrolidinophenyl group was adopted as the fluorophore, which has a strong absorption

band in the 400 nm region, emits at long wavelengths with large Stokes shifts and possesses high quantum yield with detectable fluorescence intensity.

Unlike the Zn(II) sensors developed to date, many of which consist of two bis(2-pyridylmethyl)amine units as the Zn(II) receptor,[143] our sensor employs a novel 5,5''-nitrile-2,2':6',2''-terpyridine receptor. This ensures a great polarity sensitivity in the relevant sensing environment at the same time as providing the high selectivity and excellent affinity for Zn(II) over other biologically competitive ions. Employing the PCT principle is advantageous as, if correctly designed, the sensor does not release too much fluorescence except upon coordinating to the target cation, which can actually 'turn up the emission'.

The PCT Zn(II) sensor **80g** and its non-amino substituted analogue **80a**, are the subjects of our investigation.

80a R = H

80g R = —N⟨ ⟩ (pyrrolidinyl)
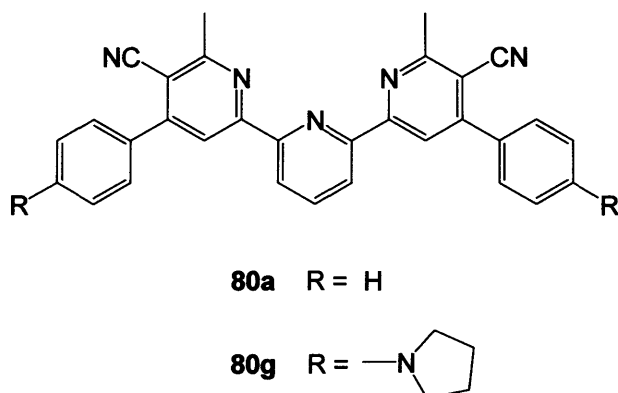
4.4.2.1 Spectroscopic polarity evaluation of 80a and 80g

The lowest absorption maxima of the two compounds in solution displayed a very small red-shift with increasing solvent polarity (Table 20). In contrast, the fluorescence maximum of **80g** underwent very large shifts to longer wavelengths. Such behaviour is strongly indicative of the ICT character of this compound in its S^1 excited state.

Table 20. Photophysical properties of **80a** and **80g** in solvents of varying polarity.

Compound	Solvent	UV/vis[a]		Fluorescence[a]		
		λ_{max} (nm)	$\log\varepsilon$	λ_{max} (nm)	Φ_f^{b}	$\Delta\nu$ (cm^{-1})
80a	Cyclohexane	312	4.66	345	0.24	3060
	Chloroform	316	4.70	350	0.22	3081
	Acetonitrile	320	4.64	355	0.23	3102
	DMSO	324	4.60	360	0.21	3097
80g	Cyclohexane	372	4.16	424	0.48	3271
	Chloroform	388	4.65	468	0.33	4383
	Acetonitrile	398	4.83	512	0.26	5600
	DMSO	440	4.90	574	0.09	5266

[a.] The average concentration: 1.0×10^{-6} M; [b.] External standard: fluorescein ($\Phi_f = 0.79$ in 0.1 M NaOH); estimated uncertainty: ±15%.

The fluorescence of the 4'-aryl substituted-2,2':6',2''-terpyridine analogues has been interpreted in this way in a recent report (Figure 20),[144] where a theoretical calculation revealed that the amino substituent can actually raise the energy level of the pendent phenyl to such an extent that the lowest energy excited state corresponding to an ICT transition ($\pi_{ph} \rightarrow \pi^*_{tpy}$), as opposed to the locally excited states of other 4'-aryl-substituted terpyridines ($\pi_{tpy} \rightarrow \pi^*_{tpy}$).

Figure 20. The electronic transition states of 4'-aryl-substituted terpyridines.
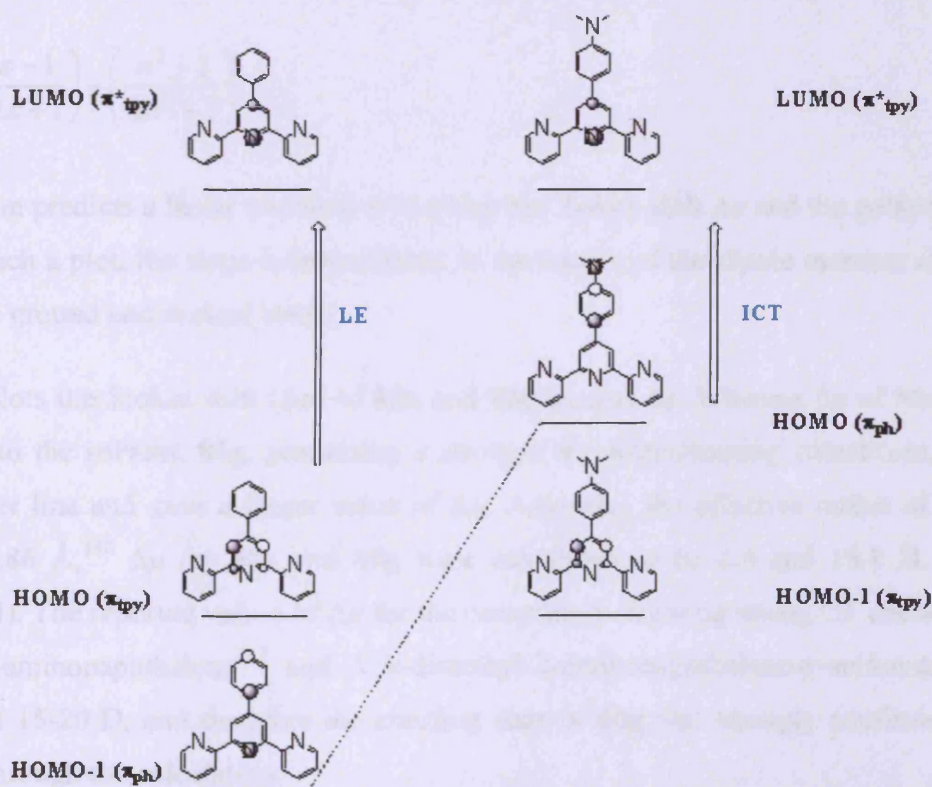
The present results indicate that the pyrrolidino substituent has a similar effect, with comparable emission maxima in each solvent examined. However, whereas the emission intensity of **80g** was greatly influenced by polar solvents such as DMSO, **80a** was weakly fluorescent in all solvents investigated. As mentioned above, according to the 4'-aryl-substituted analogue, the lowest emission maximum of **80a** was corresponding to a locally excited $\pi \rightarrow \pi^*$ transition in which there had not been any charge transfer characters involved in its S^1 emitting excited state, and therefore, no significant solvent-dependence should be observed from its emission spectrum.

To examine the photon-excitation and relaxation processes of **80a** & **80g**, the difference of the dipole moments between the ground and excited states, $\Delta\mu$, was calculated by using the Lippert-Mataga equation **(3)**.

$$\Delta\upsilon = \frac{2(\Delta\mu)^2}{hca^3}\Delta f \tag{3}$$

In such an equation, h is Plank's constant, c is the speed of light, a, the Onsager radius, is the radius of the cavity in which the solute resides and Δf is the polarity parameter which can be calculated from the dielectric constant (ε) and the refractive index (n) of the solvent of interest,[145] as shown in equation **(4)**.

$$\Delta f = \left(\frac{\varepsilon - 1}{2\varepsilon + 1}\right) - \left(\frac{n^2 - 1}{2n^2 + 1}\right) \tag{4}$$

This equation predicts a linear correlation between the Stokes shift $\Delta\upsilon$ and the polarity pararmeter Δf and in such a plot, the slope is proportional to the square of the dipole moment change, $(\Delta\mu)^2$, between the ground and excited states.

Figure 21 plots the Stokes shift ($\Delta\upsilon$) of **80a** and **80g** against Δf. Whereas $\Delta\upsilon$ of **80a** was almost insensitive to the solvent, **80g**, possessing a stronger electron-donating substituent, presented a much steeper line and gave a larger value of $\Delta\mu$. Assuming the effective radius of the Onsager cavity as 7.86 Å,[146] $\Delta\mu$ for **80a** and **80g** were calculated to be 2.6 and 18.8 D, respectively (Appendix-I). The reported values of $\Delta\mu$ for the compounds showing strong CT characters such as N-phenyl-2-aminonaphthalene[147] and N,N-dimethyl-2-aminonaphthalene-6-sulfonate[148] were in the range of 15-20 D, and therefore the emitting state of **80g** was strongly confirmed to be ICT orientated through the calculation.
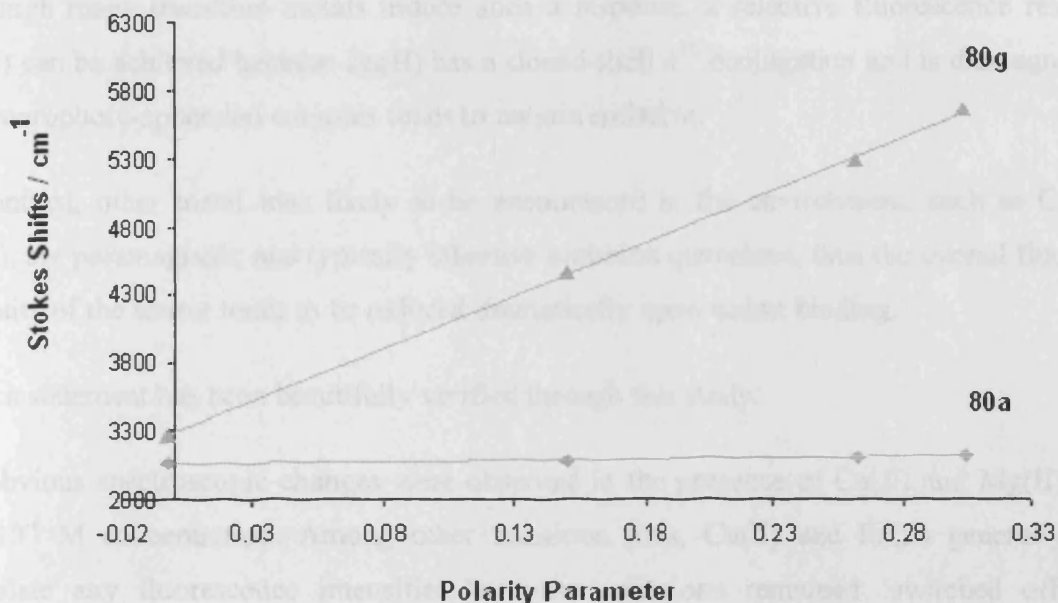
Figure 21. Lippert-Mataga plot for terpyridine **80a** and **80g**. Solvent properties [the value of dielectric constant (ε) and refractive index (n)] used to calculate Δf are available from the reference 145.

Thus, benefiting from the high efficiency offered by the microwave assisted C-N bond formation, the introduction of a strong electron donating group at the *p*-position of the phenyl unit altered the emitting character from the LE to the ICT state by increasing the π_{ph} energy level, which at the same time caused a significant red shift of the fluorescence to the entire terpyridine architecture.

4.4.2.2 Selectivity of 80g to Zn(II) over other competition ions

Having established the polarity dependence of fluorescent sensor **80g**, we evaluated its emission and absorption response towards group II & transition metal ions such as Zn(II), Cu(II), Fe(II) and Cd(II) in aerated acetonitrile.

As discussed previously, regarding PCT-based chemosensors, the ion binding generally leads to a red-shift in absorption and emission maxima in response to the planarization of the ionophore moiety (*i.e.*, the terpyridine unit, in this study), extending the effective conjugation length, in conjunction with perturbation of the electronic system.[149]

100

Although many transition metals induce such a response, a selective fluorescence response to Zn(II) can be achieved because Zn(II) has a closed-shell d^{10} conjugation and is diamagnetic; thus the fluorophore-appended complex tends to remain emissive.

In contrast, other metal ions likely to be encountered in the environment, such as Cu(II) and Fe(II), are paramagnetic and typically effective emission quenchers, thus the overall fluorescence intensity of the sensor tends to be reduced dramatically upon cation binding.

Such a statement has been beautifully verified through this study.

No obvious spectroscopic changes were observed in the presence of Ca(II) and Mg(II), even at 0.5×10^{-6} M concentration. Among other transition ions, Cu(II) and Fe(II) generally did not modulate any fluorescence intensities, and the emissions remained 'switched off'. Minor fluorescence enhancements, however, were observed at the higher concentration of Cd(II).

Table 21. The fluorescence response of **80g** to various metal ions (aerated acetonitrile).

Ion	I/I_0 ($\lambda_{ex} = 410$ nm)[a]	Φ/Φ_0 ($\lambda_{ex} = 410$ nm)[b]	Brightness (10^3 Int $M^{-1}cm^{-1}$)[c]
Ca^{2+}	0.6	0.5	8.8
Mg^{2+}	0.7	0.4	7.1
Cu^{2+}	1.4	1.1	19.5
Fe^{2+}	1.1	0.9	16.0
Cd^{2+}	3.6	1.2	21.2
Zn^{2+}	41.4	2.6	46.0

[a.] The average range of the concentration: 0.5×10^{-6} - 1×10^{-6} M. I and I_0 are the fluorescence intensities with and without added metal ions, respectively; [b.] External standard: fluorescein ($\Phi_f = 0.79$ in 0.1 M NaOH) and the initial quantum yield of the sensor: $\Phi_0 = 0.26$; [c.] This value is equal to $\varepsilon_0 \times \Phi$, where ε_0 is the extinction coefficient of the free sensor and Φ is the quantum yield of the bound complex.

Nevertheless, in the presence of Zn(II), dramatic changes were observed from the emission spectra and the fluorescence was 'switched on' as the results shown in Figure 22.
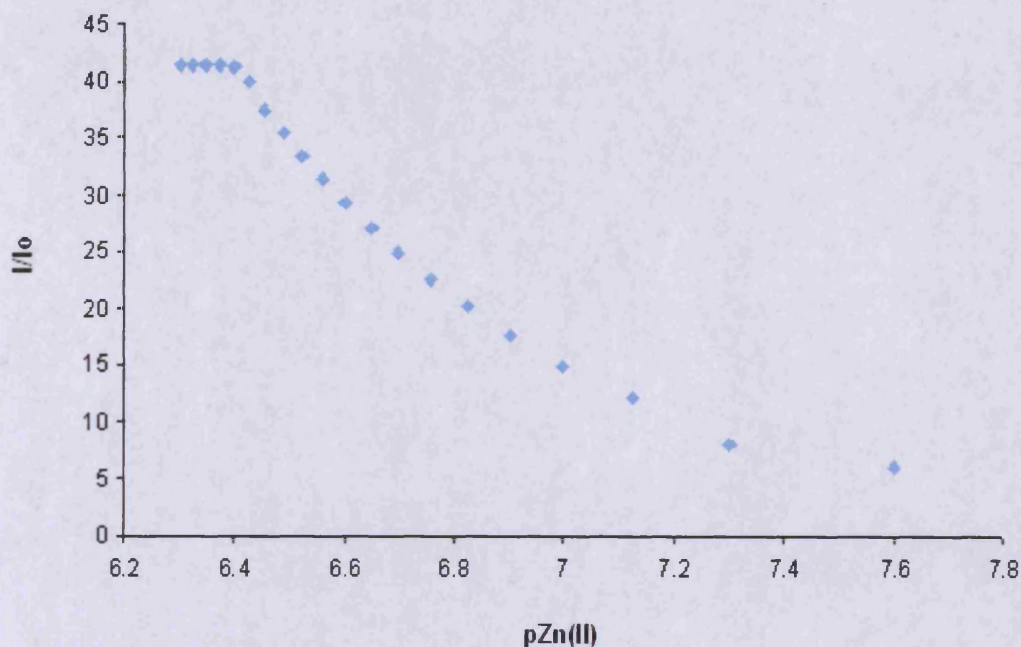
Figure 22. The changes in the fluorescence spectra of **80g** as a function of –log[Zn(II)], the pZn. (λ_{ex}: 410 nm; [Zn(II)]: 0.025 µM – 0.5 µM).

For the un-bound sensor **80g**, the fluorescence quantum yield at 512 nm (Φ_{512}) was measured to be 0.26, which increased to 0.68 at 544 nm (Φ_{544}) in the presence of 0.5 equivalents of Zn(II). This was a fluorescence enhancement of 2.6 fold upon Zn(II) binding, which demonstrated that sensor **80g** can be generally considered as a luminescence-switcher for Zn(II).

Using the value of extinction coefficient (ε_o), which was calculated from the absorption spectra of the free sensor, the brightness of the Zn(II) bound complex was determined as 4.6×10^4 Int M⁻¹cm⁻¹. Such results clearly indicated that **80g** fulfils all of the criteria set out above for an up-to-date development of highly selective Zn(II) sensing under biologically-relevant conditions, with a detectable fluorescent response.

To evaluate the selectivity of **80g** towards Zn(II), we further carried out competitive measurements. The results of these titrations are shown in Fig. 23, where the emission response of a 1×10^{-6} M solution of **80g** containing an excess amount of each competing metal ion was measured after the addition of 0.5×10^{-6} M Zn(II).
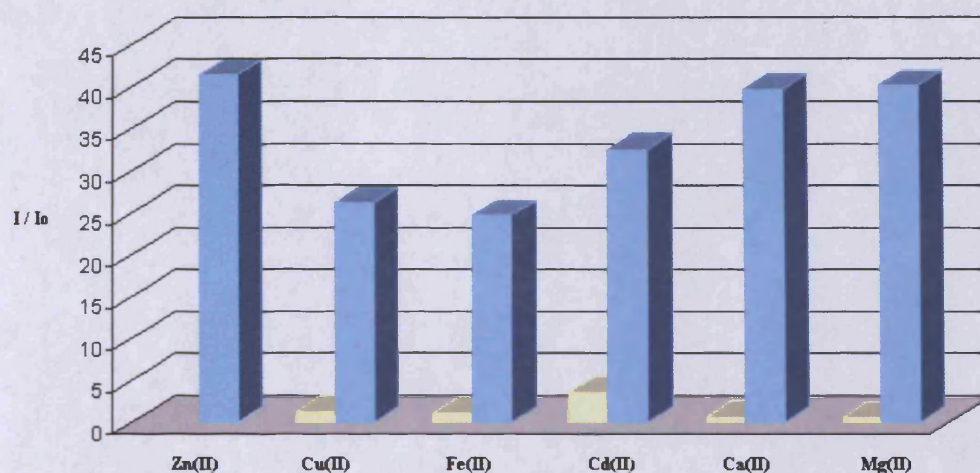
Figure 23. Relative fluorescence intensity responses of **80g** to various metal ions. Grey bars represent the emission without Zn(II) for a particular metal ion. Blue bars (starting from the second left) represent the emission induced by Zn(II) in the presence of an excess amount of the respective metal ion. The first blue bar represents the response to Zn(II) in the absence of any competitive ions.

When excitation was provided at 410 nm, an immediate 41 fold increase in the fluorescence intensity at 544 nm was evident upon the addition of 0.5 equivalent of Zn(II). The ability to observe such emissive turning in response to Zn(II) was basically not affected by any biologically ubiquitous ions such as Ca(II) & Mg(II). Surprisingly, even in the presence of 4 equivalents of Cu(II), Fe(II) or Cd(II), the Zn(II) induced fluorescence was still 9 to 23 times greater than the competing ions alone in the absence of Zn(II) (Figure 23).

Such a result clearly confirmed that sensor **80g** has excellent affinity to Zn(II) over other metal ions, as under all of the conditions explored, the fluorescence intensity increased significantly upon the addition of Zn(II). To the best of our knowledge, **80g** is the first example of a PCT-based chemosensor reported to date, which can uphold such a strict selectivity to Zn(II).

4.4.2.3 Spectroscopic evaluation of 80g towards free Zn(II) ions

Having established the high selectivity of **80g** towards Zn(II), the ability of **80g** to determine the free Zn(II) concentration was evaluated. The biological functions of Zn(II) have been reported in the protein-bound form, however, the biological function of free or chelatable Zn(II) is less certain. It is always found at high concentrations, especially in the brain and pancreas, and can be visualized by a fluorescent dye.[150]

To determine the affinity of **80g** towards free Zn(II), twenty chloroform solutions that each contained 1 μM **80g** and 0.01 M inert salt tetrabutylammonium hexafluorophosphate were prepared and to each of these, varying volumes of $Zn(ClO_4)_2$ (0.05 mM) were added, giving free Zn(II) concentrations ranging from 0.025 to 0.5 μM; then the absorption and the emission spectra were recorded. As seen in Figure 24, an evident red shift was observed in the absorption spectra upon cation binding and this can be explained in terms of the charge-dipole interaction.[151]

When the dipole moment in the excited state is larger than that in the ground state and the cation interacts with the donor group, the excited state is more strongly destabilized by the cation than the ground state, and a blue shift of the absorption is expected. Conversely, when the cation interacts with the acceptor group, the excited state is stabilized more by the cation than the ground state and, as such, a red-shift of the absorption can be observed.
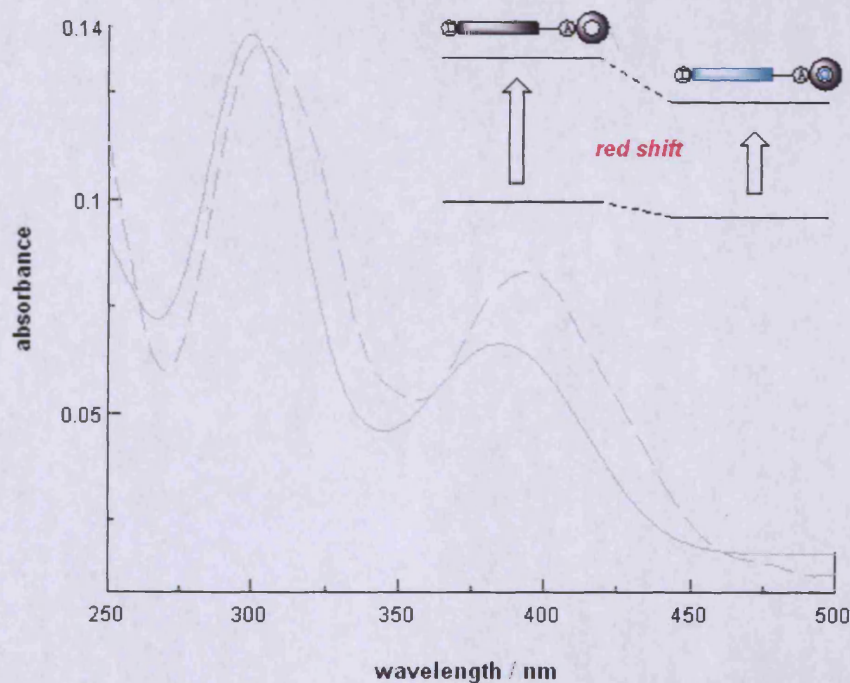
Figure 24. UV-Vis absorption spectra of **80g** (solid line); **80g** after addition of 0.5 equivalent of zinc perchlorate (dashed line). [**80g**] = 1.5 μM in chloroform.

The emissive intensity of **80g** was also significantly affected upon the addition of Zn(II), which was switched on with fluorescent enhancement of almost 42-fold; the emission colour rapidly turned to luminescent green (Figure 25).

From these changes a dissociation equilibrium constant, K_d, was obtained by plotting the $\log[(I_F - I_{Fmin})/(I_{Fmax} - I_F)]$, where I_F is the initial emission and I_{Fmax} is the saturated emission, *versus* the log of free Zn(II). A Hill plot was obtained, with a log K_d = -9.60 ± 0.1 and therefore a K_d = 2.51 × 10^{-7} $\mu M^{1/2}$ (Appendix-II).[1(a)]
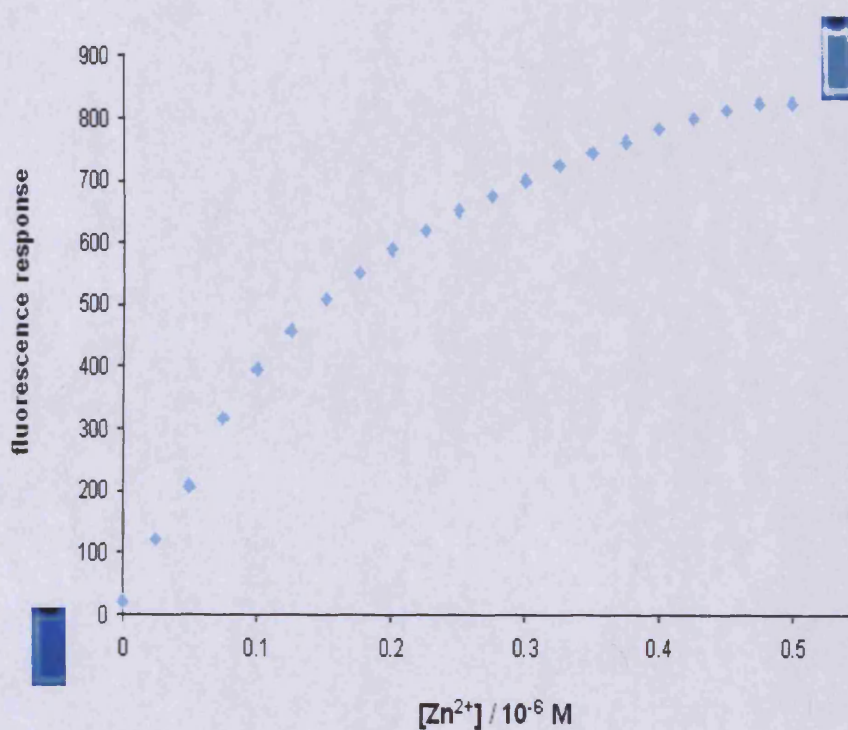
Figure 25. Changes in fluorescence intensity at 540 nm for **80g** (1 μM) as a function of free Zn(II); λ_{ex}: 400 nm, solvent: chloroform which contains 0.01 M TBAH.

These data clearly demonstrate that ligand **80g** has a high affinity and positive fluorescence response to the free Zn(II) concentration even at room temperature, under aerated conditions.

Such results have not only encouraged for study as a potential sensing system to this biologically important ion but also, elegantly, verified the overall synthetic versatility of our molecular design.

4.5 Conclusions

The microwave-assisted Bohlmann-Rahtz heteroannelation of 3-aminocrotononitrile with 3,3'-(4-bromophenyl)-1,1'-(pyridine-2-yl)-biprop-2-yn-1-one has been shown to be a viable method for the preparation of 4,4''-(4-bromophenyl)-substituted-2,2':6',2'' terpyridine **80e**, which can be applied as a flexible synthetic intermediate and readily transformed into a range of functionally-designed electron luminescent terpyridine targets.

Although compounds with simple aryl substituents at the 4'-position of the terpyridine moiety have been conventionally prepared using the Kröhnke methodology,[152] the microwave-assisted heterocondensation and the subsequent cross-coupling procedures allow the use of easily accessible materials, to provide a facile, diverse route to a range of novel 4,4''-diaryl substituted systems under very mild conditions. In particular, the 5,5''-nitrile moieties have been successfully incorporated into the terpyridine architecture by using these methods, overcoming the relative inaccessibility of the appropriately functionalized 6-cyano-2-acetyl pyridine which otherwise would be required from a conventional approach.

The 5,5''-nitrile substituted analogue has enhanced electron-withdrawing ability around the ionophore site and, more importantly, through design, can display unique luminescent properties upon investigation of their solvatochromism.

The chemosensor **80g** discussed herein exhibits a high affinity and selectivity to Zn(II) ions and as such, display a dramatic fluorescence response to cation binding that is unprecedented under all conditions explored. Our future efforts will focus on preparing water-soluble analogues for improved bio-compatibility in the cellular environment and at the same time, a luminescent sensing library to other biologically important ions could be established thereafter, by appending versatile molecular recognition units, for example, various crown ethers, onto the existing terpyridine framework.

References

114. Czarnik, A. W. *Chem. Biol.*, **1995**, *2* 423.

115. Grynkiewicz, G.; Poenie, M.; Ysien, R. Y. *J. Biol. Chem.*, **1985**, *260*, 3440.

116. Haugland, R. P. *Handbook of Fluorescent Probes and Research Chemicals*, ed. by M. T. Z. Spence, Molecular Probes, Eugene, 6th edn., **1996**, 503.

117. Koike, T.; Watanabe, T.; Aoki, S.; Kimura, E.; Shiro, M. *J. Am. Chem. Soc.*, **1996**, *118*, 12696.

118. Fra'usto da Silva J. J.; Williams, R. J. P. *The Biological Chemistry of the Elements*, Clarendon Press, Oxford, **1991**, 302.

119. Frederickson, C. J.; Kasarskis, E. J.; Ringo, D.; Frederickson, R. E. *J. Neurosci. Methods*, **1987**, *20*, 91.

120. Zalewski, P. D.; Forbes, I. J.; Betts, W. H. *Biochem. J.*, 1993, **296**, 403.

121. Zalewski, P. D.; Forbes, I. J.; Seamark, R. F.; Borlinghaus, R.; Betts, W. H.; Lincoln, S. F.; Ward, A. D. *Chem. Biol.*, **1994**, *3*, 153.

122. Huston, M. H.; Haider, K. W.; Czarnik, A. W.; *J. Am. Chem. Soc.*, **1988**, *110*, 4460.

123. Akkaya, E. U.; Huston, M. H.; Czarnik, A. W.; *J. Am. Chem. Soc.*, **1990**, *112*, 3590.

124. Czarnik, A. W. *Acc. Chem. Res.*, **1994**, *27*, 302.

125. Weiss, J. H.; Sensi, S. L.; Koh, J. Y. *Trends Pharm Sci.*, **2000**, *21*, 395.

126. Federickson, C. J.; Moncrieff, D. W. *Biol. Signals.* **1994**, *3*, 127.

127. Truong-Tran, A.Q.; Carter, J.; Ruffin, R.E.; Zalewski, P.D. *BioMetals.* **2001**, *14*, 315.

128. Bagley, M. C.; Brace, C.; Dale, J. W.; Ohnesorge, M.; Phillips, N. G.; Xiong, X.; Bower, J. *J. Chem. Soc., Perkin Trans. 1* **2002**, 1663.

129. Brikofer, L.; Hansel, E.; Steigel, A. *Chem. Ber.* **1982**, *115*, 2574.

130. Bagley, M. C.; Glove, C.; Merritt, E. A.; Xiong, X. *Synlett.* **2004**, 811.

131. Sinsky, M. S.; Bass, R. J. *J. Heterocyclic Chem.* **1984**, *21*, 759.

132. Mille, R. D.; Reiser, O. *J. Heterocyclic Chem.* **1993**, *30*, 755.

133. Bowden, K.; Jones, E. R. H. *J. Chem. Soc.*, **1946**, 953.

134. Adlington, R. M.; Baldwin, J. E.; Catterick, D.; Pritchard, G. J.; Tang, L. T. *J. Chem. Soc., Perkin Trans. 1* **2000**, 2311.

135. Baldwin, J. E.; Pritchard, G. J.; Rathmell, R. E.; *J. Chem. Soc., Perkin Trans. 1* **2001**, 2906.

136. Larock, R. C.; Dubrovsky, A. V.; Zhou, C. *J. Org. Chem.* **2006**, 71, 1626.

137. Bohlmann, F.; Rahtz, D. *Chem. Ber.* **1957**, *90*, 2265.

138. Bagley, M. C.; Hughes, D. D. *Synlett.* **2002**, *8*, 1332.

139. (a) Zhang, S.; Zhang, D.; Liebeskind, L. S. *J. Org. Chem.* **1997**, *62*, 2312. (b) Ma, D.; Zhang, Y.; Yao, J.; Wu, S.; Tao, F. *J. Am. Chem. Soc.,* **1998**, *120*, 12459. (c) Kalinin, A. V.; Bower, J. F.; Riebel, P.; Snieckus, V. *J. Org. Chem.* **1999**, *64*, 2986. (d) Goodbrand, H. B.; Hu, N. *J. Org. Chem.* **1999**, *64*, 670. (e) Fagan, P. J.; Hauptman, E.; Shapiro, R.; Casalnuovo, A. *J. Am. Chem. Soc.,* **2000**, *122*, 5043.

140. Lindley, J. *Tetrahedron* **1984**, *40*, 1433.

141. Valeur, B. *Molecular Luminescence Spectroscopy, Part 3*, Wiley, New York, **1993**.

142. Rettig, W.; Lapouyade, R. *Fluorescence Spectroscopy, Vol. 4*, Plenum, New York, **1994**.

143. Lippard, S. J.; Nolan, E. M.; Jaworski, J. Racine, M. E.; Sheng, M. *Inorg. Chem.* **2006**, *45*, 9748.

144. Tung, C.; Wu, L.; Han, X.; Si, G.; Pan, J.; Yang, Q.; Zhang, L. *Chem. Eur. J.* **2007**, *13*, 1231.

145. Laurence, C.; Nicolet, P.; Dalati, M. T.; Abboud, J. M.; Notario, R. *J. Phys. Chem.* **1994**, *98*, 5807.

146. Letard, J. F.; Lapouyade, R.; Rettig, W. *J. Am. Chem. Soc.* **1993**, *115*, 2441.

147. Lakowicz, J. R. *Principles of Fluorescence Spectroscopy*; Kluwer Academic/Plenum: New York, 1999.

148. Seliskar, C. J.; Brand, L. *J. Am. Chem. Soc.,* **1971**, *93*, 5414.

149. Valeur, B.; Leray, I.; O'reilly, F.; Habib Jiwan, J.; Soumillion, J. *J. Chem. Soc., Chem. Commun.* **1999**, 795.

150. Lippard, S. J.; Nolan, E. M. *Inorg. Chem.* **2004**, *43*, 8310.

151. Lohr, H.; Vogtle, F. *J. Chem. Soc., J. Chem. Res.* **1985**, *18*, 65 and references therein.

152. Krőhnke, F. *Synthesis* **1976**, 1.

Chapter Five – Results and Discussion

5.2 Structural properties of Zn(II) (BS)₂(NN) type complexes

According to a previous study, the complexes listed in Table 22 were synthesized and investigated spectroscopically by Crosby and co-workers.[159]

Table 22. Sample Zn(II) (BS)₂(NN) type complexes and abbreviations.[159]

Compound	Abbreviation
bis(benzenethiolate) (1,10-phenanthroline)zinc(II)	Zn(PhS)₂(phen)
bis(pentafluorobenzenethiolate) (1,10-phenanthroline)zinc(II)	Zn(F₅PhS)₂(phen)
bis(triphenylmethylthiolate) (1,10-phenanthroline)zinc(II)	Zn(Ph₃CS)₂(phen)
bis(4-chrolrobenzenethiolate) (ethylenediamine)zinc(II)	Zn(4-Cl-PhS)₂(en)
bis(4-chrolrobenzenethiolate) (1,10-phenanthroline)zinc(II)	Zn(4-Cl-PhS)₂(phen)
bis(4-methylbenzenethiolate) (1,10-phenanthroline)zinc(II)	Zn(4-Me-PhS)₂(phen)
bis(4-methoxylbenzenethiolate) (1,10-phenanthroline)zinc(II)	Zn(4-MeO-PhS)₂(phen)

When the Zn(Ph₃CS)₂(phen) complex, a white solid, was dissolved in an organic glass at 77 K, both fluorescence and phosphorescence were observed (Figure 26). Both bands were highly structured and exhibited the known characteristics of the spectra of the uncoordinated phen ligand, although slight shifts in the band energies and a lengthening of the lifetime of the phosphorescence had also been observed.[159-161] There was also a noticeable increase in the fluorescence to phosphorescence ratio (I_{fl}/I_{ph}).
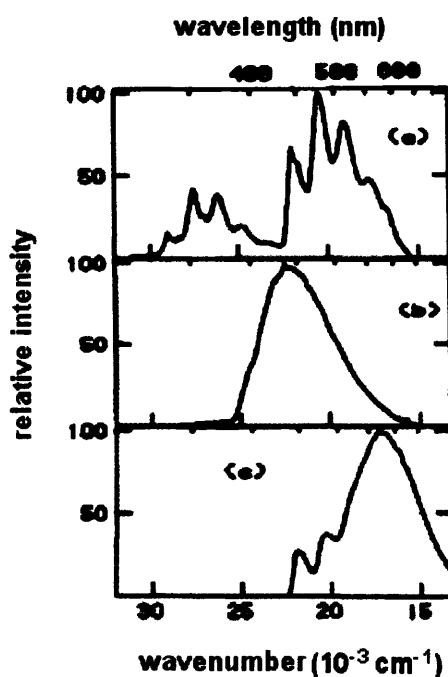
Figure 26. Steady state emission spectra of Zn(II) complexes at 77 K. (a) Zn(Ph₃CS)₂(phen), 6.0×10^{-5} M, excited at 310 nm. (b) Zn(4-Cl-PhS)₂(en), 1.1×10^{-4} M, excited at 310 nm. (c) Zn(4-Cl-PhS)₂(phen), 1.1×10^{-4} M, excited at 350 nm.[159]

These visible luminescence bands were confidently assigned to the lowest $^{1\&3}\pi{\rightarrow}\pi^*$ states of the phen ligand. In the spectrum no trace of a third transition occurs below 30 000 cm^{-1}. Crosby et al. concluded that, in the Zn(Ph$_3$CS)$_2$(phen) complex, the Zn(II) ion plays an *unimportant* role in determining the nature of the low-lying excited state manifold of the system. Although two coordinated sulfur atoms are present, they, neither, appear to play essential roles in defining the lowest excited state orientation (Figure 26a).

In Figure 26b, Crosby *et al.* had reproduced the emission spectrum of Zn(4-Cl-PhS)$_2$(en) in an organic glass. The broad band maximizing at approximately 22 500 cm^{-1} was a phosphorescence band since it appeared at essentially the same energy as the phosphorescence from the uncoordinated thiol ligand in the same solvent. The role of the Zn(II) ion appeared to increase somewhat the ratio of phosphorescence to fluorescence from the thiol ligand. There was no evidence for a third transition in the region below 30 000 cm^{-1}. The ethylenediamine moiety, as expected, had been spectroscopically transparent in this region. This saturated ligand also played no essential role in defining the low-lying excited state structure of the complex.

When the Zn(4-Cl-PhS)$_2$(phen) complex was synthesized, a yellow solid was obtained. Upon irradiation with UV light of approximately 330 nm in a glass at 77 K, a strong emission had occurred that was comprised of two easily recognizable components (Figure 26c).

There was a prominent structured blue-green emission that decayed in 0.76 s and obviously originated from a perturbed $^3\pi{\rightarrow}\pi^*$ state of the phen ligand. This structured long-lived emission band was overlapped by a new broad transition maximizing at *ca.* 17 000 cm^{-1}.

This broad band decayed on the order of 10 μs and was demonstrably not related to the $^3\pi{\rightarrow}\pi^*$ states of either the phen or thiol ligands. The appearance of this band signalled the existence of a new low-lying excited state in the complex that had not presented in either of the coordinated ligands.

Extensive spectroscopic studies of a range of Zn(BS)$_2$(NN) & Zn(SS)(NN) type complexes (SS = aromatic dithiol) confirmed the existence of the new low-lying excited configuration. However, it was also concluded by Crosby *et al* that this newly found emission band only presented whilst both *N*-heterocyclic and the aromatic thiol ligands were coordinated to the central Zn(II) ion at same time.

5.3 Tunability of Zn(II) (BS)₂(NN) type complex

The energy of the low-lying excited configuration can actually be tuned in several ways. Modification of the thiol portion of the complex produced substantial shifts in the emission wavelength.[159]

This has been clearly seen in Figure 27 where the time-resolved photoluminescence bands from Zn(4-Me-PhS)₂(phen) and Zn(4-MeOPhS)₂(phen) were compared. An evident red shift occurred when the methyl group on the thiol ligand was replaced by the methoxy substituent. More dramatic shifts in this low-lying emission band can be tuned by introducing substituents on the N-heterocycle or by switching to a different heterocycle altogether.
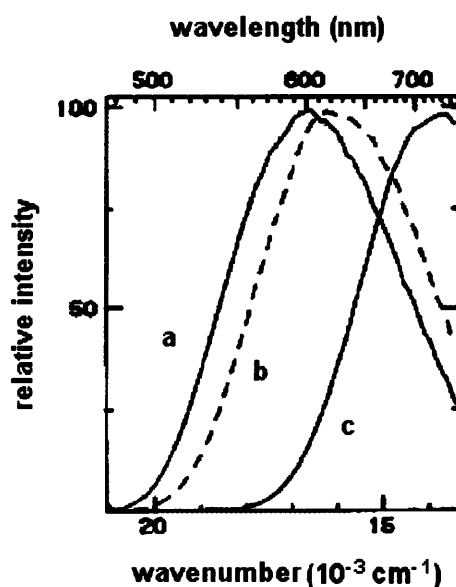
Figure 27. Time-resolved emission spectra of Zn(II) complexes at 77 K. (a) Zn(4-Me-PhS)₂(phen); (b) Zn(4-MeO-PhS)₂(phen); (c) Zn(4-Me-PhS)₂(biq).[159]

In Figure 27 Crosby *et al.* had included the time-resolved emission band from Zn(4-Me-PhS)₂(biq). One sees that replacing the 1,10-phenanthroline with 2,2'-biquinoline, while retaining the identity of the sulfur moiety, caused a *ca.* 3000 cm^{-1} red shift in the band energy. For the corresponding Zn(4-MeO-PhS)₂(biq) complex the band fell even farther in the red.[159] Thus, it is apparent that the energy of the excited state(s) corresponding to the broad new luminescence band can be tuned chemically by adjusting the electro-transporting characters both for the intrinsic (N-heterocyclic) and ancillary (benzenethiol) ligands.

In general, both electron donating groups on the thiol ligand and electron withdrawing groups on the N-heterocycle decreased the band energy. Meanwhile, significant shifts of the band maximum could also be induced via the solvent perturbation.

5.4 Solvent effect upon excited state properties

It was also found by Crosby *et al.* that the novel low-lying emitting state(s) had a set of interesting spectroscopic properties upon changing the solvent medium. The spectrum was generally unstructured, even at very low temperatures (10 K), and spanned a broad spectral range. It also had a characteristic decay time. For most of the species the measured decay curve was approximately bimodal, consisting of an extremely fast component (ns) and a longer-lived tail in the range of 10-50 μs. This latter component was somewhat non-exponential (Table 23), both the short (ns) and the long (μs) bands spanned the same spectral region.

Table 23. Luminescence decay data for sample Zn(II) (BS)₂(NN) type complexes.[159]

Compound[a]	$\pi \rightarrow \pi^*_{(phen)}$[b]	LLCT
phen	1.4 s	–
$ZnCl_2$(phen)	2.3 s	–
$Zn(Ph_3CS)_2$(phen)	1.9 s	–
$Zn(F_5PhS)_2$(phen)	1.3 s	F & P[c]
Zn(4-Cl-PhS)₂(phen)	0.76 s	F & P
Zn(PhS)₂(phen)	0.79 s	F & P
Zn(4-Me-PhS)₂(phen)	0.83 s	F & P
Zn(4-MeO-PhS)₂(phen)	–	F & P

[a] All measurements on were made on samples dissolved in 77 K rigid glasses composed of $CHCl_3$-EtOH (1:19); [b] Ligand centred transition; [c] Decay consisting of a prompt fluorescence (<15 ns) and a non-exponential tail of 5-50 μs mean lifetime.

Generally, the solvent medium affected the emission spectrum in two ways (Figure 28). For $Zn(PhS)_2$(phen), increasing the alcoholic content of the glass both decreased the relative amount of $^3\pi \rightarrow \pi^*$ contribution from the N-heterocycle ligand and also shifted the new broad band to the red side of the spectrum. Such behaviour was somehow representative for most of the complexes studied and the solvent effects upon the specific decay times of the emitting components are actually insignificant.

5.5 Proposed decay model for excited states

Finally in order to rationalize the nature of this newly emerged low-lying excited state giving rise to the red shifted broad emission, Crosby *et al.* adopted the model first proposed by Koester to interpret the visible absorption spectra of analogous Zn(II) (BS)$_2$(NN) type complexes.[159]

In this view, a new low-lying excited state should be introduced into the relaxation system whenever a good π-acceptor (phen) had been coordinated to a d^{10} metal, which had also been instantaneously coordinated to a π-donor such as the aromatic thiol. Excitation of the complex to this state can be viewed as an electronic charge transfer from the thiol moiety to the N-heterocycle. Thus the broad emission can be viewed as arising from a ligand-ligand charge-transfer (LLCT) excited configuration in which incipient oxidation and reduction had occurred at the thiol and N-heterocyclic ligands, respectively.

Koester labelled the corresponding absorption band as an *interligand transmetallic charge-transfer* band (ITCT), thus implying a transfer of charge across the metal. A schematic orbital diagram and consequent energy level scheme are depicted in Scheme 52.
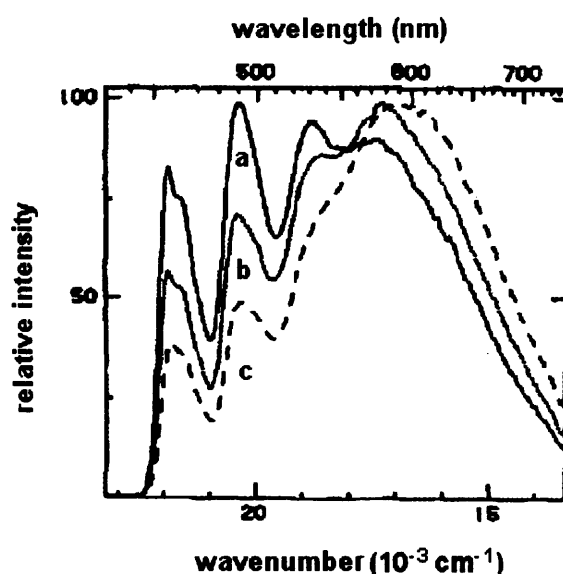
Figure 28. Solvent dependence of the emission spectrum of Zn(PhS)$_2$(phen) at 77K. (a) CHCl$_3$-EtOH (1:9), 6.5 × 10^{-5} M; (b) CHCl$_3$-EtOH (1:19), 5.6 × 10^{-5} M; (c) MeOH-EtOH (4:1), 8.6 × 10^{-5} M.[159]

A consideration of Scheme 52 reveals that several modes of excitation and de-excitation of these complexes are possible. Excitation of the thiol moiety could produce characteristic thiol fluorescence or phosphorescence or conversion to the $^{1\&3}$LLCT state(s) followed by quenching or LLCT luminescence. Alternatively the *N*-heterocycle could be excited leading to fluorescence or

114

phosphorescence from that ligand or conversion to the $^{1\&3}$LLCT manifold, and the direct energy transfer from thiol to N-heterocycle (or *vice versa*) could occur instantaneously as well.
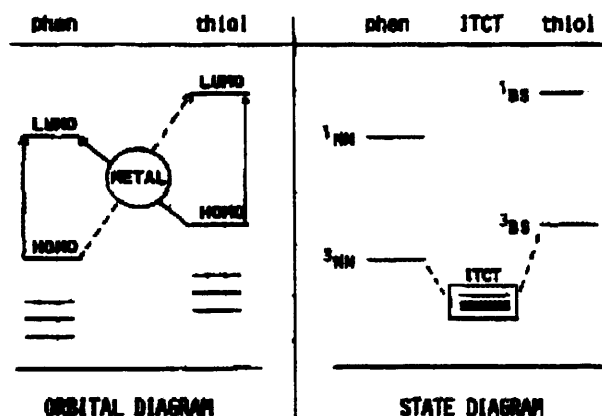
Scheme 52. Schematic energy-level and obitals schemes for closed-shell metal complexes displaying ligand-ligand CT excited states.[159]

What emission spectrum would arise experimentally would actually depend upon the excitation wavelength and the relative magnitudes of various rate constants associated with the possible radiative and non-radiative de-excitation processes thereafter.

5.6 Synthetic application: microwave-assisted synthesis of luminescent cyanobipyridyl-zinc(II) bis(thiolate) complexes and their photophysical investigation.

In chapter 2, we described the synthesis of a new series of solvatochromic 3-cyanopyridine-derived chromophores **53** with visible absorption and charge transfer (CT)-based emission properties, significant Stokes shifts, excellent quantum yields and usable nanosecond fluorescent lifetimes.[162] Our route to this motif was both rapid and efficient and employed a novel microwave-assisted tandem oxidation/Bohlmann-Rahtz heteroannulation to establish the central tetrasubstituted pyridine. Furthermore, incorporated into this scaffold was capability for two-dimensional tunability through modification of substituents, and this was varied in order to modulate photophysical behaviour. In this section, we report on the photophysical properties of a series of new cyanobipyridines prepared and modified by microwave-assisted methods for rapid access to structural variants. The addition of a second pyridyl unit provides the basic chromophoric framework with an additional dimension for modulating luminescent behaviour, through complexation with a metal ion (Scheme 53). Furthermore, simply by changing the ligands coordinating to the zinc it was anticipated that the photophysical properties of these novel chromophores could be further modulated.

5.6.1 Design and synthesis

The starting point for this study (Scheme 53) was cyanobipyridine **53g**, prepared by our previously reported method in good yield.[163] This versatile precursor contains a bromide substituent that it was envisaged could be transformed rapidly and effiently by cross-coupling methods in order to provide good variation in electronic properties. Two different methods for bipyridine functionalization were investigated under microwave dielectric heating: a Pd-mediated Suzuki cross-coupling reaction or Cu-mediated *N*-arylation. Microwave irradiation of bromide **53g** and phenylboronic acid at 150 °C for 30 min in DMSO in the presence of Pd(PPh$_3$)$_4$ under basic conditions gave (biphenyl)bipyridine **53n**, whereas reaction with diphenylamine at 120 °C for 1 h in toluene using the pre-formed Cu(I) catalyst Cu(neocup)(PPh$_3$)Br under basic conditions, according to our established procedure,[111] gave (aminophenyl)bipyridine **53o**, both reactions proceeding in excellent yield.
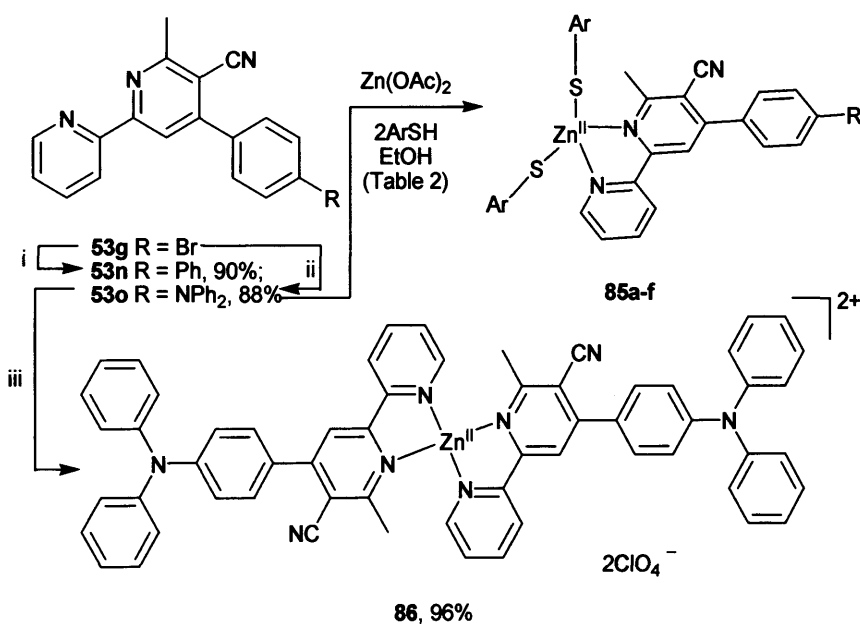
Scheme 53. Synthesis of zinc bipyridine complexes **85a-f** and **86**. *Reagents & conditions*: (i) PhB(OH)$_2$, Pd(PPh$_3$)$_4$ (10 mol%), Na$_2$CO$_3$, DMSO, microwaves, 150 °C, 30 min; (ii) diphenylamine, Cu(neocup)(PPh$_3$)Br (10 mol%), ^{t}BuOK, PhMe, microwaves, 120 °C, 1 h; (iii) Zn(ClO$_4$)$_2$.6H$_2$O, CH$_2$Cl$_2$, SiC PHE, microwaves, 120 °C, 10 min.

The formation of cyanobipyridyl-zinc(II) bis(thiolate) complex **85a** was first investigated by stirring bipyridine **53n**, Zn(OAc)$_2$ and thiophenol (2 equiv.) in EtOH at room temperature for 24 h (Scheme 53; Table 24) but surprisingly only proceeded in poor yield. Furthermore, the efficiency of this process was improved only a little by carrying out the complexation at reflux over a prolonged period (entry 2).

116

Table 24. Conditions for the synthesis of Zn(II) complex **85a**.

Entry	Conditions	Yield (%)[a]
1	25 °C, 24 h	36
2	Conductive heating, reflux, 24 h	44
3	Microwave, 120 °C, 10 min	82
4	Microwave, SiC passive heating element, 120 °C, 10 min	94

[a.] Isolated yield withou any chromatographic purifications

The use of controlled microwave dielectric heating to promote the formation of metallo complexes has hitherto been reported only recently, for example in the synthesis of Ru[II] coordination complexes,[163] despite long standing recognition of the benefits of microwave-assisted autoclave reactions for bipyridine complexation by Greene and Mingos.[164] Gratifyingly, under microwave dielectric heating at greatly elevated temperature (entry 3), Zn[II] complex **85a** was formed in high yield without the need for further purification. In order to investigate if this dramatic improvement in chemical yield was attributed to Arrhenius behaviour, or whether a specific microwave effect[165] was in evidence, the reaction was repeated under microwave irradiation in the presence of a SiC passive heating element (PHE)[166] (entry 4). Under these conditions, the thermal profile of the reaction improved (Figure 29), an observation that we have made before in microwave-assisted tandem oxidation processes,[167] and Zn[II] complex **4a** was formed in excellent yield. Although firm conclusions regarding rate accelerations under microwave dielectric heating would require much more detailed experimentation, we believe these findings are indicative of Arrhenius behaviour for this complexation reaction and not specific, or indeed non-thermal, microwave effects in contrary to other suggestions.
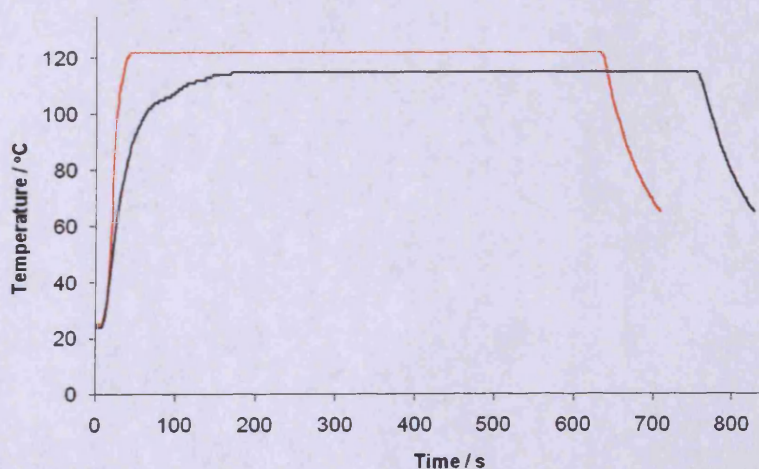
Figure 29. Heating profile under microwave irradiation in the presence (red) or absence (black) of a SiC passive heating element.

A series of bipyridyl-zinc(II) bis(thiolate) complexes **85a-f** was prepared using this approach and compared with the zinc(II) bis(bipyridyl) perchlorate complex **86**, prepared in high yield by microwave-mediated complexation, in order to establish the role of the metal, intrinsic functionality and the ancillary ligands upon CT character. In so doing, the high efficiency of both microwave-assisted complexation procedures was established by comparison with conductive heating methods. Microwave irradiation of bipyridine **53n-o** $Zn(OAc)_2$ (1 equiv.) and the corresponding thiophenol (2 equiv.) in EtOH at 120 °C in a sealed tube in the presence of a SiC passive heating element (Scheme 53) gave a series of complexes **85a-f** suitable for photophysical study in excellent (94-98%) yield (Table 25); far in excess of the chemical yield at reflux in EtOH after 24 h. Similarly, irradiation of bipyridine **3b** (2 equiv.) and zinc perchlorate in CH_2Cl_2 at 120 °C gave complex **86** in excellent yield (96%) after 10 min whereas a known conductive heating method[167] was poorly efficient (42% yield after 24 h).

Table 25. Synthesis of Zn(II) complexes **85a-f** under microwave dielectric heating and at reflux.

Entry	53	85	R	Ar	Yield (%)[a]	Yield (%)[b]
1	n	a	Ph	Ph	44	94
2	n	b	Ph	4-MeOC₆H₄	52	97
3	n	c	Ph	2-naphthyl	50	96
4	o	d	NPh₂	Ph	54	96
5	o	e	NPh₂	4-MeOC₆H₄	48	95
6	o	f	NPh₂	2-naphthyl	56	98

[a] Isolated yield without any chromatographic purification (thermal reflux); [b] Isolated yield without any chromatographic purification (microwave heating).

5.6.2 Photophysical study

Electronic absorption spectra were obtained for each of the complexes in chloroform (10^{-6} M). Comparison with the free ligands **53n-o** revealed the presence of ligand-centred transitions together with an additional broadened low-energy shoulder at *ca.* 390 (**85a-c**) and *ca.* 485 nm (**85d-f**) (Figure 30). In accordance with previous reports this transition was assigned to an inter-ligand thiolate-to-bipyridine charge transfer (LLCT),[168] further evidenced by a subtle wavelength dependence upon the electron donating ability of the coordinated thiolate.[169] For **85d-f** the LLCT band was red-shifted, presumably as a consequence of the greater dipolar CT character of the parent bipyridine (**53o**). Further confirmation was provided with the homoleptic complex **86**, which gave an absorption spectrum lacking the LLCT feature at *ca.* 490 nm.
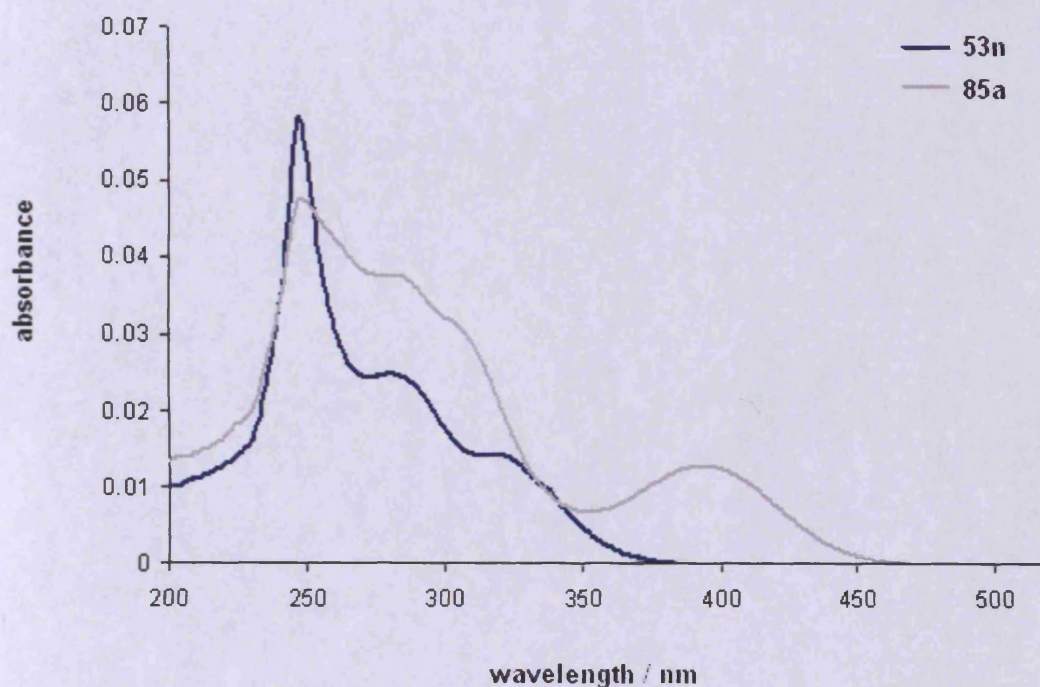
Figure 30. Electronic absorption spectra of the cyanobipyridyl-Zn^{II}-bis(thiolate) complex and its corresponding free bipyridine ligand in 10^{-6} M aerated chloroform at 298 K. **85a** (grey) and the free ligand **53n** (black).

The emission characteristics of the Zn(II) complexes (Table 26) were probed in both solid and solution-states. Room temperature measurements on solid samples showed a featureless fluorescence band (< 1 ns in all cases) in the visible region, which was independent of excitation wavelength and was therefore attributed to emission from a LLCT excited state.

Table 26. Absorption and photophysical properties oc complexes **85a-f**.

Entry	85	λ_{abs} (logε) / nm[a]	λ_{em} / nm[b]	λ_{em} / nm[a] (τ / ns)	λ_{em} / nm[a] (τ / ns)	$(\phi)^{a,g}$
1	a	325 (4.37), 390 (4.03)	584	410[c] (2.7)	520[e] (1.6)	0.24
2	b	322 (4.40), 392 (3.96)	625	402[c] (2.5)	510[e] (2.6)	0.20
3	c	328 (4.32), 388 (4.06)	512	398[c] (1.6)	512[e] (7.2)	0.28
4	d	392 (4.18), 486 (3.86)	590	540[d] (3.9)	604[f] (6.5)	0.05
5	e	390 (4.20), 490 (3.78)	615	539[d] (3.1)	618[f] (7.6)	0.01
6	f	394 (4.14), 484 (3.90)	627	524[d] (6.9)	612[f] (< 1)	0.08

[a] aerated CHCl$_3$ solution; [b] solid; [c] λ_{ex} = 320 nm; [d] λ_{ex} = 390 nm; [e] λ_{ex} = 390 nm; [f] λ_{ex} = 500 nm; [g] obtained for LLCT emission.

However, in chloroform solution each of the complexes' emission profiles were dependent upon the wavelength of excitation: for **85a-c** two emission bands at *ca.* 400 and *ca.* 510 nm resulted from excitation at 330 and 400 nm respectively (*i.e.*, Figure 31 clearly shows the emission profile dependence of **85a** upon variable excitation wavelength).
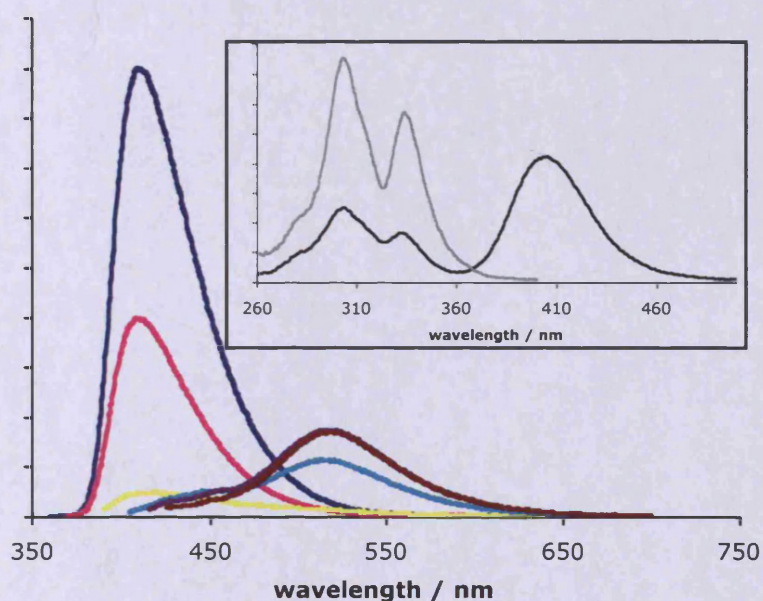
Figure 31. Main: Emission profiles for **85a** in CHCl$_3$ (λ_{ex} = 330 (blue), 350 (pink), 370 (yellow), 390 (turquoise), 400 (purple) and 410 (brown) nm. Inset: excitation spectra for **85a** λ_{em} = 410 nm (grey) and 520 nm (black).

The corresponding excitation spectra showed that the longer wavelength emission was associated with a unique excitation peak at *ca.* 400 nm, consistent with the LLCT assignment in the corresponding absorption spectra. Similar observations were noted for compounds **85d-f**, although with notable red-shifts in all cases. Time-resolved luminescence lifetime measurements showed that each of the emission peaks were relatively short-lived (< 10 ns) and indicative of a fluorescence in each case, whilst the quantum yields of the low energy emissions are significantly reduced for **85d-f**.

Taken together with the data obtained for the corresponding free ligands **53n-o**, and the solid-state fluorescence (assigned to a LLCT emitting state), these results indicate that the longer wavelength emission in chloroform solution can again be attributed to the LLCT excited state, but that the shorter wavelength band probably arises from an intra-ligand charge transfer (ILCT) associated with the cyanobipyridine. In this context, the extent of restricted motion of the coordinated thiol can be invoked to explain disparities in single (LLCT) or dual emission (Figure 32).[170]
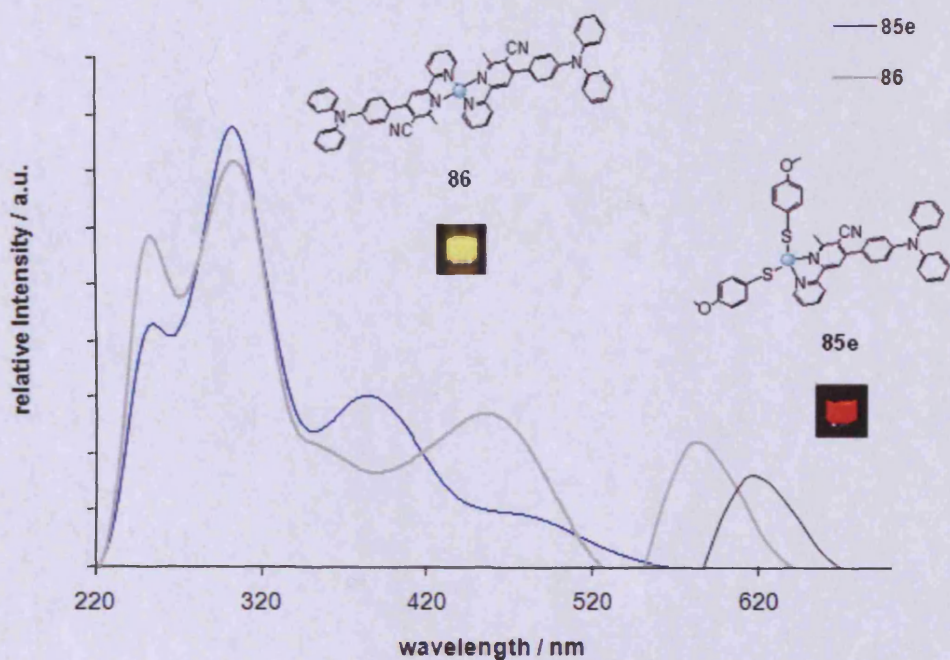
Figure 32. Electronic absorption and steady state emission spectra of the cyanobipyridyl-Zn^{II}-bis(thiolate) complex and its corresponding Zn^{II}-bis{4-[4-(diphenylamino)phenyl]-bipyridyl} perchlorate analogue in 10^{-6} M aerated chloroform at 298 K; emission spectra were recorded following initial excitation at 450 nm and 490 nm, respectively. $Zn(bipy)_2(ClO_4)_2$ **86** (grey) and **85e** (black). Inset: visualization of the pure compounds irradiated at corresponding wavelengths using a handheld UV lamp.

The solvatochromic behaviour of **85f** was probed and revealed that the emission in acetonitrile (λ_{em}= 573 nm) and DMSO (λ_{em}= 593 nm) was independent of excitation wavelength (390, 450 or 500 nm). Comparison with the free ligand **53o** [λ_{em} = 576 nm (MeCN); 580 nm (DMSO)] suggests that in polar solvent the red-shifted emission of **85f** is likely to be dominated by Zn(II)-perturbed $IL_{(bpy)}CT$ character. This observation is consistent with our previous studies into solvatochromic cyanopyridines[162] and related reports in the literature into classical *N,N*-dimethylaminobenzonitrile (DMABN) species.[24]

5.7 Conclusions

In conclusion, a series of cyanobipyridine-derived Zn(II) bisthiolate complexes can be prepared rapidly and in high yield by the microwave-assisted complexation of cyanobipyridine **53n-o**, a thiophenol and Zn(OAc)$_2$ using a passive heating element. The complexes display LLCT fluorescence in the solid-state, but tunable dual emission in chloroform, arising from co-emissive excited states. In general, the luminescence from the complexes can be tuned through changes in bipyridine functionality and subtly modulated by changes in the ancillary thiolate co-ligands.

References

[153.] State of the Art Symposium VII, 185th National Meeting of the American Chemical Society, 1983, Seattle, Wa, *J. Chem. Ed.*, 60, 1983, 784.

[154.] Adamson, A. W.; Fleischauer, P. W. *Concepts in Inorganic Photochemistry*, Wiley-Interscience, New York, **1975**.

[155.] Belzani, V.; Bolleta, F.; Gandolfi, M. T.; Maestri, H. *Top. Curr. Chem.*, **1978**, *1*, 75.

[156.] Kutal, C. *J. Chem. Ed.*, **1983**, *60*, 882.

[157.] Del Paggio, A. A.; Mctiillin, O. R. *Inorg. Chem.*, **1983**, *22*, 691.

[158.] Galin, A. M.; Razskazovsky, Y. V.; Mel'nikov, M. Y. *J. Photochem. Photobiol. A*, **1993**, *72*, 35.

[159.] Crosby, C. A.; Highland, R. G.; Truesdell, K. A. *Coord. Chem. Rev.*, **1985**, *64*, 41.

[160.] Koester, V. J. *Chem. Phys. Lett.*, **1975**, *32*, 575.

[161.] Ohno, T. *Bull. Chem. Soc. Jap.*, **1974**, *47*, 2953.

[162.] Bagley, M. C.; Lin, Z.; Pope, S. J. A. *J. Chem. Soc., Chem. Commun.*, **2009**, 5165.

[163.] (a) Anderson, T. J.; Scott, J. R.; Millett, F.; Durham, B. *Inorg. Chem.*, **2006**, *45*, 3843; (b) Sun, Y.; Machala, M. L.; Castellano, F. N. *Inorg. Chim. Acta.*, **2010**, *363*, 283 and references cited therein.

[164.] Greene, D. L. Mingos, D. M. P. *Transition Met. Chem.*, **1991**, *16*, 71.

[165.] De la Hoz, A.; Moreno, A. *Chem. Soc. Rev.*, **2005**, *34*, 164.

[166.] (a) Razzaq, T.; Kremsner, J. M.; Kappe, C. O. *J. Org. Chem.*, **2008**, *73*, 6321; (b) Kremsner, J. M.; Kappe, C. O. *J. Org. Chem.*, **2006**, *71*, 4651.

[167.] Fu, W-F.; Xu, Q-Q.; Wang, D-H.; Chi, S-M. Gan, X. *Inorg. Chim. Acta.*, **2009**, 2529.

[168.] Truesdell, K. A.; Crosby, G. A.; *J. Am. Chem. Soc.*, **1985**, *107*, 1787.

[169.] Ngan, T.W.; Ko, C. C.; Zhu, N. Yam, V.W.W. *Inorg. Chem.*, **2007**, *46*, 1144.

[170.] Gronland, P. J.; Burt, J. A.; Wacholtz, W. F. *Inorg. Chim. Acta.*, **1995**, *234*, 13.

Chapter Six – Experimental

6 Experimental

6.1 General measurements

Commercially available reagents were used without further purification; solvents were dried by standard procedures. Light petroleum refers to the fraction with bp 40–60 °C, ether (Et$_2$O) refers to diethyl ether and EtOAc refers to ethyl acetate. Column chromatography was carried out using Merck Kieselgel 60 H silica or Matrex silica 60. Analytical thin layer chromatography was carried out using aluminium–backed plates coated with Merck Kieselgel 60 GF$_{254}$ that were visualised under UV light (at 254 and/or 360 nm). Melting points (mp) were determined on a Kofler hot stage apparatus and are uncorrected. Infra–red (IR) spectra were recorded in the range 4000–600 cm^{-1} on a Perkin–Elmer 1600 series FTIR spectrometer using KBr disks for solid samples and thin films between NaCl plates for liquid samples or as a Nujol mull and are reported in cm^{-1}. Nuclear magnetic resonance (NMR) spectra were recorded in CDCl$_3$ at 25 °C unless stated otherwise using a Bruker DPX 400 instrument operating at 400 MHz for ^{1}H spectra and 100 MHz for ^{13}C spectra and were reported in ppm; J values were recorded in Hz and multiplicities were expressed by the usual conventions (s=singlet, d=doublet, t=triplet, app=apparent, m=multiplet). Low–resolution mass spectra (MS) were determined using a Fisons VG Platform II Quadrupole instrument using atmospheric pressure chemical ionization (APcI) unless otherwise stated. ES refers to electrospray ionization, CI refers to chemical ionization (ammonia) and EI refers to electron impact. High-resolution mass spectra were obtained courtesy of the EPSRC Mass Spectrometry Service at Swansea, UK using the ionisation methods specified. Microanalyses were recorded using a Perkin–Elmer 240C Elemental Analyzer. *In vacuo* refers to evaporation at reduced pressure using a rotary evaporator and diaphragm pump, followed by the removal of trace volatiles using a vacuum (oil) pump. Microwave experiments were carried out in a CEM Discovery® microwave synthesiser at the temperature and initial power stated. Temperature measurement utilized the instrument's in-built IR sensor and the power was modulated to maintain constant reaction temperature. The reaction time for microwave heated experiments refers to the hold time at the reaction temperature and do not account for the ramp time. Electronic absorption spectra were measured upon 1.0 × 10^{-6} mol L^{-1} solutions in aerated chloroform, methanol, acetonitrile and DMSO for selected compounds at room temperature from 200 to 600 nm on a Varian Cary 500 Scan UV-vis NIR spectrophotometer using Cary WinUV Scan Application software, estimated errors are ±1 nm for λ_{max} and ±5% for ε. Steady-state luminescence analyses were processed using the same 1.0 × 10^{-6} mol L^{-1} solutions as for the absorption measurements. A Perkin-Elmer Luminescence Spectrometer LS55 with FL Winlab v. 4.00.02 software was used over the range 300-800 nm. Radiative lifetimes were measured using a

JobinYvon-Horiba Fluorolog spectrometer fitted with a JY TBX picosecond photodetection module. Aerated solution samples for luminescence lifetime decays were irradiated using a pulsed NanoLED configured for 330 nm or 400 nm output and emission detected at emission maxima. Data sets were obtained using the JY-Horiba FluorHub single photon counting module and lifetimes determined using the provided decay analysis software package, v6.1. Fluorescence quantum yields, Φ_f, were measured in various solvents using 1.0×10^{-6} mol L^{-1} fluorescein in 0.1 mol L^{-1} NaOH as the reference standard ($\Phi_{std} = 0.79$).[1] Each was diluted with the appropriate solvent until the absorbance [λ_{max}(ICT/LLCT)] at 300-500 nm was eventually calibrated between 0.05 and 0.01.[65] The fluorescence spectra were then recorded with excitation wavelengths between 320-490 nm. The peak was integrated using Microsoft Excel. This process was repeated three times at different optical densities. The integrated intensity was plotted against the absorbance of each sample. The slopes of the resulting lines were calculated using Microsoft Excel. The quantum yield was then determined by the following equation, taking into account the respective refractive indices:[1]

$$\phi_{sample} = \phi_{std} \frac{\left(Slope_{sample}\right)\left(\eta^2_{sample}\right)}{\left(Slope_{std}\right)\left(\eta^2_{std}\right)}$$

All solutions used for the spectroscopic analysis (i.e. λ_{abs}, λ_{em}, τ_f & Φ_f) were freshly prepared before each measurement.

6.2 General experimental procedures

6.2.1 General procedure for the microwave-assisted synthesis of 3-cyanopyridines 53

A solution of 3-aminocrotononitrile **10c** (0.57 mmol, 1 equiv.), 1-phenyl-2-propyn-1-ol **52a** (1.14 mmol, 2 equiv.) and barium manganate (1.70 mmol, 3 equiv.) in ethanol–acetic acid (5.0 mL) (5:1) was irradiated at 170 °C at an initial power of 150 W (which was moderated to maintain constant temperature) in a sealed Pyrex™ vessel for 15 min in a self-tuned single-mode CEM Discover® microwave synthesizer. The mixture was cooled rapidly to room temperature, by passing compressed air through the microwave cavity for 5 min, and then filtered through Celite®. The filtrate was poured into water (15 mL) and extracted with ethyl acetate (8 mL). The aqueous layer was further extracted with ethyl acetate (8 mL) and the organic extracts were combined, washed sequentially with saturated aqueous sodium hydrogen carbonate solution (10 mL) and brine (10 mL), dried (Na2SO4) and evaporated *in vacuo*. Purification by flash chromatography on silica, eluting with EtOAc–light petroleum (1:6), gave the *title compound* **53a**.

6.2.2 General procedure for the copper(I)-mediated N-arylation 3-cyanopyridine bromides

A solution of pyrrolidine (2 mmol, 2 equiv.), Cu(phen)(PPh$_3$)Br[81] (10 mol%), neocuproine (10 mol%) and potassium tert-butoxide (2 mmol, 2 equiv.) in toluene (10 mL) was stirred at room temperature for 5 min. A solution of 2-methyl-4-(4-bromophenyl)-6-(4-methoxphenyl)nicotinonitrile **53d** (1 mmol, 1 equiv) in toluene (5 mL) was added dropwise and the reaction mixture was heated at reflux overnight. After cooling rapidly to room temperature, the mixture was filtered through Celite®. The filtrate was poured into water (15 mL) and extracted with diethyl ether (15 mL). The aqueous layer was further extracted with ether (15 mL) and organic extracts were combined, dried (Na$_2$SO$_4$) and evaporated in vacuo. Purification by flash chromatography on silica, eluting with EtOAc–light petroleum (1:6), gave the 4-[4-(pyrrolidino)phenyl]-substituted 3-cyanopyridine **53k**.

6.2.3 General procedure for the microwave-assisted synthesis of 2,4,6-triarylpyrimidines 68

A mixture of benzamidine **67** (0.57 mmol, 1 equiv.), 1-(4-cyanophenyl)-3-[4-bromophenyl]prop-2-yn-1-ol **52m** (0.57 mmol, 1 equiv.) and barium manganate (1.70 mmol, 3 equiv.) in EtOH–AcOH (5:1) (5 mL) was irradiated at 150 °C in a sealed pressure-rated reaction tube (10 mL), at an initial power of 150 W, for 45 min in a self-turned single mode CEM Discover® Focused Synthesiser. The mixture was cooled rapidly to room temperature, by passing compressed air through the microwave cavity for 5 min, and then filtered through Celite®. The filtrate was poured into water (15 mL) and extracted with EtOAc (8 mL). The aqueous layer was further extracted with EtOAc (8 mL) and the organic extracts were combined, washed sequentially with saturated aqueous sodium hydrogen carbonate (10 mL) and brine (10 mL), dried (Na$_2$SO$_4$) and evaporated in vacuo. Purification by column chromatography on silica gel, eluting with EtOAc–petroleum ether (1:6 v/v), gave the 4-[6-(4-bromophenyl)-2-phenylpyrimidin-4-yl]benzonitrile **68m**.

6.2.4 General procedure for the microwave-assisted copper(I)-mediated N-arylation of 2,4,6-triarylpyrimidine bromides

A solution of benzonitrile **68m** (0.57 mmol, 1 equiv.) in toluene (3 mL) was added to a stirred solution of pyrrolidine (1.13 mmol, 2 equiv.), Cu(neocup)(PPh$_3$)Br[81] (10 mol %) and potassium tert-butoxide (0.85 mmol, 1.5 equiv.) in toluene (3 mL) in a pressure-rated Pyrex reaction tube (10 mL). The vessel was sealed and irradiated at 120 °C, at an initial power of 150 W, in a self-turned single mode CEM Discover® Focused Synthesiser for 1 h. The mixture was then cooled rapidly to room temperature, by passing compressed air through the microwave cavity for 5 min, and then filtered through Celite®. The filtrate was poured into water (15 mL) and extracted with

Et₂O (15 mL). The aqueous layer was further extracted with Et₂O (15 mL) and the organic extracts were combined, dried (Na₂SO₄) and evaporated *in vacuo*. Purification by column chromatography on silica gel, eluting with EtOAc–petroleum ether (1:6 v/v), gave 4-{2-phenyl-6-[4-(pyrrolidin-1-yl)phenyl]pyrimidin-4-yl}benzonitrile **68o**.

6.2.5 General procedure for the microwave-assisted synthesis of 2,6-bis(alkynone)pyridine 79 catalysed by CuI

A solution of 2,6-pyridinecarbonyldichloride (0.566 mol, 1 equiv.), phenylacetylene (2.2 equiv.), CuI (15 mol%) and PdCl₂(PPh₃)₂ (15mol%) were dissolved in dry triethylamine (6 ml) and filled in a sealed pressure-rated reaction tube. Then the reaction mixture was irradiated at 100 °C *(Initial Power: 150 W, Pressure: 200 Psi and Running Time: 5 min)* for 45 min in a self turned single mode CEM Discover® Focused Synthesiser. The mixture was cooled rapidly to room temperature, by passing compressed air through the microwave cavity for 5 min, then filtered through Celite® and evaporated *in vacuo*. The crude product was purified by column chromatography on alumina, eluted with light petroleum-ethyl acetate (3:1 v/v) to give the *title compound* **79a**.

6.2.6 General procedure for the microwave-assisted one-pot heteroannelation of terpyridine 80 catalysed by ZnBr₂

A solution of 3,3'-(4-aryl)-1,1'-(pyridin-2-yl)-biprop-2-yn-1-one **79** (0.849 mmol, 1.5 equiv.), 3-aminocrotononitrile **10c** (2 equiv.) and ZnBr₂ (15 mol%) were dissolved in ethanol (6 ml) and filled in a sealed pressure-rated reaction tube. Then the reaction mixture was irradiated at 150 °C *(Initial Power: 150 W, Pressure: 200 Psi and Running Time: 5 min)* for 45 min in a self turned single mode CEM Discover® Focused Synthesiser. The mixture was cooled rapidly to room temperature, by passing compressed air through the microwave cavity for 5 min, then poured into water (15 mL) and extracted with ethyl acetate (8 mL). The aqueous layer was further extracted with ethyl acetate (8 mL) and the organic extracts were combined, washed sequentially with saturated sodium hydrogen phosphate (10 mL) to remove the excess ZnBr₂, brine (10 mL), dried over sodium sulfate and evaporated *in vacuo*. The crude product was purified by column chromatography on silica gel, eluted with ethyl acetate-hexane (1:6 v/v) to give the *title compound* **80**.

6.2.7 General procedure for the microwave-assisted copper(I)-mediated N-arylation terpyridine bromide

A solution of pyrrolidine (4.2 equiv.), CuI (10 mol%) neocuproine (10 mol%) and sodium ethoxide (4.2 equiv.) was dissolved in toluene (4 mL) and filled in a sealed pressure-rated reaction

tube. The mixture was irradiated at 150 °C for 5 min, then left cooled to room temperature and 4,4''-(4-bromophenyl)-5,5''-nitrile-6,6''-methyl-2,2':6',2''-terpyridine **80e** (0.566 mmol, 1 equiv.) in toluene (2 mL) was added. The reaction mixture was irradiated at 150 °C *(Initial Power: 150 W, Pressure: 200 Psi and Running Time: 5 min)* for 60 min in a self turned single mode CEM Discover® Focused Synthesiser. The mixture was then cooled rapidly to room temperature, by passing compressed air through the microwave cavity for 5 min, and then filtered through Celite®. The filtrate was poured into water (15 mL) and extracted with diethyl ether (15 mL). The aqueous layer was further extracted with ether (15 mL) and the organic extracts were combined, dried over sodium sulfate and evaporated in *vacuo*. The crude product was purified by column chromatography on silica gel, eluted with ethyl acetate-petroleum ether (1:6 v/v) to give the *title compound* **80g**.

6.2.8 General procedure for the microwave-assisted suzuki-miyaura reaction: synthesis of 2-2-Methyl-4-(4-biphenyl)-6-(2-pyridyl)nicotinonitrile 53n[171]

A solution of 2-methyl-4-(4-bromophenyl)-6-(2-pyridyl)nicotinonitrile **53g** (0.57 mmol, 2 equiv.) in DMSO (3 mL) was added to a suspension of Pd(PPh$_3$)$_4$ (0.029 mmol, 10 mol%) in the same solvent (1 mL). The mixture was stirred for 5 min while degassing with nitrogen in a pressure-rated Pyrex reaction tube (10 mL). To this solution was added phenylboronic acid (0.29 mmol, 1 equiv) and Na$_2$CO$_3$ (0.86 mmol, 3 equiv) in DMSO (2 mL), and then the mixture was stirred for a further 5 min under nitrogen. The reaction tube was sealed and irradiated at 150 °C, at an initial power of 150 W, in a self-tuned single mode CEM Discover® Focused Synthesizer for 30 min. The mixture was cooled rapidly to room temperature, by passing compressed air through the microwave cavity for 5 min, and then filtered through Celite®. The filtrate was poured into water (15 mL) and extracted with acetonitrile (15 mL). The aqueous layer was further extracted with acetonitrile (15 mL) and the organic extracts were combined, washed sequentially with water (10 mL) and brine (10 mL), dried (Na$_2$SO$_4$) and evaporated *in vacuo*. Purification by flash chromatography on silica gel, eluting with acetonitirle-acetone (1:1), gave the *title compound* **53n**.

6.2.9 General procedure for the microwave-assisted copper(I) mediated N-arylation: synthesis of 2-2-Methyl-4-[4-(diphenylamino)phenyl]-6-(2-pyridyl)nicotinonitrile 53o[81]

A solution of 2-methyl-4-(4-bromophenyl)-6-(2-pyridyl)nicotinonitrile **53g** (0.57 mmol, 2 equiv) in toluene (3 mL) was added to a stirred solution of diphenylamine (1.13 mmol, 2 equiv), Cu(neocup)(PPh$_3$)Br[81] (10 mol%) and potassium-*tert*-butoxide (0.85 mmol, 1.5 equiv) in toluene (3 mL) in a pressure-rated Pyrex reaction tube (10 mL). The vessel was sealed and irradiated at

120 °C, at an initial power of 150 W, in a self-turned single mode CEM Discover® Focused Synthesiser for 1 h. The mixture was then cooled rapidly to room temperature, by passing compressed air through the microwave cavity for 5 min, and then filtered through Celite®. The filtrate was poured into water (15 mL) and extracted with diethyl ether (15 mL). The aqueous layer was further extracted with ether (15 mL) and then the organic extracts were combined, dried (Na_2SO_4) and evaporated *in vacuo*. Purification by flash chromatography on silica gel, eluting with ethyl acetate-light petroleum ether (1:6), gave the *title compound* **53o**.

6.2.10 General procedure for the microwave-assisted complexation: cyanobipyridyl-Zn^{II}-bis(thiolate) complexes 85[172]

To a solution of zinc acetate dihydrate (0.4 mmol, 1 equiv) dissolved in 3 mL of hot ethanol in a pressure-rated Pyrex reaction tube (10 mL), thiophenol (0.8 mmol, 2 equiv) was added dropwise with rapid stirring. As the second portion was added, a white precipitate formed immediately. After 5 min of continual stirring, a solution of 2-2-methyl-4-(4-biphenyl)-6-(2-pyridyl)nicotinonitrile **53n** (0.4 mmol, 1 equiv) in ethanol (3 mL) was added dropwise. After another 5 min of vigorous stirring, a SiC passive heating element (*Anton Paar Ltd.*) was added to the mixture and the vessel was sealed and irradiated at 120 °C, at an initial power of 150 W, in a self-turned single mode CEM Discover® Focused Synthesiser for 10 min. The mixture was then cooled rapidly to room temperature, by passing compressed air through the microwave cavity for 5 min, and then filtered through a sinter funnel. The crude sample was collected and washed thoroughly with ethanol (10 mL) and diethyl ether (10 mL). The solid product was redissolved in CH_2Cl_2 and diffusion of diethyl ether vapour into its concentrated solution, gave the *title compound* **85a**.

6.2.11 General procedure for the microwave-assisted complexation: Zn^{II}-bis{3-cyano-4-[4-(diphenylamino)phenyl]bipyridyl} perchlorate complex 86[173]

To a solution of 2-2-methyl-4-[4-(diphenylamino)phenyl]-6-(2-pyridyl)nicotinonitrile **53o** (0.4 mmol, 2 equiv) dissolved in 3 mL of hot dichloromethane in a pressure-rated Pyrex reaction tube (10 mL), zinc perchlorate hexahydrate (0.2 mmol, 1 equiv) in hot dichloromethane (3 mL) was added dropwise. After 5 min of vigorous stirring, a SiC passive heating element (*Anton Paar Ltd.*) was added into the mixture and the vessel was sealed and irradiated at 120 °C, at an initial power of 150 W, in a self-turned single mode CEM Discover® Focused Synthesiser for 10 min. The mixture was then cooled rapidly to room temperature, by passing compressed air through the microwave cavity for 5 min, and then filtered through a sinter funnel. The filtrate was concentrated in vacuum to *ca.* 3 mL, and then

vapour diffusion of diethyl ether (3 mL) into the remaining solution gave the *title compound* **86**.

6.3 Experimental procedures

Literature procedure for the synthesis of propargylic alcohols (52).[78]
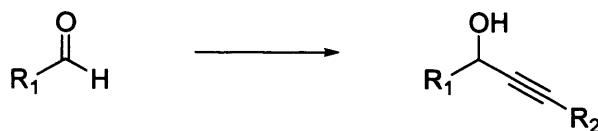
A solution of *n*-butyllithium (11.2 mmol, 1 equiv.) in toluene (1.4 M; 8 mL) was added to a stirred solution of 4-ethynylanisole (1.17 mL, 11.2 mmol) in anhydrous THF (60 mL) at -78 °C under a nitrogen atmosphere. After the mixture was stirred for 1 h, *p*-anisaldehyde (1.00 mL, 8.00 mmol) was added and the temperature was maintained at -78 °C under nitrogen overnight. After the reaction was complete, the mixture was poured over ice (10 g) and partitioned between saturated aqueous ammonium chloride solution (30 mL) and diethyl ether (30 mL). The aqueous layer was further extracted with diethyl ether (2 × 25 mL) and the combined ethereal extracts were washed sequentially with water (50 mL) and brine (50 mL), dried (MgSO$_4$) and evaporated *in vacuo*. Purification by column chromatography on silica gel, eluting with hexane–light petroleum (1:6), gave propargylic alcohols **52** as clear oils, with satisfactory spectroscopic and spectrometric characterisation data.

2-Methyl-6-phenylnicotinonitrile (53a)
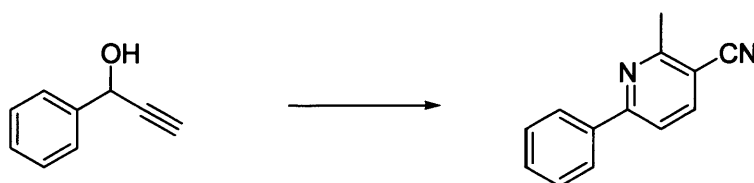
2-Methyl-6-phenylnicotinonitrile (**53a**) (0.10 g, 86%) was prepared according to the given procedure **6.2.1** using 1-phenyl-2-propyn-1-ol **52a** (0.14 mL, 1.14 mmol) and was obtained as colourless crystals, mp 137–139 °C (Lit.,[59] mp 139–140 °C) (Found: MH$^+$ 195.0916. C$_{13}$H$_{11}$N$_2$ [MH$^+$] requires 195.0917); ν_{max} 2222, 1640, 1579, 1444, 1384, 1285, 783, 741, 694; λ_{max}(CHCl$_3$)/nm 224 (log ε 4.62), 302 (log ε 4.18); δ_H (400 MHz; CDCl$_3$) 8.96 (2H, m, 2',6'-H), 7.86 (1H, d, *J* 8.2, 4-H), 7.58 (1H, d, *J* 8.2, 5-H), 7.43 (3H, m, 3',4',5'-H), 2.76 (3H, s, 2-Me); δ_C (100 MHz; CDCl$_3$) 161.6 (C), 159.8 (C), 140.7 (CH), 137.7 (C), 133.1 (C), 130.4 (CH), 129.0 (CH), 127.4 (CH), 117.4 (CH), 106.7 (CN), 23.9 (CH$_3$); *m/z* (APcI) 195 (MH$^+$, 100%).

4,6-Bis(4-methoxyphenyl)-2-methylnicotinonitrile (53b)
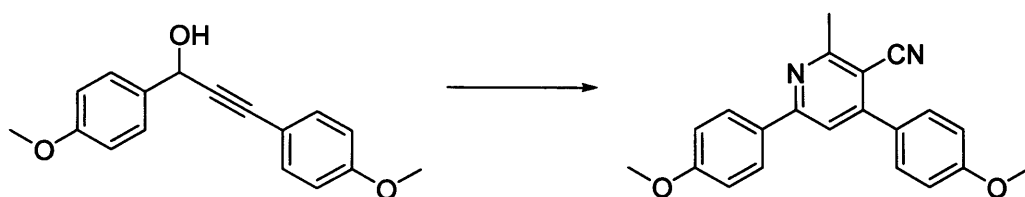
4,6-Bis(4-methoxyphenyl)-2-methylnicotinonitrile (**53b**) (0.17 g, 88%) was prepared according to the given procedure **6.2.1** using 1,3-bis(4-methoxyphenyl)prop-2-yn-1-ol **52b** (0.28 mL, 1.14 mmol) and was obtained as colourless crystals, mp 172-173 °C (Lit.,[59] mp 172-173 °C) (Found: MH^+, 331.1435. $C_{21}H_{19}N_2O_2$ [MH^+] requires 331.1447); v_{max} 3050, 2210, 1640, 1600, 1450, 1314, 1250, 1090, 912; λ_{max}(CHCl$_3$)/nm 236 (log ε 4.58), 322 (log ε 4.18); δ_H (400 MHz; CDCl$_3$) 8.08 (2H, app. d, J 8.9, 2',6'-H), 7.63 (2H, app. d, J 8.9, 2'',6''-H), 7.61 (1H, s, 5-H), 7.08 (2H, app. d, J 8.9, 3',5'-H), 7.04 (2H, app. d, J 8.9, 3'',5''-H), 3.94 (3H, s, OMe), 3.92 (3H, s, OMe), 2.90 (3H, s, 2-Me); δ_C (100 MHz; CDCl$_3$) 166.2 (C), 157.2 (C), 156.6 (C), 155.4 (C), 153.1 (C), 147.7 (C), 134.4 (C), 124.9 (C), 124.3 (CH), 123.4 (CH), 112.3 (CH), 111.2 (CH), 108.9 (CH), 106.2 (CN), 59.9 (CH$_3$), 58.9 (CH$_3$), 28.9 (CH$_3$); m/z 331 (MH$^+$, 100%).

2-Methyl-4-[4-(dimethylamino)phenyl]-6-(4-methoxyphenyl)nicotinonitrile (53c)
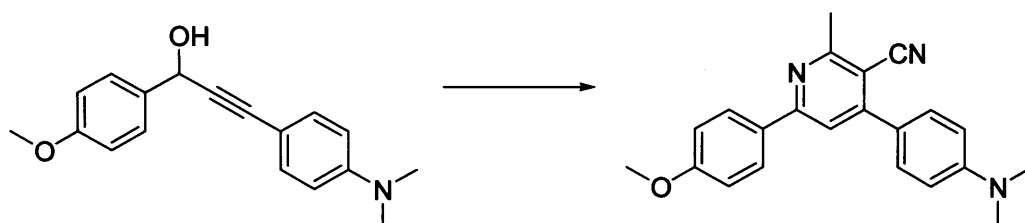
2-Methyl-4-[4-(dimethylamino)phenyl]-6-(4-methoxyphenyl)nicotinonitrile (**53c**) (0.18 g, 92%) was prepared according to the given procedure **6.2.1** using 3-[4-(dimethylamino)phenyl]-1-(4-methoxyphenyl)prop-2-yn-1-ol **52c** (0.30 mL, 1.14 mmol) and was obtained as iridescent yellow coloured crystals, mp 195-196 °C (Lit.,[59] mp 194-196 °C) (Found: MH$^+$, 344.1759. $C_{22}H_{22}N_3O$ [MH^+] requires 344.1763); v_{max} 3042, 2992, 2211, 1634, 1598, 1461, 1300, 1250, 1100, 1004, 920; λ_{max}(CHCl$_3$)/nm 240 (log ε 4.56), 374 (log ε 4.15); δ_H (400 MHz; CDCl$_3$) 7.96 (2H, app. d, J 8.9, 2',6'-H), 7.54 (2H, app. d, J 8.9, 2'',6''-H), 7.52 (1H, s, 5-H), 6.94 (2H, app. d, J 8.9, 3',5'-H), 6.76 (2H, app. d, J 8.9, 3'',5''-H), 3.82 (3H, s, OMe), 2.98 (6H, s, NMe$_2$), 2.88 (3H, s, 2-Me); δ_C (100 MHz; CDCl$_3$) 164.8 (C), 163.6 (C), 161.5 (C), 152.7 (C), 151.5 (C), 150.9 (C), 148.6 (C), 143.3 (C), 129.9 (CH), 128.9 (CH), 124.0 (CH), 116.8 (CH), 114.4 (CH), 106.9 (CN), 55.5 (CH$_3$), 40.4 (CH$_3$×2), 24.5 (CH$_3$); m/z 344 (MH$^+$, 100%).

2-Methyl-4-(4-bromophenyl)-6-(4-methoxyphenyl)nicotinonitrile (53d)
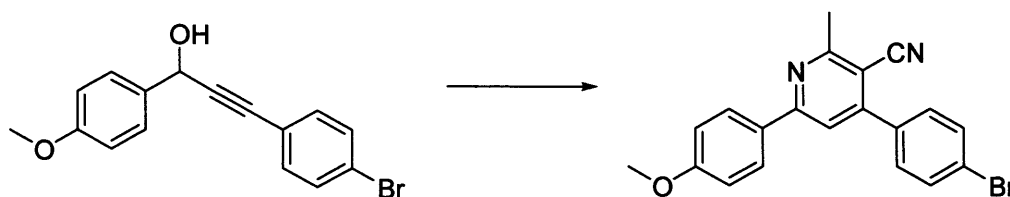
2-Methyl-4-(4-bromophenyl)-6-(4-methoxyphenyl)nicotinonitrile **(53d)** (0.19 g, 89%) was prepared according to the given procedure **6.2.1** using 3-(4-bromophenyl)-1-(4-methoxyphenyl)prop-2-yn-1-ol **52d** (0.33 mL, 1.14 mmol) and was obtained as colourless crystals, mp 224-226 °C (Found: MH$^+$, 379.2498. $C_{20}H_{16}BrN_2O$ [MH$^+$] requires 379.0368); v_{max} 3032, 2972, 2213, 1632, 1588, 1451, 1229, 1240, 1102, 1006, 918; λ_{max}(CHCl$_3$)/nm 228 (log ε 4.60), 314 (log ε 4.28); δ$_H$ (400 MHz; CDCl3) 7.98 (2H, app. d, *J* 8.9, 2',6'-H), 7.64 (2H, app. d, *J* 8.8, 3'',5''-H), 7.54 (1H, s, 5-H), 6.92 (2H, app. d, *J* 8.9, 3',5'-H), 6.82 (2H, app. d, *J* 8.8, 2'',6''-H), 3.82 (3H, s, OMe), 2.90 (3H, s, 2-Me); δ$_C$ (100 MHz; CDCl$_3$) 165.8 (C), 164.8 (C), 162.5 (C), 154.7 (C), 153.5 (C), 152.4 (C), 149.6 (C), 144.4 (C), 130.2 (CH), 129.4 (CH), 125.0 (CH), 118.8 (CH), 116.4 (CH), 105.2 (CN), 55.4 (CH$_3$), 26.4 (CH$_3$); *m/z* (ES) 379 (MH$^+$, 100%), 381 (97).

2-Methyl-6-4-(4-methoxyphenyl)-(2-pyridyl)nicotinonitrile (53e)
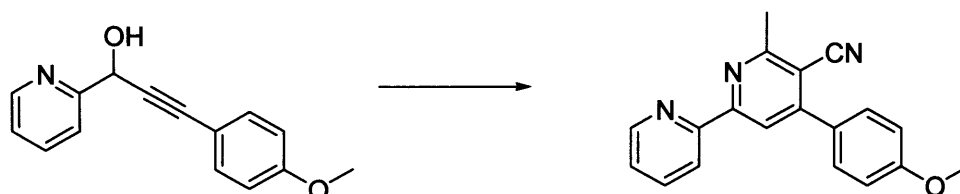
2-Methyl-6-4-(4-methoxyphenyl)-(2-pyridyl)nicotinonitrile **(53e)** (0.14 g, 84%) was prepared according to the given procedure **6.2.1** using 3-[4-methoxyphenyl]-1-(2-pyridyl)prop-2-yn-1-ol **52e** (0.25 mL, 1.14 mmol) and was obtained as colourless crystals, mp 197-199 °C (Lit.,[59] mp 197-199 °C) (Found: MH$^+$, 302.3419. $C_{19}H_{16}N_3O$ [MH$^+$] requires 302.1215); v_{max} 3042, 2982, 2233, 1630, 1568, 1450, 1326, 1230, 1106, 1008, 922; λ_{max}(CHCl$_3$)/nm 238 (log ε 4.76), 336 (log ε 4.56); δ$_H$ (400 MHz; CDCl$_3$) 8.72 (1H, d, *J* 6.4, 2'-H), 8.56 (1H, d, *J* 7.9, 5'-H), 8.46 (1H, s, 5-H), 7.88 (1H, m, 4'-H), 7.72 (2H, app. d, *J* 8.8, 2'',6''-H), 7.48 (1H, m, 3'-H), 7.08 (2H, app. d, *J* 8.8, 3'',5''-H), 3.90 (3H, s, OMe), 2.96 (3H, s, 2-Me); δ$_C$ (100 MHz; CDCl$_3$) 161.2 (C), 161.0 (C), 159.6 (C), 155.4 (C), 154.4 (C), 149.3 (CH), 137.2 (CH), 130.3 (C), 128.4 (CH), 128.0 (CH), 124.0 (CH), 120.0 (CH), 118.7 (CH), 117.0 (CH), 105.6 (CN), 55.6 (CH$_3$), 24.4 (CH$_3$); *m/z* 302 (MH$^+$, 100%).

2-Methyl-4-[4-(dimethylamino)phenyl]-6-(2-pyridyl)nicotinonitrile (53f)
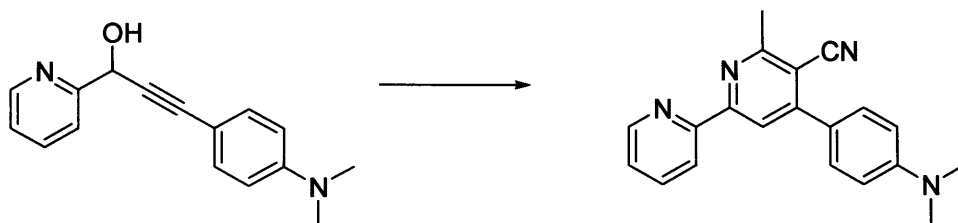
2-Methyl-4-[4-(dimethylamino)phenyl]-6-(2-pyridyl)nicotinonitrile (**53f**) (0.14 g, 80%) was prepared according to the given procedure **6.2.1** using 3-[4-(dimethylamino)phenyl]-1-(2-pyridyl)prop 2-yn-1-ol **52f** (0.26 mL, 1.14 mmol) and was obtained as iridescent green coloured crystals, mp 263-265 °C (Lit.,[59] mp 263-265 °C) (Found: MH$^+$, 315.3835. $C_{20}H_{19}N_4$ [MH$^+$] requires 315.1531); v_{max} 3046, 2984, 2221, 1632, 1565, 1452, 1323, 1230, 1104, 1006, 920; λ_{max}(CHCl$_3$)/nm 246 (log ε 4.68), 385 (log ε 4.38); δ_H (400 MHz; CDCl$_3$) 8.62 (1H, d, J 6, 2'-H), 8.42 (1H, d, J 8.0, 5'-H), 8.32 (1H, s, 5-H), 7.78 (1H, m, 4'-H), 7.62 (2H, app. d, J 8.8, 2'',6''-H), 7.28 (1H, m, 3'-H), 6.74 (2H, app. d, J 8.8, 3'',5''-H), 2.98 (6H, s, NMe$_2$), 2.82 (3H, s, 2-Me); δ_C (100 MHz; CDCl$_3$) 160.2 (C), 159.0 (C), 158.6 (C), 153.2 (C), 152.4 (C), 148.2 (CH), 135.8 (CH), 129.8 (C), 127.4 (CH), 127.0 (CH), 122.0 (CH), 119.8 (CH), 116.9 (CH), 115.0 (CH), 106.2 (CN), 40.6 (CH$_3$×2), 23.6 (CH$_3$); m/z 315 (MH$^+$, 100%).

2-Methyl-4-(4-bromophenyl)-6-(2-pyridyl)nicotinonitrile (53g)
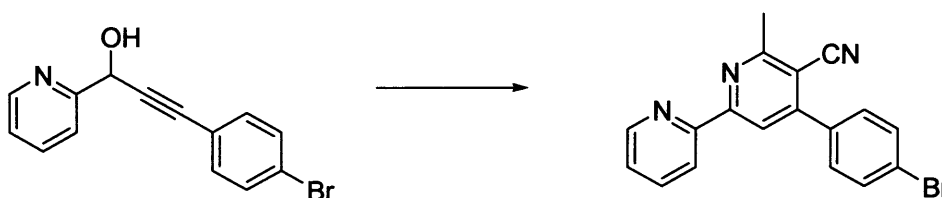
Methyl-4-(4-bromophenyl)-6-(2-pyridyl)nicotinonitrile (**53g**) (0.17 g, 87%) was prepared according to the given procedure **6.2.1** using 3-(4-bromophenyl)-1-(2-pyridyl)prop-2-yn-1-ol **52g** (0.30 mL, 1.14 mmol) and was obtained as colourless crystals, mp 296-298 °C (Found: MH$^+$, 350.2124. $C_{18}H_{13}BrN_3$ [MH$^+$] requires 350.0215); v_{max} 3052, 2988, 2216, 1630, 1558, 1450, 1322, 1228, 1102, 1004, 916; λ_{max}(CHCl$_3$)/nm 226 (log ε 4.64), 310 (log ε 4.26); δ_H (400 MHz; CDCl$_3$) 8.68 (1H, d, J 6, 2'-H), 8.52 (1H, d, J 8.0, 5'-H), 8.40 (1H, s, 5-H), 7.87 (1H, m, 4'-H), 7.72 (2H, app. d, J 8.8, 3'',5''-H), 7.34 (1H, m, 3'-H), 6.80 (2H, app. d, J 8.8, 2'',6''-H), 2.98 (3H, s, 2-Me); δ_C (100 MHz; CDCl$_3$) 164.2 (C), 160.0 (C), 159.6 (C), 156.2 (C), 154.6 (C), 150.2 (CH), 138.8 (CH), 130.8 (C), 128.4 (CH), 127.9 (CH), 124.0 (CH), 120.8 (CH), 119.6 (CH), 118.0 (CH), 104.8 (CN), 26.4 (CH$_3$); m/z 350 (MH$^+$, 100%), 352(97).

133

2-Methyl-4-(4-methoxyphenyl)-6-[4-(piperidino)phenyl]nicotinonitrile (53h)
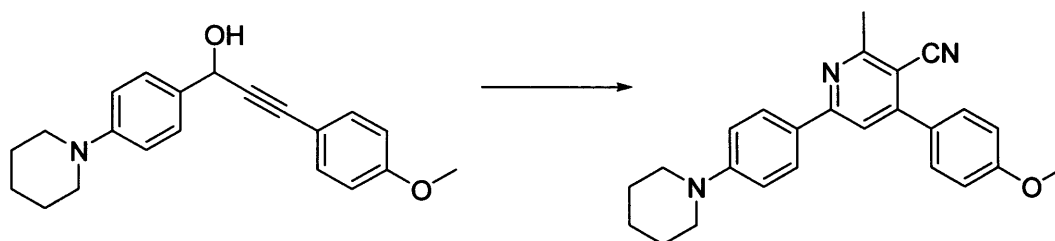
2-Methyl-4-(4-methoxyphenyl)-6-[4-(piperidino)phenyl]nicotinonitrile **(53h)** (0.19 g, 88%) was prepared according to the given procedure **6.2.1** using 3-(4-methoxyphenyl)-1-[4 (piperidino)phenyl]prop-2-yn-1-ol **52h** (0.33 mL, 1.14 mmol) and was obtained as pale yellow crystals, mp 212-214 °C (Found: MH^+, 384.4854. $C_{25}H_{26}N_3O$ $[MH^+]$ requires 384.1998); v_{max} 3054, 2994, 2218, 1636, 1560, 1456, 1326, 1230, 1106, 1008, 922; $\lambda_{max}(CHCl_3)$/nm 238 (log ε 4.38), 336 (log ε 4.50); δ_H (400 MHz; $CDCl_3$) 8.00 (2H, app. d, J 8.9, 2',6'-H), 7.82 (2H, app. d, J 8.8, 2''',6'''-H), 7.66 (1H, s, 5-H), 7.02 (2H, app. d, J 8.8, 3''',5'''-H), 6.90 (2H, app. d, J 8.9, 3',5'-H), 3.70 (3H, s, OMe), 3.34 (4H, t, J 4.9, 2'',6''-CH_2), 2.88 (3H, s, 2-Me), 1.68 (6H, m, 3'',4'',5''-CH_2); δ_C (100 MHz; $CDCl_3$) 161.2 (C), 161.0 (C), 158.9 (C), 154.4 (C), 148.2 (C), 130.4 (C), 128.5 (CH), 128.4 (CH), 125.8 (C), 118.6 (CH), 117.0 (CH), 114.8 (CH), 114.6 (CH), 106.2 (CN), 55.9 (CH_3), 52.4 (CH_2×2), 25.9 (CH_2×2), 25.5 (CH_2), 24.4 (CH_3); m/z 384 (MH^+, 100%).

2-Methyl-4-[4-(dimethylamino)phenyl]-6-[4-(piperidino)phenyl]nicotinonitrile (53i)
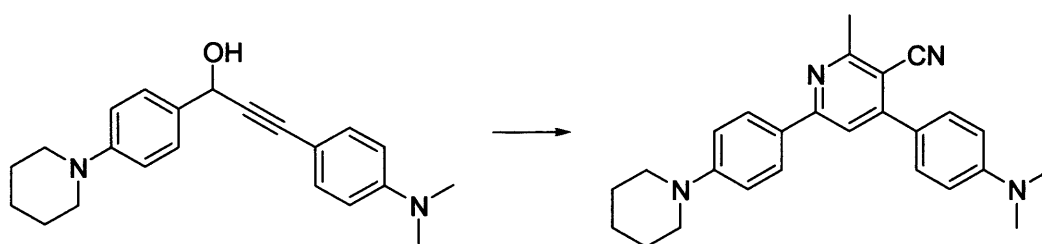
2-Methyl-4-[4-(dimethylamino)phenyl]-6-[4-(piperidino)phenyl]nicotinonitrile **(53i)** (0.19 g, 86%) was prepared according to the given procedure **6.2.1** using 3-[4-(dimethylamino)phenyl]-1-[4- (piperidino)phenyl]prop-2-yn-1-ol **52i** (0.35 mL, 1.14 mmol) and was obtained as iridescent green coloured crystals, mp 214-216 °C (Found: MH^+, 397.5214. $C_{26}H_{29}N_4$ $[MH^+]$ requires 397.2314); v_{max} 3056, 2998, 2219, 1636, 1562, 1457, 1328, 1231, 1104, 1008, 924; $\lambda_{max}(CHCl_3)$/nm 248 (log ε 4.24), 364 (log ε 4.60); δ_H (400 MHz; $CDCl_3$) 7.98 (2H, app. d, J 8.9, 2',6'-H), 7.62 (2H, app. d, J 8.8, 2''',6'''-H), 7.53 (1H, s, 5-H), 7.00 (2H, app. d, J 8.9, 3',5'-H), 6.84 (2H, app. d, J 8.8, 3''',5'''-H), 3.34 (4H, t, J 4.9, 2'',6''-CH_2), 3.08 (6H, s, NMe_2), 2.86 (3H, s, 2-Me), 1.70 (6H, m, 3'',4'',5''-CH_2); δ_C (100 MHz; $CDCl_3$) 160.2 (C), 159.0 (C), 158.6 (C), 153.4 (C), 148.0 (C), 129.4 (C), 127.5 (CH), 127.4 (CH), 124.8 (C), 116.6 (CH), 116.0 (CH),

113.8 (CH), 112.6 (CH), 106.8 (CN), 55.4 (CH3), 52.6 (CH₂×2), 40.6 (CH₃×2), 26.0 (CH₂×2), 25.8 (CH₂), 24.2 (CH₃); *m/z* 397 (MH⁺, 100%).

2-Methyl-4-(4-bromophenyl)-6-[4-(piperidino)phenyl]nicotinonitrile (53j)
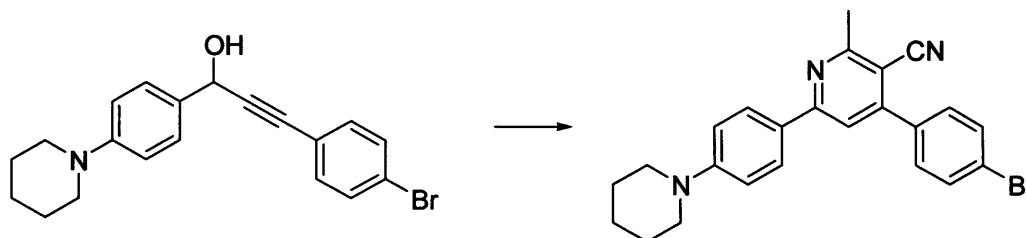
2-Methyl-4-(4-bromophenyl)-6-[4-(piperidino)phenyl]nicotinonitrile **(53j)** (0.20 g, 82%) was prepared according to the given procedure **6.2.1** using 3-(4-bromophenyl)-1-[4-(piperidino)phenyl]prop-2-yn-1-ol **52j** (0.39 mL, 1.14 mmol) and was obtained as pale white crystals, mp 296-298 °C (Found: MH⁺, 432.3558. C₂₄H₂₃BrN₃ [MH⁺] requires 432.0997); νmax 3052, 2994, 2216, 1630, 1554, 1450, 1320, 1230, 1100, 1004, 918; λmax(CHCl₃)/nm 220 (log ε 4.48), 312 (log ε 4.10);δH (400 MHz; CDCl₃) 8.00 (2H, app. d, *J* 8.9, 2',6'-H), 7.68 (2H, app. d, *J* 8.8, 3''',5'''-H), 7.60 (1H, s, 5-H), 7.00 (2H, app. d, *J* 8.8, 2''',6'''-H), 6.90 (2H, app. d, *J* 8.9, 3',5'-H), 3.36 (4H, t, *J* 4.9, 2'',6''-CH₂), 2.89 (3H, s, 2-Me), 1.72 (6H, m, 3'',4'',5''-CH₂); δC (100 MHz; CDCl₃) 162.2 (C), 161.0 (C), 160.4 (C), 156.4 (C), 150.0 (C), 132.4 (C), 130.5 (CH), 128.4 (CH), 126.8 (C), 118.6 (CH), 117.0 (CH), 116.8 (CH), 114.6 (CH), 105.0 (CN), 55.6 (CH₃), 52.8 (CH₂×2), 28.0 (CH₂), 25.8 (CH₂×2), 24.8 (CH₃); *m/z* 432 (MH⁺, 100%), 434 (97).

2-Methyl-6-(4-methoxphenyl)-4-[4-(pyrrolidino)phenyl]nicotinonitrile (53k)
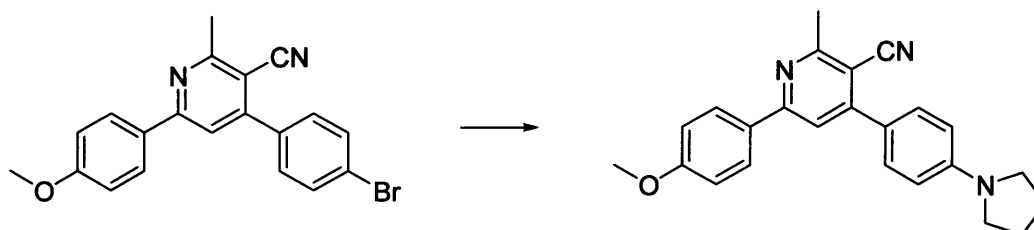
2-Methyl-6-(4-methoxphenyl)-4-[4-(pyrrolidino)phenyl]nicotinonitrile **(53k)** (0.32 g, 86%) was prepared according to the given procedure **6.2.2** using 2-methyl-4-(4-bromophenyl)-6-(4-methoxphenyl)nicotinonitrile **53d** (0.38 g, 1.00 mmol) and was obtained as iridescent green coloured crystals, mp 196-198 °C (Found: MH⁺, 370.4588. C₂₄H₂₄N₃O [MH⁺] requires 370.1841); vmax 3044, 2998, 2218, 1639, 1599, 1464, 1302, 1254, 1106, 1008, 922; λmax(CHCl₃)/nm 252 (log ε 4.48), 386 (log ε 4.03); δH (400 MHz; CDCl₃) 7.98 (2H, app. d, *J* 8.9, 2',6'-H), 7.52 (2H, app. d, *J* 8.8, 2'',6''-H), 7.50 (1H, s, 5-H), 6.98 (2H, app. d, *J* 8.9, 3',5'-H), 6.70 (2H, app. d, *J*

8.8, 3'',5''-H), 3.82 (3H, s, OMe), 3.20 (4H, t, J 6.6, 2''',5'''-CH$_2$), 2.86 (3H, s, 2-Me), 1.96 (4H, t, J 6.6, 3''',4'''-CH$_2$); δ_C (100 MHz; CDCl$_3$) 162.8 (C), 160.6 (C), 161.2 (C), 150.7 (C), 150.5 (C), 150.8 (C), 146.6 (C), 143.0 (C), 129.4 (CH), 128.6 (CH), 124.0 (CH), 116.8 (CH), 114.6 (CH), 107.0 (CN), 55.5 (CH$_3$), 46.4 (CH$_2$×2), 28.6 (CH$_2$×2), 24.2 (CH$_3$); m/z 370 (MH$^+$, 100%).

2-Methyl-4-[4-(pyrrolidino)phenyl]-6-(2-pyridyl)nicotinonitrile (53l)
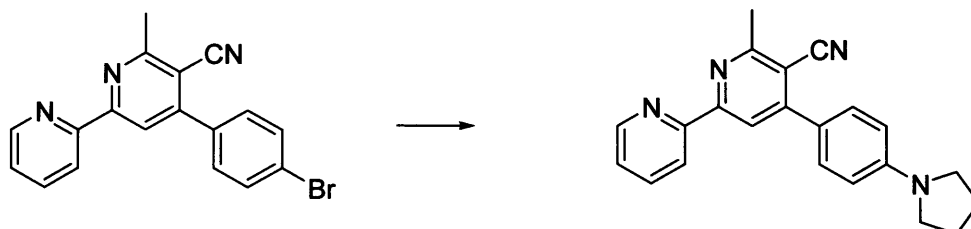
2-Methyl-4-[4-(pyrrolidino)phenyl]-6-(2-pyridyl)nicotinonitrile (53l) (0.25 g, 72%) was prepared according to the given procedure **6.2.2** using 2-methyl-4-(4-bromophenyl)-6-(2-pyridyl)nicotinonitrile **53g** (0.35 g, 1.00 mmol), catalysed by Cu(neocup)(PPh$_3$)Br[81] (10 mol%), and was obtained as iridescent green coloured crystals, mp 266-268 °C (Found: MH$^+$, 341.1780. C$_{22}$H$_{21}$N$_4$ [MH$^+$] requires 341.1766); ν_{max} 3048, 2988, 2216, 1634, 1569, 1458, 1329, 1232, 1105, 1008, 923; λ_{max}(CHCl$_3$)/nm 258 (log ε 4.60), 397 (log ε 4.16); δ_H (400 MHz; CDCl$_3$) 8.64 (1H, d, J 6.4, 2'-H), 8.42 (1H, d, J 8.0, 5'-H), 8.31 (1H, s, 5-H), 7.78 (1H, m, 4'-H), 7.60(2H, app. d, J 8.8, 2'',6''-H), 7.28 (1H, m, 3'-H), 6.60 (2H, app. d, J 8.8, 3'',5''-H), 3.20 (4H, t, J 6.6, 2''',5'''-CH$_2$), 2.82 (3H, s, 2-Me), 1.96 (4H, t, J 6.6, 3''',4'''-CH$_2$); δ_C (100 MHz; CDCl$_3$) 160.0 (C), 158.0 (C), 158.6 (C), 152.2 (C), 151.4 (C), 148.0 (CH), 133.8 (CH), 129.6 (C), 126.8 (CH), 127.0 (CH), 121.0 (CH), 119.4 (CH), 116.8 (CH), 114.8 (CH), 106.6 (CN), 46.4 (CH$_2$×2), 28.6 (CH$_2$×2), 23.6 (CH$_3$); m/z (APcI) 341 (MH$^+$, 100%).

2-Methyl-4-[4-(pyrrolidino)phenyl)]-6-[4-(piperidino)phenyl]nicotinonitrile (53m)
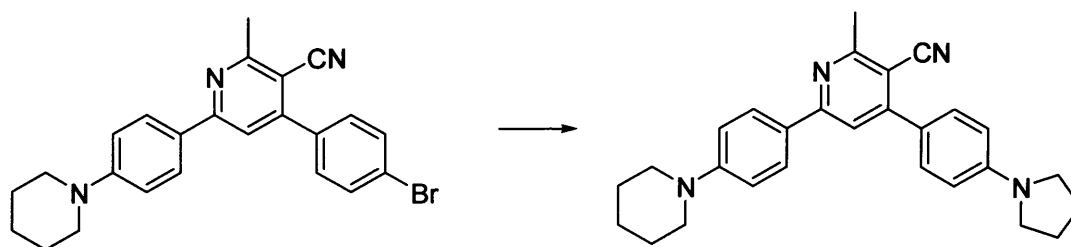
2-Methyl-4-[4-(pyrrolidino)phenyl)]-6-[4-(piperidino)phenyl]nicotinonitrile (53m) (0.37 g, 88%) was prepared according to the given procedure **6.2.2** using 2-methyl-4-(4-bromophenyl)-6-[4-(piperidino)phenyl]nicotinonitrile **53j** (0.44 g, 1.00 mmol) and was obtained as iridescent yellow coloured crystals, mp 216-218 °C (Found: MH$^+$, 423.2532. C$_{28}$H$_{31}$N$_4$ [MH$^+$] requires 423.2549);

v_{max} 3058, 2999, 2220, 1637, 1564, 1459, 1329, 1233, 1106, 1008, 926; λ_{max}(CHCl$_3$)/nm 252 (log ε 4.20), 370 (log ε 4.58); δ_H (400 MHz; CDCl$_3$) 7.98 (2H, app. d, *J* 8.9, 2',6'-H), 7.60 (2H, app. d, *J* 8.8, 2''',6'''-H), 7.58 (1H, s, 5-H), 7.00 (2H, app. d, *J* 8.9, 3',5'-H), 6.68 (2H, app. d, *J* 8.8, 3''',5'''-H), 3.48 (4H, t, *J* 6.6, 2'''',5''''-CH$_2$), 3.34 (4H, t, *J* 4.9, 2'',6''-CH$_2$), 2.88 (3H, s, 2-Me), 2.06 (4H, t, *J* 6.6, 3'''',4''''-CH$_2$), 1.70 (6H, m, 3'',4'',5''-CH$_2$); δ_C (100 MHz; CDCl$_3$) 159.8 (C), 159.0 (C), 158.4 (C), 153.3 (C), 148.1 (C), 129.2 (C), 126.9 (CH), 127.3 (CH), 124.5 (C), 116.4 (CH), 115.8 (CH), 113.6 (CH), 112.4 (CH), 107.2 (CN), 55.2 (CH$_3$), 52.6 (CH$_2$×2), 50.4 (CH$_2$×2), 28.6 (CH$_2$×2), 26.0 (CH$_2$), 25.8 (CH$_2$×2), 24.0 (CH$_3$); *m/z* (APcI) 423 (MH$^+$, 100%).

2,6-Diphenyl-pyrimidine (68a)
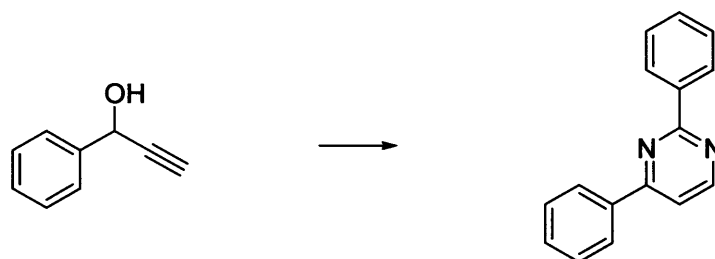
2,6-Diphenyl-pyrimidine (**68a**) (0.12 g, 92%) was prepared according to the given procedure **6.2.3** using 1-phenyl-2-propyn-1-ol **52** (0.57 mmol, 1 equiv.) and was obtained as colourless crystals, mp 140–142 °C (Lit.,[107] mp 139–140 °C) (Found: MH$^+$, 233.1026. C$_{16}$H$_{13}$N$_2$ [MH$^+$] requires 233.1000); v_{max} (KBr) 2988, 1634, 1600, 816; λ_{max}(CHCl$_3$)/nm 278 (log ε 4.26); δ_H (400 MHz; CDCl$_3$) 8.21 (1H, d, *J* 8.2, 3-H), 7.46 (4H, m, 2',6',2'',6''-H), 7.30 (6H, m, 3',4',5',3'',4'',5''-H), 7.10 (1H, d, *J* 8.2, 4-H); δ_C (100 MHz; CDCl$_3$) 162.5 (C), 158.3 (C), 157.6 (CH), 131.1 (C), 128.7 (C), 127.3 (CH×2), 127.0 (CH×2), 126.8 (CH), 126.0 (CH), 125.5 (CH×2), 125.0 (CH×2), 110.5 (CH); *m/z* 233 (MH$^+$, 100%).

2-Phenyl-4-(4-methoxyphenyl)-6-(4-methoxyphenyl)-pyrimidine (68b)
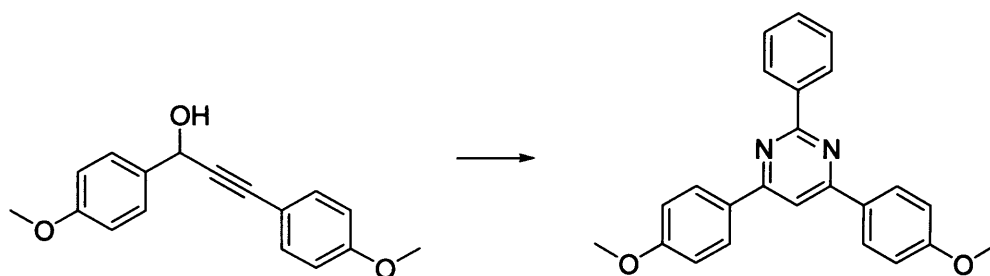
2-Phenyl-4-(4-methoxyphenyl)-6-(4-methoxyphenyl)-pyrimidine (**68b**) (0.15 g, 72%) was prepared according to the given procedure **6.2.3** using 1,3-bis(4-methoxyphenyl)prop-2-yn-1-ol
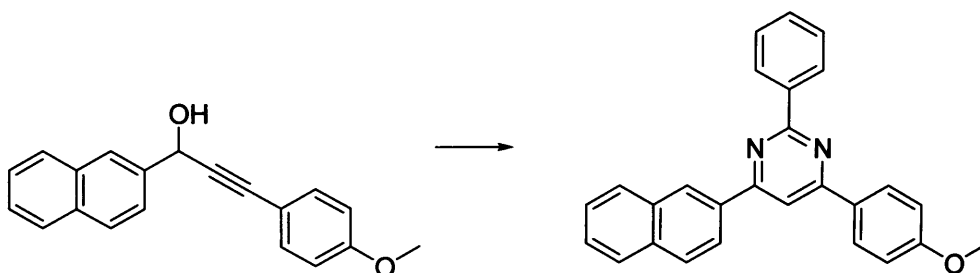
52 (0.57 mmol, 1 equiv.) and was obtained as colourless crystals, mp 174–176 °C (Found: MH$^+$, 369.1532. C$_{24}$H$_{21}$N$_2$O$_2$ [MH$^+$] requires 369.1525); ν$_{max}$ (KBr) 2986, 1632, 1602, 1260, 816; λ$_{max}$(CHCl$_3$)/nm 328 (log ε 4.20); δ$_H$ (400 MHz; CDCl$_3$) 7.46 (2H, m, 2'',6''-H), 7.35 (4H, app. d, *J* 8.8, 2',6',2''',6'''-H), 7.30 (3H, m, 3'',4'',5''-H), 7.26 (1H, s, 5-H), 6.80 (4H, app. d, *J* 8.8, 3',5',3''',5'''-H), 3.90 (6H, s, OCH$_3$×2); δ$_C$ (100 MHz; CDCl$_3$) 162.7 (C), 160.0 (C×2), 158.7 (C×2), 130.7 (C), 127.3 (CH×2), 126.5 (CH×4), 126.0 (CH), 125.5 (CH×2), 122.4 (C×2), 112.8 (CH×4), 102.0 (C), 58.9 (CH$_3$×2); *m/z* 369 (MH$^+$, 100%).

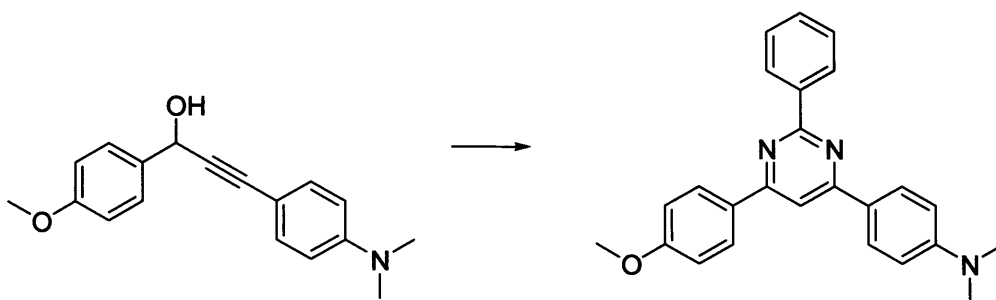## 2-Phenyl-4-(3-thienyl)-6-(4-methoxyphenyl)-pyrimidine (68c)
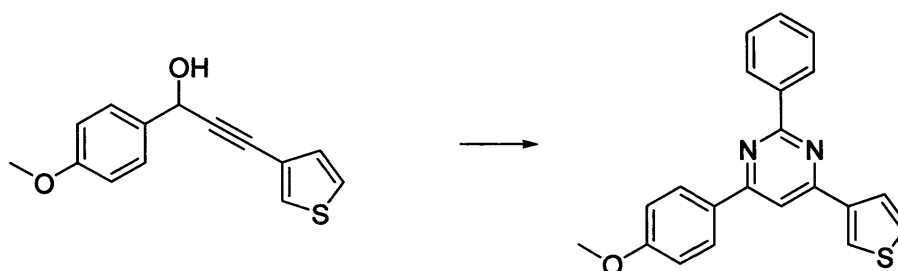
2-Phenyl-4-(3-thienyl)-6-(4-methoxyphenyl)-pyrimidine (**68c**) (0.16 g, 79%) was prepared according to the given procedure **6.2.3** using 1-(4-methoxyphenyl)-3-(3-thienyl)-prop-2-yn-1-ol **52** (0.57 mmol, 1 equiv.) and was obtained as pale yellow crystals, mp 168–170 °C (Found: MH$^+$, 345.1202. C$_{21}$H$_{17}$N$_2$OS [MH$^+$] requires 345.0983); ν$_{max}$ (KBr) 2988, 1630, 1602, 1264, 814; λ$_{max}$(CHCl$_3$)/nm 332 (log ε 4.22); δ$_H$ (400 MHz; CDCl$_3$) 7.46 (2H, m, 2'',6''-H), 7.35 (2H, app. d, *J* 8.8, 2',6'-H), 7.32 (1H, s, 5-H), 7.28 (3H, m, 3'',4'',5''-H), 7.20 (1H, dd, *J* 3, 1, 2'''-H), 7.18 (1H, dd, *J* 5, 3, 5'''-H), 6.82 (2H, app. d, *J* 8.8, 3',5'-H), 6.80 (1H, dd, *J* 5, 1, 4'''-H), 3.70 (3H, s, OCH$_3$); δ$_C$ (100 MHz; CDCl$_3$) 162.7 (C), 160.5 (C), 159.5 (C), 158.7 (C), 140.3 (C), 130.0 (C), 129.0 (CH×2), 126.8 (CH), 126.5 (CH×2), 126.3 (CH), 126.0 (CH), 125.5 (CH×2), 123.4 (C), 121.0 (CH), 112.8 (CH×2), 100.5 (C), 56.0 (CH$_3$); *m/z* 345 (MH$^+$, 100%).

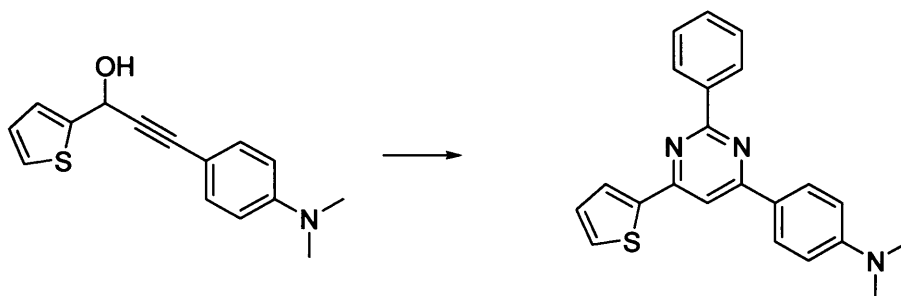## 2-Phenyl-4-(4-methoxyphenyl)-6-(2-thienyl)-pyrimidine (68d)
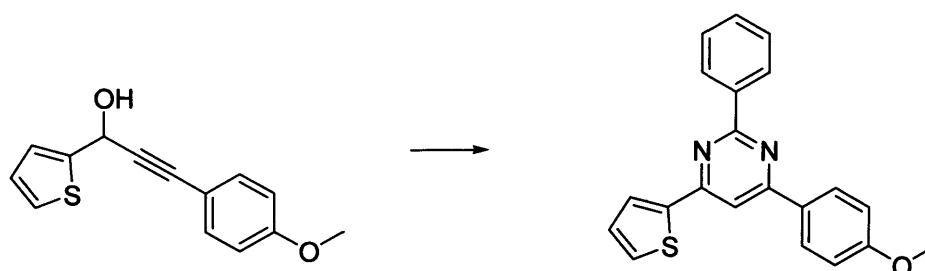
2-Phenyl-4-(4-methoxyphenyl)-6-(2-thienyl)-pyrimidine (**68d**) (0.17 g, 82%) was prepared according to the given procedure **6.2.3** using 1-(2-thienyl)-3-(4-methoxyphenyl)-prop-2-yn-1-ol

52 (0.57 mmol, 1 equiv.) and was obtained as colourless crystals, mp 169–171 °C (Found: MH$^+$, 345.1204. C$_{21}$H$_{17}$N$_2$OS [MH$^+$] requires 345.0983); ν_{max} (KBr) 2989, 1632, 1604, 1264, 816; λ_{max}(CHCl$_3$)/nm 334 (log ε 4.20); δ_H (400 MHz; CDCl$_3$) 7.46 (2H, m, 2'',6''-H), 7.35, (2H, app. d, *J* 8.8, 2''',6'''-H), 7.30 (1H, s, 5-H), 7.28 (3H, m, 3'',4'',5''-H), 7.20 (1H, d, *J* 3.9, 3'-H), 7.02 (1H, d, *J* 4.8, 5'-H), 6.96 (1H, dd, *J* 4.8, 3.9, 4'-H), 6.80 (2H, app. d, *J* 8.8, 3''',5'''-H), 3.70 (3H, s, OCH$_3$); δ_C (100 MHz; CDCl$_3$) 162.6 (C), 160.3 (C), 159.4 (C), 158.2 (C), 140.0 (C), 130.0 (C), 129.2 (CH×2), 126.5 (CH×2), 126.4 (CH), 126.3 (CH), 126.0 (CH), 125.3 (CH×2), 123.0 (C), 121.0 (CH), 112.6 (CH×2), 100.53 (C), 56.2 (CH$_3$); *m/z* 345 (MH$^+$, 100%).

2-Phenyl-4-(3-thienyl)-6-(2-thienyl)-pyrimidine (68e)
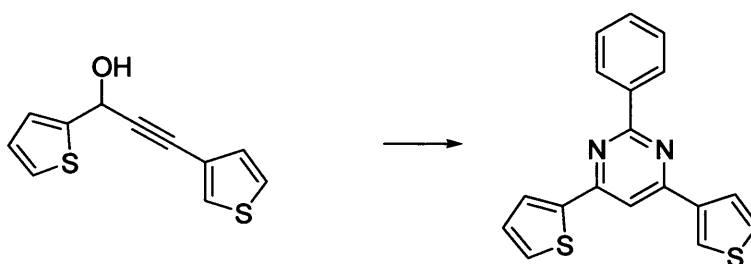
2-Phenyl-4-(3-thienyl)-6-(2-thienyl)-pyrimidine (**68e**) (0.16 g, 86%) was prepared according to the given procedure **6.2.3** using 1-(2-thienyl)-3-(3-thienyl)-prop-2-yn-1-ol **52** (0.57 mmol, 1 equiv.) and was obtained as light yellow crystals, mp 174–176 °C (Found: MH$^+$, 321.0456. C$_{18}$H$_{13}$N$_2$S$_2$ [MH$^+$] requires 321.0442); ν_{max} (KBr) 2990, 1634, 1606, 816; λ_{max}(CHCl$_3$)/nm 342 (log ε 4.18); δ_H (400 MHz; CDCl$_3$) 7.46 (2H, m, 2'',6''-H), 7.38 (1H, s, 5-H), 7.30 (3H, m, 3'',4'',5''-H), 7.26 (1H, d, *J* 3.9, 3'-H), 7.24 (1H, d, *J* 4.8, 5'-H), 7.22 (1H, dd, *J* 3, 1, 2'''-H), 7.20 (1H, dd, *J* 5, 3, 5'''-H), 7.06 (1H, dd, *J* 5, 1, 4'''-H), 7.02 (1H, dd, *J* 4.8, 3.9, 4'-H); δ_C (100 MHz; CDCl$_3$) 164.5 (C), 162.4 (C), 160.2 (C), 142.2 (C), 140.0 (C), 130.7 (C), 129.3 (CH×2), 128.8 (CH), 128.5 (CH), 128.2 (CH), 127.9 (CH), 127.6 (CH), 127.4 (CH×2), 125.5 (CH), 121.4 (CH), 102.4 (CH); *m/z* 321 (MH$^+$, 100%).

2-Phenyl-4-(4-methoxyphenyl)-6-(10-naphthyl)-pyrimidine (68f)

2-Phenyl-4-(10-naphthyl)-6-(4-methoxyphenyl)-pyrimidine (**68f**) (0.16 g, 73%) was prepared according to the given procedure **6.2.3** using 1-(10-naphthyl)-3-(4-methoxyphenyl)-prop-2-yn-1-ol **52** (0.57 mmol, 1 equiv.) and was obtained as colourless crystals, mp 182–184 °C (Found: MH^+, 389.1620. $C_{27}H_{21}N_2O$ [MH^+] requires 389.1576); v_{max} (KBr) 2989, 1640, 1610, 1266, 820; λ_{max}(CHCl$_3$)/nm 330 (log ε 4.22); δ_H (400 MHz; CDCl$_3$) 7.90 (1H, s, 1'-H), 7.74 (1H, d, J 8.6, 4'-H), 7.70 (2H, m, 6',7'-H), 7.54 (1H, d, J 8.6, 3'-H), 7.48 (2H, m, 2'',6''-H), 7.37 (2H, app. d, J 8.8, 2''',6'''-H), 7.32 (2H, m, 5',8'-H), 7.30 (3H, m, 3'',4'',5''-H), 7.28 (1H, s, 5-H), 6.84 (2H, app. d, J 8.8, 3''',5'''-H), 3.70 (3H, s, OCH$_3$); δ_C (100 MHz; CDCl$_3$) 164.5 9 (C), 162.4 (C), 161.3 (C), 160.7 (C), 134.3 (C), 133.8 (C), 132.6 (C), 130.7 (C), 129.3 (CH×2), 128.6 (CH), 128.4 (CH×2), 128.3 (CH), 128.1 (CH×2), 127.4 (CH×2), 127.0 (CH), 126.0 (CH×2), 125.4 (C), 124.5 (CH), 114.0 (CH×2), 102.0 (CH), 55.0 (CH$_3$); m/z 389 (MH^+, 100%).

2-Phenyl-4-(3-thienyl)-6-(10-naphthyl)-pyrimidine (68g)
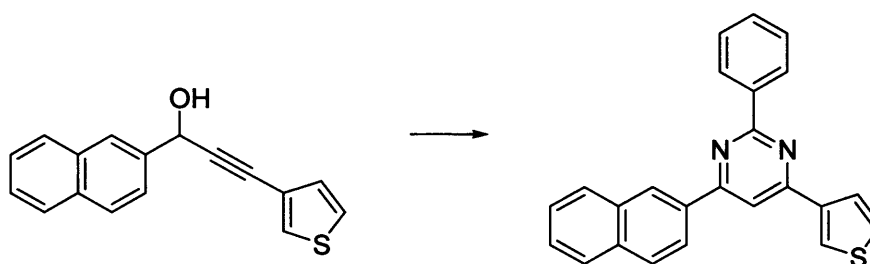
2-Phenyl-4-(10-naphthyl)-6-(3-thienyl)-pyrimidine (**68g**) (0.14 g, 68%) was prepared according to the given procedure **6.2.3** using 1-(10-naphthyl)-3-(3-thienyl)-prop-2-yn-1-ol **52** (0.57 mmol, 1 equiv.) and was obtained as pale yellow crystals, mp 176–178 °C (Found: MH^+, 365.1102. $C_{24}H_{17}N_2S$ [MH^+] requires 365.1034); v_{max} (KBr) 2990, 1642, 1608, 822; λ_{max}(CHCl$_3$)/nm 336 (log ε 4.24); δ_H (400 MHz; CDCl$_3$) 7.90 (1H, s, 1'-H), 7.75 (1H, d, J 8.6, 4'-H), 7.67 (2H, m, 6',7'-H), 7.56 (1H, d, J 8.6, 3'-H), 7.48 (2H, m, 2'',6''-H), 7.32 (3H, m, 3'',4'',5''-H), 7.30 (2H, m, 5',8'-H), 7.28 (1H, s, 5-H), 7.22 (1H, dd, J 3, 1, 2'''-H), 7.20 (1H, dd, J 5, 3, 5'''-H), 7.02 (1H, dd, J 5, 1, 4'''-H); δ_C (100 MHz; CDCl$_3$) 164.0 (C), 162.4 (C), 161.3 (C), 142.2 (C), 134.3 (C), 133.6 (C), 132.6 (C), 130.5 (C), 129.2 (CH×2), 128.8 (CH), 128.6 (CH), 128.3 (CH), 128.2 (CH), 128.1 (CH×2), 127.4 (CH×2), 126.0 (CH×2), 125.8 (CH), 124.5 (CH), 121.0 (CH), 102.0 (CH); m/z 365 (MH^+, 100%).

2-Phenyl-4-[4-(dimethylamino)phenyl]-6-(4-methoxyphenyl)-pyrimidine (68h)

2-Phenyl-4-[4-(dimethylamino)phenyl]-6-(4-methoxyphenyl)-pyrimidine (**68f**) (0.16 g, 72%) was prepared according to the given procedure **6.2.3** using 1-(4-methoxyphenyl)-3-[4-(dimethylamino)phenyl]-prop-2-yn-1-ol **52** (0.57 mmol, 1 equiv.) and was obtained as intense yellow crystals, mp 186–188 °C (Found: MH^+, 382.1856. $C_{25}H_{24}N_3O$ [MH^+] requires 382.1841); v_{max} (KBr) 2989, 2206, 1640, 1610, 1266, 821; λ_{max}(CHCl$_3$)/nm 376 (log ε 4.82); δ_H (400 MHz; CDCl$_3$) 7.46 (2H, m, 2'',6''-H), 7.38 (2H, app. d, J 8.8, 2',6'-H), 7.32 (3H, m, 3'',4'',5''-H), 7.30 (2H, app. d, J 8.9, 2''',6'''-H), 7.26 (1H, s, 5-H), 6.84 (2H, app. d, J 8.8, 3',5'-H), 6.66 (2H, app. d, J 8.9, 3''',5'''-H), 3.70 (3H, s, OCH$_3$), 2.80 (6H, s, N(CH$_3$)$_2$); δ_C (100 MHz; CDCl$_3$) 166.7 (C), 164.5 (C), 162.5 (C), 160.7 (C), 149.6 (C), 132.7 (C), 129.4 (CH×2), 128.9 (CH), 128.6 (CH×2), 128.4 (CH×2), 127.5 (CH×2), 125.6 (C), 122.8 (C), 114.9 (CH×2), 114.6 (CH×2), 102.4 (CH), 55.0 (CH$_3$), 40.4 (CH$_3$×2); m/z 382 (MH^+, 100%).

2-Phenyl-4-[4-(dimethylamino)phenyl]-6-(2-theinyl)-pyrimidine (68i)

2-Phenyl-4-[4-(dimethylamino)phenyl]-6-(2-thienyl)-pyrimidine (**68i**) (0.14 g, 68%) was prepared according to the given procedure **6.2.3** using 1-(2-thienly)-3-[4-(dimethylamino)phenyl]-prop-2-yn-1-ol **52** (0.57 mmol, 1 equiv.) and was obtained as golden crystals, mp 190–192 °C (Found: MH^+, 358.1402. $C_{22}H_{20}N_3S$ [MH^+] requires 358.1300); v_{max} (KBr) 2989, 1640, 1610, 820; λ_{max}(CHCl$_3$)/nm 371 (log ε 4.64); δ_H (400 MHz; CDCl$_3$) 7.50 (2H, m, 2'',6''-H), 7.34 (1H, s, 5-H), 7.32 (3H, m, 3'',4'',5''-H), 7.30 (2H, app. d, J 8.9, 2''',6'''-H), 7.21 (1H, d, J 3.9, 3'-H), 7.02 (1H, d, J 4.8, 5'-H), 7.00 (1H, dd, J 4.8, 3.9, 4'-H), 6.65 (2H, app. d, J 8.9, 3''',5'''-H), 2.80 (6H, s, N(CH$_3$)$_2$); δ_C (100 MHz; CDCl$_3$) 165.6 (C), 163.6 (C), 160.4 (C), 150.2 (C), 142.0 (C), 131.9

(C), 129.3 (CH×2), 128.9 (CH), 128.6 (CH×2), 128.0 (CH), 127.9 (CH), 127.6 (CH×2), 125.6 (CH), 122.8 (C), 115.2 (CH×2), 102.8 (CH), 40.2 (CH$_3$×2); m/z 358 (MH$^+$, 100%).

2-Phenyl-4-[4-(dimethylamino)phenyl]-6-(10-naphthyl)-pyrimidine (68j)
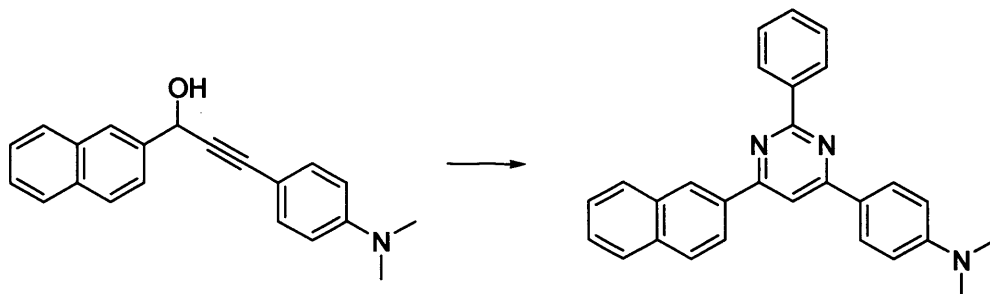
2-Phenyl-4-[4-(dimethylamino)phenyl]-6-(10-naphthyl)-pyrimidine **(68j)** (0.17 g, 74%) was prepared according to the given procedure **6.2.3** using 1-(10-naphthyl)-3-[4-(dimethylamino)phenyl]-prop-2-yn-1-ol **52** (0.57 mmol, 1 equiv.) and was obtained as orange crystals, mp 196–198 °C (Found: MH$^+$, 402.1904. C$_{28}$H$_{24}$N$_3$ [MH$^+$] requires 402.1892); v_{max} (KBr) 2990, 1642, 1612, 822; λ_{max}(CHCl$_3$)/nm 379 (log ε 4.84); δ_H (400 MHz; CDCl$_3$) 7.90 (1H, s, 1'-H), 7.78 (1H, app. d, J 8.6, 4'-H), 7.70 (2H, m, 6',7'-H), 7.56 (1H, app. d, J 8.6, 3'-H), 7.49 (2H, m, 2'',6''-H), 7.34 (2H, m, 5',8'-H), 7.32 (3H, m, 3'',4'',5''-H), 7.30 (2H, app. d, J 8.9, 2''',6'''-H), 7.26 (1H, s, 5-H), 6.68 (2H, app. d, J 8.9, 3''',5'''-H), 2.88 (6H, s, N(CH$_3$)$_2$); δ_C (100 MHz; CDCl$_3$) 166.7 (C), 163.4 (C), 162.3 (C), 150.2 (C), 135.3 (C), 133.8 (C), 132.6 (C), 130.8 (C), 129.5 (CH×2), 128.9 (CH), 128.8 (CH), 128.5 (CH×2), 128.2 (CH×2), 127.6 (CH×2), 126.6 (CH×2), 125.9 (CH), 124.6 (CH), 122.8 (C), 116.8 (CH×2), 104.6 (CH), 40.2 (CH$_3$×2); m/z 402 (MH$^+$, 100%).

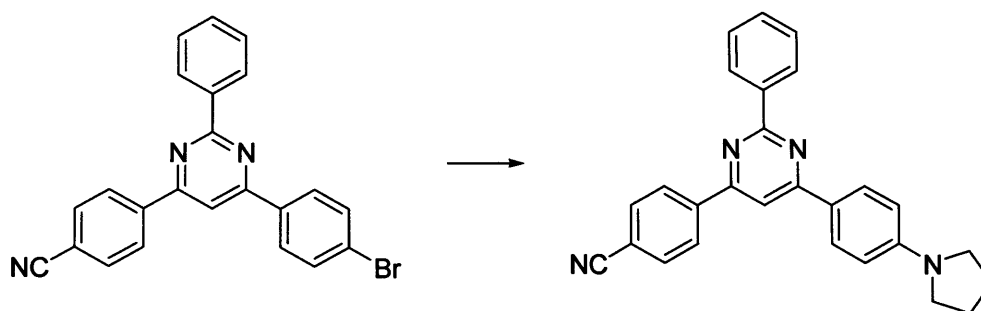## 2-Phenyl-4-[4-bromophenyl]-6-(10-naphthyl)-pyrimidine (68k)
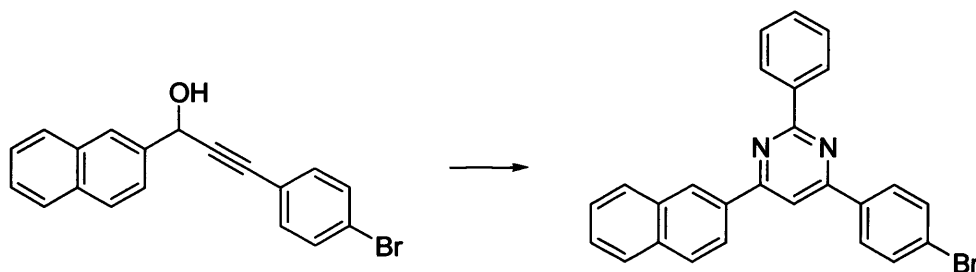
2-Phenyl-4-[4-bromophenyl]-6-(10-naphthyl)-pyrimidine **(68k)** (0.20 g, 74%) was prepared according to the given procedure **6.2.3** using 1-(10-naphthyl)-3-(4-bromophenyl)-prop-2-yn-1-ol **52** (0.57 mmol, 1 equiv.) and was obtained as colourless crystals, mp 210–212 °C (Found: MH$^+$, 437.0592. C$_{26}$H$_{18}$BrN$_2$ [MH$^+$] requires 437.0575); v_{max} (KBr) 2989, 1640, 1611, 820, 756; λ_{max}(CHCl$_3$)/nm 325 (log ε 4.20); δ_H (400 MHz; CDCl$_3$) 7.92 (1H, s, 1'-H), 7.75 (1H, d, J 8.6, 4'-

H), 7.69 (2H, m, 6',7'-H), 7.56 (1H, d, *J* 8.6, 3'-H), 7.52 (2H, app. d, *J* 8.9, 3''',5'''-H), 7.50 (2H, m, 2'',6''-H), 7.38 (2H, app. d, *J* 8.9, 2''',6'''-H), 7.36 (2H, m, 5',8'-H), 7.32 (3H, m, 3'',4'',5''-H), 7.29 (1H, s, 5-H); δ_C (100 MHz; CDCl$_3$) 168.7 (C), 164.5 (C), 163.5 (C), 135.3 (C), 134.8 (C), 133.6 (C), 132.4 (CH×2), 132.2 (C), 131.8 (C), 130.8 (CH×2), 129.6 (CH×2), 128.9 (CH), 128.6 (CH), 128.2 (CH×2), 127.6 (CH×2), 126.4 (CH×2), 125.9 (CH), 124.6 (CH), 123.4 (C), 106.5 (CH); *m/z* 437 (MH$^+$, 100%), 439 (97).

2-Phenyl-4-[4-(dimethylamino)phenyl]-6-(4-cyanophenyl)-pyrimidine (68l)
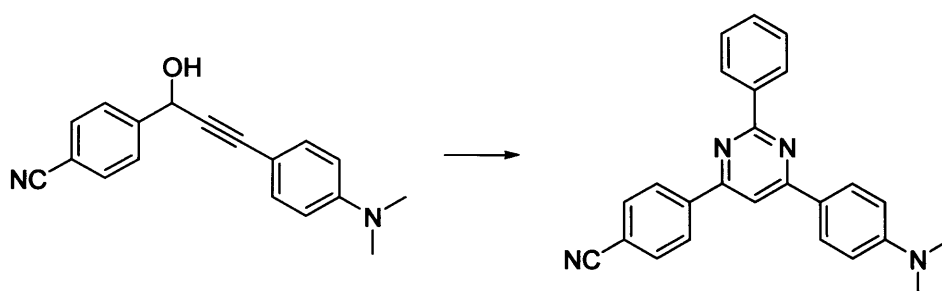
2-Phenyl-4-[4-(dimethylamino)phenyl]-6-(4-cyanophenyl)-pyrimidine (**68l**) (0.17 g, 74%) was prepared according to the given procedure **6.2.3** using 1-(4-cyanophenyl)-3-[4-(dimethylamino)phenyl]-prop-2-yn-1-ol **52** (0.57 mmol, 1 equiv.) and was obtained as intense yellow crystals, mp 186–188 °C (Found: MH$^+$, 377.1702. C$_{25}$H$_{21}$N$_4$ [MH$^+$] requires 377.1689); v_{max} (KBr) 2989, 2206, 1640, 1610, 821; λ_{max}(CHCl$_3$)/nm 379 (log ε 4.84); δ_H (400 MHz; CDCl$_3$) 7.87 (2H, app. d, *J* 8.8, 2',6'-H), 7.68 (2H, app. d, *J* 8.8, 3',5'-H), 7.52 (2H, m, 2'',6''-H), 7.32 (3H, m, 3'',4'',5''-H), 7.29 (2H, app. d, *J* 8.9, 2''',6'''-H), 7.26 (1H, s, 5-H), 6.66 (2H, app. d, *J* 8.9, 3''',5'''-H), 2.82 (6H, s, N(CH$_3$)$_2$); δ_C (100 MHz; CDCl$_3$) 166.7 (C), 164.5 (C), 162.5 (C), 152.6 (C), 139.4 (C), 133.7 (CH×2), 130.7 (C), 129.9 (CH×2), 129.0 (CH), 128.9 (CH×2), 128.4 (CH×2), 127.6 (CH×2), 122.8 (C), 115.2 (CH×2), 113.0 (C), 105.8 (CN), 102.8 (CH), 40.2 (CH$_3$×2); *m/z* 377 (MH$^+$, 100%).

2-Phenyl-4-(4-bromophenyl)-6-(4-cyanophenyl)-pyrimidine (68m)
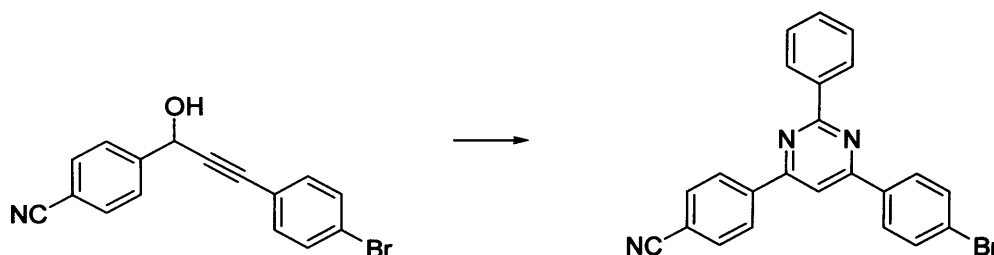
2-Phenyl-4-(4-bromophenyl)-6-(4-cyanophenyl)-pyrimidine (**68m**) (0.18 g, 76%) was prepared according to the given procedure **6.2.3** using 1-(4-cyanophenyl)-3-[4-bromophenyl]prop-2-yn-1-

ol **52** (0.57 mmol, 1 equiv.) and was obtained as colourless crystals, mp 231–232 °C (found: M^+, 411.0356. $C_{23}H_{14}{}^{79}BrN_3$ [*M*] requires 411.0371); λ_{max}(CHCl$_3$)/nm 320 (log ε 4.20); ν_{max} (KBr) 2990, 2208, 1640, 1610, 821, 758; δ_H (400 MHz, CDCl$_3$) 7.71 (2H, m, 2'',6''-H), 7.41 (2H, app. d, *J* 8.8, 3',5'-H), 7.19 (2H, app. d, *J* 8.9, 3''',5'''-H), 7.01 (1H, s, 5-H), 6.88 (2H, app. d, *J* 8.8, 2',6'-H), 6.73 (2H, app. d, *J* 8.9, 2''',6'''-H), 6.56 (3H, m, 3'',4'',5''-H); δ_C (100 MHz; CDCl$_3$) 165.1 (C), 163.2 (C), 162.8 (C), 142.4 (C), 138.2 (C), 137.4 (C), 136.4 (C), 133.1 (CH), 132.0 (CH), 131.6 (CH), 131.4 (CH), 129.6 (CH), 128.9 (CH), 127.8 (CH), 126.0 (C), 114.0 (CN), 110.6 (CH); *m/z* (EI) 413 (M[^{81}Br]$^+$, 97%), 411 (M[^{79}Br]$^+$, 100).

2-Phenyl-4-[4-(pyrrolydino)phenyl]-6-(10-naphthyl)-pyrimidine (68n)
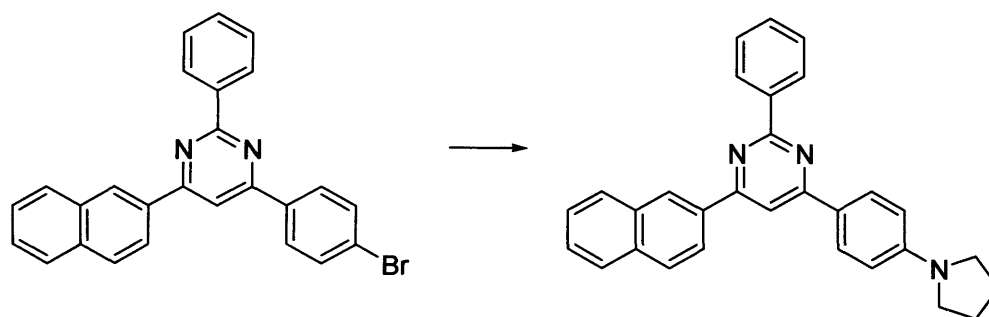
2-Phenyl-4-[4-(pyrrolidino)phenyl]-6-(10-naphthyl)-pyrimidine (**68n**) (0.17 g, 68%) was prepared according to the given procedure **6.2.4** using 2-phenyl-4-[4-bromophenyl]-6-(10-naphthyl)-pyrimidine **68k** (0.57 mmol, 1 equiv.) and was obtained as orange crystals, mp 202–204 °C (Found: MH$^+$, 428.2052. $C_{30}H_{26}N_3$ [MH$^+$] requires 428.2048); ν_{max} (KBr) 2992, 1640, 1610, 824; λ_{max}(CHCl$_3$)/nm 430 (log ε 4.40); δ_H (400 MHz; CDCl$_3$) 7.89 (1H, s, 1'-H), 7.72 (1H, d, *J* 8.6, 4'-H), 7.66 (2H, m, 6',7'-H), 7.52 (1H, d, *J* 8.6, 3'-H), 7.49 (2H, m, 2'',6''-H), 7.34 (2H, m, 5',8'-H), 7.32 (3H, m, 3'',4'',5''-H), 7.30 (2H, app. d, *J* 8.9, 2''',6'''-H), 7.28 (1H, s, 5-H), 6.66 (2H, app. d, *J* 8.9, 3''',5'''-H), 2.80 (4H, t, *J* 6.6, 2'''',5''''-CH$_2$), 1.58 (4H, t, *J* 6.6, 3'''',4''''-CH$_2$); δ_C (100 MHz; CDCl$_3$) 164.6 (C), 162.4 (C), 161.2 (C), 149.4 (C), 134.2 (C), 133.8 (C), 132.8 (C), 130.6 (C), 129.2 (CH×2), 128.6 (CH), 128.5 (CH), 128.3 (CH×2), 128.1 (CH×2), 127.6 (CH×2), 126.2 (CH×2), 125.6 (CH), 124.3 (CH), 122.4 (C), 114.8 (CH×2), 102.6 (CH), 51.6 (CH$_2$×2), 24.8 (CH$_2$×2); *m/z* 428 (MH$^+$, 100%).

2-Phenyl-4-[4-(pyrrolydino)phenyl]-6-(4-cyanophenyl)-pyrimidine (68o)

2-Phenyl-4-[4-(pyrrolydino)phenyl]-6-(4-cyanophenyl)-pyrimidine **(68o)** (0.17 g, 74%) was prepared according to the given procedure **6.2.4** using 2-phenyl-4-(4-bromophenyl)-6-(4-cyanophenyl)-pyrimidine **68m** (0.57 mmol, 1 equiv.) and was obtained as yellow crystals, mp 190-192 °C (Found: MH^+, 403.1862. $C_{27}H_{23}N_4$ [MH^+] requires 403.1862); λ_{max}(CHCl$_3$)/nm 385 (log ε 4.38); v_{max} (KBr) 2990, 2208, 1641, 1612, 820; δ_H (400 MHz, CDCl$_3$) 7.68 (2H, app. d, J 8.8, 2',6'-H), 7.58 (2H, app. d, J 8.8, 3',5'-H), 7.49 (2H, m, 2'',6''-H), 7.32 (3H, m, 3'',4'',5''-H), 7.30 (2H, app. d, J 8.9, 2''',6'''-H), 7.28 (1H, s, 5-H), 6.68 (2H, app. d, J 8.9, 3''',5'''-H), 2.82 (4H, t, J 6.6, 2'''',5''''-CH$_2$), 1.54 (4H, t, J 6.6, 3'''',4''''-CH$_2$); δ_C (100 MHz; CDCl$_3$) 165.7 (C), 164.2 (C), 162.5 (C), 150.2 (C), 138.4 (C), 133.7 (CH×2), 132.7 (C), 130.3 (CH×2), 129.8 (CH), 128.6 (CH×2), 128.4 (CH×2), 128.0 (CH×2), 124.6 (C), 116.8 (CN), 115.8 (CH×2), 113.6 (C), 103.6 (CH), 52.4 (CH$_2$×2), 26.5 (CH$_2$×2); *m/z* 403 (MH^+, 100%).

2,6-Bis(3-phenylprop2-yn-1-oyl)pyridine (79a)
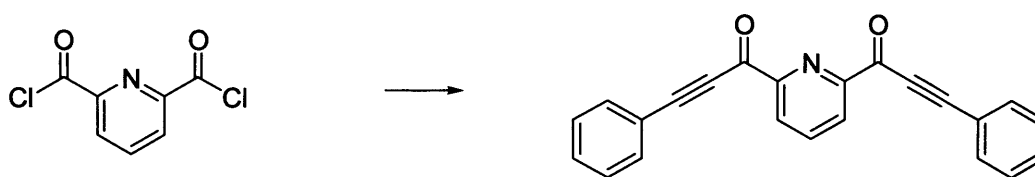
2,6-Bis(3-phenylprop2-yn-1-oyl)pyridine **(79a)** (0.14 g, 72%) was prepared according to the given procedure **6.2.5** using 2,6-pyridinecarbonyldichloride (0.57 mol, 1 equiv.) and was obtained as colourless crystals, mp 92-94 °C (Found: MH^+, 336.0961. $C_{23}H_{14}NO_2$ [MH^+] requires 336.0946); λ_{max}(CHCl$_3$)/nm 302 (log ε 4.68); v_{max} (KBr) 2208, 1726, 1652, 1600, 780; δ_H (400 MHz, CDCl$_3$) 8.62 (2H, d, J 7.8, 3',5'-H), 8.41 (1H, t, J 7.8, 4'-H), 7.72 (4H, m, 2,6,2'',6''-H), 7.51 (6H, m, 3,4,5,3'',4'',5''-H); δ_C (100 MHz; CDCl$_3$) 177.7 (CO×2), 153.2 (C×2), 140.2 (CH), 138.4 (CH×4), 136.4 (CH×4), 136.2 (CH×2), 128.2 (CH×2), 124.0 (C×2), 98.8 (C×2), 90.8 (C×2); *m/z* 336 (MH^+, 100%).
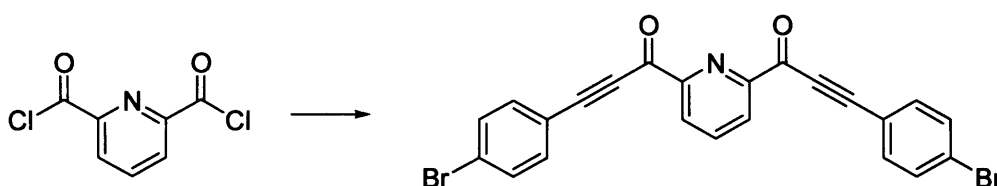
145

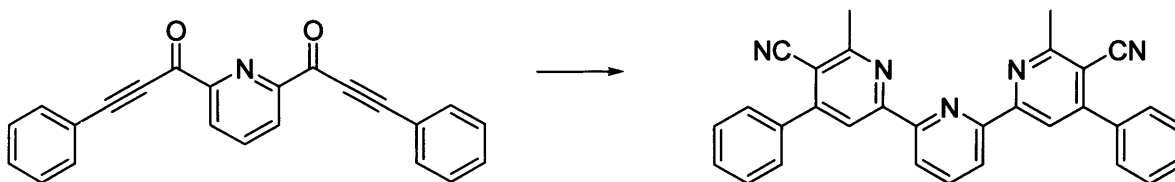## 2,6-Bis[3-(4-methoxyphenyl)prop2-yn-1-oyl]pyridine (79b)
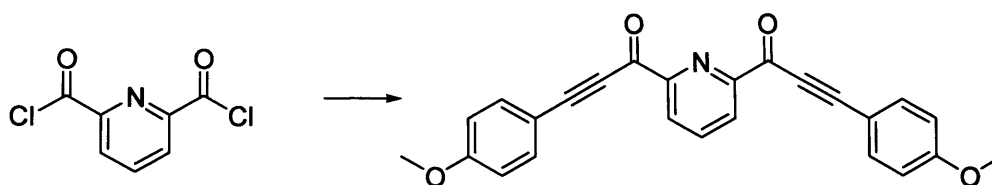
2,6-bis[3-(4-methoxyphenyl)prop2-yn-1-oyl]pyridine (**79b**) (0.17 g, 74%) was prepared according to the given procedure **6.2.5** using 2,6-pyridinecarbonyldichloride (0.57 mol, 1 equiv.) and was obtained as colourless crystals, mp 96-98 °C (Found: MH^+, 396.1206. $C_{25}H_{18}NO_4$ [MH^+] requires 396.1158); $\lambda_{max}(CHCl_3)$/nm 322 (log ε 4.78); ν_{max} (KBr) 2209, 1724, 1650, 1602, 1280, 780; δ_H (400 MHz, CDCl$_3$) 8.52 (2H, d, J 7.8, 3',5'-H), 8.21 (1H, t, J 7.8, 4'-H), 7.62 (4H, app. d, J 8.8, 2,6,2'',6''-H), 7.31 (4H, app. d, J 8.8, 3,5,3'',5''-H), 3.52 (6H, s, OCH$_3$×2); δ_C (100 MHz; CDCl$_3$) 172.2 (CO×2), 160.6 (C×2), 154.2 (C×2), 138.8 (CH), 133.6 (CH×4), 124.8 (CH×2), 115.2 (C×2), 114.0 (CH×4), 96.4 (C×2), 88.4 (C×2), 55.8 (CH$_3$×2); m/z 396 (MH^+, 100%).

2,6-Bis[3-(4-dimethylamino-phenyl)prop2-yn-1-oyl]pyridine (79c)
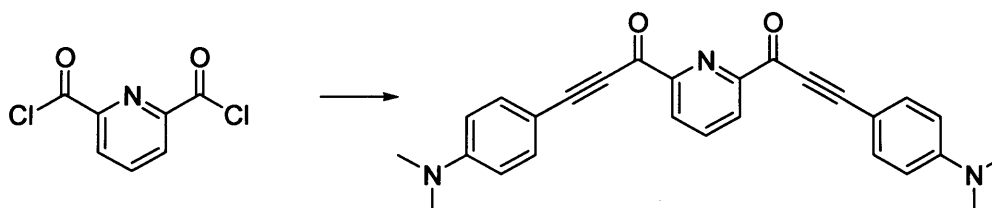
2,6-Bis[3-(4-dimethylamino-phenyl)prop2-yn-1-oyl]pyridine (**79c**) (0.17 g, 69%) was prepared according to the given procedure **6.2.5** using 2,6-pyridinecarbonyldichloride (0.57 mol, 1 equiv.) and was obtained as yellow crystals, mp 106-108 °C (Found: MH^+, 422.1802. $C_{27}H_{24}N_3O_2$ [MH^+] requires 422.1790); $\lambda_{max}(CHCl_3)$/nm 360 (log ε 4.64); ν_{max} (KBr) 2208, 1720, 1652, 1600, 784; δ_H (400 MHz, CDCl$_3$) 8.40 (2H, d, J 7.8, 3',5'-H), 8.02 (1H, t, J 7.8, 4'-H), 7.22 (4H, app. d, J 8.8, 2,6,2'',6''-H), 7.01 (4H, app. d, J 8.8, 3,5,3'',5''-H), 2.80 (12H, s, N(CH$_3$)$_2$×2); δ_C (100 MHz; CDCl$_3$) 170.2 (CO×2), 152.0 (C×2), 147.3 (C×2), 136.6 (CH), 132.2 (CH×4), 122.9 (CH×2), 112.9 (C×2), 110.2 (CH×4), 96.0 (C×2), 87.6 (C×2), 40.0 (CH$_3$×4); m/z 422 (MH^+, 100%).

2,6-Bis[3-(4-chlorophenyl)prop2-yn-1-oyl]pyridine (79d)
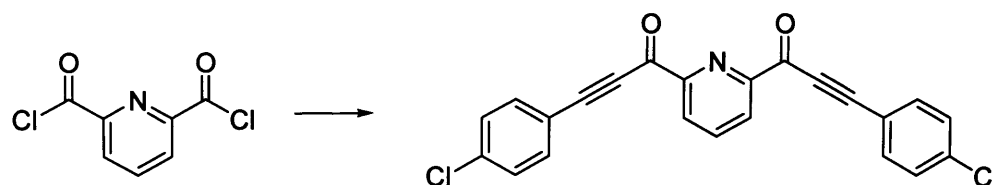
2,6-Bis[3-(4-chlorophenyl)prop2-yn-1-oyl]pyridine (**79d**) (0.18 g, 76%) was prepared according to the given procedure **6.2.5** using 2,6-pyridinecarbonyldichloride (0.57 mol, 1 equiv.) and was obtained as colourless crystals, mp 94-96 °C (Found: MH$^+$, 404.0167. C$_{23}$H$_{12}$Cl$_2$NO$_2$ [MH$^+$] requires 404.0167); λ_{max}(CHCl$_3$)/nm 308 (log ε 4.82); ν_{max} (KBr) 2206, 1722, 1650, 1602, 784, 726; δ_H (400 MHz, CDCl$_3$) 8.58 (2H, d, *J* 7.8, 3',5'-H), 8.32 (1H, t, *J* 7.8, 4'-H), 7.62 (4H, app. d, *J* 8.8, 2,6,2'',6''-H), 7.41 (4H, app. d, *J* 8.8, 3,5,3'',5''-H); δ_C (100 MHz; CDCl$_3$) 173.0 (CO×2), 156.0 (C×2), 140.6 (CH), 136.0 (C×2), 134.7 (CH×4), 129.5 (CH×4), 126.9 (CH×2), 122.8 (C×2), 98.2 (C×2), 90.2 (C×2); *m/z* 404 (MH$^+$, 100%).

2,6-Bis[3-(4-bromophenyl)prop2-yn-1-oyl]pyridine (79e)

2,6-Bis[3-(4-bromophenyl)prop2-yn-1-oyl]pyridine (**79e**) (0.18 g, 76%) was prepared according to the given procedure **6.2.5** using 2,6-pyridinecarbonyldichloride (0.57 mol, 1 equiv.) and was obtained as colourless crystals, mp 100-102 °C (Found: MH$^+$, 491.9302. C$_{23}$H$_{12}$Br$_2$NO$_2$ [MH$^+$] requires 491.9157); λ_{max}(CHCl$_3$)/nm 306 (log ε 4.80); ν_{max} (KBr) 2208 1720, 1652, 1600, 782, 728; δ_H (400 MHz, CDCl$_3$) 8.60 (2H, d, *J* 7.8, 3',5'-H), 8.34 (1H, t, *J* 7.8, 4'-H), 7.64 (4H, app. d, *J* 8.8, 2,6,2'',6''-H), 7.44 (4H, app. d, *J* 8.8, 3,5,3'',5''-H); δ_C (100 MHz; CDCl$_3$) 173.6 (CO×2), 157.0 (C×2), 141.0 (CH), 136.6 (CH×4), 134.6 (CH×4), 127.2 (CH×2), 123.2 (C×2), 122.2 (C×2), 98.6 (C×2), 90.6 (C×2); *m/z* 491 (MH$^+$, 100%), 493 (97).

4,4''-Phenyl-5,5''-cyano-6,6''-methyl-2,2':6',2''-terpyridine (80a)

4,4''-Phenyl-5,5''-cyano-6,6''-methyl-2,2':6',2''-terpyridine (**80a**) (0.23 g, 88%) was prepared according to the given procedure **6.2.6** using 2,6-bis(3-phenylprop2-yn-1-oyl)pyridine **79a** (0.85 mmol, 1.5 equiv.) and was obtained as colourless crystals, mp 276-278 °C (Found: MH$^+$, 464.1812. C$_{31}$H$_{22}$N$_5$ [MH$^+$] requires 464.1797); λ_{max}(CHCl$_3$)/nm 316 (log ε 4.70); ν_{max} (KBr) 2990, 2206, 1640, 1610, 822; δ_H (400 MHz, CDCl$_3$) 8.96 (2H, s, 3,3''-H), 8.26 (2H, d, *J* 7.8, 3',5'-H), 7.58 (1H, t, *J* 7.8, 4'-H), 7.48 (4H, m, 2'''',6'''',2''''',6'''''-H), 7.36 (6H, m,

3''',4''',5''',3'''',4'''',5''''-H), 2.53 (6H, s, CH$_3$×2); δ$_C$ (100 MHz; CDCl$_3$) 162.0 (C×2), 160.6 (C×2), 156.6 (C×2), 154.4 (C×2), 139.6 (CH), 139.0 (C×2), 130.0 (CH×6), 128.2 (CH×4), 121.2 (CH×2), 119.7 (CH×2), 118.0 (CN×2), 110.6 (C×2), 20.2 (CH$_3$×2); *m/z* 464 (MH$^+$, 100%).
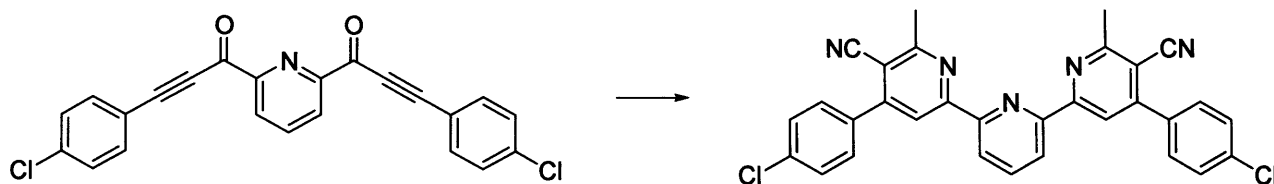
4,4''-(4-Methoxyphenyl)-5,5''-cyano-6,6''-methyl-2,2':6',2''-terpyridine (80b)
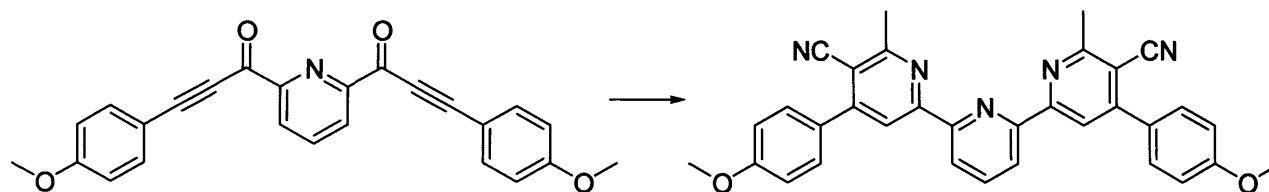
4,4''-(4-Methoxyphenyl)-5,5''-cyano-6,6''-methyl-2,2':6',2''-terpyridine **(80b)** (0.24 g, 82%) was prepared according to the given procedure **6.2.6** using 2,6-bis[3-(4-methoxyphenyl)prop2-yn-1-oyl]pyridine **79b** (0.85 mmol, 1.5 equiv.) and was obtained as colourless crystals, mp 280-282 °C (Found: MH$^+$, 524.2016. C$_{33}$H$_{26}$N$_5$O$_2$ [MH$^+$] requires 524.2008); λ$_{max}$(CHCl$_3$)/nm 320 (log ε 4.65); ν$_{max}$ (KBr) 2989, 2205, 1642, 1612, 1260, 820; δ$_H$ (400 MHz, CDCl$_3$) 8.98 (2H, s, 3,3''-H), 8.28 (2H, d, *J* 7.8, 3',5'-H), 7.59 (1H, t, *J* 7.8, 4'-H), 7.38 (4H, app. d, *J* 8.8, 2''',6''',2'''',6''''-H), 6.80 (4H, app. d, *J* 8.8, 3''',5''',3'''',5''''-H), 3.76 (6H, s, OCH$_3$×2), 2.56 (6H, s, CH$_3$×2); δ$_C$ (100 MHz; CDCl$_3$) 162.4 (C×2), 161.6 (C×2), 159.8 (C×2), 155.8 (C×2), 154.6 (C×2), 138.6 (CH), 130.6 (C×2), 128.8 (CH×4), 121.6 (CH×2), 118.9 (CH×2), 117.4 (CN×2), 114.9 (CH×4), 110.6 (C×2), 55.8 (CH$_3$×2), 19.2 (CH$_3$×2); *m/z* 524 (MH$^+$, 100%).

4,4''-[4-(dimethylamino)phenyl]-5,5''-cyano-6,6''-methyl-2,2':6',2''-terpyridine (80c)
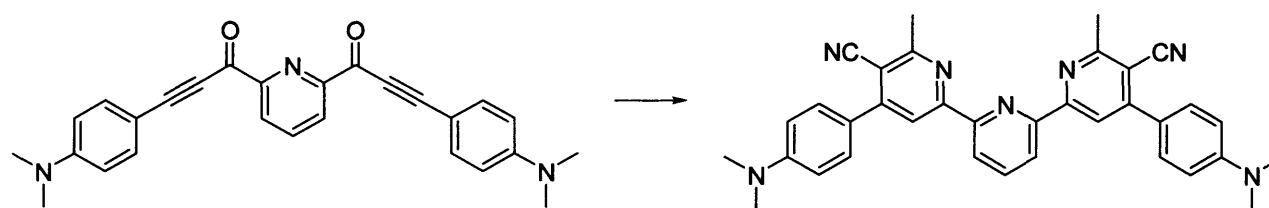
4,4''-[4-(Dimethylamino)phenyl]-5,5''-cyano-6,6''-methyl-2,2':6',2''-terpyridine **(80c)** (0.20 g, 64%) was prepared according to the given procedure **6.2.6** using 2,6-bis[3-(4-dimethylamino-phenyl)prop2-yn-1-oyl]pyridine **79c** (0.85 mmol, 1.5 equiv.) and was obtained as yellow crystals, mp 286-288 °C (Found: MH$^+$, 550.2682. C$_{35}$H$_{32}$N$_7$ [MH$^+$] requires 550.2641); λ$_{max}$(CHCl$_3$)/nm 380 (log ε 4.72); ν$_{max}$ (KBr) 2990, 2206, 1644, 1614, 822; δ$_H$ (400 MHz, CDCl$_3$) 8.92 (2H, s, 3,3''-H), 8.24 (2H, d, *J* 7.8, 3',5'-H), 7.56 (1H, t, *J* 7.8, 4'-H), 7.26 (4H, app. d, *J* 8.8, 2''',6''',2'''',6''''-H), 6.62 (4H, app. d, *J* 8.8, 3''',5''',3'''' ,5''''-H), 2.84 (12H, s, N(CH$_3$)$_2$×2), 2.52 (6H, s, CH$_3$×2); δ$_C$ (100 MHz; CDCl$_3$) 160.0 (C×2), 159.8 (C×2), 156.2 (C×2), 154.6 (C×2),

150.2 (C×2), 138.2 (CH), 128.2 (CH×4), 127.6 (C×2), 121.4 (CH×2), 118.6 (CH×2), 117.2 (CN×2), 114.9 (CH×4), 110.6 (C×2), 40.2 (CH$_3$×4), 17.6 (CH$_3$×2); *m/z* 550 (MH$^+$, 100%).

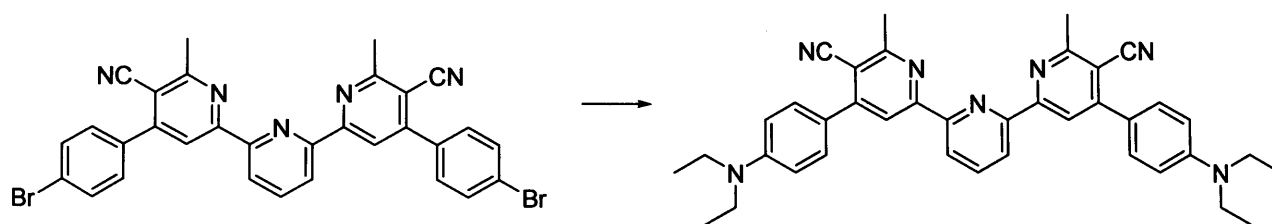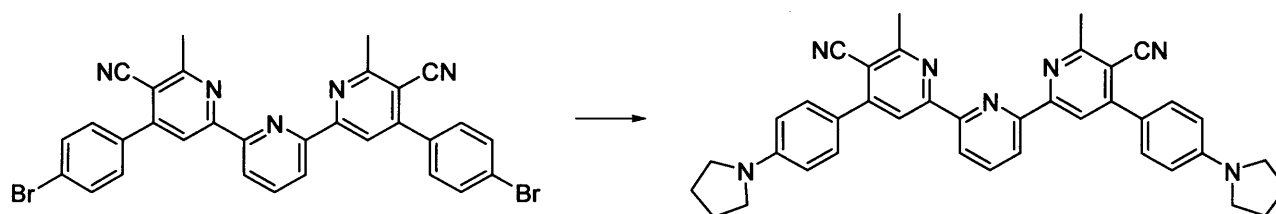## 4,4''-(4-Chlorophenyl)-5,5''-cyano-6,6''-methyl-2,2':6',2''-terpyridine (80d)

4,4''-(4-Chlorophenyl)-5,5''-cyano-6,6''-methyl-2,2':6',2''-terpyridine (**80d**) (0.26 g, 86%) was prepared according to the given procedure **6.2.6** using 2,6-bis[3-(4-chlorophenyl)prop2-yn-1-oyl]pyridine **79d** (0.85 mmol, 1.5 equiv.) and was obtained as colourless crystals, mp 276-278 °C (Found: MH$^+$, 532.1026. C$_{31}$H$_{20}$Cl$_2$N$_5$ [MH$^+$] requires 532.1018); λ$_{max}$(CHCl$_3$)/nm 318 (log ε 4.82); ν$_{max}$ (KBr) 2992, 2206, 1646, 1614, 824, 726; δ$_H$ (400 MHz, CDCl$_3$) 9.02 (2H, s, 3,3''-H), 8.26 (2H, d, *J* 7.8, 3',5'-H), 7.58 (1H, t, *J* 7.8, 4'-H), 7.44 (4H, app. d, *J* 8.8, 2''',6''',2''''',6'''''-H), 7.34 (4H, app. d, *J* 8.8, 3''',5''',3''''' ,5'''''-H), 2.56 (6H, s, CH$_3$×2); δ$_C$ (100 MHz; CDCl$_3$) 161.0 (C×2), 160.6 (C×2), 158.2 (C×2), 156.6 (C×2), 152.2 (C×2), 140.2 (CH), 130.2 (CH×4), 129.6 (C×2), 123.2 (CH×2), 119.6 (CH×2), 118.2 (CN×2), 116.9 (CH×4), 112.6 (C×2), 18.4 (CH$_3$×2); *m/z* 532 (MH$^+$, 100%).

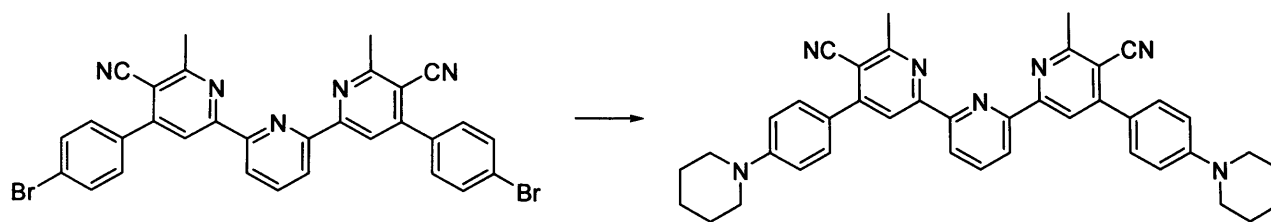## 4,4''-(4-Bromophenyl)-5,5''-cyano-6,6''-methyl-2,2':6',2''-terpyridine (80e)
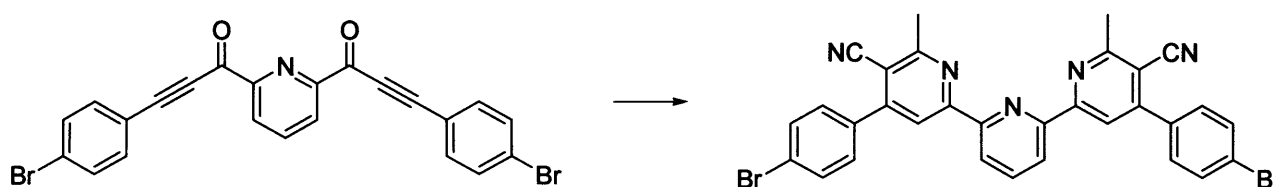
4,4''-(4-Bromophenyl)-5,5''-cyano-6,6''-methyl-2,2':6',2''-terpyridine (**80e**) (0.30 g, 84%) was prepared according to the given procedure **6.2.6** using 2,6-bis[3-(4-bromophenyl)prop2-yn-1-oyl]pyridine **79e** (0.85 mmol, 1.5 equiv.) and was obtained as colourless crystals, mp 284-286 °C (Found: MH$^+$, 620.0038. C$_{31}$H$_{20}$Br$_2$N$_5$ [MH$^+$] requires 620.0026); λ$_{max}$(CHCl$_3$)/nm 326 (log ε 4.76); ν$_{max}$ (KBr) 2990, 2206, 1642, 1612, 826, 722; δ$_H$ (400 MHz, CDCl$_3$) 9.04 (2H, s, 3,3''-H), 8.28 (2H, d, *J* 7.8, 3',5'-H), 7.62 (1H, t, *J* 7.8, 4'-H), 7.46 (4H, app. d, *J* 8.8, 2''',6''',2''''',6'''''-H), 7.36 (4H, app. d, *J* 8.8, 3''',5''',3''''' ,5'''''-H), 2.58 (6H, s, CH$_3$×2); δ$_C$ (100 MHz; CDCl$_3$) 161.4 (C×2), 160.8 (C×2), 158.6 (C×2), 157.2 (C×2), 152.6 (C×2), 140.6 (CH), 130.4 (CH×4), 129.8 (C×2), 123.6 (CH×2), 120.4 (CH×2), 118.6 (CN×2), 118.2 (CH×4), 112.8 (C×2), 18.6 (CH$_3$×2); *m/z* 620 (MH$^+$, 100%), 622 (97).

4,4''-[4-(Diethylamino)phenyl]-5,5''-cyano-6,6''-methyl-2,2':6',2''-terpyridine (80f)


4,4''-[4-(Diethylamino)phenyl]-5,5''-cyano-6,6''-methyl-2,2':6',2''-terpyridine **(80f)** (0.30 g, 86%) was prepared according to the given procedure **6.2.7** using 4,4''-(4-bromophenyl)-5,5''-cyano-6,6''-methyl-2,2':6',2''-terpyridine **80e** (0.57 mmol, 1.0 equiv.) and was obtained as yellow crystals, mp 288-290 °C (Found: MH^+, 606.3286. $C_{39}H_{40}N_7$ [MH^+] requires 606.3267); λ_{max}(CHCl$_3$)/nm 384 (log ε 4.68); ν_{max} (KBr) 2992, 2208, 1644, 1616, 826; δ_H (400 MHz, CDCl$_3$) 8.90 (2H, s, 3,3''-H), 8.22 (2H, d, J 7.8, 3',5'-H), 7.56 (1H, t, J 7.8, 4'-H), 7.24 (4H, app. d, J 8.8, 2''',6''',2''''',6'''''-H), 6.62 (4H, app. d, J 8.8, 3''',5''',3''''',5'''''-H), 3.36 (8H, q, J 6.0, N(CH$_2$)$_2$(CH$_3$)$_2$×2), 2.54 (6H, s, CH$_3$×2), 1.12 (12H, t, J 6.0, N(CH$_2$)$_2$(CH$_3$)$_2$×2); δ_C (100 MHz; CDCl$_3$) 159.0 (C×2), 158.6 (C×2), 154.6 (C×2), 152.8 (C×2), 149.1 (C×2), 137.6 (CH), 128.0 (CH×4), 126.4 (C×2), 120.1 (CH×2), 118.0 (CH×2), 116.0 (CN×2), 113.8 (CH×4), 110.2 (C×2), 44.0 (CH$_2$×4), 18.0 (CH$_3$×2), 12.8 (CH$_3$×4); m/z 606 (MH^+, 100%).

4,4''-[4-(Pyrrolydino)phenyl]-5,5''-cyano-6,6''-methyl-2,2':6',2''-terpyridine (80g)

4,4''-[4-(Pyrrolydino)phenyl]-5,5''-cyano-6,6''-methyl-2,2':6',2''-terpyridine **(80g)** (0.30 g, 84%) was prepared according to the given procedure **6.2.7** using 4,4''-(4-bromophenyl)-5,5''-cyano-6,6''-methyl-2,2':6',2''-terpyridine **80g** (0.57 mmol, 1.0 equiv.) and was obtained as orange crystals, mp 292-294 °C (Found: MH^+, 602.3012. $C_{39}H_{36}N_7$ [MH^+] requires 602.2954); λ_{max}(CHCl$_3$)/nm 388 (log ε 4.65); ν_{max} (KBr) 2990, 2205, 1642, 1614, 825; δ_H (400 MHz, CDCl$_3$) 8.88 (2H, s, 3,3''-H), 8.20 (2H, d, J 7.8, 3',5'-H), 7.52 (1H, t, J 7.8, 4'-H), 7.22 (4H, app. d, J 8.8, 2''',6''',2''''',6'''''-H), 6.58 (4H, app. d, J 8.8, 3''',5''',3''''',5'''''-H), 2.80 (8H, t, J 6.6, 2''''''',5''''''',2''''''''',5'''''''''-CH$_2$), 2.52 (6H, s, CH$_3$×2), 1.58 (8H, t, J 6.6, 3''''''',4''''''',3''''''''',4'''''''''-CH$_2$); δ_C (100 MHz; CDCl$_3$) 158.0 (C×2), 157.6 (C×2), 154.6 (C×2), 153.4 (C×2), 149.1 (C×2), 136.4 (CH), 127.3 (CH×4), 125.4 (C×2), 120.1 (CH×2), 116.7 (CH×2), 115.0 (CN×2), 112.8 (CH×4), 108.2 (C×2), 51.0 (CH$_2$×4), 25.2 (CH$_2$×4), 17.6 (CH$_3$×2); m/z 602 (MH^+, 100%).

4,4''-[4-(Pipperidino)phenyl]-5,5''-cyano-6,6''-methyl-2,2':6',2''-terpyridine (80h)


4,4''-[4-(Pipperidino)phenyl]-5,5''-cyano-6,6''-methyl-2,2':6',2''-terpyridine **(80h)** (0.32 g, 89%) was prepared according to the given procedure **6.2.7** using 4,4''-(4-bromophenyl)-5,5''-cyano-6,6''-methyl-2,2':6',2''-terpyridine **80g** (0.57 mmol, 1.0 equiv.) and was obtained as orange crystals, mp 296-298 °C (Found: MH$^+$, 630.3296. C$_{41}$H$_{40}$N$_7$ [MH$^+$] requires 630.3267); λ$_{max}$(CHCl$_3$)/nm 384 (log ε 4.68); ν$_{max}$ (KBr) 2992, 2206, 1644, 1616, 828; δ$_H$ (400 MHz, CDCl$_3$) 8.92 (2H, s, 3,3''-H), 8.24 (2H, d, *J* 7.8, 3',5'-H), 7.57 (1H, t, *J* 7.8, 4'-H), 7.32 (4H, app. d, *J* 8.8, 2''',6''',2'''',6''''-H), 6.60 (4H, app. d, *J* 8.8, 3''',5''',3'''',5''''-H), 2.70 (8H, t, *J* 6.4, 2''''',6''''',2''''''',6'''''''-CH$_2$), 2.55 (6H, s, CH$_3$×2), 1.50 (8H, m, 3''''',5''''',3''''''',5'''''''-CH$_2$), 1.48 (4H, q, *J* 6.4, 4''''',4'''''''-CH$_2$); δ$_C$ (100 MHz; CDCl$_3$) 160.0 (C×2), 158.0 (C×2), 154.6 (C×2), 153.2 (C×2), 150.1 (C×2), 138.4 (CH), 128.3 (CH×4), 126.4 (C×2), 121.1 (CH×2), 117.8 (CH×2), 117.0 (CN×2), 114.5 (CH×4), 110.0 (C×2), 52.2 (CH$_2$×4), 25.8 (CH$_2$×2), 25.4 (CH$_2$×4), 18.0 (CH$_3$×2); *m/z* 630 (MH$^+$, 100%).

2-Methyl-4-(4-biphenyl)-6-(2-pyridyl)nicotinonitrile (53n)
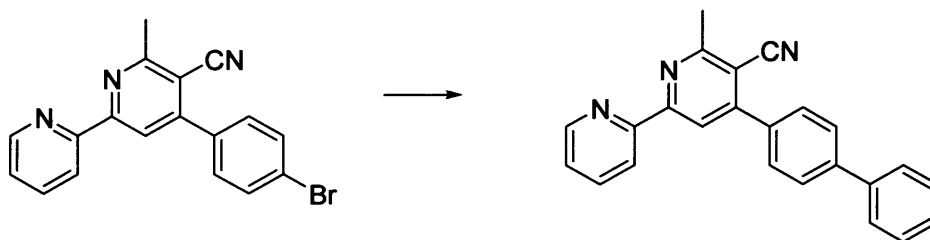
2-Methyl-4-(4-biphenyl)-6-(2-pyridyl)nicotinonitrile **(53n)** (0.18 g, 90%) was prepared according to the given procedure **6.2.8** using 2-methyl-4-(4-bromophenyl)-6-(2-pyridyl)nicotinonitrile **53g** (0.20 g, 0.57 mmol), catalysed by Pd(PPh$_3$)$_4$ (10 mol%), and was obtained as colourless crystals, mp 198–200 °C (EtOH) (Found: MH$^+$, 348.1419. C$_{24}$H$_{18}$N$_3$ [MH$^+$] requires 348.1422); ν$_{max}$ (KBr) 2989, 2208, 1630, 1558, 816; λ$_{max}$ (CHCl$_3$)/nm 328 (log ε 4.06), 285 (log ε 4.20); δ$_H$ (400 MHz; CDCl$_3$) 8.66 (1H, d, *J* 6.4, 6'-H), 8.18 (1H, d, *J* 7.9, 3'-H), 8.15 (1H, s, 5-H), 7.85 (1H, m, 4'-H), 7.70 (2H, app. d, *J* 8.8, 2'',6''-H), 7.32 (1H, m, 5'-H), 7.40 (3H), 7.30 (2H, m, 2''',6'''-H), 6.72 (2H, app. d, *J* 8.8, 3'',5''-H), 2.94 (3H, s, 2-Me); δ$_C$ (100 MHz; CDCl$_3$) 162.2 (C), 159.6 (C), 155.6 (C), 154.6 (C), 149.6 (CH), 137.2 (CH), 137.0 (C), 136.8 (C), 136.4 (C), 129.3 (CH×2),

128.4 (CH×2), 127.9 (CH×2), 127.6 (CH×2), 127.5 (CH), 124.2 (CH), 120.8 (CH), 118.7 (CH), 110.2 (C), 103.8 (CN), 26.2 (CH₃); *m/z* 348 (MH⁺, 100%).

2-Methyl-4-[4-(diphenylamino)phenyl]-6-(2-pyridyl)nicotinonitrile (53o)
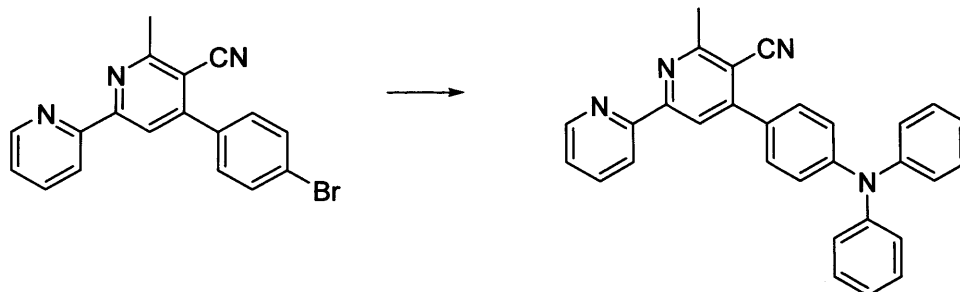
2-Methyl-4-[4-(diphenylamino)phenyl]-6-(2-pyridyl)nicotinonitrile (**53o**) (0.22 g, 88%) was prepared according to the given procedure **6.2.9** using 2-methyl-4-(4-bromophenyl)-6-(2-pyridyl)nicotinonitrile **53g** (0.20 g, 0.57 mmol), catalysed by Cu(neocup)(PPh₃)Br⁸¹ (10 mol%), and was obtained as green crystals, mp 268-270 °C (EtOH) (Found: MH⁺, 439.1838. C₃₀H₂₃N₄ [MH⁺] requires 439.1844); ν_max (KBr) 2986, 2206, 1628, 1556, 814; λ_max (CHCl₃)/nm 302 (log ε 4.70), 393 (log ε 4.52); δ_H (400 MHz; CDCl₃) 8.72 (1H, d, *J* 6.4, 2'-H), 8.54 (1H, d, *J* 7.9, 5'-H), 8.44 (1H, s, 5-H), 7.88 (1H, m, 4'-H), 7.62 (2H, app. d, *J* 8.8, 2'',6''-H), 7.40 (1H, m, 3'-H), 7.35 (6H, m, 3''',4''',5''',3'''',4'''',5''''-H), 7.20 (2H, app. d, *J* 8.8, 3'',5''-H), 7.18 (4H, m, 2''',6''',2'''',6''''-H), 2.92 (3H, s, 2-Me); δ_C (100 MHz; CDCl₃) 161.2 (C), 159.8 (C), 155.6 (C), 154.6 (C), 149.5 (CH), 141.7 (C), 141.2 (C×2), 137.2 (CH), 132.6 (C), 129.9 (CH×4), 128.5 (CH×2), 124.4 (CH), 123.4 (CH×2), 123.2 (CH×2), 122.7 (CH×4), 120.8 (CH), 118.9 (CH), 117.2 (C), 102.6 (CN), 26.0 (CH₃); *m/z* 439 (MH⁺, 100%).
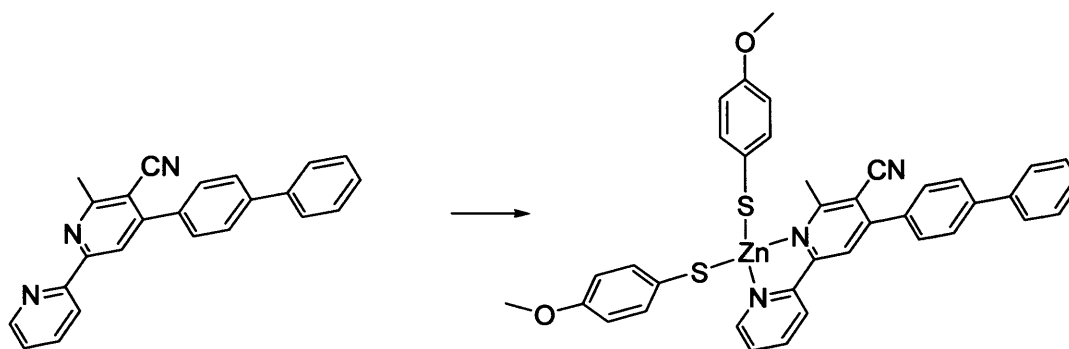
2-Methyl-3-cyano-4-(4-biphenyl)-6-(2-pyridyl)pyridyl-Znᴵᴵ-bis(benzenethiolate) (85a)
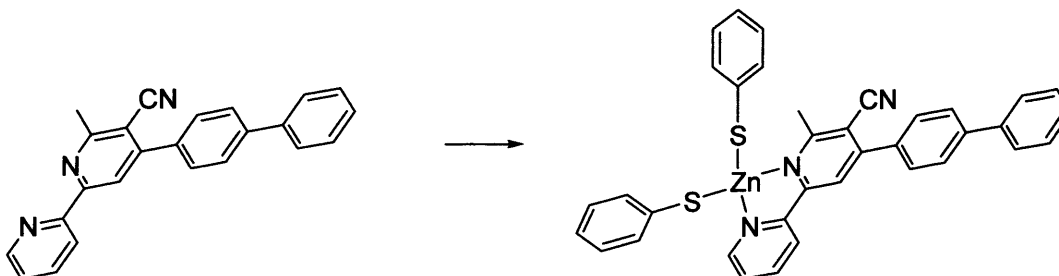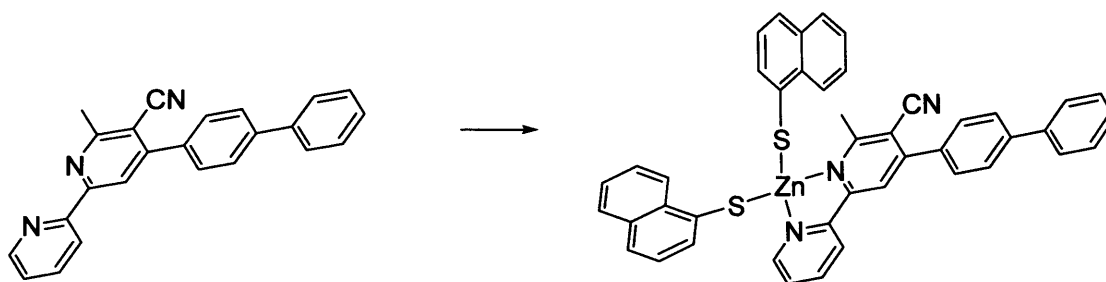

2-Methyl-3-cyano-4-(4-biphenyl)-6-(2-pyridyl)pyridyl-Znᴵᴵ-bis(benzenethiolate) (**85a**) (0.24 g, 94%) was prepared according to the given procedure **6.2.10** using thiophenol (0.08 mL, 0.8 mmol) and 2-methyl-4-(4-biphenyl)-6-(2-pyridyl)nicotinonitrile **53n** (0.4 mmol, 1 equiv.) and was obtained as bright yellow crystals, mp 220–222 °C (Found: M⁺, 629.0926. C₃₆H₂₈N₃S₂Zn [M⁺]

requires 629.0938); v_{max} (KBr) 2990, 2209, 1630, 1556, 1250, 818; λ_{max} (CHCl$_3$)/nm 390 (log ε 4.03), 325 (log ε 4.37); δ_H (400 MHz; CDCl$_3$) 8.86 (1H, d, *J* 6.4, 6'-H), 8.38 (1H, d, *J* 7.9, 3'-H), 8.36 (1H, s, 5-H), 8.09 (1H, m, 4'-H), 7.88 (2H, app. d, *J* 8.8, 2'',6''-H), 7.78 (3H), 7.69 (2H, m, 2''',6'''-H), 7.52 (6H), 7.40 (4H, m), 6.92 (1H, m, 5'-H), 6.88 (2H, app. d, *J* 8.8, 3'',5''-H), 3.29 (3H, s, 2-Me); δ_C (100 MHz; CDCl$_3$) 164.8 (C), 161.6 (C), 158.6 (C), 154.4 (C), 145.2 (CH), 137.4 (CH), 137.0 (C), 136.8 (C), 136.4 (C), 132.5 (C×2), 129.4 (CH×4), 129.2 (CH×2), 129.0 (CH×4), 128.4 (CH×2), 127.9 (CH×2), 127.6 (CH×2), 127.4 (CH), 125.6 (CH×2), 124.2 (CH), 120.8 (CH), 118.7 (CH), 117.0 (C), 108.2 (CN), 28.4 (CH$_3$); *m/z* 629 (M$^+$, 100%).
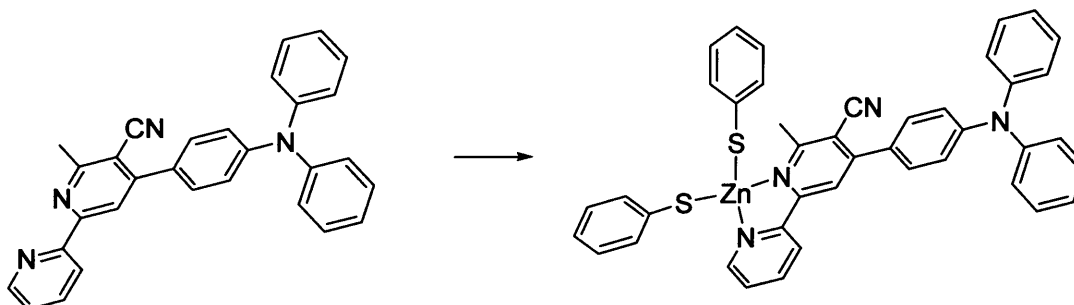
2-Methyl-3-cyano-4-(4-biphenyl)-6-(2-pyridyl)pyridyl-Zn^{II}-bis(4-methoxybenzenethiolate) (85b)

2-Methyl-3-cyano-4-(4-biphenyl)-6-(2-pyridyl)pyridyl-Zn^{II}-bis(4-methoxybenzenethiolate) (85b) (0.28 g, 96%) was prepared according to the given procedure **6.2.10** using 4-methoxythiophenol (0.10 mL, 0.8 mmol) and 2-methyl-4-(4-biphenyl)-6-(2-pyridyl)nicotinonitrile **53n** (0.4 mmol, 1 equiv.) and was obtained as deep yellow crystals, mp 230–232 °C (Found: M$^+$, 689.1134. C$_{38}$H$_{32}$N$_3$O$_2$S$_2$Zn [M$^+$] requires 689.1149); v_{max} (KBr) 2994, 2208, 1628, 1554, 1252, 1200, 816; λ_{max} (CHCl$_3$)/nm 392 (log ε 3.96), 322 (log ε 4.40); δ_H (400 MHz; CDCl$_3$) 8.84 (1H, d, *J* 6.4, 6'-H), 8.36 (1H, d, *J* 7.9, 3'-H), 8.30 (1H, s, 5-H), 8.04 (1H, m, 4'-H), 7.86 (2H, app. d, *J* 8.8, 2'',6''-H), 7.76 (4H, app. d, *J* 8.9), 7.70 (3H), 7.64 (2H, m), 7.20 (4H, app. d, *J* 8.9), 6.90 (1H, m, 3'-H), 6.86 (2H, app. d, *J* 8.8, 3'',5''-H), 3.86 (6H, s, 2×OMe), 3.26 (3H, s, 2-Me); δ_C (100 MHz; CDCl$_3$) 162.6 (C), 161.4 (C), 157.5 (C×2), 157.0 (C), 154.4 (C), 145.0 (CH), 137.2 (CH), 137.0 (C), 136.8 (C), 136.5 (C), 130.4 (CH×4), 129.3 (CH×2), 128.4 (CH×2), 127.9 (CH×2), 127.6 (CH×2), 127.2 (CH), 124.8 (C×2), 124.2 (CH), 120.8 (CH), 118.7 (CH), 114.6 (CH×4), 110.2 (C), 108.0 (CN), 58.9 (CH$_3$×2), 27.6 (CH$_3$); *m/z* 689 (M$^+$, 100%).

2-Methyl-3-cyano-4-(4-biphenyl)-6-(2-pyridyl)pyridyl-Zn^{II}-bis(2-naphthalenethiolate) (85c)

2-Methyl-3-cyano-4-(4-biphenyl)-6-(2-pyridyl)pyridyl-Zn^{II}-bis(2-naphthalenethiolate) **(85c)** (0.28 g, 96%) was prepared according to the given procedure 6.2.10 using 2-naphthalenethiol (0.13 g, 0.8 mmol) and 2-methyl-4-(4-biphenyl)-6-(2-pyridyl)nicotinonitrile **53n** (0.4 mmol, 1 equiv.) and was obtained as light yellow crystals, mp 238–240 °C (Found: M$^+$, 729.1169. C$_{44}$H$_{32}$N$_3$S$_2$Zn [M$^+$] requires 729.1251); ν_{max} (KBr) 2990, 2210, 1626, 1556, 1250, 816; λ_{max} (CHCl$_3$)/nm 388 (log ε 4.06), 328 (log ε 4.32); δ_H (400 MHz; CDCl$_3$) 8.86 (1H, d, *J* 6.4, 6'-H), 8.38 (1H, d, *J* 7.9, 3'-H), 8.34 (1H, s, 5-H), 8.06 (1H, m, 4'-H), 7.88 (2H, app. d, *J* 8.8, 2'',6''-H), 7.78 (2H, s, 1-NapH), 7.70 (3H), 7.62 (2H, m, 2''',6'''-H), 7.58 (2H, d, *J* 8.6, 4-NapH), 7.46 (4H, 5,8-NapH), 7.32 (2H, d, *J* 8.6, 3-NapH), 7.16 (4H, 6,7-NapH), 6.96 (1H, m, 3'-H), 6.89 (2H, app. d, *J* 8.8, 3'',5''-H), 3.32 (3H, s, 2-Me); δ_C (100 MHz; CDCl$_3$) 163.4 (C), 161.8 (C), 157.6 (C), 154.6 (C), 145.0 (CH), 137.4 (CH), 137.0 (C), 136.9 (C), 136.6 (C), 134.1 (C×2), 131.6 (CH×2), 130.6 (C×2), 129.9 (C×2), 129.3 (CH×2), 128.4 (CH×2), 128.2 (CH×2), 128.0 (CH×4), 127.6 (CH×2), 127.4 (CH×2), 127.0 (CH), 126.6 (CH×2), 126.2 (CH×4), 124.2 (CH), 120.8 (CH), 118.7 (CH), 117.0 (C), 108.4 (CN), 28.8 (CH$_3$); *m/z* 729 (M$^+$, 100%).
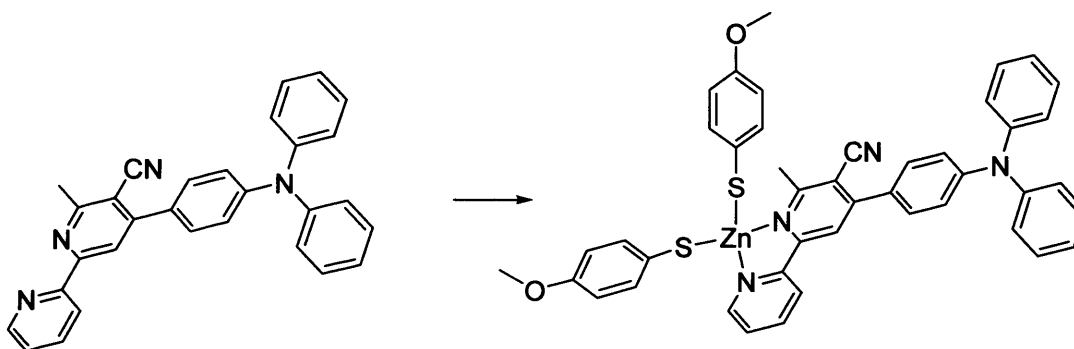
2-Methyl-3-cyano-4-[4-(diphenylamino)phenyl]-6-(2-pyridyl)pyridyl-Zn^{II}-bis-(benzenethiolate) (85d)

2-Methyl-3-cyano-4-[4-(diphenylamino)phenyl]-6-(2-pyridyl)pyridyl-Zn^{II}-bis(benzenethiolate) **(85d)** (0.28 g, 96%) was prepared according to the given procedure **6.2.10** using thiophenol (0.08 mL, 0.8 mmol) and 2-methyl-4-[4-(diphenylamino)phenyl]-6-(2-pyridyl)nicotinonitrile **53o** (0.4 mmol, 1 equiv.) and was obtained as bright red crystals, mp 236–238 °C (Found: M$^+$, 720.1328.

$C_{42}H_{33}N_4S_2Zn$ [M$^+$] requires 720.1360); v_{max} (KBr) 2988, 2204, 1628, 1556, 1252, 816; λ_{max} (CHCl$_3$)/nm 486 (log ε 3.86), 392 (log ε 4.18); δ_H (400 MHz; CDCl$_3$) 8.86 (1H, d, J 6.4, 6'-H), 8.26 (1H, d, J 7.9, 3'-H), 8.20 (1H, m, 4'-H), 8.01 (1H, s, 5-H), 7.79 (1H, m, 5'-H), 7.61 (2H, app. d, J 8.8, 2'',6''-H), 7.53 (6H), 7.46 (4H, m), 7.38 (6H), 7.20 (4H, m), 6.89 (2H, app. d, J 8.8, 3'',5''-H), 3.24 (3H, s, 2-Me); δ_C (100 MHz; CDCl$_3$) 163.9 (C), 161.4 (C), 157.2 (C), 154.6 (C), 145.0 (CH), 141.5 (C), 141.0 (C×2), 137.2 (CH), 132.6 (C×2), 132.2 (C), 129.7 (CH×4), 129.4 (CH×4), 129.1 (CH×4), 128.3 (CH×2), 125.6 (CH×2), 124.2 (CH), 123.2 (CH×2), 123.0 (CH×2), 122.7 (CH×4), 120.6 (CH), 118.4 (CH), 116.0 (C), 103.6 (CN), 28.0 (CH$_3$); m/z 720 (M$^+$, 100%).

2-Methyl-3-cyano-4-[4-(diphenylamino)phenyl]-6-(2-pyridyl)pyridyl-Zn^{II}-bis(4-methoxy-benzenethiolate) (85e)
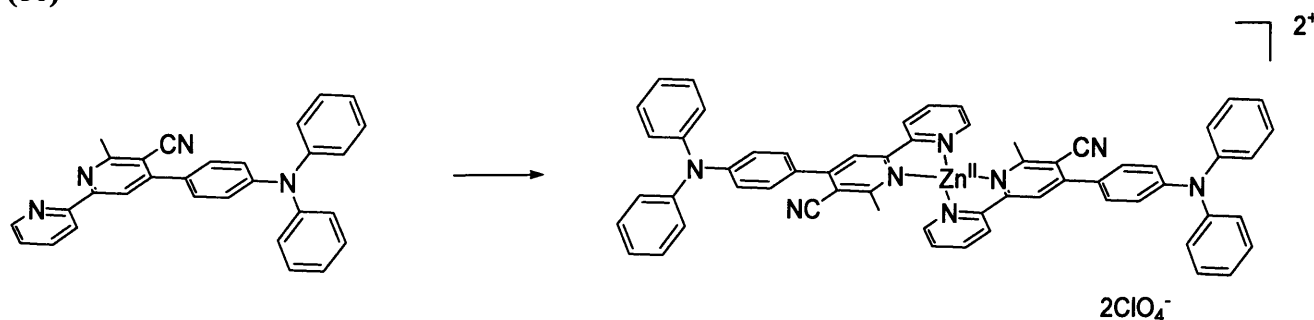

2-Methyl-3-cyano-4-[4-(diphenylamino)phenyl]-6-(2-pyridyl)pyridyl-Zn^{II}-bis(4-methoxy-benzenethiolate) (85e) (0.30 g, 96%) was prepared according to the given procedure **6.2.10** using 4-methoxythiophenol (0.10 mL, 0.8 mmol) and 2-methyl-4-[4-(diphenylamino)phenyl]-6-(2-pyridyl)nicotinonitrile **53o** (0.4 mmol, 1 equiv.) and was obtained as deep red crystals, mp 248–250 °C (Found: M$^+$, 780.1560. $C_{44}H_{37}N_4O_2S_2Zn$ [M$^+$] requires 780.1571); v_{max} (KBr) 2989, 2206, 1629, 1558, 1254, 1202, 818; λ_{max} (CHCl$_3$)/nm 490 (log ε 3.78), 390 (log ε 4.20); δ_H (400 MHz; CDCl$_3$) 8.84 (1H, d, J 6.4, 6'-H), 8.24 (1H, d, J 7.9, 3'-H), 8.19 (1H, m, 4'-H), 8.00 (1H, s, 5-H), 7.77 (1H, m, 5'-H), 7.60 (2H, app. d, J 8.8, 2'',6''-H), 7.48 (4H, app. d, J 8.9), 7.36 (6H), 7.18 (4H, m), 6.96 (4H, app. d, J 8.9), 6.84 (2H, app. d, J 8.8, 3'',5''-H), 3.84 (6H, s, 2×OMe), 3.22 (3H, s, 2-Me); δ_C (100 MHz; CDCl$_3$) 162.4 (C), 161.4 (C), 157.5 (C×2), 157.0 (C), 152.4 (C), 144.0 (CH), 141.2 (C), 140.8 (C×2), 137.2 (CH), 132.4 (C), 130.2 (CH×4), 129.5 (CH×4), 128.0 (CH×2), 124.8 (C×2), 124.0 (CH), 123.2 (CH×2), 123.0 (CH×2), 122.5 (CH×4), 120.6 (CH), 118.5 (CH), 117.0 (C), 114.4 (CH×4), 102.8 (CN), 58.0 (CH$_3$×2), 27.6 (CH$_3$); m/z 780 (M$^+$, 100%).

2-Methyl-3-cyano-4-[4-(diphenylamino)phenyl]-6-(2-pyridyl)pyridyl-Zn^{II}-bis(2-naphthalenethiolate) (85f)
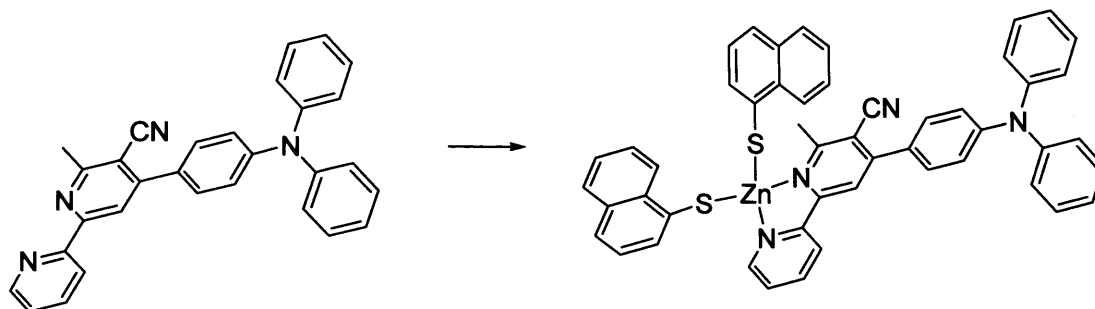
2-Methyl-3-cyano-4-[4-(diphenylamino)phenyl]-6-(2-pyridyl)pyridyl-Zn^{II}-bis(2-naphthalenethiolate) (**85f**) (0.32 g, 98%) was prepared according to the given procedure **6.2.10** using 2-naphthalenethiol (0.13 g, 0.8 mmol) and 2-methyl-4-[4-(diphenylamino)phenyl]-6-(2-pyridyl)nicotinonitrile **53o** (0.4 mmol, 1 equiv.) and was obtained as pale red crystals, mp 256–258 °C (Found: M$^+$, 820.1588. C$_{50}$H$_{37}$N$_4$S$_2$Zn [M$^+$] requires 820.1673); v$_{max}$ (KBr) 2994, 2208, 1630, 1559, 1254, 820; λ_{max} (CHCl$_3$)/nm 484 (log ε 3.90), 394 (log ε 4.14); δ$_H$ (400 MHz; CDCl$_3$) 8.89 (1H, d, *J* 6.4, 6'-H), 8.26 (1H, d, *J* 7.9, 3'-H), 8.23 (1H, m, 4'-H), 8.12 (1H, s, 5-H), 7.84 (1H, m, 5'-H), 7.59 (2H, app. d, *J* 8.8, 2'',6''-H), 7.44 (2H, s, 1-NapH), 7.34 (6H), 7.24 (2H, d, *J* 8.60, 4-NapH), 7.16 (4H, m), 7.12 (4H, 5,8-NapH), 6.88 (2H, d, *J* 8.60, 3-NapH), 6.80 (2H, app. d, *J* 8.8, 3'',5''-H), 6.72 (4H, 6,7-NapH), 3.26 (3H, s, 2-Me); δ$_C$ (100 MHz; CDCl$_3$) 164.8 (C), 163.6 (C), 159.4 (C), 157.4 (C), 147.0 (CH), 143.5 (C), 143.0 (C×2), 140.2 (CH), 137.1 (C×2), 135.4 (C), 134.5 (CH×2), 133.6 (C×2), 132.9 (C×2), 130.7 (CH×4), 129.4 (CH×2), 128.6 (CH×2), 128.2 (CH×4), 127.6 (CH×2), 127.0 (CH×4), 126.2 (CH), 124.2 (CH×2), 123.8 (CH×2), 123.4 (CH×4), 121.8 (CH), 119.7 (CH), 118.0 (C), 104.2 (CN), 28.6 (CH$_3$); m/z 820 (M$^+$, 100%).

Zn^{II}-bis{3-cyano-4-[4-(diphenylamino)phenyl]-6-(2-pyridyl)pyridyl} perchlorate complex (86)

Zn^{II}-bis{3-cyano-4-[4-(diphenylamino)phenyl]-6-(2-pyridyl)pyridyl} perchlorate complex (**86**) (0.22 g, 96%) was prepared according to the given procedure **6.2.11** using zinc perchlorate

hexahydrate (0.2 mmol, 1 equiv.) and 2-methyl-4-[4-(diphenylamino)phenyl]-6-(2-pyridyl)nicotinonitrile **53o** (0.4 mmol, 2 equiv.) and was obtained as bright orange crystals, mp 296–298 °C (Found: M^+, 1138.1940. $C_{60}H_{45}Cl_2N_8O_8Zn$ [M^+] requires 1138.1951); v_{max} (KBr) 2988, 2208, 1630, 1556, 816; λ_{max} (CHCl$_3$)/nm 450 (log ε 4.16), 302 (log ε 4.51); δ_H (400 MHz; CDCl$_3$) 8.90 (2H, d, *J* 6.4, 2×6'-H), 8.74 (2H, d, *J* 7.9, 2×3'-H), 8.66 (2H, s, 2×5-H), 8.02 (2H, m, 2×4'-H), 7.88 (4H, app. d, *J* 8.8, 2×2'',6''-H), 7.66 (2H, m, 2×5'-H), 7.56 (12H), 7.40 (4H, app. d, *J* 8.8, 2×3'',5''-H), 7.36 (8H, m), 3.28 (6H, s, 2×2-Me); δ_C (100 MHz; CDCl$_3$) 162.8 (C×2), 161.6 (C×2), 157.6 (C×2), 155.6 (C×2), 150.5 (CH×2), 143.8 (C×2), 143.4 (C×4), 139.2 (CH×2), 134.6 (C×2), 131.9 (CH×8), 130.5 (CH×4), 126.4 (CH×2), 124.4 (CH×4), 124.0 (CH×4), 123.7 (CH×8), 122.8 (CH×2), 119.9 (CH×2), 118.0 (C×2), 103.8 (CN×2), 28.8 (CH$_3$×2); *m/z* 1138 (M$^+$, 100%).

References

[1.] Lakowicz, J. R. *'Principles of Fluorescence Spectroscopy'* 3rd Ed, Springer, New York, **2006**.

[59.] Matsui, M.; Oji, A.; Hiramatsu, K.; Shibata, K.; Maramatsu, H. *J. Chem. Soc., Perkin Trans. 2.* **1992**, *2*, 201.

[65.] Bowman, M. D.; Jacobsen, M. M.; Blackwell, H. E. *Org. Lett.*, **2006**, *8*, 1645.

[78.] Shi Shun, A. L. K.; Chernick, E. T.; Eisler, S.; Tykwinski, R. R. *J. Org. Chem.*, **2003**, *68*, 1339.

[81.] Venkataraman, D.; Gujadhur, R. K.; Bates, C. G. *Org. Lett.*, **2001**, *3*, 4315.

[107.] Bagley, M. C.; Hughes, D. D.; Lubinu, M. C.; Merritt, E. A.; Taylor, P. H.; Tomkinson, N. C. O. *QSAR Comb. Sci.*, **2004**, *23*, 859.

[171.] Williams, J. A. G.; Aspley, C. J. *New J. Chem.*, 2001, **25**, 1136.

[172.] For related complexes, see Yam, V.; Ngan, T-W.; Ko, C-C.; Zhu, Z. *Inorg. Chem.*, **2007**, *46*, 1144.

[173.] For related complexes, Fu, W.; Xu, Q-Q.; Wang, D-H.; Chi, S-M.; Gan, X. *Inorg. Chim. Act.*, **2009**, 2529.

Appendix

Appendix –I

Chapter 4.4.2.1: Dipole difference between ground and excited states

80g
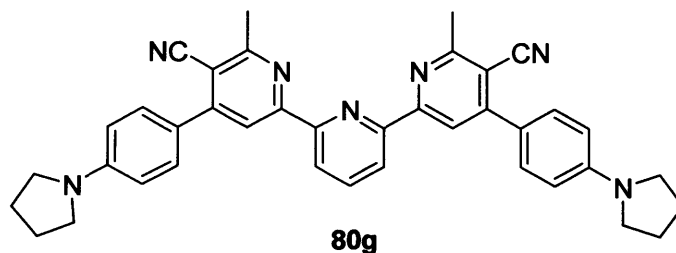
Lippert-Mataga plot: 80g in various solvents

$y = 7323.3x + 3251.1$

Polarity parameter
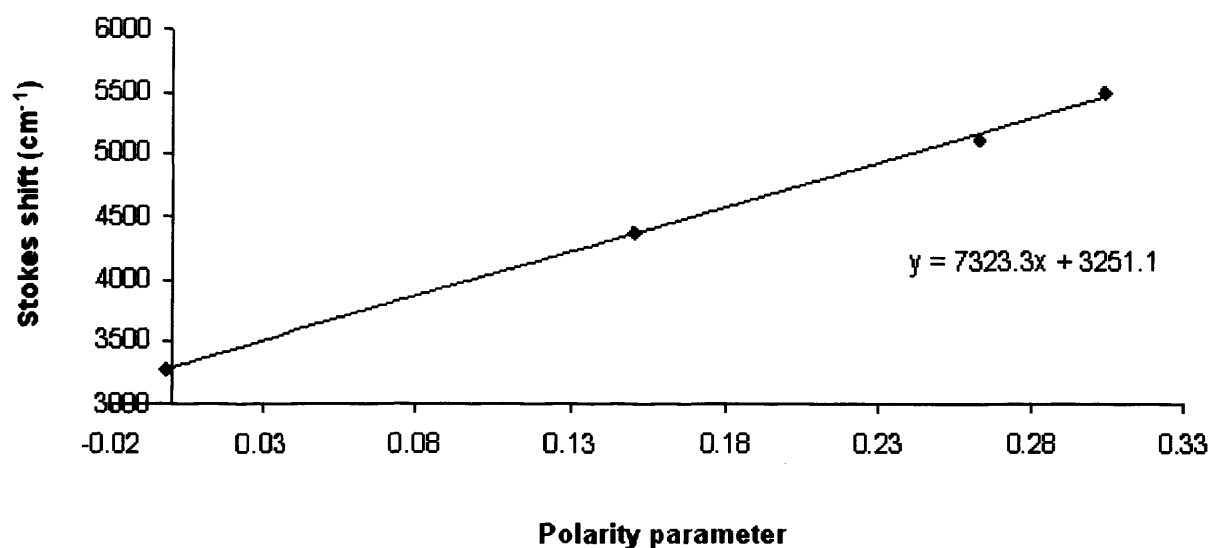
Solvent	ε	n	Δf	$\Delta\upsilon_{st}$ (cm^{-1})	Slope (cm^{-1})	$\Delta\mu_{eg}$ (D)
Cyclohexane	2.02	1.426	-0.02	3271	7323	**18.8**
Chloroform	4.89	1.446	0.05	4383		
Acetonitrile	37.5	1.342	0.31	5600		
DMSO	46.71	1.479	0.26	5266		

The change of the dipole moment $\Delta\mu_{eg}$ between the ground and the excited states can be calculated using the Lippert-Mataga equation, where:

$$\Delta\upsilon_{st} = \frac{2\Delta\mu_{eg}^2}{hca^3}\Delta f + const \quad \&$$

$$\Delta f = \frac{\varepsilon-1}{2\varepsilon+1} - \frac{n^2-1}{2n^2+1}$$

i

From the slope of the plot shown above, the magnitude of $\Delta\mu_{eg}$ can be obtained as **18.8 D** by estimating the cavity radius a equals to **7.86 Å** from the molecular volume as calculated from the molecular weight of **80g** and the molecular density for general D-A type molecules,[146] which equals to 0.95 g cm^{-3}.

Calculation

Slope = 7323 cm^{-1}

This value equals to $2\Delta\mu_{eg}^2 / hca^3$, assuming a radius of 7.86 Å:

$\Delta\mu_{eg}^2 = (7323/2) \, hca^3 = 3661.6(6.626 \times 10^{-27})(3 \times 10^{10})(7.86 \times 10^{-8})^3$

$\quad\quad = 3.53 \times 10^{-34} \, (\text{cm}^{-1})(\text{erg s})(\text{cm s}^{-1})(\text{cm}^3)$

Using erg = g cm^2 s^{-2}, one obtains $\Delta\mu_{eg}^2 = 3.53 \times 10^{-34} \, (\text{g cm}^3 \, \text{s}^{-2}) \, \text{cm}^2$

So $\Delta\mu_{eg} = 1.88 \times 10^{-17} \, (\text{g}^{1/2} \, \text{cm}^{3/2} \, \text{s}^{-1}) \, \text{cm}$

Since esu = g$^{1/2}$ cm$^{3/2}$ s^{-1}, thus the result can be expressed either:

in *esu* unit: $\Delta\mu_{eg} = 18.8 \times 10^{-18}$ *esu cm* or,

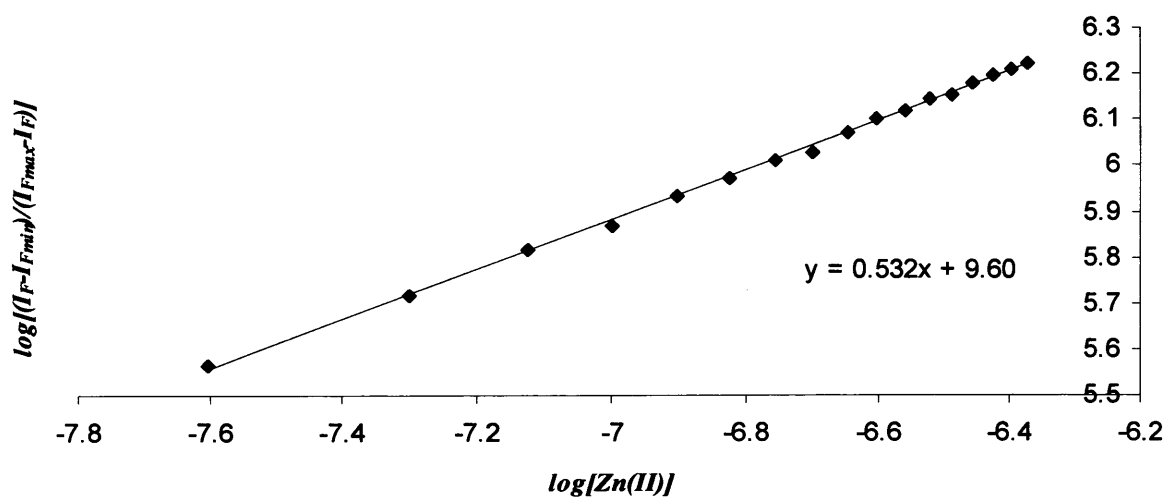in *Debye* unit: $\Delta\mu_{eg} = 18.8$ *D*

Appendix – II

Chapter 4.4.2.3: Calculation of the dissociation constant K_d[1]

$$nM \quad + \quad L \quad \underset{Kd}{\overset{Ka}{\rightleftharpoons}} \quad M_nL$$

$K_d = [M]^n[L]/[M_nL]$

If $[L_o] \gg [M_o]$

$[(I_F - I_{Fmin})/(I_{Fmax} - I_F)] \approx [M_nL]/[L] = [M]^n/K_d$

So $\log[(I_F - I_{Fmin})/(I_{Fmax} - I_F)] = n \times \log[M] - \log K_d$

The Hill Plot

Thus $n \approx 0.5$ (confirmed the 1:2 binding),

$\log K_d = -9.60$;

$K_d = 2.51 \times 10^{-7} \ \mu M^{1/2}$

Appendix – III

<u>Research Publications</u>

1. 'Rapid synthesis of 3-cyanopyridine-derived chromophores with two-dimensional tunability and solvatochromic photophysical properties', Bagley, M. C.; Lin, Z.; Pope, S. J. A. *J. Chem. Soc., Chem. Commun.*, **2009**, 5165 – 5167. (*I.F.: 5.504*)

2. 'Barium manganate in microwave-assisted oxidation reactions: synthesis of solvatochromic 2,4,6-triarylpyrimidines', Bagley, M. C.; Lin, Z.; Pope, S. J. A. *Tetrahedron Lett.*, **2009**, *50*, 6818 – 6822. (*I.F.: 2.660*)

3. 'Barium manganate in microwave-assisted oxidation reactions: synthesis of lactones by oxidative cyclization of diols', Bagley, M. C.; Lin, Z.; Phillips, D. J.; Graham, A. E. *Tetrahedron Lett.*, **2009**, *50*, 6823 - 6825. (*I.F.: 2.660*)

4. 'Microwave-assisted synthesis and complexation of luminescent cyanobipyridyl-zinc(II)-bis(thiolate) complexes with intrinsic and ancillary photophysical tunability', Bagley, M. C.; Lin, Z.; Pope, S. J. A. *J. Chem. Soc., Dalton. Trans.*, **2010**, *39*, 3163 - 3166. (*I.F.: 4.081*)

5. 'Bohlmann-Rahtz synthesis of a novel terpyridine PCT fluorescent sensor for the detection of Zn(II) ions in the near physiological environment', Lin, Z.; Bagley, M. C.; Pope, S. J. A. *J. Chem. Soc., Chem. Commun.*, **2011**, in preparation – *obtained full experimental results.*

6. 'Novel microwave-mediated synthesis of luminescent chromophores for photophysical study', Bagley, M. C.; Lin, Z.; Pope, S. J. A. *J. Am. Chem. Soc.*, **2011**, in preparation – *obtained full experimental results.*

References

[1.] Lakowicz, J. R. *'Principles of Fluorescence Spectroscopy'* 3rd Ed, Springer, New York, **2006**.

[146.] Letard, J. F.; Lapouyade, R.; Rettig, W. *J. Am. Chem. Soc.* **1993**, *115*, 2441.